Bond Performance between Lightweight Concrete with Crumb Rubber and Glass Fibre Reinforced Polymer Bar

by

Rupak Mutsuddy

A thesis submitted in partial fulfillment of the requirements for the degree of

Doctor of Philosophy

in

Structural Engineering

Department of Civil and Environmental Engineering
University of Alberta

ABSTRACT

For any reinforced concrete structure, the bond between concrete and the reinforcement bar is the most important parameter from structural standpoint. Notwithstanding numerous prior studies on describing this interaction for different reinforcing bars, not enough understanding exists for fibre reinforced polymer bars in structural lightweight concrete. In the research reported here, the bond between Glass Fibre Reinforced Polymer (GFRP) bar and a structural lightweight concrete is examined. Crumb rubber derived from recycled tires was used as fine aggregate in the concrete mix. A variety of industrial waste were utilized as supplementary cementing materials to further render the mix sustainable.

The experimental aspect focused on the development of the lightweight concrete mixes with potential structural use. Based on their mechanical performance, a particular basic mixture that was prepared with a blend of silica fume and Portland cement, was selected for further examination of bond performance with GFRP. Through their compressive and flexural performance, one notes up to 70% compressive strength loss was observed with the mixes with 100% crumb rubber replacement. An optimal replacement of fine aggregates with 50% crumb rubber was obtained.

Two different sizes of GFRP bar were used for the experimental pullout test where the concrete mixes were prepared with the optimal mix, as found earlier. Cylindrical samples with rebar embedded were tested for bond performance as the rebar pulled out from each matrix. This study examined the effect of crumb rubber replacement dosage as well as that of the bar diameter. Results show that the bond strength decreases with an increase in the replacement of

conventional fine aggregate with crumb rubber. As expected, in beams, an increase in the bar diameter resulted in a drop in the bond strength. However, when each bar was pulled out of a cylindrical concrete matrix, the bond strength was sensitive to the amount of crumb rubber. An increasing crumb rubber to fine aggregate content resulted in a better performance for larger bar diameter. This was true both in plain concrete and in the presence of steel fibres. In single rebar pullout, the presence of microfibres was seen to benefit the larger bar diameter. This was attributed to the relatively less disturbance created by the fiber at the surface of contact, which promotes better stress transfer through friction.

The analytical approach consists of exploring established bond-slip relationships for various concrete compositions and reinforcement types. The results from pullout testing obtained here were used to verify the bond-slip relationship and determine the parameters for the specific mix proportions and bar size in the present case.

ACKNOWLEDGEMENTS

First, I would like to express my sincere thanks to Dr. Vivek Bindiganavile, my research supervisor, for giving me the opportunity to pursue my interest on concrete technology and sustainability. His professional guidance, innovative insights, technical expertise and continuous encouragement are helpful to overcome all the challenges towards successful completion of this program. I am also very grateful to Dr. J.J. Roger Cheng for his invaluable guidance, support and constructive comments. I would like to extend my gratitude to all the committee members for their precious time, comments and suggestions during my Doctoral Final exam: Dr. Carlos Cruz-Noguez, Dr. Alireza Bayat and Dr. Ashutosh Bagchi. Special gratitude is given to Dr. Alireza Bayat and Dr. Adam Lubell for their support during doctoral candidacy exam.

I would like to express my heartfelt gratitude towards Arlene Figley, Graduate Advisor, for her continuous support and encouragement to overcome many challenges during the program. Again, as experimental work formed a significant part of this research program, I am deeply thankful to Mr. Rizaldy Mariano of Concrete Lab for helping with concrete samples preparation and Mr. Greg Miller and Mr. Cameron West of Structural Lab for their help with carrying out compressive tests, flexural test, pull out test and beam test.

During the entire program I had the opportunity to associate with many graduate students and research associates. I would like to express my special gratitude to Mr. Mamun and Mr. Toihidul for their valuable help during sample preparation, conducting various tests and analyzing data from the test as well as helping with the drafting. Not only that, their supports in personal life helped me a lot to overcome many other challenges.

Finally, I would like to dedicate my grateful words to my wife Nilantika for her unconditional love and support during my entire program. Nilantika, along with my two kids Dhrubojyoti and Avantika, and our parents are the true inspiration in completing this program.

TABLE OF CONTENTS

LIST OF TABLES

LIST OF FIGURES

LIST OF SYMBOLS

Chapter 2

l_d = development or splice length,

d_b = diameter of rebar

f_y = yield strength of reinforcing bar being developed,

f'_c = concrete compressive strength,

α = reinforcement location factor (Equation (2.1) and (2.2))

β = coating factor (Equation (2.1) and (2.2))

γ = reinforcement size factor

λ = light-weight concrete factor

c = spacing or cover dimension,

K_{tr} = transverse reinforcement index = $K_{tr} = \frac{A_{tr} f_{yt}}{10sn}$,

A_{tr} = area of each stirrup or tie crossing the potential plane of splitting adjacent to the reinforcement being developed, spliced or anchored,

f_{yt} = yield strength of transverse reinforcement

s = spacing of transverse reinforcement

n = number of bars being developed or spliced

d_b = diameter of the reinforcement bar

F, G = Empirical constant in Malvar Model for each bar type

P = the tensile load

p = softening branch slope defining parameter in BPE and mBPE model

s = slip

s_m/s_1 = slip at maximum bond stress

$s_{m,ue}$ = unloaded end slip at maximum bond stress

$s_{m,ue}{}^b$ = average unloaded end slip at maximum bond stress

$s_{m,le}$ = loaded end slip at maximum bond stress

$s_{m,le}{}^b$,= average loaded end slip at maximum bond stress

s_r = curve fitting parameter in Cosenza Manfredi Realfonzo (CMR) model

s_2 = maximum slip at constant maximum bond stress (as per BPE model)

s_3 = slip at the end of softening branch (as per BPE and mBPE model)

α = curve fitting parameter for BPE model and modified BPE model (Equation (5.4))

β = curve fitting parameter in Cosenza Manfredi Realfonzo (CMR) model (Equation (5.6))

τ_m/τ_1 = maximum bond stress

τ^*_{max} = maximum normalized bond stress

τ_3 = bond stress at the end of softening branch (as per BPE and mBPE model)

Chapter 3

b = average width of the specimen at fracture,

d = average depth of the specimen at fracture.

E_c = Modulus of Elasticity of concrete

f_1 = first Peak Strength,

f'_c = Compressive strength of concrete

f_r = Modulus of rupture

K_{IC} = Fracture Toughness

$R^D_{T,150}$ = equivalent flexural strength ratio

T^D_{150} = toughness up to a net deflection of $L/150$

Δ = Midspan beam deflection

Chapter 4

$LVDT$ = Linear variable Displacement Transducer

E_c = Modulus of Elasticity of concrete

f'_c = Compressive strength of concrete

γ_c = Density of concrete

CoV = Coefficient of Variation

P = tensile load in reinforcement bar during pullout test,

d_b = diameter of the bar,

l_b = embedment length

Chapter 5

d_b = diameter of the reinforcement bar

F, G = Empirical constant in Malvar Model for each bar type

$f'c$ = compressive strength of concrete

l_b = embedment length

P = the tensile load

p = softening branch slope defining parameter in BPE and mBPE model

s = slip

s_m/s_1 = slip at maximum bond stress

$s_{m,ue}$ = unloaded end slip at maximum bond stress

$s_{m,ue}^b$ = average unloaded end slip at maximum bond stress

$s_{m,le}$ = loaded end slip at maximum bond stress

$s_{m,le}^b$,= average loaded end slip at maximum bond stress

s_r = curve fitting parameter in Cosenza Manfredi Realfonzo (CMR) model

s_2 = maximum slip at constant maximum bond stress (as per BPE model)

s_3 = slip at the end of softening branch (as per BPE and mBPE model)

α = curve fitting parameter for BPE model and modified BPE model

β = curve fitting parameter in Cosenza Manfredi Realfonzo (CMR) model

τ_m/τ_1 = maximum bond stress

$\tau^*_{\max}$ = maximum normalized bond stress

τ_3 = bond stress at the end of softening branch (as per BPE and mBPE model)

Chapter 6

τ = average bond stress (MPa);

P = axial tensile force in the rebar,

l_e = embedment length of rebar (mm);

d_b = rebar diameter (mm).

F = Applied load on the beam during testing

Chapter 7

A = cross sectional area

B = constant in stress rate sensitivity Equation (7.7) proposed by Nadeau et al. (1982)

b = average width of the specimen at fracture,

d = average depth of the specimen at fracture.

E_c = Modulus of Elasticity of concrete

f_l = first Peak Strength,

f'_c = Compressive Strength of concrete

f_r = Modulus of rupture

K_{IC} = Fracture Toughness

l = overhang span

L = Span of the beam specimen

m = slope of deflection-CMOD line

N = constant in stress rate sensitivity Equation (7.7) proposed by Nadeau et al. (1982), which particularly related to stress rate sensitivity of parameters

ρ = mass density;

$R^D_{T,150}$ = Equivalent flexural strength ratio

S = Span;

T^D_{150}= toughness up to a net deflection of L/150,

$\ddot{u}$ (t) = acceleration at mid span at any time t.

Δ_0 = deflection history

Δ = deflection at midspan

σ_f = stress at final condition,

σ_i = stress at initial condition

$\dot{\sigma}$= stress rate

LIST OF ABBREVIATIONS

OPC – Ordinary Portland Cement

SF – Silica Fume

MK – Metakaolin

LVDT – Linear Variable Displacement Transducer

CoV – Coefficient of Variation

CMOD – Crack mouth opening displacement

GFRP – Glass Fibre Reinforced Polymer

FRC – Fibre reinforced concrete

SFRC – Steel fibre reinforced concrete

.

CHAPTER 1. INTRODUCTION

1.1 Introduction

The proper understanding of the bond between a reinforcing bar and the concrete matrix is the key to characterize and predict the mechanical performance of reinforced concrete structures. A satisfactory bond ensures that forces in the surrounding concrete transfer fully to the reinforcement. Many studies have been conducted on this aspect of reinforced concrete structures, but, the development of sustainable concrete mixtures, introduces innovative industrial and recycled waste. Along with the production of newer reinforcement, this introduces a scope for further improvement of the existing understanding of rebar bond behavior.

Portland cement concrete is the most widely used material in per capita usage with global consumption of 3 billion m^3 (as of 2016). It comprises of Portland cement, fine aggregate and coarse aggregate as the main constituents to which water is added to react with cement in order to form a composite. Usually, a typical concrete mix contains 10-15% cement, 40% coarse aggregate (gravel or crushed stone) and 25% of fine aggregate (sand). Though the major portion of greenhouse gas emitted from concrete production is due to the production of cement, the process of mining sand and gravel and crushed stones, mixing the materials in concrete plant and transporting concrete to the site also require energy and hence emit greenhouse gases in to the atmosphere (Gonçalves and Margarido 2015; Mehta and Monteiro 2014; NRMCA 2012). Cement and concrete industries around the world take many steps to reduce the emission of greenhouse gases. Introduction of supplementary cementitious materials, which are waste products from other industries, in the binder along with cement is a proven method to reduce greenhouse gas emission associated with cement manufacture.

On the other hand, fine and coarse aggregate comprise approximately 60-75% of concrete volume. The concrete industry is searching for lightweight concrete mixes to achieve higher performance to weight ratio which will help with structural efficiency and construction efficiency. By using lightweight concrete, it is expected to have reduced dead load, longer

span, reduced substructure and less transportation cost. In order to achieve higher performance to weight ratio, alternate lightweight aggregates are being used to replace fine and coarse aggregate. Among various available sources, rubber from scrap tires has shown promising use as both coarse and fine aggregate. The use of alternative aggregate source to replace the coarse and fine aggregate will also help reduce environmental impact. An optimal use of such lightweight aggregate renders structural lightweight concrete with adequate mechanical properties that possesses an improved performance-to-weight ratio.

In many countries including Canada & the USA, the scrap tire waste is becoming a major concern for waste management. As reported by U.S. Scrap Tire market, 2016, 4 million tons of scrap tires were generated by US at the end of 2015. Approximately 80% of those scrap tires were consumed for fuel production, civil engineering applications and other products. And the remaining scrap tires were disposed in landfills or stock piled, which may cause environmental degradation to the surrounding sites. However, incorporation of crumb rubber within concrete as its constituent may serve as a possible disposal method of scrap tire. The use of crumb rubber also saves natural resources and thus makes the resultant concrete more sustainable.

In recent years, alternates to steel have been sought as reinforcement to offset the corrosion induced deterioration of reinforced concrete infrastructure. Fiber reinforced polymer (FRP) bars are increasingly being used as concrete reinforcement in view of their better corrosion resistance as well as higher stiffness to weight ratio and superior fatigue properties, as compared to steel reinforcement.

This study has its primary focus on applications which require structural lightweight reinforced concrete. The bond behavior of steel reinforcement with lightweight concrete has been previously studied and the effect of concrete density was incorporated into the bond equation. But the bond behavior of FRP in lightweight concrete introduces an as yet untested variable. Especially since the bond with steel rebar is mechanical in nature whereas that with lower modulus rebar such as FRP bar might be frictional or both frictional and mechanical in nature depending on its surface condition. This study evaluates the various factors that affect this bond and explains the underlying mechanisms.

1.2 Research objectives

The main objective of this research project is to understand the bond behavior of Glass Fibre Reinforced Polymer (GFRP) Bar embedded in lightweight concrete. As is well known, the bond behavior is dependent on factors including: (i) concrete strength and density, (ii) reinforcing material, (iii) bar size, (iv) bar surface condition, (v) loading rate, etc. To assess the effect of strength and density of the concrete on bond performance, lightweight concrete mixes were developed in this study by incorporating crumb rubber as partial replacement to fine aggregate. The bond behavior was determined using pullout testing and quasi static beam tests. The pullout test is a widely used test method that provides a simple means to compare the relative bond performance between FRP bars and surrounding material. This test doesn't consider the emergence of flexural cracking in concrete. On the other hand, the beam test is used to assess the bond performance considering the flexure cracks in the concrete. The objectives of this study were the following:

- Development of structural lightweight concrete mix incorporating crumb rubber, based on quasi-static compressive and flexural response.
- Determination of the bond characteristics between sand coated GFRP bar and lightweight concrete mix that developed in this study.
- Evaluate the applicability of prominent bond-slip analytical models for bond-slip relationship for GFRP bars embedded in structural lightweight concrete.

1.3 Scope of the research

Bond characteristics between reinforcement and surrounding concrete is dependent on various factors, which includes concrete strength, concrete density, reinforcement bar size, bar surface condition, bar location, casting position. Now days, concrete with a wide range of strength and density are being used in various applications. This study examined the bond characteristics of concrete mixes with compressive strength that varies from 10-40 MPa and the density varies from 1400-2200 kg/m^3. As a result, this study would provide a better understanding about structural lightweight concrete prepared with crumb rubber as fine aggregates. In addition to that, discrete steel fiber reinforcement was employed to assess its role on the bond performance

between FRP and lightweight concrete. Among various FRP types and surface conditions, the Glass Fibre Reinforced Polymer (GFRP) bars with sand coated surface were used in this study. Moreover, this study represented the bond performance of two different bar sizes, 10 mm and 16 mm bars. The structural lightweight concrete mixture together with the bond slip relationship with lightweight GFRP rebar offers tremendous opportunity for applications that include crash cushions, traffic barriers.

1.4 Thesis outline

This thesis is presented in a paper based format, wherein Chapter 3 to Chapter 7 describe the major contributions to lightweight concrete mix development and the bond performance between Fibre Reinforced Polymer (FRP) bar of different bar diameter and concrete mixes with different crumb rubber proportions and short steel fibre. To begin with, Chapter 2 narrates the literature reviewed on the performance of lightweight concrete, including those contained crumb rubber. Further, the bond behavior of steel and FRP bars with different types of concrete mixes, is discussed based on experimental data. Thereafter, various analytical models to predict bond performance of specific types of reinforcement are also outlined.

Chapter 3 describes the development of lightweight concrete mixes, designed with crumb rubber as fine aggregate and the evolution of the optimal mix composition. Various mechanical and physical properties of the mixes prepared with crumb rubber were investigated. These mixes were designed according to the proportions typical of lightweight concrete. In addition to the crumb rubber replacement for fine aggregate, lightweight expanded shale was used as the coarse aggregate. In all such cases, the fine aggregate was replaced by volume. Concrete mixes with supplementary cementitious materials (metakaolin and silica fume) as mass replacement of cement were compared for their mechanical properties under static loading. Seeing that silica fume emerged the most efficient supplementary cementitious material, subsequent mixes were developed with a wider range of crumb rubber as volume replacement to fine aggregate.

Chapters 4 to 6 emphasize the bond performance between FRP bar and lightweight concrete developed in this study. Chapter 4 presents the bond performance of Glass Fibre Reinforced Polymer (GFRP) bar of different sizes and concrete mixes with various percentages of crumb rubber as replacement to fine aggregate. Pullout tests on cylindrical specimens were performed to determine the bond response. It was found that higher crumb rubber percentage decreases bond strength. Chapter 5 explores the applicability of various established bond-slip analytical models proposed by previous researchers to the bond slip responses of GFRP bar and concrete mixes. Chapter 6 aims to explore the beam tests for bond strength determination. The beam tests were performed to better simulate stress condition of reinforced concrete structures component. The results showed that the level of fine aggregate replacement with crumb rubber, the bar size and the presence of steel fibre affect the bond performance.

In Chapter 7, as a pilot study, the author explored the effect of higher loading rate on the mechanical strength of various concrete mixes optimized for static performance. A drop weight impact hammer was used to generate the higher loading rates through flexural loading. Stress rate sensitivity for the mechanical properties has been highlighted.

The key findings from this study are summarized in Chapter 8. Alongside, certain recommendations are made for future extension of this work.

References

Gonçalves, M. C., and Margarido, F. (Eds.). (2015). *Materials for Construction and Civil Engineering*. Springer International Publishing, Cham.

Mehta, P. K., and Monteiro, P. J. M. (2014). *Concrete. Structure, properties and materials*. New York, McGraw-Hill Professional.

NRMCA. (2012). National Ready Mixed Concrete Association Concrete CO2 Fact Sheet.

CHAPTER 2. LITERATURE REVIEW

Concrete is one of the most widely used construction materials today. Significant parts of the infrastructure constructed over the last century were built with reinforcing concrete, wherein the tensile forces are taken by continuous reinforcement. Proper bond between reinforcement and surrounding concrete is very important for overall performance of reinforced concrete structures. In this Chapter, firstly, structural lightweight concrete is reviewed with a focus on crumb rubber as aggregate. Following that, the mechanisms underlying the bond between the reinforcement bar and concrete are described. In addition, the factors affecting bond performance as governed by existing formulations to capture this behavior has been described.

2.1 Use of rubber as aggregate

The global aggregate consumption for concrete is approximately 4.5 billion tons (Alexander and Mindess 2005) and the aggregate demand is increasing day by day. This continuous growth in demand has shifted the attention towards alternative aggregate resources. Use of these alternative materials not only reduces the environmental effect through aggregate extraction but also reduces the landfill and recycling cost of those materials, such as use of crumb rubber from scrap tires.

Utilization of scrap tires may play a significant role in sustainable development considering the existing stockpile of scrap tires and the increase in the number of vehicles around the world. In the USA alone, around 290 million tires are generated annually of which 80% were used for fuel production, civil engineering application and other products. In mid 2000s, it was estimated that 40 million tires were disposed of to landfill. By early 2000, over 275 million tires were stockpiled ("U.S. Scrap Tire Market" 2003). This stockpile of tires is dangerous, not only due to potential environmental concern but also from fire hazard. Also those stockpiles often served as the breeding ground of insects and rats which pose health risks. As a result, land filling of the tires is becoming unacceptable. Innovative solutions to solve the tire disposal

problem have been explored by various researchers. Use of tire chips as aggregate is one of the many ways to dispose tires in a reasonable way.

2.1.1 Use of rubber as aggregates in cement composites

In the last 20 years the potential use of crumb rubber as replacement of fine and/or coarse aggregate has been studied by many researchers. Previous studies (Eldin and Senouci 1993; Khatib and Bayomy 1999; Topçu and Avcular 1997; Topçu 1995; Toutanji 1996; Wong and Ting 2009; Zheng et al. 2008) reported that the addition of rubber as aggregate changes the mechanical properties of concrete. The ductility or deformability of regular concrete could be increased with the addition of rubber. Another study (Fattuhi and Clark 1996) suggested various applications where rubber could be used in concrete. Those applications are; i) foundation pads for machinery and in railway station where vibration damping is required, ii) road traffic barriers and railway buffers where resistance to impact or explosion is required, iii) pipe bedding, artificial reef construction, trench filling, pipe heads and paving slabs where high strength requirement is not important. The use of rubber in concrete thus makes the concrete economical as well as sustainable.

2.1.1.1 Physical properties

Several studies (Hooton et al. 2001; Siddique and Naik 2004) were conducted on the physical properties of crumb rubber to assess its applicability as aggregate in concrete mixtures. They found that maximum size and grading of rubber granules used by different researchers varied considerably. Khatib and Bayomy (1999) developed a characteristic function to quantify the reduction in strength due to the addition of rubber. Another study (Huang et al. 2004) was carried out to evaluate the effect of maximum rubber chip sizes and stiffness of coarse aggregate on the composite strength of concrete. Najim and Hall (2012) recommended that rubber aggregates can be loosely classified into four types depending on their particle size and distribution, whether they were shredded, chipped or ground. Whereas shredded and chipped particles represent the coarse aggregate, crumb rubber (typically between 4.75mm and 0.425mm) and ground tire rubber (passing through No 40 sieve) are potential fine aggregate. There also exists fibrous rubber aggregate, which are short fibres typically between 8.5mm and

21.5mm in length. In all case, the recycled rubber is characterized as having negligible water absorption and low density (0.866 kg/m^3).

2.1.1.2 Fresh concrete properties

It was reported (Raghavan et al. 1998a) that mortar with rubber shreds as aggregate achieved a workability comparable to or better than the mortar with conventional aggregate. Another study (Khatib and Bayomy 1999) reported that the workability decreases with an increase in rubber content. Also, mixtures with fine crumb rubber aggregates showed better workability when compared to concrete mixes with coarse tire chip or combination of coarse tire chips and crumb rubber.

Various studies (Fedroff et al. 1996; Khatib and Bayomy 1999) reported higher air content with rubberized concrete mixtures compare to control mixtures which is due to the non-polar nature of rubber particles and their tendency to entrap air on their rough surface. Due to the low specific gravity of rubber particles, the unit weight of concrete mixes containing rubber decreases with an increase in rubber content (Khatib and Bayomy 1999).

2.1.1.3 Compressive and tensile strength

Past researchers (Eldin and Senouci 1993; Khatib and Bayomy 1999; Topçu 1995) have found the reduction in compressive strength resulting from using rubber in concrete. Those results of various studies indicated that the size, proportions and surface texture of rubber particles have significant influence on the compressive strength. Eldin and Senouci (1993) reported that concrete mixtures with crumb rubber and tire chips showed lower compressive and splitting tensile strength. There was approximately an 85% reduction in compressive strength and a 50% reduction in splitting tensile strength when coarse aggregate was fully replaced by coarse crumb rubber. However a 65% reduction in compressive strength and a 50% reduction in splitting tensile strength were observed when the fine aggregate portion was fully replaced with fine crumb rubber. The failure of these materials was ductile in nature and had the ability to absorb a large amount of energy under both compressive and tensile loads. Other studies (Khatib and Bayomy 1999; Topçu 1995) also reported that the addition of coarse rubber chips in concrete lowered the compressive strength more than the addition of fine crumb rubber.

Some researchers showed that surface treatment of rubber particles enhanced bond strength between the rubber particle and cement paste (Chung and Hong 1999; Lee et al. 1998; Raghavan et al. 1998a; Taha et al. 2008). Treating rubble particles using Sodium Hydroxide (NaOH) and Calcium Hydroxide ($Ca(OH_2)$) demonstrated enhanced bond and thus increased compressive and flexural properties (Chung and Hong 1999; Raghavan et al. 1998a; Segre and Joekes 2000). Moreover, Biel and Lee (1996) showed that Magnesium Oxychloride cement noticeably enhanced the mechanical properties of concrete with rubber, whereas Lee et al. (1998) showed that addition of styrenebutadiene rubber polymer latex to the tire particle was enhanced mechanical and durability of rubberized concrete.

2.1.1.4 Shrinkage

A very little amount of research work was done to explore the plastic shrinkage of concrete containing rubber particles. Raghavan et al. (1998a) demonstrated that with higher content of rubber shreds, the crack length and width got smaller, and also the onset time of cracking was delayed.

2.1.1.5 Toughness and impact resistance

Few studies (Eldin and Senouci 1993; Khatib and Bayomy 1999) demonstrated that the failure mode of concrete containing rubber was more quasi-brittle as opposed to conventional concrete. Other studies (Eldin and Senouci 1993; Topçu and Avcular 1997; Topçu 1995) also found that the impact resistance of concrete increased when rubber aggregates were introduced into the concrete mixtures. This increase in impact resistance was generated from the enhanced ability of the rubberized composite to absorb energy. Besides these, the rubberized concrete was found to improve freeze and thaw performance to some extent (Dhir et al. 2002a; b; Savas et al. 1997)

2.1.1.6 Use of supplementary cementitious material in rubberized concrete

Supplementary cementitious materials are widely used to improve various properties of concrete. Several authors reported the effect of supplementary cementitious material on the various properties of rubberized concrete, especially to offset the drop in mechanical properties. Notable improvement is reported due to silica fume and ground granulated blast

furnace slag (Guneyisi 2010; Wong and Ting 2009). Besides improving the mechanical properties, the use of silica fume in concrete reduces its permeability and in turn benefits the long-term durability of the matrix (Duval and Kadri 1998; Sabir 1997). Many other researchers also explored the applicability of metakaolin as supplementary cementitious material in conventional concrete (Gruber et al. 2001; Qian and Li 2001; Wild et al. 1996). However, no data exists regarding its performance in concrete with crumb rubber aggregates.

2.1.2 Use of rubber as aggregates in other civil engineering applications

Though the current study focused on the utilization of rubber tire as aggregate in cement composites, it was found that rubber tire has already been widely and effectively used in asphalt concrete and in various highway projects such as embankment application, backfill behind retaining walls. A brief description of these usages is given in this section.

2.1.2.1 Recycled tire rubber in asphalt concrete

The application of rubber in bitumen is an old concept where it was attempted to capture the flexible nature of rubber in a longer lasting pavement surface. In 1960s, the scrap tires were processed and used in pavements as secondary material. During that period, “dry process” was introduced where a surface asphalt mixture was produced with the addition of a small quantity of ground rubber derived from scrap tires as partial replacement of mineral aggregates (Epps 1994). Besides, another technology was introduced by Charles McDonald which is known as “wet process”. He found that thoroughly mixing crumb rubber from scrap tires with bitumen and allowing it to react for 45 minutes to an hour result an asphalt mix which had the beneficial engineering characteristics of both base materials. The definition for rubberized asphalt was included in ASTM D8 in 1988 and later ASTM specification (ASTM D6114 2009) was introduced specially for Asphalt-Rubber composite. Various researchers have explored the characteristics of asphalt-rubber composites. From those studies it was found that the asphalt pavements, where recycled tire rubber was used as aggregate, have improved ductility, improved surface crack resistance, improved oxidation and aging resistance, and lower maintenance cost with improved pavement durability (Bertollo 2004; Caltrans 2006; Jung et al. 2003; Kaloush et al. 2003; Lo Presti 2013) . It also showed improved skid resistance, lower

traffic noise generation, and improved night time visibility due to the contrast in pavement and stripping (Leung et al. 2006; Terrel and Walter 1986).

In spite of all these benefits, asphalt-rubber has some limitations as well. These limitations include; challenging construction due to critical temperature requirements, high initial cost, and hazardous emission.

2.1.2.2 Recycled tire rubber in highway projects

Tire rubber aggregate (TDA) has low unit weight, which is the primary benefit of using it as a construction material in highway projects. In addition, TDA was found to have good vibration damping, high thermal capacity, and high compressibility. These are suitable characteristics for some applications for which ASTM D6270 (2009) provides necessary. The aggregates derived from recycled tires have been used for embankment fills and subgrade, bridge abutments and backfill for retaining walls, subgrade insulation for highways, and vibration damping below rail lines (Drescher and Newcomb 1994; Hoppe 1998; Humphrey et al. 1998; Humphrey 2008; Mills and McGinn 2010; Nelson 2009; Reid et al. 1998; Tatlisoz et al. 1998; Tweedie et al. 1998a; Whetten et al. 1997) . The at-rest horizontal stress for TDA back fill was found to be 45% less than that for conventional granular back fill (Tweedie et al. 1998b).

However, due to its high compressibility, TDA fill experiences immediate and long term settlements which need to be considered in engineering design. While short term settlement may be addressed immediately, the time dependent settlement is more critical since it affects the long term performance and serviceability of pavements and other supported structures (Wartman et al. 2007).

2.2 Bond response of reinforcement bar and concrete

2.2.1 Bond behavior of concrete reinforced with steel bar

Bond may be referred to as the load transfer mechanism on which the load carrying capacity of a structure depends. The bond between steel reinforcement and normal weight concrete has been well documented and understood. Previously, plain bars were used as reinforcement

where the friction between the surface of the bar and surrounding concrete provided necessary bond. Later, deformed bars were produced with lug deformation. The transfer mechanism of forces from reinforcement to surrounding concrete for a deformed bar can be described as follows (ACI 318 2014; Azizinamini et al. 1993; Brettmann et al. 1986);

1) The adhesion between the concrete and the rebar;
2) Friction forces generated from the roughness of the interface, relative slip of rebar with the surrounding concrete;
3) Mechanical anchorage of the rebar and the bearing of ribs (in deformed bars) on the surrounding concrete.

Initially the force in the reinforcement is resisted by the adhesion. This adhesion is generally developed by enhancement of mechanical interlock, due to shrinkage of the concrete matrix around the rebar. But when the bar slips with respect to the surrounding concrete, the adhesion is lost and the applied force is then resisted by the bearing of ribs (the deformation) and friction of ribs and barrels (part of rebar without any deformation) with the surrounding concrete. The compressive bearing forces increase the value of the friction forces. With an increase in the slip, the friction between the barrels and surrounding concrete diminishes and the force is solely transfer through the friction developed by the forces at the contact faces between the ribs and surrounding concrete. The forces of the bar surface from bearing generates compressive stress and shear stress on the concrete contact surface (as shown in Figure 2-1).

These forces then resolved into radial and longitudinal components as shown in Figure 2-2. The radial components generates crack both parallel and perpendicular to the reinforcement, and the longitudinal component is the effective bond stress, as shown in Figure 2-3. The transverse cracks shown in Figure 2-4(a) form if there is not enough concrete cover or the spacing between bars is small. These lead to splitting cracks as shown in Figure 2-4(b). But the presence of sufficient concrete cover, suitable bar spacing and transverse reinforcement delay the splitting failure so that the failure eventually occurs by shearing along the surface of the top of the ribs around the rebar. This is known as pullout failure.

For both cases, splitting failure and pullout failure, crushing of concrete may occur in the region of bearing surfaces. If the anchorage to the concrete is sufficient then the stress in reinforcement becomes high enough to reach its yield stress.
Hence bond failure in the reinforced concrete may be categorized as follows (ACI 408R-03 2012; Darwin et al. 1992; Esfahani and Rangan 1998; Mor 1993; Tepfers 1979; Zuo and Darwin 2000);

- Splitting failure (without adequate reinforcement cover, bar spacing and transverse reinforcement);
- Pullout failure (when concrete cover and bar spacing are adequate but frictional forces are not sufficient to transfer the applied load);
- Rupture/yielding of rebar (anchorage of rebar is adequate to prevent pullout failure but the load applied is beyond the capacity of the rebar.

From the above description it was identified that the bond resistance in concrete with steel reinforcement under quasi static loading is governed by (ACI 408R-03 2012; Altowaiji et al. 1986; Azizinamini et al. 1993, 1995; Darwin et al. 1996; Darwin and Graham 1993; Esfahani and Rangan 1998);

- The mechanical properties of concrete (tensile strength and bearing strength);
- The volume of concrete surrounding the rebar which includes the concrete cover and the bar spacing;
- The surface condition of the reinforcement;
- The geometry of the rebar which includes the size of rebar, the rib height and rib spacing;
- The mechanical properties of reinforcement
- The presence of transverse reinforcement which can delay the crack propagation;

Adequate bond resistance in the reinforced concrete structures is measured by a length, called “development length”. This is the embedment length of reinforcement in concrete required to ensure development of yield stress in the reinforcement.

In the following sections the effect of various factors on bond performance has been discussed.

2.2.1.1 Effect of concrete mix properties on bond performance

2.2.1.1.1 Effect of concrete compressive strength on bond behavior

Bond strength is significantly affected by the various mechanical properties of concrete. These properties include the compressive strength (f'_c) as well as the flexural strength (f_r) of concrete. In the previous studies (Darwin et al. 1992; Esfahani and Rangan 1998a; Esfahani and Rangan 1998b; Orangun et al. 1977) effect of concrete compressive strength on bond strength is represented by $f'_c{}^{1/2}$. This relation is adequate for a maximum compressive strength of 55 MPa. But at higher strength concrete, the average bond strength at failure after normalization by $f'_c{}^{1/2}$ decreases with increase in compressive strength (Azizinamini et al. 1995; Azizinamini et al. 1993; Zuo and Darwin 2000a). According to some studies (Darwin et al. 1996; Zuo and Darwin 2000b), $f'_c{}^{1/4}$ provides the best representation to the effect of compressive strength on the development and splice strength which is reflected in the Equation 2.2.

2.2.1.1.2 Effect of concrete density on bond performance

Bond strength of steel with lightweight concrete is different compared to that with normal weight concrete. Lightweight concrete (prepared from lightweight coarse aggregate) demonstrated lower tensile strength, fracture energy and local bearing capacity than normal weight concrete with similar compressive strength. Hence the bond strength of bars cast in lightweight concrete is lower than that of bars cast in normal weight concrete, irrespective of presence of transverse reinforcement. Mor (1993) showed that the bond strength in lightweight concrete varies in the range of 82% to 85% compared to normal weight concrete. ACI 318 (2014) includes a factor (λ) of 1.3 for the development length in lightweight concrete to reflect the lower tensile strength when compared with normal weight concrete. Again, if the average splitting strength, f_{ct} of lightweight concrete is known, then the factor can be taken as $6.7\sqrt{f'_c}/f_{ct} \geq 1$.

2.2.1.1.3 Effect of supplementary cementitious material on bond performance

Long term durability of concrete is an important issue and it is enhanced by improving its impermeability. Use of supplementary cementitious material such as silica fume, fly ash and

metakaolin in the concrete mix enhances the performance of concrete. Due to its finer particle size compared to fly ash or metakaolin, silica fume is a highly reactive pozzolan. After casting the steel with concrete, a calcium hydroxide crystal layer is formed around the reinforcement. This layer is partly covered by the calcium silicate hydrate (CSH) formed due to the pozzolanic reaction between calcium hydroxide and silica fume. The calcium hydroxide layer is also united with the concrete matrix by a dense interlocking. Overall, the densification of concrete-steel interface occur which leads to the reduction of porosity in the transition zone. This densification at the steel-concrete interface and improvement in strength due to the pozzolanic reaction improve the bond strength (Gjorv et al. 1990). However, another study (Mor 1993) showed that silica fume has little effect on bond strength, with an increase less than 2% for normal weight concrete and a within 5%, for lightweight concrete. But some studies (Hwang et al. 1994; Hamad and Itani 1998) found that the addition of silica fume decreases the bond strength by 5% to 7%. The presence of supplementary cementitious material is not directly included in the bond prediction models.

2.2.1.2 Effect of steel fiber reinforcement on bond performance

Presence of short discrete fibers is known to significantly affect the bond strength of concrete. Steel fiber reinforced concrete (SFRC) has better tensile strength than normal weight concrete. Concrete subjected to tension usually have cracks. These cracks decrease the bond strength between rebar and concrete. Addition of short steel fibers is effective in bridging cracks around both longitudinal and transverse reinforcement in the concrete. This mechanism improves the bond strength between SFRC and reinforcement. But one study (Ezeldin and Balaguru 1990) shows that steel fibers with 0.25% volume fraction decreased the bond strength whereas 0.5 to 0.75% volume fractions of steel fibers increased the bond strength by 18%. Again, few other studies (Soroushian et al. 1994; Hota and Naaman 1997) found that 0.5% volume fraction of steel fibers (hooked) may improve the bond strength by 33%. But further increase in volume fraction doesn't affect the bond strength significantly. These studies also found that neither the aspect ratio of the steel fiber nor the fiber geometry (hooked end or undeformed) has any influence on the bond strength.

2.2.1.3 Effect of concrete cover on bond performance

It was observed in different studies (Orangun et al. 1977; Darwin et al. 1996) that bond strength increases with an increase in the concrete cover and the bar spacing. Pullout failure may be obtained for larger cover and bar spacing whereas splitting tensile failure occurs for smaller concrete cover and bar spacing. The influence of concrete cover on bond performance is taken into consideration as shown in Equations (2.1) and (2.2).

2.2.1.4 Effect of bar size and embedment length on bond performance

Increasing the development length or splice length of a reinforcing bar increases the bond strength of the member but the bond strength gained is not proportional to the increase in development length. According to ACI 318 (2014), it is conservative to establish a proportional relationship between bond force and bonded length for short bonded lengths but less conservative for larger bonded length.

Bar position also has a significant effect on the bond strength. The bars cast lower in a member have higher bond strength than the top-cast bars (Altowaiji et al. 1986; Jeanty et al. 1988). ACI 318 (2014) addressed this behavior and introduced a factor, α. They mentioned that the top reinforcement with more than 300mm of fresh concrete cast in the member below the development length and splice requires a 30% increase in development length.

Again, for an increase in the bar diameter, longer development length is required (Darwin et al. 1992; Orangun et al. 1977; Darwin et al. 1996). Therefore, for a given confinement, it is suggested to use a larger number of smaller bar diameters than a smaller number of larger bar diameters, as the former provide greater bar area which in turn develop greater strength.

2.2.1.5 Effect of transverse reinforcement on bond strength

Presence of transverse reinforcement also increases the bond strength as it confines the developed and spliced bars by limiting the progress of splitting crack (Orangun et al. 1977; Darwin and Graham 1993). Also an increase in the transverse reinforcement results in an increase in the bond strength. ACI has addressed the issue by incorporating a factor K_{tr} which

depends on the yield property of transverse reinforcement, and the number and spacing of transverse reinforcement.

2.2.1.6 Effect of reinforcement surface condition and mechanical properties on the bond performance

In their study, Darwin and Graham (1993) found that the bond strength with steel rebars is independent of the surface deformation of the bar under relatively low confinement (i.e. small concrete cover and no transverse reinforcement). But, with the presence of transverse reinforcement, the bond strength increases with an increase in rib area.

Yield strength of steel is important in determining the bond strength. Some studies (Darwin et al. 1996; Zuo and Darwin 2000b) have found that the bond strength of bars that yield will average only 2% less when not confined by transverse reinforcement and 10% more when confined by transverse reinforcement when compared to a similar bar of same development length but of higher strength steel that doesn't yield. This is considered in the predictive bond Equation (2.1) and Equation (2.2) by introducing t_d and t_r.

2.2.1.7 Effect of higher loading rate on the bond performance

A study by Yan (1992a) has shown the effect of rate of loading on the bond strength. In that study the dynamic load was generated by using a 345-kg mass drop weight impact machine. The experiments consisted of both pullout and push-in tests. For all types of tests, the experimental work was carried out for a stress rate ranging from 0.5×10^{-8} to 0.5×10^{-2} MPa/s. The other important variables considered in the experimental study were: two different types of reinforcing bars (smooth and deformed), two different concrete compressive strengths (normal and high), two different fibers (polypropylene and steel), different fiber contents (0.1 %, 0.5 %, and 1.0 % by volume), and surface conditions (epoxy coated and uncoated). It was observed that for smooth rebars, the stress rate has no significant effect on the bond strength. But for deformed bars, a higher loading rate causes a significant increase in the bond-resistance capacity and fracture energy associated with the bond failure. Weathersby (2003) also showed that bond strength increased (approximately 300%) when load is applied at higher rates (as

high as $4.1x10^6$ kPa/s). The effect of loading rate wasn't included in the bond prediction model (seen later in Chapter 5 as Equation (5.4, 5.5, and 5.6)) for this study.

2.2.2 Bond behavior of concrete reinforced with FRP bar

Steel bars have been used as the primary reinforcement in concrete structures for a long time. Performance of steel bars as reinforcement is suspect when they are subjected to corrosive environment. Due to corrosion, steel expands in volume and generates excessive tensile stress in concrete. This causes spalling of concrete and eventually, the premature deterioration of structure. In the last couple of decades, the use of fiber reinforced polymer (FRP) reinforcing bar as main reinforcement in concrete structures has found wide acceptance due to their superior corrosion resistance, lightweight and sometimes, higher strength.

A Fibre Reinforced Polymer (FRP) rebar consists of a polymer matrix either thermoset or thermoplastic which is reinforced with a fibre with a significantly large aspect ratio. Its reinforcing fibres are continuous and have higher stiffness and strength than the surrounding matrix. The matrix holds the fibre in place and influences the physical properties of the FRP and the fibres provide the mechanical strength. Unlike other reinforcement, FRP composites are anisotropic in nature as their mechanical properties are different in the longitudinal and transverse direction.

Currently FRP composites have been used as internal reinforcement in new structures and as external reinforcement in the rehabilitation of existing structures. Though FRP bars can be used both as internal and external reinforcement, FRP plates are used for the structural rehabilitation in the form of external reinforcement. The bond behavior of FRP bars and plates are different due to the difference in their application. Here, only the bond behavior of FRP bar as internal reinforcement will be discussed.

2.2.2.1 Bond mechanism

From the preceding studies it is observed that the bond of FRP bar in concrete is controlled by several factors (Achillides and Pilakoutas 2004; Azizinamini et al. 1995; Baena et al. 2009; Benmokrane et al. 1996; Chaallal and Benmokrane 1993a) including; chemical bond, friction

due to surface roughness of FRP bars, mechanical interlocking of deformed FRP bars against the concrete, hydrostatic pressure generated from the shrinkage of hardened concrete, and any volumetric increase of FRP bar due to change in temperature and moisture absorption. The chemical bond between concrete and FRP is extremely low. Hence the main mechanism of stress transfer is the friction and/or mechanical interlock depending on the type of FRP bar whether straight or deformed.

2.2.2.2 Effect of FRP bar surface condition

The surface of the straight bars is usually smooth; grain covered or sandblasted whereas deformed bar surface is usually ribbed, indented, twisted or braided.

In case of straight FRP bars two components may be present; a) adhesion and b) friction. Studies show that smooth FRP bars depict very low values of bond strength as the friction mechanism alone is involved here. In case of sanded rebars, sanding leads to an increase in chemical bond and friction which in turns increase the bond strength. However, the bond failure is brittle in this case.

The deformed bar is intended to increase the friction as well as to obtain some contribution from mechanical interlocking. The contribution from mechanical interlocking depends on the type, size and shape of the surface deformation. Some researchers found that specific surface deformation (glued fibre spiral) has negligible improvement in bond strength as compared to smooth rebar but other types of surface deformations (indented and ribbed rods) increased the bond strength significantly (Benmokrane et al. 1996; Malvar 1994). One study (Nanni et al. 1997) found that only friction-type bond behavior is present in case of deformed FRP bar. Al-Zahrani et al. (1999) demonstrated that mechanical interlock and shear strength of the lugs are stress transfer mechanisms but after the shearing of the lugs, only friction between rebar and concrete becomes the main bond mechanism.

2.2.2.3 Effect of concrete compressive strength on bond

Previous studies (Achillides and Pilakoutas 2004; Ametrano 2011; Baena et al. 2009; Chaallal and Benmokrane 1993b; Ehsani et al. 1997; Esfahani et al. 2005; Tighiouart et al. 1998)

reported that for higher compressive strength concrete (*f'c*>30 MPa) bond failure interface happens at the surface of FRP bar. Hence, in such concrete, bond strength value doesn't depend much on the compressive strength of concrete. However, for lower strength concrete (around 15 MPa) the mode of bond failure changes. In this type of concrete, the failure interface takes place in the concrete matrix. As a result, the bond behavior of FRP bar is depends directly on the compressive strength of concrete.

2.2.2.4 Effect of bar size

As with steel rebars, the size of the FRP bar is also an important parameter on which the bond strength depends. Many researches (Benmokrane et al. 1996; Chaallal and Benmokrane 1993; Tao 1994) were performed to study the bond performance of FRP bars of different diameters. It was observed that the increase in bar size decreases the average bond strength. This may be due to the reason of Poisson's effect of FRP bar. The larger size of FRP bar will exhibit larger contraction when they will be subjected to tensile stress. This reduces the friction as well as mechanical interlocking mechanism of bond.

2.2.2.5 Effect of bar position

Bar position has significant impact on the bond strength. Ehsani et al. (1996) reported that bond stress in top bar (with cover of 280mm below and 19mm above the bar) was 66% of the bottom bar. Chaallal and Benmokrane (1993a; b) also demonstrated the effect of concrete compressive strength in combination with FRP bar position. It showed that for high strength concrete top bar effect was less prominent when compared to normal strength concrete.

2.2.3 Development length equation considering factors affecting bond

Adequate bond resistance in the reinforced concrete structures is measured by a length, called "development length". This is the embedment length of reinforcement in concrete required to ensure development of yield stress in the reinforcement.

2.2.3.1 ACI 318 (2014)

ACI 318 (2014) provided an equation to determine the development length of straight steel reinforcement in reinforced concrete structure. The equation is shown below;

$$\frac{l_d}{d_b} = 0.9\,\frac{\alpha\beta\gamma\lambda f_y}{\sqrt{f_c'}\left(\frac{c + K_{tr}}{d_b}\right)} \qquad (2.1)$$

Here, l_d = development or splice length, d_b = diameter of rebar, f_y = yield strength of reinforcing bar being developed, f'_c = concrete compressive strength, α = reinforcement location factor, β = coating factor, γ = reinforcement size factor, λ = light-weight concrete factor, c = spacing or cover dimension, K_{tr} = transverse reinforcement index= $\frac{A_{tr} f_{yt}}{10sn}$,

A_{tr} = area of each stirrup or tie crossing the potential plane of splitting adjacent to the reinforcement being developed, spliced or anchored, f_{yt} = yield strength of transverse reinforcement, s = spacing of transverse reinforcement, n = number of bars being developed or spliced.

2.2.3.2 ACI Committee 408R-03 (2012)

Later ACI Committee 408R-03 (2012) has modified the development length equation as below by considering other factors and incorporating a strength reduction factor.

$$\frac{l_d}{d_b} = \frac{\left(\frac{f_y}{f_c'^{1/4}} - \varphi 57.4\omega\right)\alpha\beta\lambda}{\varphi 1.83\left(\frac{c\omega + K_{tr}}{d_b}\right)} \qquad (2.2)$$

Here, φ =strength reduction factor, $\omega = 0.1\ c_{max}/c_{min} + 0.9 \le 1.25$, $K_{tr} = (6.26\ t_r\ t_d\ A_{tr}/sn) f'^{0.5}_c$

$t_d = 0.03 d_b + 0.22$, $t_r = 9.6\ R_r + 0.28 \le 1.72$, R_r = relative rib area of the reinforcement

c_{max} = maximum cover, c_{min} = minimum cover

2.2.3.3 CSA S806-12

CSA S806-12 (2012) provided a much simpler equation for the development length for FRP bar which is shown below,

$$l_d = 1.15\ \frac{k_1 k_2 k_3 k_4 k_5}{d_{cs}} . \frac{f_F}{\sqrt{f_c'}} A_b \qquad (2.3)$$

d_{cs} = factor depending on bar spacing, shall not be greater than $2.5 d_b$

k_1 = bar location factor, k_2 = concrete density factor, k_3 = bar size factor, k_4 = bar fibre factor k_5 = bar surface profile factor, f_F = design stress in FRP tension reinforcement at ultimate limit state

2.3 Development of bond-slip analytical models

In a typical flexural member as shown in Figure 2-5(a), the FRP bars act as main reinforcement to carry the tension in a section. And due to the difference in moment between adjacent sections, the bond stress needs to be developed to maintain the equilibrium.
To derive the theory of bond mechanism of FRP bar as internal reinforcement, it is assumed that;

- The constitutive law of the FRP material is linear in the longitudinal direction
- The displacement of the points on concrete are negligible when compared to the points on the FRP bar. This means, the slip at each interface point is equal to the displacement of the corresponding cross section of the bar.

If the bond charactersitics of the FRP bar are analytically described by the relationship, $\tau = \tau(s)$, where τ is the shear stress acting on the contact surface between bar and concrete, and s is the slip or relative displacement between bar and concrete, then from the equilibrium of rebar as shown in Figure 2-5(b), we get;

$$A_b d\sigma = \pi d_b \tau dx \qquad (2.3)$$

Here d_b =diameter of the bar, A_b = cross section of the bar

For a linear elastic behavior of the bar,

$$\sigma_b = E\varepsilon_b \cong E\frac{ds}{dx} \qquad (2.4)$$

Here, E = Young'smodulus of FRP bar and $s = s(x)$ with x a reference axis along the bar.
From equation (1) and (2), the following differential equation is obtianed,

$$\frac{d^2s}{dx^2} = \frac{\pi d_b}{E_{db}A_b}\tau(s) \qquad (2.5)$$

The Equation (2.3) is useful for the numerical analysis of behavior of reinforced concrete members including the interaction between concrete and reinforcement. The development length, transfer length and achorage length of FRP reinforcement can be determined if a consistent bond-slip relationship $\tau = \tau(s)$ for the FRP bar in the concrete is available.

2.4 Existing bond-slip analytical models

Many researchers have developed the analytical local bond (τ) – slip (s) relationship for steel and FRP bars.

(Malvar 1994) has developed a model for FRP bar which is as follows,

$$\frac{\tau}{\tau_m} = \frac{F\left(\frac{s}{s_m}\right) + (G-1)(\frac{s}{s_m})^2}{1 + (F-2)\left(\frac{s}{s_m}\right) + G(\frac{s}{s_m})^2} \qquad (2.6)$$

Here, τ_m, s_m = peak bond stress, slip at peak bond stress and F, G = empirical constants determined for each bar type.

The model proposed by (Eligehausen et al. 1983) is a well known model known as the Betero-Popov-Eligehausen (BPE) for deformed steel bar. But it has been successfully used for FRP bar also. Referring to Figure 2-6, in the BPE model, the ascending branch of the bond-slip ($s \leq s_1$) relationship is expressed as follows:

$$\frac{\tau}{\tau_1} = (\frac{s}{s_1})^{\alpha} \qquad (2.7)$$

Here, τ_1, s_1 = peak bond stress and corresponding slip respectively α is the curve fitting parameter, which must not be greater than 1 to be physically meaningful.

BPE model presents a second branch with constant bond up to slip $s = s_2$, a linearly descending branch from s_2, τ_1 to s_3, τ_3 and a horizontal branch for $s > s_3$, as shown in Figure 2-6 (a). Values of s_2, s_3 and t_3 have to be calibrated on the basis of experimental results.

In their study, Cosenza et al. (1997) proposed an alternative analytical model which is a slight modification of BPE model. For the FRP bars when analytical response using original BPE model was compared with the experimental curve it lacks the second branch. Hence, for bond response between FRP bar and concrete the original BPE model doesn't consider. In the modified BPE model as shown in Figure 2-6(b) the ascending branch is the same as presented by original BPE model, and a softening branch with a slope of $\rho.\tau_1/s_1$ from (s_1,τ_1) to (s_3,τ_3) which is given by Equation (2.8) and then a horizontal branch for $s>s_3$ to represent the frictional component.

$$\frac{\tau}{\tau_1} = 1 - p\left(\frac{s}{s_1} - 1\right) \qquad (2.8)$$

Therefore, for the case of modified BPE model only three parameters have to be estimated: parameter α, on which the ascending branch depends; parameter p, on which softening branch depends; and the frictional component, τ_3, of bond resistance.

Cosenza-Manfredi-Realfonzo (CMR) developed another model to represent the ascending branch of FRP-concrete bond-slip response more precisely;

$$\tau(s) = \tau_m \left[1 - exp\left(-\frac{s}{s_r}\right)\right]^{\beta} \qquad (2.9)$$

Here the unknown parameters are τ_m, s_r and β.

The unknown parameters of equations (2.7), (2.8) and (2.9) can be determined from the various bond tests. These parameters depend on various factors such as bar type and bar surface condition, bar size, compressive and tensile strength of concrete mixtures, presence of steel fibre in the concrete mixes, concrete cover. Pullout test and beam test are widely used to determine the bond-slip responses.

On the basis of the literature review presented here, the following comments may be made,

1. To date, many studies were conducted to understand bond behavior of GFRP bar in various concrete matrices but the bond performance of GFRP bar in lightweight matrix has not been examined yet.
2. No data exist on bond performance between GFRP bar and concrete with very low compressive strength.
3. The effect of short steel fibre on the bond performance between sand grained GFRP bar and normal weight or lightweight concrete matrices has not yet been studied.

Figures

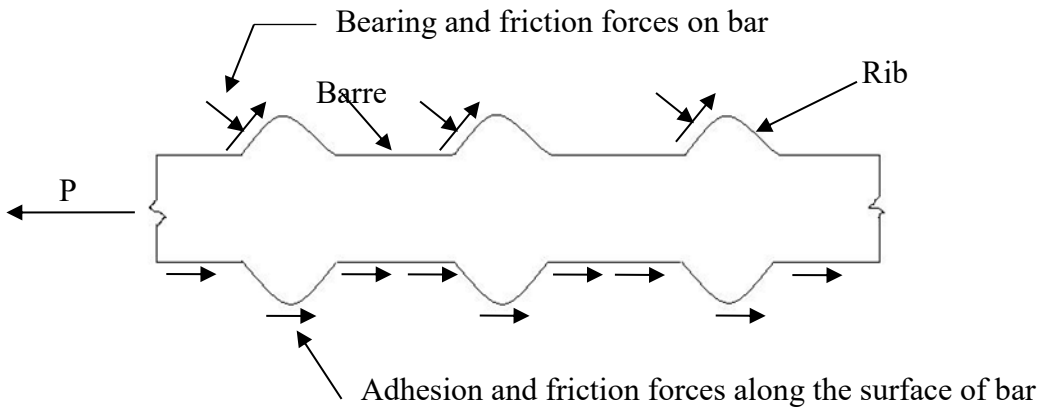

Figure 2-1: Bond force transfer mechanism (Forces on bar)

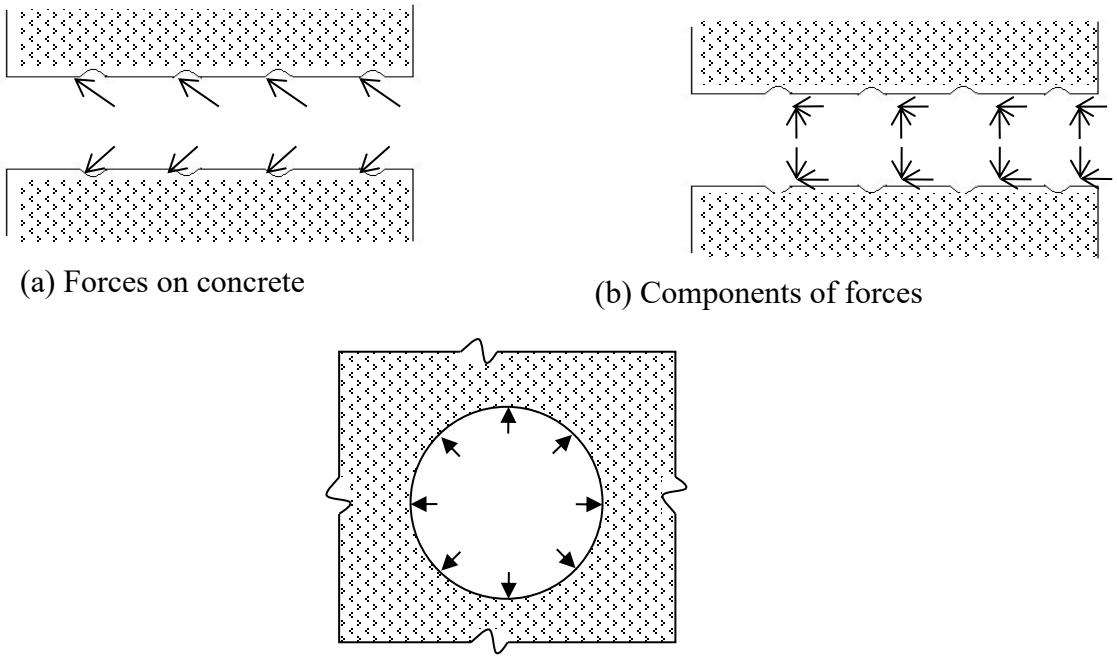

Figure 2-2: Component of forces during bond development

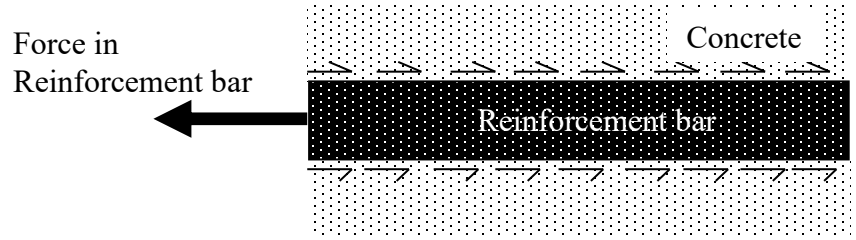

Figure 2-3: Bond stress in reinforcement bar

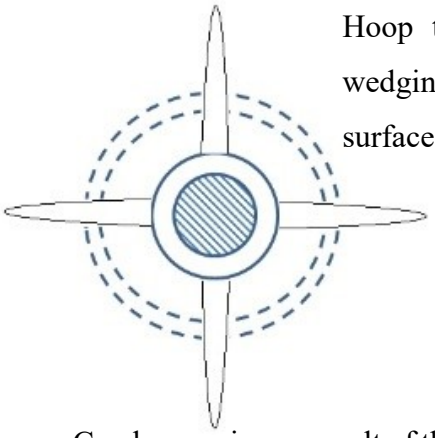

Hoop tensile stresses as result of wedging action of the reinforcement surface deformation

Cracks opening as result of the tension stress

(a): Crack opening

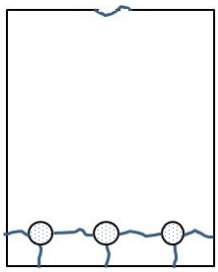

(b): Splitting Cracks

Figure 2-4: Formation of cracks due to tensile stress component (a) Crack opening; (b) Splitting crack

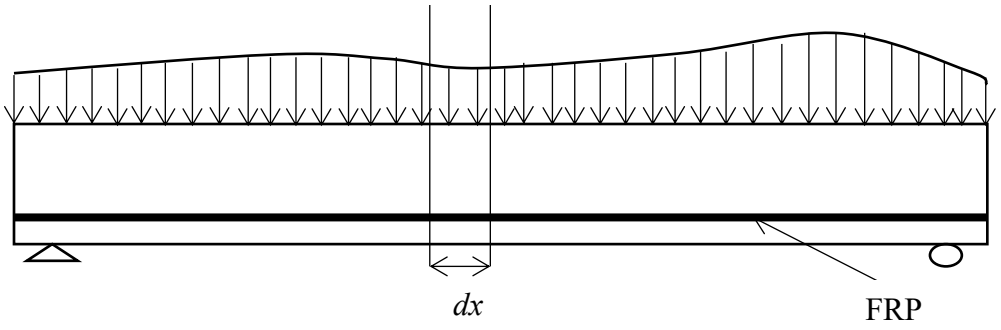

(a): A typical flexural member

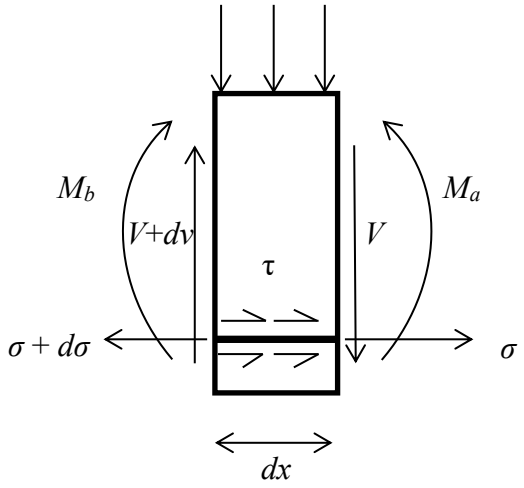

(b): An infinitesimal element of the beam

Figure 2-5: Mathematical derivation of bond stress

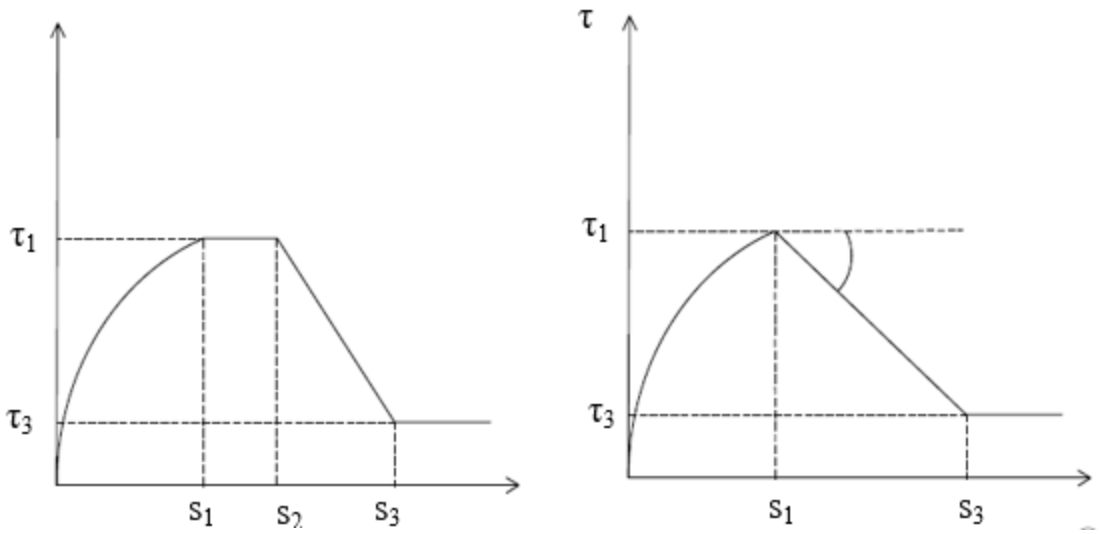

(a) BPE Model **(b)** Modified BPE Model

Figure 2-6: (a) BPE Model, (b) Modified BPE Model

References

Achillides, Z., and Pilakoutas, K. (2004). "Bond behavior of fiber reinforced polymer bars under direct pullout conditions." *Journal of Composites for construction*, 8, 173.

ACI 318. (2014). *Building Code Requirements for Structural Concrete and Commentary*. American Concrete Institute, Farmington Hills, MI.

ACI 408R-03. (2012). *Bond and Development of Straight Reinforcing Bars in Tension*. American Concrete Institute, Farmington Hills, MI.

Alexander, M., and Mindess, S. (2005). *Aggregates in Concrete*. Taylor and Francis, 270 Madison Ave, New York, NY.

Altowaiji, W. A. K., Darwin, D., and Donahey, R. C. (1986). "Bond of Reinforcement to Revibrated Concrete." *Journal Proceedings*, 83(6), 1035–1042.

Al-Zahrani, M. M., Al-Dulaijan, S. U., Nanni, A., Bakis, C. E., and Boothby, T. E. (1999). "Evaluation of bond using FRP rods with axisymmetric deformations." *Construction and Building Materials*, 13(6), 299–309.

Ametrano, D. (2011). "Bond characteristics of glass fibre reinforced polymer bars embedded in high performance and ultra-high performance concrete." *Ryerson University, Toronto, Ontario, Canada*, 1–132.

ASTM D6114. (2009). *Standard Specification for Asphalt-Rubber Binder, ASTM D6114/D6114M*. ASTM International, West Conshohocken, PA.

ASTM D6270. (2009). *Standard practice for use of scrap tires in civil engineering applications. ASTM D6270*. West Conshohocken, PA.

Azizinamini, A., Chisala, M., and Ghosh, S. K. (1995). "Tension development length of reinforcing bars embedded in high-strength concrete." *Engineering structures*, 17(7), 512–522.

Azizinamini, A., Stark, M., Roller, J. J., and Ghosh, S. (1993). "Bond performance of reinforcing bars embedded in high-strength concrete." *ACI Structural Journal*, 90(5), 554–561.

Baena, M., Torres, L., Turon, A., and Barris, C. (2009). “Experimental study of bond behaviour between concrete and FRP bars using a pull-out test.” *Composites Part B: Engineering*, 40(8), 784–797.

Benmokrane, B., Tighiouart, B., and Chaallal, O. (1996). “Bond strength and load distribution of composite GFRP reinforcing bars in concrete.” *ACI Materials Journal*, 93(3).

Bertollo, S. (2004). *Mechanical properties of asphalt mixtures using recycled tyre rubber produced in Brazil – a laboratory evaluation*. 83rd TRB Annual Meeting, Washington.

Biel, T., and Lee, H. (1996). “Magnesium Oxychloride Cement Concrete with Recycled Tire Rubber.” *Transportation Research Record: Journal of the Transportation Research Board*, 1561, 6–12.

Brettmann, B. B., Darwin, D., and Donahey, R. C. (1986). “Bond of Reinforcement to Superplasticized Concrete.” *ACI Journal Proceedings*, 83(1), 98–107.

Caltrans. (2006). *Caltrans. Asphalt Rubber Usage Guide*. State of California Department of Transportation, Materials Engineering and Testing Services.

Chaallal, O., and Benmokrane, B. (1993a). “Pullout and bond of glass-fibre rods embedded in concrete and cement grout.” *Materials and structures*, 26(3), 167–175.

Chaallal, O., and Benmokrane, B. (1993b). “Physical and mechanical performance of an innovative glass-fiber-reinforced plastic rod for concrete and grouted anchorages.” *Canadian Journal of Civil Engineering*, 20(2), 254–268.

Chung, K.-H., and Hong, Y.-K. (1999). “Introductory Behavior of Rubber Concrete.” *JOURNAL OF APPLIED POLYMER SCIENCE*, 72(1), 35–40.

Cosenza, E., Manfredi, G., and Realfonzo, R. (1997). “Behavior and modeling of bond of FRP rebars to concrete.” *Journal of composites for construction*, 1(2), 40–51.

CSA S806-12. (2012). “Design and construction of building structures with fibre-reinforced polymers.” Canadian Standards Association, Mississauga, ON.

Darwin, D., and Graham, E. K. (1993). “Effect of Deformation Height and Spacing on Bond Strength of Reinforcing Bars.” *Structural Journal*, 90(6), 646–657.

Darwin, D., McCabe, S. L., Idun, E. K., and Schoenekase, S. P. (1992). "Development Length Criteria: Bars Not Confined by Transverse Reinforcement." *Structural Journal*, 89(6), 709–720.

Darwin, D., Tholen, M. L., Idun, E. K., and Zuo, J. (1996). "Splice Strength of High Relative Rib Area Reinforcing Bars." *Structural Journal*, 93(1), 95–107.

Dhir, R. K., Dyer, T. D., and Halliday, J. E. (Eds.). (2002a). *Challenges of Concrete Construction: Volume 5, Sustainable Concrete Construction: Proceedings of the International Conference held at the University of Dundee, Scotland, UK on 9–11 September 2002*. Thomas Telford Publishing.

Dhir, R. K., McCarthy, M. J., and Newlands, M. D. (Eds.). (2002b). *Challenges of Concrete Construction: Volume 6, Concrete for Extreme Conditions: Proceedings of the International Conference held at the University of Dundee, Scotland, UK on 9–11 September 2002*. Thomas Telford Publishing.

Drescher, A., and Newcomb, D. E. (1994). *Development of design guidelines for use of shredded tires as a lightweight fill in road subgrade and retaining walls*. Report, Minnesota Department of Transportation.

Duval, R., and Kadri, E. H. (1998). "Influence of Silica Fume on the Workability and the Compressive Strength of High-Performance Concretes." *Cement and Concrete Research*, 28(4), 533–547.

Ehsani, M., Saadatmanesh, H., and Tao, S. (1996). "Design recommendations for bond of GFRP rebars to concrete." *Journal of Structural Engineering*, 122(3), 247–254.

Ehsani, M., Saadatmanesh, H., and Tao, S. (1997). "Bond behavior of deformed GFRP rebars." *Journal of Composite Materials*, 31(14), 1413–1430.

Eldin, N., and Senouci, A. (1993). "Rubber-Tire Particles as Concrete Aggregate." *Journal of Materials in Civil Engineering*, 5(4), 478–496.

Epps, J. A. (1994). "USES OF RECYCLED RUBBER TIRES IN HIGHWAYS." *NCHRP Synthesis of Highway Practice*, (198).

Esfahani, M. R., Kianoush, M. R., and Lachemi, M. (2005). "Bond strength of glass fibre reinforced polymer reinforcing bars in normal and self-consolidating concrete." *Canadian Journal of Civil Engineering*, 32(3), 553–560.

Esfahani, M. R., and Rangan, B. V. (1998). "Bond between Normal Strength and High-Strength Concrete (HSC) and Reinforcing Bars in Splices in Beams." *Structural Journal*, 95(3), 272–280.

Fattuhi, N. I., and Clark, L. A. (1996). "Cement-based materials containing shredded scrap truck tyre rubber." *Construction and Building Materials*, 10(4), 229–236.

Fedroff, D., Ahmad, S., and Savas, B. (1996). "Mechanical Properties of Concrete with Ground Waste Tire Rubber." *Transportation Research Record: Journal of the Transportation Research Board*, 1532, 66–72.

Gruber, K. A., Ramlochan, T., Boddy, A., Hooton, R. D., and Thomas, M. D. A. (2001). "Increasing concrete durability with high-reactivity metakaolin." *Cement and Concrete Composites*, 23(6), 479–484.

Guneyisi, E. (2010). "Fresh properties of self-compacting rubberized concrete incorporated with fly ash." *Materials and Structures/Materiaux et Constructions*, 43(8), 1037–1048.

Hooton, R., Nehdi, M., and Khan, A. (2001). "Cementitious Composites Containing Recycled Tire Rubber: An Overview of Engineering Properties and Potential Applications." *Cement, Concrete and Aggregates*, 23(1), 3.

Hoppe, E. (1998). "Field Study of Shredded-Tire Embankment." *Transportation Research Record: Journal of the Transportation Research Board*, 1619, 47–54.

Huang, B., Li, G., Pang, S.-S., and Eggers, J. (2004). "Investigation into Waste Tire Rubber-Filled Concrete." *Journal of Materials in Civil Engineering*, 16(3), 187–194.

Humphrey, D. N. (2008). *Civil engineering application of tire derived aggregate.* Alberta Recycling Management Authority, Edmonton.

Humphrey, D. N., Whetten, N., Weaver, J., Recker, K., and Cosgrove, T. A. (1998). "TDA as lightweight fill for embankments and retaining walls." *Conf. on Recycled Materials in Geotechnical Applications*, Arlington, VA.

Jung, J., Kaloush, K., and Way, G. (2003). *Life cycle cost analysis: conventional versus asphalt rubber pavements.* Rubber Pavement Association.

Kaloush, K., Witczak, M., Sotil, A., and Way, G. (2003). *Laboratory evaluation of asphalt rubber mixtures using the dynamic modulus (E∗) Test.* Washington.

Khatib, Z. K., and Bayomy, F. M. (1999). "Rubberized Portland Cement Concrete." *Journal of Materials in Civil Engineering*, 11(3), 206–213.

Lee, H. S., Lee, H., Moon, J. S., and Jung, H. W. (1998). "Development of tire-added latex concrete." *ACI Materials Journal*, 95(4), 356–364.

Leung, F., Tighe, S., Macdonald, G., and Penton, S. (2006). "Noise Reducing Asphalt Pavements: A Canadian Case Study."

Lo Presti, D. (2013). "Recycled Tyre Rubber Modified Bitumens for road asphalt mixtures: A literature review." *Construction and Building Materials*, 49, 863–881.

Malvar, L. J. (1994). *Bond Stress-Slip Characteristics of FRP Rebars.* Office of Naval Research, naval Cailities Engineering Service Center, port Hueneme, California.

Mills, B., and McGinn, J. (2010). "Design, Construction, and Performance of a Highway Embankment Failure Repaired with Tire-Derived Aggregate." *Transportation Research Record: Journal of the Transportation Research Board*, 2170, 90–99.

Mor, A. (1993). "Steel-Concrete Bond in High-Strength Lightweight Concrete." *Materials Journal*, 89(1), 76–82.

Najim, K. B., and Hall, M. R. (2012). "Mechanical and dynamic properties of self-compacting crumb rubber modified concrete." *Construction and Building materials*, 27(1), 521–530.

Nanni, A., Nenninger, J. S., Ash, K. D., and Liu, J. (1997). "Experimental bond behavior of hybrid rods for concrete reinforcement." *Structural Engineering and Mechanics*, 5(4), 339–354.

Nelson, B. E. (2009). "Using tire chips for roadway embankment fill." Centre for Integrated Waste management, Buffalo, NY.

Qian, X., and Li, Z. (2001). “The relationships between stress and strain for high-performance concrete with metakaolin.” *Cement and Concrete Research*, 31(11), 1607–1611.

Raghavan, D., Huynh, H., and Ferraris, C. (1998). “Workability, mechanical properties, and chemical stability of a recycled tyre rubber-filled cementitious composite.” *Journal of Materials Science*, 33(7), 1745–1752.

Reid, R. A., Soupir, S. P., and Schaefer, V. R. (1998). “Mitigation of Void Development under Bridge Approach Slabs Using Rubber Tire Chips.” ASCE, 37–50.

Sabir, B. B. (1997). “Mechanical properties and frost resistance of silica fume concrete.” *Cement and Concrete Composites*, 19(4), 285–294.

Savas, B., Ahmad, S., and Fedroff, D. (1997). “Freeze-Thaw Durability of Concrete with Ground Waste Tire Rubber.” *Transportation Research Record: Journal of the Transportation Research Board*, 1574, 80–88.

Segre, N., and Joekes, I. (2000). “Use of tire rubber particles as addition to cement paste.” *Cement and Concrete Research*, 30(9), 1421–1425.

Siddique, R., and Naik, T. R. (2004). “Properties of concrete containing scrap-tire rubber - An overview.” *Waste Management*, 24(6), 563–569.

Taha, M. M. R., El-Dieb, A. S., El-Wahab, M. A. A., and Abdel-Hameed, M. E. (2008). “Mechanical, fracture, and microstructural investigations of rubber concrete.” *Journal of Materials in Civil Engineering*, 20(10), 640–649.

Tatlisoz, N., Edil, T. B., and Benson, C. H. (1998). “Interaction between Reinforcing Geosynthetics and Soil-Tire Chip Mixtures.” *Journal of Geotechnical and Geoenvironmental Engineering*, 124(11), 1109–1119.

Tepfers, R. (1979). “Cracking of concrete cover along anchored deformed reinforcing bars.” *Magazine of concrete research*, 31(106), 3–12.

Terrel, R., and Walter, J. (1986). “Modified asphalt materials – the European Experience.” *AAPT*, 482–518.

Tighiouart, B., Benmokrane, B., and Gao, D. (1998). “Investigation of bond in concrete member with fibre reinforced polymer (FRP) bars.” *Construction and Building Materials*, 12(8), 453–462.

Topçu, lker B., and Avcular, N. (1997). “Analysis of rubberized concrete as a composite material.” *Cement and Concrete Research*, 27(8), 1135–1139.

Topçu, I. B. (1995). “The properties of rubberized concretes.” *Cement and Concrete Research*, 25(2), 304–310.

Toutanji, H. A. (1996). “The use of rubber tire particles in concrete to replace mineral aggregates.” *Cement and Concrete Composites*, 18(2), 135–139.

Tweedie, J., Humphrey, D., and Sandford, T. (1998a). “Full-Scale Field Trials of Tire Shreds as Lightweight Retaining Wall Backfill Under At-Rest Conditions.” *Transportation Research Record: Journal of the Transportation Research Board*, 1619, 64–71.

Tweedie, J. J., Humphrey, D. N., and Sandford, T. C. (1998b). “Tire Shreds as Lightweight Retaining Wall Backfill: Active Conditions.” *Journal of Geotechnical and Geoenvironmental Engineering*, 124(11), 1061–1070.

“U.S. Scrap Tire Market.” (2003). *Rubber Manufacturer Association*.

Wartman, J., Natale, M. F., and Strenk, P. M. (2007). “Immediate and Time-Dependent Compression of Tire Derived Aggregate.” *Journal of Geotechnical and Geoenvironmental Engineering*, 133(3), 245–256.

Whetten, N., Weaver, J., Humphrey, D., and Sandford, T. (1997). “RUBBER MEETS THE ROAD IN MAINE.” *Civil Engineering*, 67(9).

Wild, S., Khatib, J. M., and Jones, A. (1996). “Relative strength, pozzolanic activity and cement hydration in superplasticised metakaolin concrete.” *Cement and Concrete Research*, 26(10), 1537–1544.

Wong, S.-F., and Ting, S.-K. (2009). “Use of recycled rubber tires in normal and high-strength concretes.” *ACI Materials Journal*, 106(4).

Yan, C. (1992). “Bond between reinforcing bars and concrete under impact loading.” University of British Columbia.

Zheng, L., Huo, X. S., and Yuan, Y. (2008). “Strength, Modulus of Elasticity, and Brittleness Index of Rubberized Concrete.” *Journal of Materials in Civil Engineering*, 20(11), 692–699.

Zuo, J., and Darwin, D. (2000). “Bond Slip of High Relative Rib Area Bars under Cyclic Loading.” *Structural Journal*, 97(2), 331–334.

Notations

l_d = development or splice length,

d_b = diameter of rebar

f_y = yield strength of reinforcing bar being developed,

f'_c = concrete compressive strength,

α = reinforcement location factor (Equation (2.1) and (2.2))

β = coating factor (Equation (2.1) and (2.2))

γ = reinforcement size factor

λ = light-weight concrete factor

c = spacing or cover dimension,

d_{cs} = factor depending on bar spacing

K_{tr} = transverse reinforcement index = $K_{tr} = \frac{A_{tr} f_{yt}}{10sn}$,

k_1 = bar location factor

k_2 = concrete density factor

k_3 = bar size factor

k_4 = bar fibre factor

k_5 = bar surface profile factor

A_{tr} = area of each stirrup or tie crossing the potential plane of splitting adjacent to the reinforcement being developed, spliced or anchored

A_b = area of an individual bar

f_{yt} = yield strength of transverse reinforcement

f_F = design stress in FRP tension reinforcement at ultimate limit state

s = spacing of transverse reinforcement

n = number of bars being developed or spliced

d_b = diameter of the reinforcement bar

F, G = Empirical constant in Malvar Model for each bar type

P = the tensile load

p = softening branch slope defining parameter in BPE and mBPE model

s = slip

s_m/s_1 = slip at maximum bond stress

$s_{m,ue}$ = unloaded end slip at maximum bond stress

$s_{m,ue}^{b}$ = average unloaded end slip at maximum bond stress

$s_{m,le}$ = loaded end slip at maximum bond stress

$s_{m,le}^{b}$,= average loaded end slip at maximum bond stress

s_r = curve fitting parameter in Cosenza Manfredi Realfonzo (CMR) model

s_2 = maximum slip at constant maximum bond stress (as per BPE model)

s_3 = slip at the end of softening branch (as per BPE and mBPE model)

α = curve fitting parameter for BPE model and modified BPE model (Equation (2.7))

β = curve fitting parameter in Cosenza Manfredi Realfonzo (CMR) model (Equation (2.9))

τ_m/τ_1 = maximum bond stress

τ^*_{max} = maximum normalized bond stress

τ_3 = bond stress at the end of softening branch (as per BPE and mBPE model)

CHAPTER 3. EFFECT OF CRUMB RUBBER ON THE PROPERTIES OF LIGHTWEIGHT CONCRETE

3.1 Introduction

Concrete is one of the most widely used building materials worldwide. Annual global production of concrete is about 5 billion cubic yards (Cement Association of Canada) which is twice as much of all other building materials, including wood, steel, plastic and aluminum. In a typical concrete mix, fine and coarse aggregates comprise approximately 65% of the aggregate volume. This means, the demand for aggregates also increases with an increase in concrete demand worldwide. This continuous growth in demand has shifted the attention towards alternative aggregate resources. Use of these new materials not only reduces the environmental loss due to aggregate extraction but also reduces the landfill and recycling cost of those materials. Utilization of scrap tires may play a significant role in sustainable development considering the existing stockpile of scrap tires and the increase in the number of vehicles around the world. In the USA alone for which data is available, around 290 million tires are generated annually of which 80% were used for fuel production, civil engineering application and other products. The remaining scrap tires are land filled or stock piled which imposes an adverse impact on the environment.

In the last 20 years the potential use of crumb rubber as replacement of fine and/or course aggregate was studied by many researchers (Eldin and Senouci 1993; Khatib and Bayomy 1999; Topçu and Avcular 1997; Topçu 1995; Wong and Ting 2009; Zheng et al. 2008). The rubber aggregates can be loosely classified into four types depending on their particle size, shredded or chipped (the size representing the coarse aggregate), crumb rubber (typically between 4.75mm and 0.425mm), ground tire rubber (passing through No 40 sieve) and fibre rubber aggregate (short fibre typically between 8.5mm and 21.5mm in length) (Najim and Hall 2012) and these are characterized as having negligible water absorption and low density (0.866 kg.m3). Topçu (1995) found that the use of rubber as aggregate in concrete leads to higher amounts of energy absorption under both compressive and tensile loading. Topçu and Avcular(1997) showed that the energy absorption of concrete under impact load was increased

when rubber was used as the coarse aggregate replacement in concrete. It also been noted that the free shrinkage increases as a result of low aggregate stiffness and hence reduce the internal restraint and thus allow strain capacity enhancement. All these studies were carried out on the concrete with normal weight aggregate. The use of rubber is seen to cause a reduction in both compressive and tensile strength of concrete (Eldin and Senouci 1993; Khatib and Bayomy 1999) which is a big challenge to overcome to be able to incorporate rubber as a concrete constituent for wide range of application. Some of the structural and non-structural applications of rubberized concrete are road barriers, crash cushioning structures, railway buffers where resistance to impact or explosion is necessary, blast protection structure in military use, trench filling, pipe bedding, pipe heads and paving slabs etc. Rubberized concrete application in sacrificial shock absorbing structures is of great importance. These kind of structures absorb energy from the impact loads and thus saves lives and resources. Due to the frequent occurrence of impact load, continuous production of these sort of concrete structure is expected, and use of rubber as aggregate in that concrete matrix enhance the energy absorption capacity. In addition to that, use of rubber as replacement of fine aggregate would save natural resources as well as it may serve as a way to recycle those rubber wastes.

In order to overcome this strength loss, supplementary cementitious materials have been used with rubber aggregates in concrete with notable improvement due to silica fume and ground granulated blast furnace slag (Güneyisi et al. 2004; Wong and Ting 2009). Use of supplementary cementitious material is widely used method to improve various physical and mechanical properties of concrete. Previous studies (Detwiler and Mehta 1989; Ding and Li 2002; Hooton 1993; Mehta 1983; Mehta and Gjørv 1982) showed that silica fume as supplementary cementitious material improved mechanical properties by acting as filler and with pozzolanic reaction. Silica fume reduced bleed in fresh concrete and thus improved the density of transition zone between cement and coarse aggregate particle. Silica fume is also found to reduce pore sizes in concrete (Delage and Aitcin 1983; Mehta and Gjørv 1982) and completely eliminate them in the 500 micron to 0.5 micron range. The reduction of pore sizes reduces permeability and increase long term durability. Similar effect of metakaolin on the mechanical properties of concrete (Qian and Li 2001; Wild et al. 1996) and durability has been observed (Gruber et al. 2001).

Usually, concrete is described as a quasi brittle material, but crack nucleation in concrete occurs without much effort. Concrete barely poses any crack tip plasticity, hence crack nucleation leads to a brittle failure that does not require much energy. In order to improve crack control properties of concrete, fibre reinforcement is applied. In addition to crack control, this application of fibre reinforcement helps in maintaining serviceability and structural integrity of concrete members, improve compressive and flexural toughness, significant improvement for resistance to impact, blast or explosive loading (Balaguru and Shah 1992; Banthia et al. 1998; Bentur and Mindess 2006; Mufti et al. 1998). With the application of fibres in concrete, more efficient toughening and strengthening mechanism develop in the vicinity of fibres when compared to aggregate particles and cement paste. This is due to their elastic properties, aspect ratios and relatively large surface areas. Being brittle in nature, cement matrices usually reach failure strain before the fibres. And once the crack formed, fibres bridge the matrix cracks and act as stress transfer bridges. Thus, fibres help to maintain the material integrity of concrete section and provide post cracking tensile strength unlike plain concrete.

Nowadays, concrete industry uses different types of fibres; steel fibres, glass fibres, asbestos fibres, synthetic fibres as well as some natural fibres. Among all these types of fibres, use of steel fibre is the most popular for their effectiveness in improving post peak behavior in concrete. After the crack formation in cement matrices, steel fibre bridges the crack and provides stress transfer mechanism. At higher deformation, fibre pullout process initiates which provides toughening or energy absorption mechanisms in the concrete. The fibre pullout processes are the fundamental micro mechanisms that decide concrete composite toughness or post peak behavior. The factors affecting post peak behavior includes fibre shape, fibre geometry and fibre amount. Straight, hooked end and enlarged-end fibres are the most commonly used steel fibres and hooked and enlarged-end fibres are found to have superior pullout behavior which in turn aid in better toughening process when used in concrete. The dynamic strength of concrete reinforced with various types of fibres, subjected to dynamic flexural, tensile and compressive strength, is 3 to 10 times greater than that for plain concrete (Suaris and Shah 1984). The impact strength was derived from the higher energy required to

pullout the fibre from the concrete matrices (Wedding et al. 1981). It was also observed that the energy absorbed by steel fibre reinforced beams, subjected to impact loading and instrumented drop height and charpy-type systems, can be as much as 40 to 100 times that for unreinforced beams (Gopalaratnam et al. 1984; Gopalaratnam and Shah 1986; Naaman and Gopalaratnam 1983; Suaris and Shah 1983). Steel fibres were found effective in crack bridging and mechanical properties improvement with normal to high strength concrete due to comparable modulus of elasticity of concrete mixes and steel fibre.

On the other hand, it was observed that low modulus fibres such as polypropylene and other synthetic fibres are more suitable for the low strength and low modulus concrete mixes. These polypropylene fibre provides poor bond with surrounding cement matrix due to their hydrophobic nature unless treated prior to use. At low fibre dosage, presence of polypropylene fibre doesn't have any improvement on flexural and compressive strength. At higher fibre content, compressive strength sometimes reduced. However, at higher fibre content, polypropylene fibres have been found effective in increasing flexural strength (10% to 20%) (Banthia and Dubey 1999, 2000; Hasaba et al. 1984; Zollo 1984). This increase in flexural strength may be due to their enhanced load bearing capability in the post cracking zone as well as their effectiveness in reducing cracking. Moreover, it was found that the use of polypropylene at higher dosage (0.3% to 0.5%) improve the energy absorption capacity of composites (30 to 80%) under flexure and tension (Banthia et al. 1987; Barr and Newman 1985; Mindess et al. 1986; Mindness et al. 1989). It has also been shown that polypropylene fibres are effective in enhancing concrete performance under blast loading.

3.2 Research significance

The study reported in this Chapter describes the response of those concrete mixes where crumb rubber was used as partial replacement of fine aggregate along with lightweight shale aggregates used as coarse aggregate. Incorporating crumb rubber as fine aggregate replacements might serve as the possible recycling of scrap tires. Using crumb rubber as fine aggregate will save valuable natural resources and would make the concrete more sustainable.

In addition to this, various supplementary cementitious materials were also incorporated to compare their effect on concrete properties. Alongside a reference plain mix, a companion series was prepared to contain short discrete steel fibres.

3.3 Objectives

The objectives of this study are as follows,

a) Development of optimum concrete mixes with suitable supplementary cementitious by comparing mechanical properties of fibre reinforced concrete mixes with different rubber content and various supplementary cementitious material.
b) Expand the material characterization of the optimum concrete mix derived from (a) for wide range of crumb rubber content.
c) Evaluate the effect of short steel fibre on various mechanical properties of concrete mixes from (b)

3.4 Experimental program

The experimental program in this chapter was divided into two broad divisions;

a) At first, concrete mixes with 25% and 75% volume replacement of fine aggregate with crumb rubber were prepared. The effect of supplementary cementitious material were examined by incorporating silica fume and metakaolin separately as 10% mass replacement of ordinary Portland cement and by comparing with the concrete mixes with only ordinary Portland cement for same crumb rubber replacement. All the mixes contained 1% volume of short discreet steel fibre.
b) In the second part, based on the result from previous section, the concrete mixes with wide range of crumb rubber were prepared (0%, 25%, 50%, 75% and 100% volume replacement of fine aggregate with crumb rubber). All these mixes contained silica fume as supplementary cementitious material at 10% mass replacement of ordinary Portland cement. In addition to that, the effect of short discrete steel fibres on the physical and mechanical properties of lightweight mixes containing crumb rubber was examined with fibres up to 1% by volume.

3.4.1 Materials

The cement used was a (CSA A3001 2009) Type GU ordinary Portland cement (OPC). In addition to OPC, silica fume (SF) and metakaolin (MK) were incorporated as a supplementary cementitious material at 0 and 10% by mass of the binder. A 10mm downgraded expanded shale aggregate that would typically be used for structural lightweight concrete, was used here as the coarse aggregate. A locally available river sand and crumb rubber were used as the fine aggregate. The crumb rubber aggregate was obtained in 3 size ranges (0.85 mm to 3.35 mm) and later these three sizes were blended together. The crumb rubber and grain size distribution of coarse aggregate, fine aggregate and crumb rubber were shown in Figure 3-1. This blended crumb rubber was used at 0%, 25%, 50%, 75% and 100% volume replacement of total fine aggregates. The crumb rubber was manufactured from recycled motor vehicle tires and purchased from a local recycling company. Hooked-end steel fibres, 35 mm in length, with an aspect ratio of 70 and yield strength of 1100 MPa were employed at 1% volume fraction in corresponding mixes. The mix proportions were derived as per ACI 211 (1991) for the concrete mix composition for 28 days compressive strength of 35 MPa. This target compressive strength was deemed suitable for different structural as well as non-structural concrete applications. The water-cementitious material ratio (w/cm) was 0.40 for all mixes. A high range water reducing admixture was used to achieve adequate workability. In the initial concrete mixture development, nine (9) different concrete mixes were prepared. The detail mix proportions for those mixes are given in Table 3-1.

In addition to that, ten (10) different concrete mixes were prepared for this study which contained silica fume as supplementary cementitious material. The detail mix proportion for those mixes is given in Table 3-2

3.4.2 Specimen preparation

All specimens were prepared in accordance with ASTM C192 (2012) using a drum mixer of 75 litre capacity. From each mix, cylinders of 100mm diameter and 200mm height were also prepared to be tested in compression while prisms with dimension of 400 mm x 100 mm x 100 mm were prepared to be tested in flexure. The specimens were demolded 24 hours after casting and then cured in a moist room under controlled humidity (>99%) and temperature (22 ºC)

until testing. A 4 mm wide notch was sawn into each flexural specimen to a height of approximately 10 mm. This notch was intended to facilitate crack growth analysis under Mode-I fracture (Md Toihidul Islam 2010; Muhammad Mamun 2010).

In order to ensure the repeatability of the tests, three replicate specimens were cast for each investigation. The following protocol was adopted for the specimens ID's for mixes with silica fume and various level of fine aggregate replacements with crumb rubber: the alphabets "CR" in the first place holder represents crumb rubber and the numeral in the second place holder represents the aggregate replacement percentage, the alphabet in the third place holder stands for short steel fibre and the following numeral represents the percentage volume fraction of fibres in the concrete mix. Typical specimen identification is shown in Figure 3-2

3.4.3 Test setup

3.4.3.1 Compression test

The compression tests were performed in accordance with ASTM C469 (2010a) to evaluate the modulus of elasticity and establish the compressive stress-strain response. A displacement-controlled servo-hydraulic Materials Testing System with 2600 kN capacity was used to test the cylinders. Three Linear Variable Displacement Transducers (LVDT) were placed at 120º separation about the longitudinal axis together with two LVDTs in the transverse direction to measure axial and radial displacements, respectively. The test arrangement is shown in Figure 3-3. The data was collected through a continuous-record data acquisition system at 10 Hz. The cross-arm displacement rate was set to 1.25 mm/min as recommended by ASTM C469 (2010a).

3.4.3.2 Flexural test

From each mix, three prisms were tested in third-point bending according to ASTM C1609 (2010b). A Material Testing System of 1000kN capacity was used for this purpose. The load was applied by setting the cross-arm displacement rate to 0.15 mm/min which conformed to ASTM C1609 (2010b). As shown in Figure 3-4, a yoke was installed around the specimens to attach two LVDTs, one on either side. This yoke ensured that the displacement measured was that of the neutral axis and eliminated any errors due to support settlement. The LVDTs were

used to measure the mid-span deflection of the beam. All the loads and displacement readings were sampled at 10 Hz.

3.5 Results and discussion

3.5.1 Compressive response

3.5.1.1 Effect of supplementary cementitious materials

The compressive stress-strain responses of different mixes under compression are shown in Figure 3-5. The variations of compressive strength with different crumb rubber replacements are shown in Figure 3-6. In addition to compressive strength the modulus of elasticity for each mixes were calculated as per ASTM C469 (2010a) and those results were shown in Figure 3-7. From the results it was observed that an increase in crumb rubber content from 25% to 75% as volume replacement of sand caused a drop in the compressive strength. For mixes with only ordinary Portland cement (OPC) this drop in compressive strength was 69% whereas for mixes with silica fume and metakaolin this drop was 53% and 38% respectively. When the results of concrete mixtures with 25% and 75% crumb rubber replacement were compared with concrete mixtures of 0% crumb rubber content, it was found that 13% and 73% strength reduction took place for mixtures with only OPC, 27% and 66% strength reduction happened for mixtures with OPC and silica fume and 38% and 62% strength reduction was observed for concrete mixtures with OPC and metakaolin.

From the results of modulus of elasticity, it was observed that modulus of elasticity also decreased with an increase in crumb rubber replacement. This was due to increase in soft rubber particles in the concrete mixes at higher crumb rubber replacement. At 75% crumb rubber replacement, the reduction in modulus of elasticity was 50% for the mixture with only OPC. For same rubber content and mixes with silica fume and metakaolin, this reduction in the modulus of elasticity is 35% and 40% respectively. These results are presented in Table 3-3. In CSA A23.3-04 (2004) , the modulus of elasticity of plain concrete is calculated from the compressive strength using Equation (3.1),

$$E_c = (3300\sqrt{f_c'} + 6900)(\frac{\gamma_c}{2300})^{1.5} \quad (3.1)$$

where, γ_c = Density of concrete and f'_c = Compressive strength of concrete in MPa.

The suggested value of modulus of elasticity derived from Equation (3.1) is compared with the experimental values in Table 3-3. It was found that for all mixes, CSA Equation overestimated the modulus of elasticity values. However, the mix containing OPC and metakaolin with 0% crumb rubber replacement was closest to the value predicted by Equation (3.1). In addition to that, the Equation (3.1) predicted the values more closely for mixes with silica fume for 25% and 75% crumb rubber replacement with compare to mixes with other supplementary cementitious material.

3.5.1.2 Compressive response of mixes with silica fume with varying degree of fine aggregate replacement with crumb rubber

The variation of compressive strength and the modulus of elasticity are shown in Figure 3-8 and Figure 3-9. Table 3-4 lists the compressive strength of all mixes. From the results it was observed that an increase in crumb rubber replacement causes a drop in the compressive strength. For plain concrete and at 100% replacement of fine aggregate with crumb rubber, the compressive strength dropped by about 80% of that for mixes with no crumb rubber replacement. For each percentage of crumb rubber replacement, the introduction of steel fibre causes an improvement in compressive strength by 30% to 50%. The modulus of elasticity also decreases with an increase in crumb rubber replacement. At higher dosage of crumb rubber replcement(> 50% of the fine aggregate), introducing steel fibres leads to perceptible increase in the modulus of elasticity.

The reduction of compressive strength of concrete containing crumb rubber as aggregate can be attributed to three main reasons. First, due to high deformability of rubber particles compared with the surrounding cement paste, cracks are initiated around the rubber particles in the mix. This accelerates the failure in rubber-cement matrix (Eldin and Senouci 1993; Khatib and Bayomy 1999; Lee et al. 1998; Taha et al. 2008). Secondly due to the lack of proper adhesion or bond between rubber particle and cement paste, soft rubber particles may be viewed as voids in the concrete mix (Chung and Hong 1999; Eldin and Senouci 1993; Taha et al. 2008). The third possible reason of strength reduction is due to the resulting reduction of

density of the concrete matrix which depends greatly on the density, size and hardness of the aggregate. Of these, the deformability of soft rubber particles has more prominent effect on the compressive strength reduction of concrete mixes. When the concrete mixes with crumb rubber is subjected to a compressive stress state, the crumb rubber particles act as soft aggregate and tensile stress developed at the rubber particle surface and in the cement paste vicinity. This type of tensile stresses result in premature cracking in the cement matrix.

The significant strength loss also attributed to the low bond between rubber particles and the cement paste. All the crumb rubber particles were untreated in this study which yields low bond with the cementitious matrix. Some researchers showed that surface treatment of rubber particles enhanced bond strength between the rubber particle and cement paste (Chung and Hong 1999; Lee et al. 1998; Raghavan et al. 1998b; Taha et al. 2008). Treating rubble particle using Sodium Hydroxide (NaOH) and Calcium Hydroxide ($Ca(OH_2)$) demonstrated enhanced bond and thus increased compressive and flexural properties (Chung and Hong 1999; Raghavan et al. 1998b; Segre and Joekes 2000). Moreover, Biel and Lee (1996) showed that Magnesium Oxychloride cement noticeably enhanced the mechanical properties of concrete with rubber and Lee et al. (1998) showed that adding styrenebutadiene rubber polymer latex to the tire particle was also capable of enhancing mechanical and durability of rubberized concrete. Though the crumb rubber particles were untreated in this study, it is worth exploring the potential of using treated rubber particle to enhance its mechanical properties. Such studies shall examine effect of surface treatment of cement hydration and other long term durability characteristics of rubberized concrete.

Again, the presence of crumb rubber also affects the modulus of elasticity. From the Figure 3-10 it was evident that the Equation (3.1) overestimates the modulus of elasticity in case of rubberized concrete. In the mixes with low crumb rubber replacement, this variation is low whereas mixes with high crumb rubber replacement has wider variation. This variation is due to the presence of lightweight expanded shale as coarse aggregate and crumb rubber as fine aggregate in the concrete mixes which has comparatively lower modulus of elasticity.

Considering the deviation of modulus of elasticity obtained from CSA equation, the author of this study proposed the following equation to predict modulus of elasticity of concrete mixes containing expanded shale as coarse aggregate and various replacement level of fine aggregate with crumb rubber.

$$E_c = \left(3110\sqrt{f_c'}\right) * \left(\frac{\gamma_c}{2300}\right)^{0.825} \quad (3.2)$$

From the comparison with experimental values, this Equation (3.2) provided better approximation of modulus of elasticity for the lightweight mixes with expanded shale and crumb rubber.

3.5.2 Flexural response

3.5.2.1 Comparison between various supplementary cementitious materials

The load-deflection response under third-point bending is shown in Figure 3-11. Since a notch was introduced, the modulus of rupture, f_r was calculated using the effective cross sectional dimensions after accounting for the notch. The post peak energy dissipation was evaluated as per ASTM C1609 (2010b) for fibre reinforced concrete. This method introduced an equivalent flexural strength ratio ($R^D_{T,150}$) as calculated by using Equation (3.3)

$$R^D_{T,150} = 150 \cdot T^D_{150}/(f_1\, b \cdot d^2) \quad (3.3)$$

where, T^D_{150}= toughness up to a net deflection of $L/150$,

f_1 = first Peak Strength,

b = average width of the specimen at fracture,

d = average depth of the specimen at fracture.

A summary of the quasi-static flexural properties is provided in Table 3-5. The mix with OPC alone and the one with a blend of OPC and metakaolin showed a drop in f_r value with increased crumb rubber replacement but mixes containing OPC blended with SF do not show any significant change in f_r values. Similar change can be observed in case of equivalent flexural strength ratios as well.

Armelin and Banthia (1997) has proposed that, the mid span deflection of the beam, Δ and *CMOD* are related according to the following Equation (3.4),

$$\Delta = 0.75 \text{ x } CMOD \quad (3.4)$$

Using this relation, the stress intensity factor was calculated from the load-deflection response as propose by prior researchers (Broek 1986; Guinea et al. 1998) . The resulting fracture toughness, K_{IC} was determined and presented in Table 3-6.

3.5.2.2 Quasi static flexural response of concrete mixes with silica fume and various percentage of fine aggregate replacement with crumb rubber

The quasi static flexural test results for various mixes are provided in Figure 3-12 and summarized in Table 3-7. From the results it was observed that the flexural strength decreased with an increase in rubber concrete for the mixes without short steel fibre. Strength reduction of 22%, 45%, 42% and 65% were found for the crumb rubber replacement percentage of 25%, 50%, 75% and 100% and plain concrete. In case of fibre reinforced concrete, 8% and 27% increase in flexural strength was observed for concrete mixes with 25% and 50% rubber content respectively. For the mixes with 75% and 100% rubber content, 1% and 28% flexural strength reduction was recorded.

Again, short steel fibre has significant impact on improving flexural strength. In the present study, the presence of steel fibres found to improve flexural strength by 51%, 110%, 255%, 160% and 215% for 0%, 25%, 50%, 75% 100% crumb rubber content.

The flexural failure mode of concrete with rubber aggregate can be described as follows. The rubber aggregate can undergo large deformation before failure. Hence, a tension crack that develops in cement paste or at a mineral aggregate propagates until it reaches a piece of rubber particle. Rubber does not fail in tensile stress as easily as the surrounding matrix. Moreover, reduction in flexural strength is due to the weak bond between cement past and rubber particles. The strength reduction can be attributed both to a reduction of the solid load carrying material in the concrete mixes.

Evidence of improvement of flexural strength, even in the lightest mix, due to presence of steel fibre is a significant finding. However, the equivalent flexural strength ratio as calculated show that an increase in crumb rubber replacement provides better ductility. The equivalent flexural strength ratio gradually increases with an increase in the crumb rubber replacement. In case of steel fibre reinforced mixes, this equivalent flexural strength ratio decreases with an increase in the replacement of fine aggregate with crumb rubber.

3.6 Conclusion

In this chapter, the effect of crumb rubber inclusion on the mechanical properties was studied. In addition to that, the effect of short steel fibre and different supplementary cementitious materials were evaluated.

1) It was observed that, compressive strength of concrete mixes were decreased with higher crumb rubber replacement. For 100% replacement of fine aggregate with crumb rubber this reduction is 80% in plain concrete and 74% in fibre reinforced concrete. Modulus of elasticity was found to be decreased with increase in crumb rubber replacement.
2) At lower crumb rubber replacement, concrete mixes with only OPC showed superior compressive strength than the mixes with silica fume and metakaolin, but at higher crumb rubber replacement concrete mixes with silica fume and metakaolin showed 25% and 33% increase in compressive strength.
3) Significant drop (as high as 65%) in modulus of rupture was observed with higher crumb rubber replacement. At lower crumb rubber replacement mixes with only OPC were to achieve higher flexural strength. However, concrete mixes with supplementary cementitious material showcased higher flexural strength at higher crumb rubber replacement.

3.6.1 Limitations of the study

This study was focused on the material characterization of various concrete mixes with different crumb rubber content and supplementary cementitious material. Among various supplementary cementitious materials, only silica fume and metakaolin were used for optimum

mix determination. Effect of rubber content was studied by replacing fine aggregate portion of concrete mix with crumb rubber. Course aggregate wasn't replaced with rubber particles. Only one dosage (1%) of fibre content was employed to examine steel fibre effect on mechanical strength. Besides, no other fibre types were used to compare results with steel fibre. The gradation of crumb rubber was intended to match with fine aggregate, though an exact match wasn't possible due to unavailability of different crumb rubber sizes in the market. Compression test were performed on 100 mm x 200 mm cylinder, whereas flexural tests were performed on 100 mm x 100 mm x 400 mm prisms. Specimen size effect on the compressive strength and flexural properties weren't considered in this study.

Tables

Table 3-1: Mix Proportions for initial mix development (Water-binder ratio = 0.4, Steel fibre = 1% by volume)

Mix[1]	OPC kg/m^3	SF kg/m^3	MK kg/m^3	Sand kg/m^3	Crumb Rubber[2] %	Crumb Rubber (kg/m^3)
OPC, 0% Rubber	550	0	0	641	0	0
OPC+SF, 0% Rubber	495	55	0	641	0	0
OPC+MK, 0% Rubber	495	0	55	641	0	0
OPC, 25% Rubber	550	0	0	481	25	51
OPC+SF, 25% Rubber	495	55	0	481	25	51
OPC+MK, 25% Rubber	495	0	55	481	25	51
OPC, 75% Rubber	550	0	0	160	75	153
OPC+SF, 75% Rubber	495	55	0	160	75	153
OPC+MK, 75% Rubber	495	0	55	160	75	153

[1] Gravel content 986 kg/m^3

[2] Fine aggregate replacement

Table 3-2: Mix proportion for complete range of crumb rubber to fine aggregate percentage with silica fume

Mix[1]	OPC (kg/m^3)	SF (kg/m^3)	Sand (kg/m^3)	Crumb Rubber % (fine agg. repl.)	Crumb Rubber (kg/m^3)	Steel Fibre (Volume Fraction) %
CR0F0	495	55	640	0	0	0
CR25F0	495	55	480	25	51	0
CR50F0	495	55	320	50	102	0
CR75F0	495	55	160	75	153	0
CR100F0	495	55	0	100	204	0
CR0F1	495	55	640	0	0	1
CR25F1	495	55	480	25	51	1
CR50F1	495	55	320	50	102	1
CR75F1	495	55	160	75	153	1
CR100F1	495	55	0	100	204	1

[1] Gravel content 986 kg/m^3

[2] Water to binder ratio 0.4

Table 3-3: Summary of compression response

Mix Description	f'_c (MPa)	CoV	E_c (MPa)	CoV	E_c (Test)/ E_c (CSA)
OPC, 0% Rubber	45	0.11	17100	0.09	0.58
OPC & SF,0% Rubber	44	0.02	18590	0.10	0.65
OPC &MK,0% Rubber	42	0.04	23460	0.18	0.84
OPC, 25% Rubber	39	0.05	15300	0.44	0.67
OPC & SF,25% Rubber	32	0.03	14600	0.34	0.75
OPC &MK,25% Rubber	26	0.16	12390	0.17	0.70
OPC, 75% Rubber	12	0.07	7800	0.43	0.64
OPC & SF,75% Rubber	15	0.02	9250	0.84	0.71
OPC & MK,75% Rubber	16	0.02	7240	0.29	0.52

Table 3-4: Compressive strength

Specimen	$f'c$ (MPa)	CoV
CR0F0	37	0.16
CR25F0	22	0.14
CR50F0	15	0.04
CR75F0	10	0.09
CR100F0	8	0.01
CR0F1	44	0.02
CR25F1	32	0.03
CR50F1	20	0.13
CR75F1	15	0.02
CR100F1	11	0.10

Table 3-5: Summary of quasi-static flexural response for mixes with various supplementary cementitious materials

Mix Description	f_r (MPa)	CoV	$R^D_{T,150}$ %	CoV
OPC, 0% Rubber	9.7	0.1	76.5	0.05
OPC & SF,0% Rubber	5.17	0.06	83.0	0.05
OPC &MK,0% Rubber	7.9	0.12	82.0	0.04
OPC, 25% Rubber	7.0	0.07	84	0.03
OPC & SF,25% Rubber	5.6	0.11	78	0.08
OPC &MK,25% Rubber	6.6	0.09	76	0.05
OPC, 75% Rubber	4.6	0.11	74.0	0.02
OPC & SF,75% Rubber	5.1	0.14	75.5	0.05
OPC & MK,75% Rubber	5.0	0.02	78.0	0.04

Table 3-6: Fracture Toughness, K_{IC}

Mix Description	K_{IC} (MPa.√m)	CoV
OPC, 0% Rubber	9.0	0.35
OPC & SF, 0% Rubber	8.7	0.48
OPC & MK, 0% Rubber	9.0	0.74
OPC, 25% Rubber	6.4	0.08
OPC & SF, 25% Rubber	5.2	0.29
OPC & MK, 25% Rubber	4.7	0.17
OPC, 75% Rubber	3.4	0.16
OPC & SF, 75% Rubber	4	0.29
OPC & MK, 75% Rubber	3.9	0.04

Table 3-7: Summary of quasi-static flexural response for mixes with silica fume and various crumb rubber percentages

	f_r (MPa)	CoV	$R^D_{T,150}$	CoV
CR0F0	3.41	0.04	0.548	0.97
CR25F0	2.64	0.09	10.43	0.15
CR50F0	1.85	0.15	8.977	0.29
CR75F0	1.97	0.10	10.62	0.16
CR100F0	1.167	0.11	15.21	0.13
CR0F1	5.17	0.06	83.21	0.05
CR25F1	5.62	0.11	77.83	0.08
CR50F1	6.58	0.07	74.18	0.09
CR75F1	5.15	0.14	75.72	0.05
CR100F1	3.71	0.08	54.07	0.35

Figures

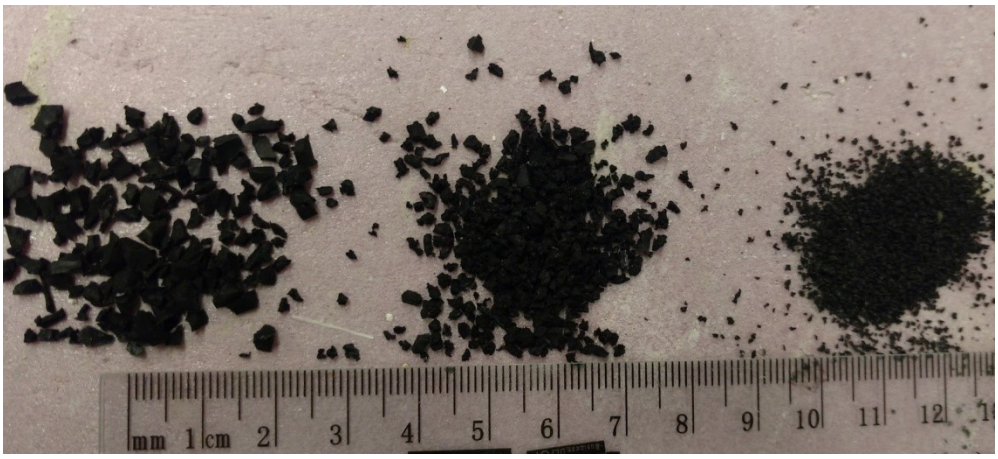

(a) Crumb rubber of different sizes

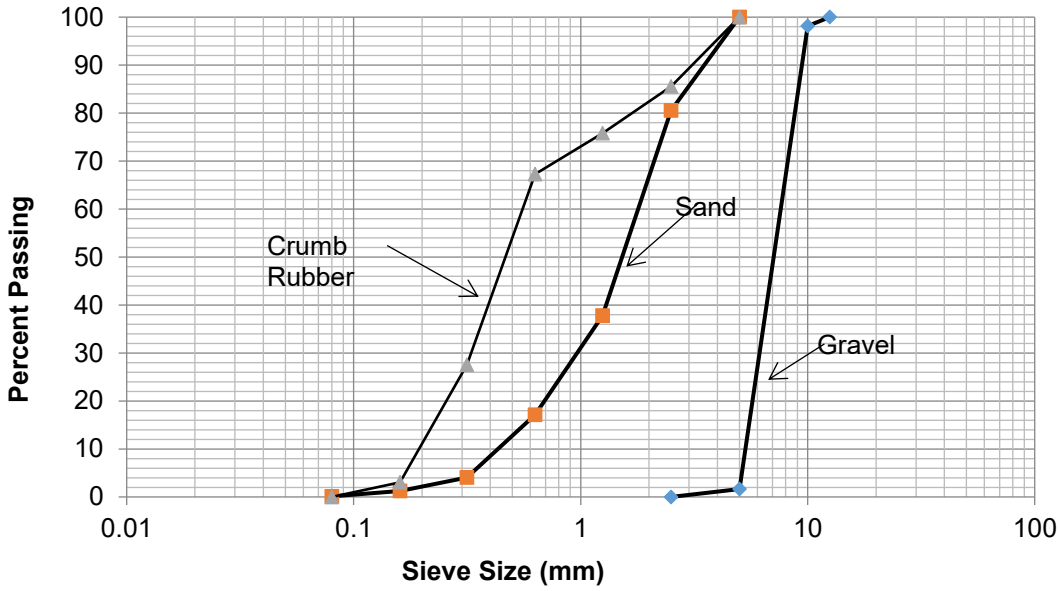

(b) Grain size distribution of coarse aggregate, fine aggregate and crumb rubber

Figure 3-1: (a) Crumb rubber of different sizes; (b) Grain size distribution of coarse aggregate, fine aggregate and crumb rubber

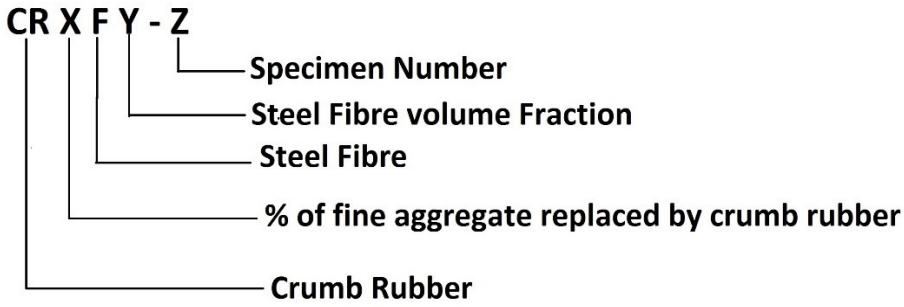

Figure 3-2: Specimen identification description

Figure 3-3: Compression test setup

Figure 3-4: Quasi-static flexural test setup

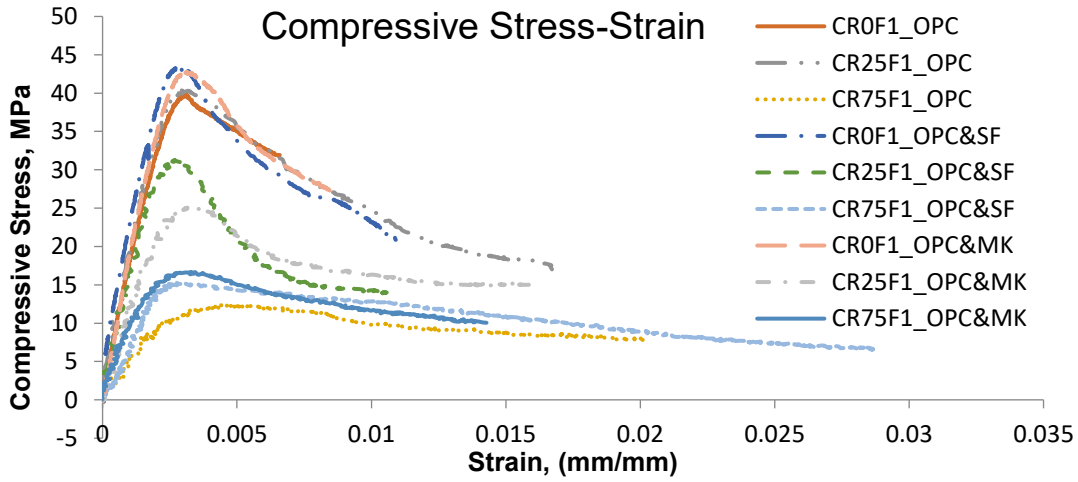

Figure 3-5: Compressive response

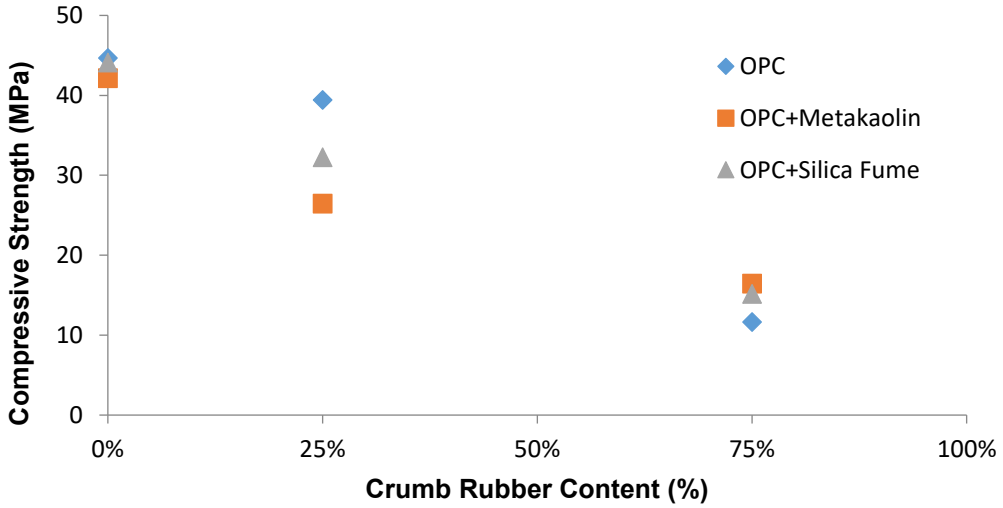

Figure 3-6: Effect of crumb rubber content on compressive strength

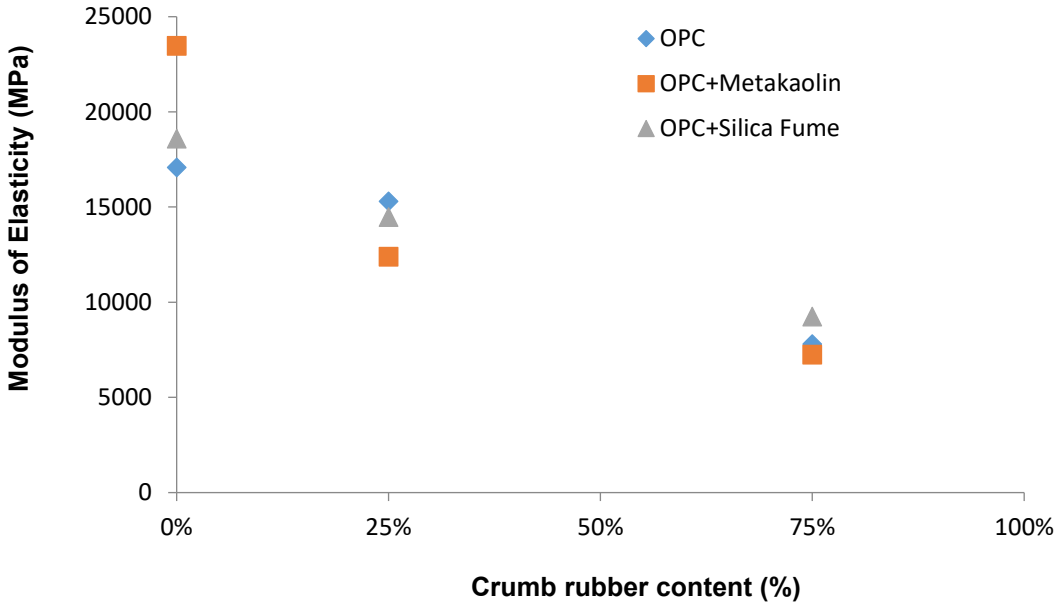

Figure 3-7: Effect of crumb rubber content on modulus of elasticity

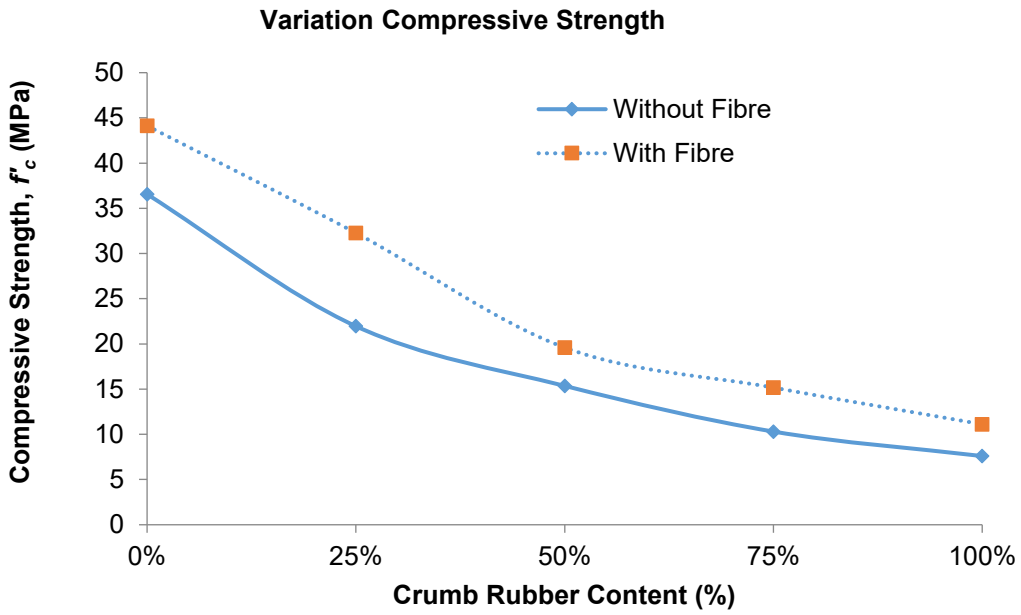

Figure 3-8: Variation of compressive strength with crumb rubber content

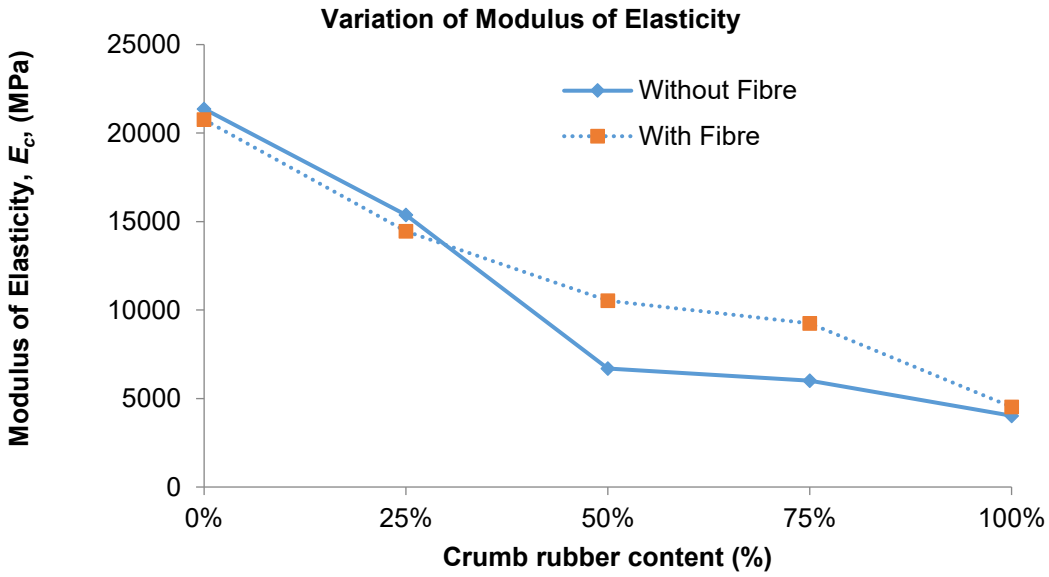

Figure 3-9: Variation of modulus of elasticity with crumb rubber content

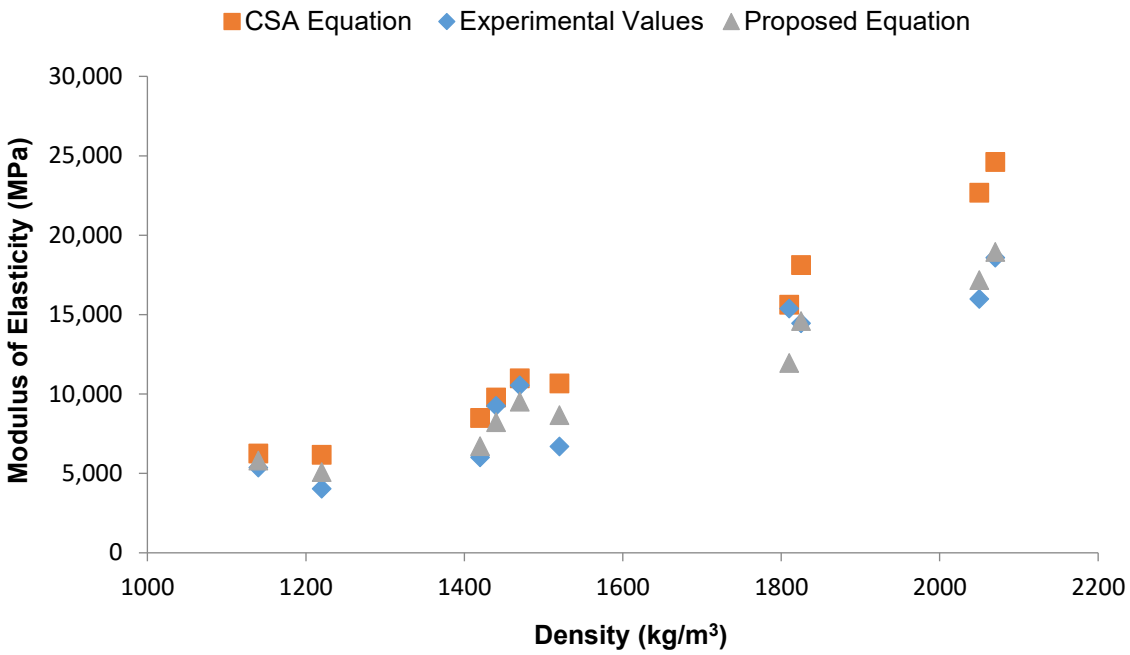

Figure 3-10: Comparison of experimental modulus of elasticity with CSA Equation and Proposed Equation

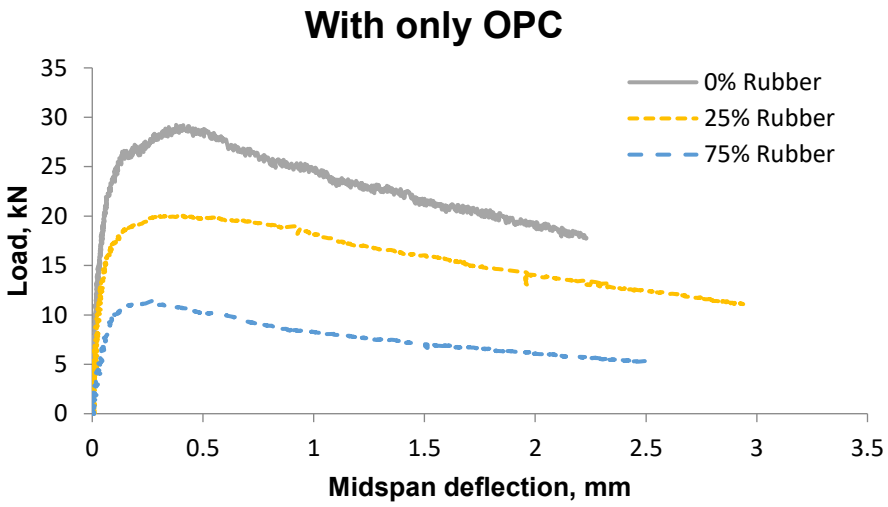

(a)

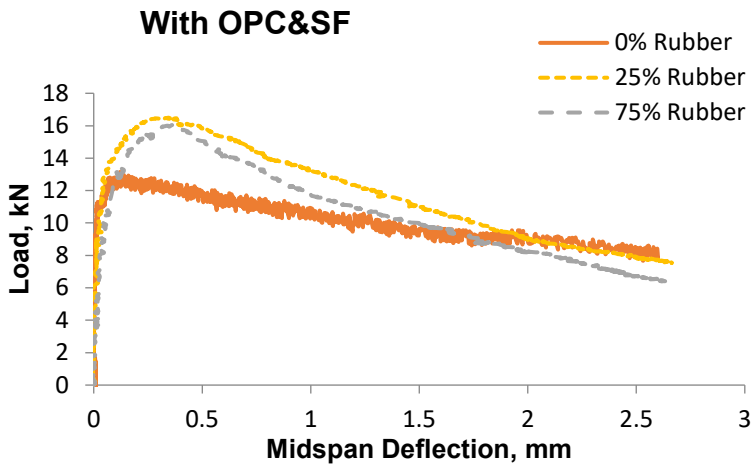

(b)

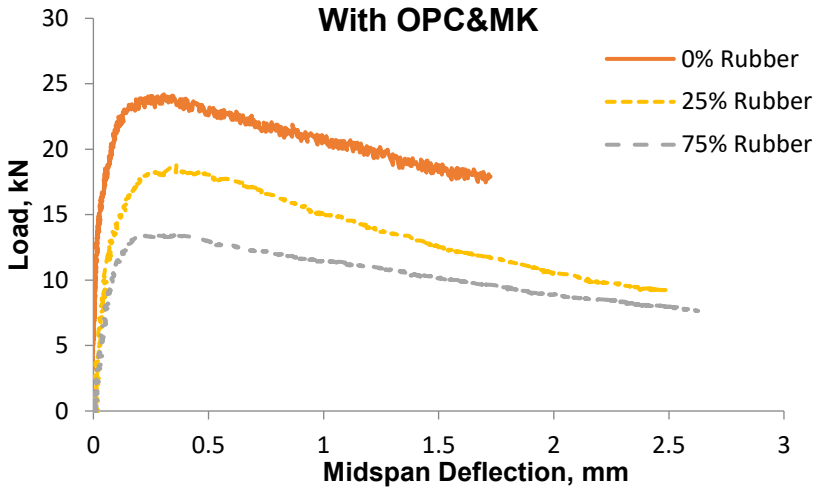

(c)

Figure 3-11: Load-deflection response for concrete mixes with various supplementary cementitious material (a) With only OPC, (b) With OPC and SF, (c) With OPC and MK

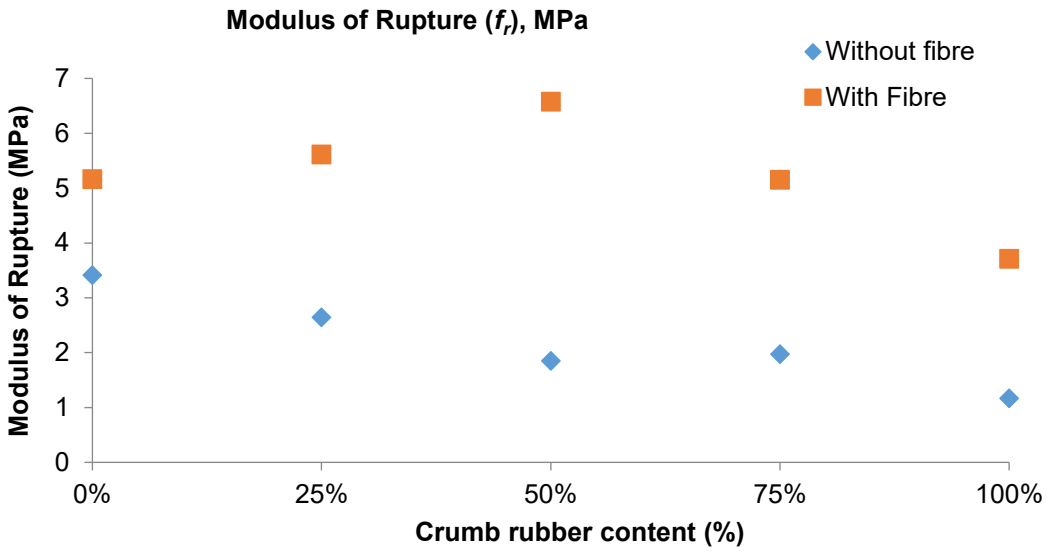

Figure 3-12: Variation of Modulus of Rupture with crumb rubber content

References

ACI Committee 211.1. (1991). "Standard Practice for Selecting Proportions for Normal, Heavyweight, and Mass Concrete ACI 211.1 (Reapproved 2009)."

Armelin, H. S., and Banthia, N. (1997). "Predicting the flexural postcracking performance of steel fiber reinforced concrete from the pullout of single fibers." *ACI materials Journal*, 94(1).

ASTM C192. (2012). *Practice for Making and Curing Concrete Test Specimens in the Laboratory (ASTM C192)*. ASTM International, West Conshohocken, PA.

ASTM C469. (2010a). *Test Method for Static Modulus of Elasticity and Poissons Ratio of Concrete in Compression ASTM C469*. ASTM International, West Conshohocken, PA.

ASTM C1609. (2010b). *Test Method for Flexural Performance of Fiber-Reinforced Concrete (Using Beam With Third-Point Loading) ASTM C1609*. ASTM International, West Conshohocken, PA.

Balaguru, P. N., and Shah, S. P. (1992). *FIBER-REINFORCED CEMENT COMPOSITES*.

Banthia, N., and Dubey, A. (1999). "Measurement of Flexural Toughness of Fiber-Reinforced Concrete Using a Novel Technique—Part 1: Assessment and Calibration." *Materials Journal*, 96(6), 651–656.

Banthia, N., and Dubey, A. (2000). "Measurement of Flexural Toughness of Fiber-Reinforced Concrete Using a Novel Technique—Part 2: Performance of Various Composites." *Materials Journal*, 97(1), 3–11.

Banthia, N. P., Mindess, S., and Bentur, A. (1987). "Impact behaviour of concrete beams." *Materials and Structures*, 20(4), 293–302.

Banthia, N., Yan, C., and Sakai, K. (1998). "Impact resistance of fiber reinforced concrete at subnormal temperatures." *Cement and Concrete Composites*, 20(5), 393–404.

Barr, B., and Newman, P. D. (1985). "Toughness of polypropylene fibre-reinforced concrete." *Composites*, 16(1), 48–53.

Bentur, A., and Mindess, S. (2006). *Fibre Reinforced Cementitious Composites, Second Edition*. CRC Press.

Biel, T., and Lee, H. (1996). "Magnesium Oxychloride Cement Concrete with Recycled Tire Rubber." *Transportation Research Record: Journal of the Transportation Research Board*, 1561, 6–12.

Broek, D. (1986). *Elementary Engineering Fracture Mechanics*. Springer.

Chung, K.-H., and Hong, Y.-K. (1999). "Introductory Behavior of Rubber Concrete." *JOURNAL OF APPLIED POLYMER SCIENCE*, 72(1), 35–40.

CSA A23.3-04. (2004). "Design of Concrete Structures." Canadian Standards Association, Mississauga, ON.

CSA A3001. (2009). "Cementitious materials compendium." Canadian Standards Association, Mississauga, ON.

Delage, P., and Aitcin, P. C. (1983). "Influence of condensed silica fume on the pore-size distribution of concretes." *Industrial & Engineering Chemistry Product Research and Development*, 22(2), 286–290.

Detwiler, R. J., and Mehta, P. K. (1989). "Chemical and Physical Effects of Silica Fume on the Mechanical Behavior of Concrete." *Materials Journal*, 86(6), 609–614.

Ding, J.-T., and Li, Z. (2002). "Effects of metakaolin and silica fume on properties of concrete." *ACI Materials Journal*, 99(4), 393–398.

Eldin, N., and Senouci, A. (1993). "Rubber-Tire Particles as Concrete Aggregate." *Journal of Materials in Civil Engineering*, 5(4), 478–496.

Gopalaratnam, V. S., and Shah, S. P. (1986). "Properties of steel fiber reinforced concrete subjected to impact loading." *ACI Journal Proceedings*.

Gopalaratnam, V. S., Shah, S. P., and John, R. (1984). "A modified instrumented charpy test for cement-based composites." *Experimental Mechanics*, 24(2), 102–111.

Gruber, K. A., Ramlochan, T., Boddy, A., Hooton, R. D., and Thomas, M. D. A. (2001). "Increasing concrete durability with high-reactivity metakaolin." *Cement and Concrete Composites*, 23(6), 479–484.

Guinea, G. V., Pastor, J. Y., Planas, J., and Elices, M. (1998). "Stress Intensity factor, compliance and CMOD for a General Three-Point-Bend Beam." *International Journal of Fracture*, 89(2), 103–116.

Güneyisi, E., Gesoğlu, M., and Özturan, T. (2004). "Properties of rubberized concretes containing silica fume." *Cement and Concrete Research*, 34(12), 2309–2317.

Hasaba, S., Kawamura, M., Koizumi, T., and Takemoto, K. (1984). "Resistibility Against Impact Load and Deformation Characteristics Under Bending Load in Polymer and Hybrid (Polymer and Steel) Fiber Reinforced Concrete." *Special Publication*, 81, 187–196.

Hooton, R. D. (1993). "Influence of Silica Fume Replacement of Cement on Physical Properties and Resistance to Sulfate Attack, Freezing and Thawing, and Alkali-Silica Reactivity." *Materials Journal*, 90(2), 143–151.

Khatib, Z. K., and Bayomy, F. M. (1999). "Rubberized Portland Cement Concrete." *Journal of Materials in Civil Engineering*, 11(3), 206–213.

Lee, H. S., Lee, H., Moon, J. S., and Jung, H. W. (1998). "Development of tire-added latex concrete." *ACI Materials Journal*, 95(4), 356–364.

Md Toihidul Islam. (2010). "Static and Dynamic Response of Sandstone Masonry Units Bound with Fibre Reinforced Mortars." Master's Thesis, University of Alberta.

Mehta, P. K. (1983). "Pozzolanic and Cementitious Byproducts as Mineral Admixtures for Concrete - A Critical Review." *Special Publication*, 79, 1–46.

Mehta, P. K., and Gjørv, O. E. (1982). "Properties of portland cement concrete containing fly ash and condensed silica-fume." *Cement and Concrete Research*, 12(5), 587–595.

Mindess, S., Banthia, N., and Bentur, A. (1986). "The response of reinforced concrete beams with a fibre concrete matrix to impact loading." *International Journal of Cement Composites and Lightweight Concrete*, 8(3), 165–170.

Mindness, S., Bentur, A., Yan, C., and Vondran, G. (1989). “Impact Resistance of Concrete Containing Both Conventional Steel Reinforcement and Fibrillated Polypropylene Fibers.” *Materials Journal*, 86(6), 545–549.

Mufti, A. A., Bentur, A., and Banthia, N. (1998). *Fiber reinforced concrete: present and future*. Canadian Society for Civil Engineering, Montreal.

Muhammad Mamun. (2010). “Loading Rate Effects and Sulphate Resistance of Fibre Reinforced Cement-based Foams.” Master’s Thesis, University of Alberta.

Naaman, A. E., and Gopalaratnam, V. S. (1983). “Impact properties of steel fibre reinforced concrete in bending.” *International Journal of Cement Composites and Lightweight Concrete*, 5(4), 225–233.

Najim, K. B., and Hall, M. R. (2012). “Mechanical and dynamic properties of self-compacting crumb rubber modified concrete.” *Construction and Building materials*, 27(1), 521–530.

Qian, X., and Li, Z. (2001). “The relationships between stress and strain for high-performance concrete with metakaolin.” *Cement and Concrete Research*, 31(11), 1607–1611.

Raghavan, D., Huynh, H., and Ferraris, C. (1998). “Workability, mechanical properties, and chemical stability of a recycled tyre rubber-filled cementitious composite.” *Journal of Materials Science*, 33(7), 1745–1752.

Segre, N., and Joekes, I. (2000). “Use of tire rubber particles as addition to cement paste.” *Cement and Concrete Research*, 30(9), 1421–1425.

Suaris, W., and Shah, S. P. (1983). “Properties of Concrete Subjected to Impact.” *Journal of Structural Engineering*, 109(7), 1727–1741.

Suaris, W., and Shah, S. P. (1984). “Test Methods for Impact Resistance of Fiber Reinforced Concrete.” *Special Publication*, 81, 247–266.

Taha, M. M. R., El-Dieb, A. S., El-Wahab, M. A. A., and Abdel-Hameed, M. E. (2008). “Mechanical, fracture, and microstructural investigations of rubber concrete.” *Journal of Materials in Civil Engineering*, 20(10), 640–649.

Topçu, lker B., and Avcular, N. (1997). “Analysis of rubberized concrete as a composite material.” *Cement and Concrete Research*, 27(8), 1135–1139.

Topçu, I. B. (1995). “The properties of rubberized concretes.” *Cement and Concrete Research*, 25(2), 304–310.

Wedding, P., Suaris, W., and Shah, S. (1981). “Inertial Effects in the Instrumented Impact Testing of Cementitious Composites.” *Cement, Concrete and Aggregates*, 3(2), 77.

Wild, S., Khatib, J. M., and Jones, A. (1996). “Relative strength, pozzolanic activity and cement hydration in superplasticised metakaolin concrete.” *Cement and Concrete Research*, 26(10), 1537–1544.

Wong, S.-F., and Ting, S.-K. (2009). “Use of recycled rubber tires in normal and high-strength concretes.” *ACI Materials Journal*, 106(4).

Zheng, L., Huo, X. S., and Yuan, Y. (2008). “Strength, Modulus of Elasticity, and Brittleness Index of Rubberized Concrete.” *Journal of Materials in Civil Engineering*, 20(11), 692–699.

Zollo, R. F. (1984). “Collated Fibrillated Polypropylene Fibers in FRC.” *Special Publication*, 81, 397–410.

Notations

b = average width of the specimen at fracture,

d = average depth of the specimen at fracture.

E_c = Modulus of Elasticity of concrete

f_1 = first Peak Strength,

f'_c = Compressive strength of concrete

f_r = Modulus of rupture

K_{IC} = Fracture Toughness

$R^D_{T,150}$ = equivalent flexural strength ratio

T^D_{150} = toughness up to a net deflection of $L/150$

Δ = Midspan beam deflection

CHAPTER 4. BOND RESPONSE OF FIBRE REINFORCED PLOYMER BAR WITH LIGHTWEIGHT CONCRETE: PULLOUT TEST

4.1 Introduction

Steel reinforcement bars are the widely used reinforcement material in reinforced concrete structures. It's high strength, ductility and above all the availability makes it a prominent reinforcement option. However, one of the major setbacks of steel reinforcement is corrosion. In recent years the infrastructure systems are deteriorating due to the corrosion of existing steel reinforcement. In order to prevent the deterioration of reinforced concrete structures, scientist and engineers were looking for alternative reinforcing materials to use instead of steel. Hence fiber reinforced polymer (FRP) bars are increasingly used in concrete structures for their better corrosion resistance as well as higher stiffness to weight ratio and good fatigue properties compare to steel reinforcement.

On the other hand there is continuous growth of concrete structural construction which requires more and more natural resources as concrete constituents. This continuous growth of demand has shifted the attention towards alternative aggregate resources. Use of these new materials not only reduces the environmental effect due to aggregate extraction but also reduces the landfill and recycling cost of those materials. Utilization of scrap tires may play a significant role in sustainable development considering the existing stockpile of scrap tires. In the last 20 years the potential use of crumb rubber as replacement of fine and/or course aggregate was studied by many researchers (Eldin and Senouci 1993; Khatib and Bayomy 2013; Topçu and Avcular 1997; Topçu 1995; Zheng et al. 2008), The rubber aggregates can be loosely classified into four types depending on their particle size, shredded or chipped (the size representing the coarse aggregate), crumb rubber (typically between 4.75mm and 0.425mm), ground tire rubber (passing through No 40 sieve) and fibre rubber aggregate (short fibre typically between 8.5mm and 21.5mm in length) (Najim and Hall 2012) and these are characterized as having negligible water absorption and low density (0.866 kg/m^3). The use of rubber is seen to cause a reduction in both compressive and tensile strength of concrete which is a big challenge to overcome.

Use of silica fume in concrete to enhance mechanical properties and durability is widely accepted. Previous studies (Detwiler and Mehta 1989; Ding and Li 2002; Hooton 1993; Mehta 1983; Mehta and Gjørv 1982) showed that silica fume as supplementary cementitious material improve mechanical properties by acting as filler and with pozzolanic reaction. Silica fume reduced bleed in fresh concrete and thus improved the density of transition zone between cement and coarse aggregate particle. Silica Fume also found to reduce pore sizes in concrete (Delage and Aitcin 1983; Mehta and Gjørv 1982). Moreover, some studies (Duval and Kadri 1998; Güneyisi et al. 2004) showed that use of silica fume with concrete where rubber chips and crumb rubber as aggregate improved the mechanical and physical properties of concrete.

Again, concrete is usually considered as a quasi brittle material. However crack nucleation in concrete occurs without much effort and the lack of crack tip plasticity leads to a brittle failure that does not necessitate much energy. Fibre reinforcement in concrete was found to improve many properties of concrete including crack control in the plastic state, compressive and flexural toughness, with substantial improvement to resistance to impact, blast or explosive loading (Balaguru and Shah 1992; Banthia et al. 1998; Bentur and Mindess 2006; Mufti et al. 1998). Fibres in concrete usually develop more efficient toughening and strengthening mechanism in their vicinity when compare to aggregate particles and cement paste because of their aspect ratios, large surface areas and elastic properties. After the crack formed, fibres bridge the matrix cracks and act as stress transfer bridges, which is important mechanism in dealing with post peak performance of concrete under flexure.

The proper bond between reinforcing bar and concrete is the key aspect to the performance of reinforced concrete structures. The bond ensures that forces in the reinforcement fully transfer to the surrounding concrete. Use of the FRP bar along with the concrete made of alternate aggregate sources requires an understanding of the mechanisms underlying the bond between these reinforcing bars and the resulting lightweight concrete.

The bond behavior of FRP bar has been evaluated by many researchers over the last two decades. There are many factors that influence bond behavior namely; surface condition of FRP bar, size and orientation of surface deformations, size of the FRP bar, mechanical

properties of the FRP bar, mechanical properties of the surrounding concrete, environmental conditions, shrinkage of FRP bar etc. Some researchers found that specific surface deformation (glued fibre spiral) has negligible improvement in bond strength as compared to smooth rebar but other types of surface deformations (indented and ribbed rods) increased the bond strength significantly (Benmokrane et al. 1996; Malvar 1994). Some studies (Nanni et al. 1995, 1997), found that only friction-type bond behavior is present in case of deformed FRP bar. But Al-Zahrani et al.(1999) demonstrated that mechanical interlock and shear strength of the lugs are stress transfer mechanisms but after the shearing of the lugs, friction between rebar and concrete becomes the main bond mechanism.

The compressive strength of concrete affects the bond performance of FRP rebar during pull out. Various studies were conducted (Ametrano 2011; Baena et al. 2009; Chaallal and Benmokrane 1993a; Nanni et al. 1995; Rossetti et al. 1995) where effect of concrete compressive strength on the bond strength were studied. Those studies were conducted with the concrete of 30 MPa to 79 MPa in compressive strength and with density range 2380 kg/m^3 to 2580kg/m^3, and in some case (Ametrano 2011) as high as 175 MPa. Those studies found that bond strength increased with the increase in compressive strength. However, at low compressive strength ($f'c \approx 30$), bond failure mechanism varies when compared to higher compressive strength.

In the reported literature (Achillides and Pilakoutas 2004; Baena et al. 2009; Benmokrane et al. 1996; Cosenza et al. 1997; Nanni et al. 1995; Rossetti et al. 1995; Tepfers 2006; Tighiouart et al. 1998), it has been found that larger diameter rebars develop lower bond strength. During a pullout test, peak bond stress moves toward free end from the loaded end with bond stress at loaded end considerably low; which develops a nonlinear distribution of bond stress along the length of the bar. As longer development length is required for larger bar diameter, this nonlinear distribution of bar produces lower average bond strength. Again, due to Poisson effect, the diameter of bar reduces under tension. For larger bar diameters, this reduction is more prominent compared to smaller bar diameter, which in turn leads to lower frictional and mechanical interlocking stresses.

Again, fibre reinforced concrete (FRC) is becoming popular in use due to the fibre's crack bridging ability and toughening mechanism. Several studies were performed to evaluate the effect of fibre presence on the bond characteristics between reinforcement bar and surrounding concrete mixes. Yan (1992) conducted an extensive research to evaluate the effect of different fibre types (steel and polypropylene) and various fibre dosage (0.1%, 0.5% and 1%) on the bond strength between normal strength (40 MPa) and high strength (75 MPa) concrete with plain and deformed steel bars. He found insignificant improvement in bond with the presence of low modulus fibre (polypropylene), whereas steel fibre was found to improve bond strength significantly. Few other studies were conducted (Ezeldin and Balaguru 1990; Hota and Naaman 1997; Soroushian et al. 1994) on the effect of steel fibre reinforced concrete on bond performance of GFRP bars. They found that steel fibre reinforced concrete provided greater (20% to 36%) bond strength with compared to plain concrete. Similar study was performed by Ding et al. (2014) to evaluate bond performance between ribbed GFRP bar and fibre reinforced concrete (short steel fibre and polypropylene fibre). It was found that, fibre reinforced concrete was found to increase bond resistance by 14% to 29% due to their splitting crack resisting ability.

All of the studies related to bond behavior of FRP bars were performed with a concrete having compressive strength of 30 MPa or higher. And most of the study was carried out on the concrete with density of 2380 kg/m^3 or higher. But few studies so far evaluate the bond performance of FRP with structural lightweight concrete (~ 1400 kg/m^3) with significantly low compressive strength (~10 MPa). Partial replacement of fine aggregate portion of concrete mixes by a lighter constituent is one of the various ways to prepare lightweight concrete. In this study crumb rubber was used as partial replacement of sand. The concrete prepared with crumb rubber as replacement of fine aggregate had a compressive strength in the range of 7 to 40 MPa and a density in the range of 1400 kg/m^3 to 2240 kg/m^3, depending on the degree of fine aggregate replacement.

4.2 Objective

The objective of this study was to evaluate bond performance between sand coated GFRP bar and lightweight concrete mixes using pullout test method. The effect of crumb rubber content on bond performance was studied by using concrete mixes prepared with lightweight expanded shale as coarse aggregate and crumb rubber as of fine aggregate replacement at various percentages. Moreover, the effect of short steel fibre on bond performance was examined by preparing specimens with hooked end steel fibre at 1% volume and then comparing with corresponding plain concrete. All the concrete mixes contain silica fume as 10% mass replacement of OPC, as previous studies showed better durability of rubberized concrete with silica fume. The detailed material characterizations of these concrete mixes were presented in Chapter 3. In addition to that, two different bar sizes (10 mm and 16 mm) were used to study bar size effect on bond performance.

4.3 Experimental method

The following parameters were examined to characterize their influence on the mechanical properties of concrete:

- Crumb rubber as aggregate replacement: varied at 0%, 25%, 50%, 75% and 100% by volume of total fine aggregates;
- Presence of short discrete steel fibre: 0% and 1% volume
- Effect of bar diameter: 10mm and 16mm

4.3.1 Materials

4.3.1.1 Concrete mix proportion

The concrete mixes were prepared by the CSA A3001-09 (2009) Type GU ordinary Portland cement (OPC). In addition to that, silica fume was incorporated as supplementary cementitious material up to 10% mass replacement of OPC. A 10mm downgraded expanded shale aggregate was used as coarse aggregate. A locally available river sand and crumb rubber were used as the fine aggregate. The crumb rubber was manufactured from recycled motor vehicle tires and purchased from a local recycling company. Three different size ranges (0.85mm to 3.35mm)

of crumb rubber will be blended for partial/full replacement of sand. To evaluate the effect of steel fibre, hooked-end steel fibres of 35 mm in length with aspect ratio of 65 and yield strength of 1100 MPa were employed at 1% volume fraction in five of the ten mixes. High range water reducing admixture was incorporated to achieve required workability. The Table 4-1 shows the detail mix composition that is used in this study.

4.3.1.2 Glass fiber reinforced polymer bar (GFRP Bar)

Nowadays there are various GFRP bar manufacturing companies in the country. For our study TUF-BAR^{TM} GFRP bars were used which were produced by a local manufacturer. The surface of the GFRP bars were sand coated. Properties of the sampled bars are provided in Table 4-2.

4.3.2 Sample preparation for compressive strength of various concrete mixes

From each mix, three cylinders of 100mmx200mm were tested for determining compressive strength and stress-strain relationship. The compression tests were performed in accordance with ASTM C469 (2010a) to evaluate the modulus of elasticity and establish the compressive stress-strain response. Three LVDTs were used to measure the longitudinal strain with 100 mm gauge length. Two LVDTs were also used to record the lateral strain during the test. An electronic data acquisition system was used to record the data at a rate of 10 Hz. The compressive strength set up is shown in Figure 4-1

4.3.3 Pullout test specimen

In this study the effect of crumb rubber content on the bond performance was examined as a function of the bar diameter and short steel fibre content. In all, ten different mix combinations and two different bar sizes were used which are summarized in the Table 4-3.

For the bond pullout test sample, 100mmx200mm concrete cylinders were cast with FRP bar in the central axis of the cylinder. The embedment length of FRP bar inside the cylinder was kept constant at 5 times diameter for all bar sizes by using rubber tube to separate the concrete and FRP bar for required length. The schematic diagram of the pullout test is presented in Figure 4-2(a). A typical pull out sample is shown in Figure 4-2(b). The samples were cured for 28 days before conducting pullout test. The setup for the pullout test is shown in Figure 4-2(c).

LVDT's have been used to determine the loaded end slip and free end slip. Appropriate load cell was used to get the load data. All data were recorded in a data acquisition system. From this test the bond strength and bond-slip response of FRP bar and various concrete mixes have been obtained.

4.3.4 Image analysis for GFRP bar surface examination

GFRP bar surface condition plays an important role with the mechanism of bond between rebar and surrounding concrete. For that reason, it is of outmost necessity to know about the surface condition of the rebar in use for bond performance evaluation. Image analysis was done with high quality images. After the acquisition of those images, desired features were isolated, which was defined as segmentation. In this study, the sand grains attached on the surface of GFRP bar were considered as features. Finally, the regions of interests (ROI) were analyzed to get average area of the feature of interest.

4.4 Results

4.4.1 Compressive response of concrete

From the results it is evident that the concrete compressive strength decreases with an increase in crumb rubber replacement. This is similar to the research previously done which is reasonable because of lower bond between crumb rubber component and cementitious materials. The variation of compressive strength and the modulus of elasticity are shown in Figure 4-3 and Figure 4-4.

From the results it is observed that an increase in crumb rubber replacement (replacement of fine aggregate with crumb rubber) causes a drop in the compressive strength. At 100% replacement, the compressive strength drops about 80% of the compressive strength of mixes with no crumb rubber replacement. For each crumb rubber replacement level, the introduction of steel fibre causes improvement of compressive strength by 30 to 50%. The modulus of elasticity also decreases with the increase in crumb rubber replacement. For 50% and 75% crumb rubber replacement the variation of modulus of elasticity is more prominent between

plain and fibre reinforced mixes. In CSA A23.3-04 (2004) , the modulus of elasticity of plain concrete is calculated from the compressive strength using Equation (4.1),

$$E_c = (3300\sqrt{f_c'} + 6900)(\frac{\gamma_c}{2300})^{1.5} \quad (4.1)$$

where, γ_c = Unit weight of concrete and f'_c = Compressive strength of concrete in MPa.

The comparison between modulus of elasticity values of various concrete mixes and the theoretical values were shown in Figure 4-5. From the results it was found that CSA equation overestimated modulus of elasticity values for all the mixes.

4.4.2 Pullout test results

The influence of the various concrete mixes, steel fibre presence and rebar diameter on the bond behavior is analyzed in this Section. During the pull-out test, the average bond stress at any stage of loading is the recorded pullout load on the bar, P, divided by the nominal surface area of the embedment length L. For a circular bar, this is given by

$$\tau = P/\pi \cdot d_b \cdot l_b \quad (4.2)$$

where, P is the tensile load, d_b = diameter of the bar, l_b= embedment length. The bond stress and the slip between concrete and FRP bar were used to analyze the bond behavior. The summary of the test results are shown in Table 4-5.

4.4.2.1 Effect of rubber content on the bond strength

From the reported results in Table 4-5 it is observed that the bond strength decreases with an increase in the crumb rubber replacement. For the plain concrete and 10mm bar, this reduction is 22%, 60%, 45% and 80% for a corresponding crumb rubber replacement of 25%, 50%, 75% and 100%, respectively. As for the mixes with steel fibre and 10mm bar, the percentage reductions in bond strength are 11%, 38%, 45%, 54% for the corresponding crumb rubber replaement of 25%, 50%, 75%, 100%, respectively. Comparing the data, the reduction is more in the presence of steel fibres. This strength loss is due to the lower density of the concrete mixes with an increase in crumb rubber replacement. The crumb rubber is much lighter when

compared to sand. Hence, more sand replaced by crumb rubber results in lower density. The lower density mixes exert lower resistance against the adhesion and friction between rebar and concrete mixes which yields lower bond strength. Also due to the difference in their stiffness crumb rubber particles deform more than the surrounding cement paste under the load. This results in micro-crack formation which causes weaker bond between rubber and cement paste.

4.4.2.2 Effect of bar diameter on the bond strength

Prior studies have evaluated the effect of bar diameter on the bond strength of GFRP bar in concrete mixes with different ranges of compressive strength (Achillides and Pilakoutas 2004; Baena et al. 2011; Chaallal and Benmokrane 1993a; Cosenza et al. 1997; Nanni et al. 1995; Tepfers 2006; Tighiouart et al. 1998). The results of the current study was shown in Figure 4-6(a) for plain concrete while that with steel fibre reinforced concrete mixes is shown in Figure 4-6(b). The comparative strength reduction in compression is shown is Table 4-6. It can be observed that the bond strength decreases with an increase in the bar size for the concrete mixes without steel fibres. A strength reduction of 4% and 5%, respectively, were observed for mixes with 0% rubber and 25% rubber. But for the mixes with 50%, 75% and 100% replacement with rubber showed 47%, 6% and 47% increase in bond strength with an increase in bar size from 10mm to 16mm. This may be attributed by the fact that the concrete mixes with higher crumb rubber replacement have significantly less compressive strength. Thus surface condition of bars provides the significant portion of bond strength but it was uniformly seen that the 10 mm FRP rebar was smoother than the 16 mm rebar. This is likely due to the difficulty for a given sand particle size to adhere onto the curved surface for a larger curvature as shown in Figure 4-7. In order to quantify sand particles, image analyses of different surface area samples of the reinforcement bars were performed. Appendix IV illustrates the multiple images taken on each of these bars. Based on the average from those images after analysis, the representative images for the 10mm and 16mm bar were shown in Figures 4-8(a) and 4-8(b), respectively. It was found that 10mm bar had 5% (average of three different surface area samples) surface area covered with sand particles whereas for 16mm bar 18% (average of six different surface area samples) surface area were covered with sand particle. The higher percentage of sand grain covered area of FRP bar surface in 16mm diameter also attributed to the higher bond strength in similar mix composition. On the other hand, the mixes with lower crumb rubber replacement

had higher compressive strength. Concrete with higher compressive strength exert significant frictional and adhesion on the rebars. Due to Poisson's effect, the lateral contraction in diameter is more prominent in 16mm bar as compared to 10 mm bar subjected to tensile force. This reduction in diameter leads to reduction in frictional and mechanical interlocking stress and thus bond strength is lower in case of 16mm compared to 10 mm bar.

In the concrete mixes with steel fibre the 16mm bar showed greater bond strength with compare to 10mm bar. The degree to which steel fibres affect the bond wasn't determined yet, but it was observed in a previous study (Ametrano et al. 2011) that the presence of steel fibre might disturb the surface between FRP bar and concrete. The fibre disturbed the surface between smaller diameter bar and concrete to greater extent. The smoother surface of 10mm bar coupled with the disturbance of steel fibre on the contact surface between FRP bar and concrete generate lower bond strength with compared to larger bar size.

Bond behavior of FRP bar with concrete is widely examined by many researchers. Among many other researchers, Chaallal and Benmokrane (1993a) and Baena et al. (2009) has done some pullout tests to analyze the bond behavior of various types of FRP bar and concrete matrices with different compressive strength. Chaallal and Benmokrane (1993a) has tested pullout samples to examine the effect of concrete compressive strength on bond strength, development length and top bar modification factor. Three different bar sizes (12.7, 15.9 and 19.1mm) have been used in that study. Baena et al.(2009) also performed 88 pullout sample various FRP bar and regular steel bar along with two different concrete mixes to examine the effect of concrete compressive strength, bar diameter, FRP bar surface condition on the bod strength. The brief results of those two studies have been presented in Table 4-7.

The compressive strength in the present study varies from 40 MPa (without any crumb rubber) to 7 MPa (with 100% crumb rubber). For the concrete mixes with no rubber content and no steel fibre, the bond strength is 11.6 MPa and 11.13 MPa for 10 mm bar and 16 mm bar, respectively. This is close to the values obtained by Baena et al. (2009) When compared to their data for steel bars, the 16 mm bar in the present study delivers 75% of the bond strength

of steel bar when used in the mix with no rubber content. In case of maximum crumb rubber replacement, this value drops to 11% of the steel bond value.

4.4.2.3 Effect of short steel fibre

The presence of short discrete steel fibre also affects the bond strength between FRP and concrete. The variation of strength due to presence of steel fibre is shown in Figure 4-9(a) and 4-9(b). In case of 10mm bar, it was found that introduction of 1% volume steel fibre reduced the bond strength by 41%, 32%, 9%, and 41% for 0%, 25%, 50% and 75% crumb rubber replacement. And for the 16mm bar, the bond strength reduction was 23%, 46%, 11% and 20% for mixes with 0%, 25%, 50% and 75% crumb rubber replacement, respectively. For both cases of plain concrete and steel fibre reinforced concrete with 100% crumb rubber to fine aggregate content, bond strength was improved by 32% and 20% for 10 mm and 16 mm diameter bar respectively.

The bond response of deformed steel bar and concrete can be characterized with three different stages; i) initial adhesion between concrete and reinforcement, ii) bearing of the ribs against the concrete after breakage of initial bond and finally iii) friction through rebar ribs on the surrounding concrete after peak bond stress, as shown in Figure 4-10. During the second stage, internal cracks occur and propagate due to ribs of rebar. In case of steel fibre reinforced concrete, fibres were found to strengthen the matrix by transmitting substantial amount of tensile force during the slippage of fibres, hence resisting further opening of cracks and carry additional tensile force. Steel fibres also found to keep the crack width small and prevent sudden formation of splitting cracks. Hence, compared to plain concrete, fibres may increase the bond strength by arresting splitting of concrete around the rebar. Studies, performed by Ezeldin and Balaguru (1990), Soroushian et al. (1994) and Hota & Naaman (1997) on the effect of steel fibre reinforced concrete on bond performance, found that fibre reinforced concrete provided greater (20% to 36%) bond strength with compared to plain concrete.

Similar study was performed by Ding et al. (2014) to evaluate bond performance between ribbed GFRP bar and fibre reinforced concrete(short steel fibre and polypropylene fibre). Due

to their splitting crack resisting ability, fibre reinforced concrete was found to increase bond resistance by 14% to 29%.

But for sand coated GFRP bar used in the current study, the bond mechanism is different compared to ribbed GFRP and deformed steel rebar. Various studies (Al-Zahrani et al. 1999; Baena et al. 2009; Cosenza et al. 1997; Makitani et al. 1993; Nanni et al. 1995; Rossetti et al. 1995) were performed to evaluate bond response of sand coated GFRP bar and concrete. It was found that, in the case of sand coated GFRP bar the bond mechanism was primarily the adhesion (initial stage) and then the surface friction between GFRP bar and surrounding concrete (later stage), no mechanical interlocking or bearing on surrounding concrete exist due to absence of prominent surface deformation.

Although many researches were done to evaluate bond properties of sand coated GFRP and normal density concrete, the effect of short steel fibre on the bond between sand coated GFRP bar and lightweight concrete is yet to be examined at large. The present study examined the effect of short steel fibre for all concrete mixes and the two different bar sizes. Unlike steel reinforcement, it was found that steel fibres led to a drop in the bond strength for the present scenario. The predominant stress-transfer mechanism for this type of GFRP bar is thought to be friction. Application of steel fibres created additional interfacial transition zone around those fibres. As a result, frictional mechanism was interfered with (as shown in Figure 4-11) due to fibre presence and thus, the bond strength was reduced compared to plain concrete (Ametrano et al. 2011). This interference is likely more dramatic in case of a smaller bar diameter, due to the smaller available surface.

4.5 Conclusion

In this chapter the interfacial bond between FRP and different kinds of concrete mixes were analyzed. The following conclusion can be drawn:

1. In the presence of crumb rubber, the bond strength between FRP bar and concrete decreases with an increase in the crumb rubber replacement. Higher crumb rubber

replacement produces lower density mixes which exert lower resistance against the adhesion and friction between rebar and concrete mixes which yields lower bond strength. Also due to the difference in their stiffness crumb rubber particles deform more than the surrounding cement paste under the load. This results in micro-crack formation which causes weak bond between rubber and cement paste.

2. The presence of short steel fibres has a negative impact on the bond strength between lightweight concrete and FRP bar. This is likely due to the fibres interfering with the surrounding matrix and thus adversely affecting the friction between the bar and concrete.
3. In most cases, the bond strength with larger bar diameter was higher than that for the smaller diameter except few mix compositions. This was likely due to the combined effect of prominent surface deformation and lower interference in case of the larger bars. For few mixes without steel fibre and 0% and 25% fine aggregate replacement with crumb rubber, smaller bar diameter showed higher bond strength.

4.5.1 Limitations of this study

This study investigated the bond performance between lightweight concrete mixes with crumb rubber as fine aggregate replacement and sand coated GFRP bar using pullout tests. In addition to that, lightweight expanded shale aggregate was used as coarse aggregate. Crumb rubber was used as fine aggregate replacement. No replacement of coarse aggregate with rubber particles was considered in this study. Again, among various supplementary cementitious materials, only silica fume was used as supplementary cementitious material. Effect of fibre presence in concrete mixes was performed using steel fibres only. Besides steel fibres, there are other types of fibres available; synthetic fibres, glass fibres, asbestos fibres, natural fibres etc. which weren't employed in this study. The result suggest that low modulus fibres such as polypropylene macro fibres might be better suited with low strength and low modulus concrete. The effect of bar size on bond strength was investigated with only two bar sizes (10 mm and 16 mm). These two bar sizes were selected for their frequent use in structures. Due to test set up limitation, larger than 16 mm bar sizes couldn't be tested in this study. Bond performance with other bar sizes would enrich the current database of bond performance between

lightweight concrete and GFRP bars. Moreover, researches can be done on other GFRP bars with different surface configuration as well as other types of FRP bar itself.

Tables

Table 4-1: Mix Proportions of various concrete mixes

Mix[a]	Water-binder ratio	OPC (kg/m^3)	Silica Fume (kg/m^3)	Gravel (Kg/m^3)	Sand (kg/m^3)	Crumb Rubber% (fine aggr. replacement)	Crumb Rubber (kg/m^3)
CR0F0	0.4	495	55	986	640	0	0
CR25F0	0.4	495	55	986	480	25	51
CR50F0	0.4	495	55	986	320	50	102
CR75F0	0.4	495	55	986	160	75	153
CR100F0	0.4	495	55	986	0	100	204
CR0F1	0.4	495	55	986	640	0	0
CR25F1	0.4	495	55	986	480	25	51
CR50F1	0.4	495	55	986	320	50	102
CR75F1	0.4	495	55	986	160	75	153
CR100F1	0.4	495	55	986	0	100	204

Table 4-2: Properties of GFRP bars

US Size	Glass Content, % weight	Nominal Size	Cross Sectional Area	Ultimate tensile strength	Guaranteed Design Tensile Strength	Modulus of Elasticity	Ultimate elongation
		mm	mm^2	MPa	MPa	GPa	%
#3	78.5	10	75.7	1054	930	45.4	2.41
#5	78.1	16	212.8	981	896	44.1	2.45

Table 4-3: Mix combination under investigation

Concrete Mixes	Bar Sizes (mm)	
CR0F0	10	16
CR25F0	10	16
CR50F0	10	16
CR75F0	10	16
CR100F0	10	16
CR0F1	10	16
CR25F1	10	16
CR50F1	10	16
CR75F1	10	16
CR100F1	10	16

Table 4-4: Compressive strength

Concrete Mixes	$f'c$(MPa)	CoV
CR0F0	37	0.16
CR25F0	22	0.14
CR50F0	15	0.04
CR75F0	10	0.09
CR100F0	8	0.01
CR0F1	44	0.02
CR25F1	32	0.03
CR50F1	20	0.13
CR75F1	15	0.02
CR100F1	11	0.10

Table 4-5: Bond Test Result

Specimen	$f'c$ (MPa)	10mm Bond Strength, τ_m (MPa)	10mm CoV	16mm Bond Strength, τ_m (MPa)	16mm CoV
CR0F0	37	11.60	0.58	11.13	0.25
CR25F0	22	8.99	0.13	8.54	0.05
CR50F0	15	4.65	0.33	6.85	0.27
CR75F0	10	6.31	0.15	6.67	0.02
CR100F0	8	2.34	0.14	3.45	0.19
CR0F1	44	6.82	0.07	8.52	0.08
CR25F1	32	6.08	0.21	4.57	0.18
CR50F1	20	4.21	0.05	6.03	0.33
CR75F1	15	3.74	0.21	5.29	0.06
CR100F1	11	3.10	0.19	4.13	0.06

Table 4-6: Change in strength for different bar sizes

	Bond strength, MPa		
Specimen	10 mm	16 mm	Change in strength in 16 mm compared to 10 mm bar
CR0F0	11.60	11.13	4.1
CR25F0	8.99	8.54	4.9
CR50F0	4.65	6.85	-47.3
CR75F0	6.31	6.67	-5.7
CR100F0	2.34	3.45	-47.1
CR0F1	6.82	8.52	-25.0
CR25F1	6.08	4.57	24.9
CR50F1	4.21	6.03	-43.2
CR75F1	3.74	5.29	-41.7
CR100F1	3.10	4.13	-33.2

'+' denotes reduction and '-'denotes increase in strength

Table 4-7: Bond test values on FRP and steel bars from previous researches

Different Studies		Bond Strength, MPa			
Challal and Bemrokane [1993]		$f'c$ = 31MPa,		$f'c$ = 79MPa,	
	Bar Dia	FRP bar	Steel bar	FRP bar	Steel Bar
	12.7mm	15	18	15.8	30
	15.9mm	12.5		15	

Baena et. al [2009]		$f'c$ = 28.63 MPa		$f'c$ = 52.19MPa	
	Bar Dia	FRP bar	Steel	FRP bar	Steel
	#3 or 10.22mm	11.2	~	16.31	29.1
	#5 or 16.44mm	12.1	15.28	22.13	26.26

Figures

Figure 4-1: Test setup for quasi static compression testing

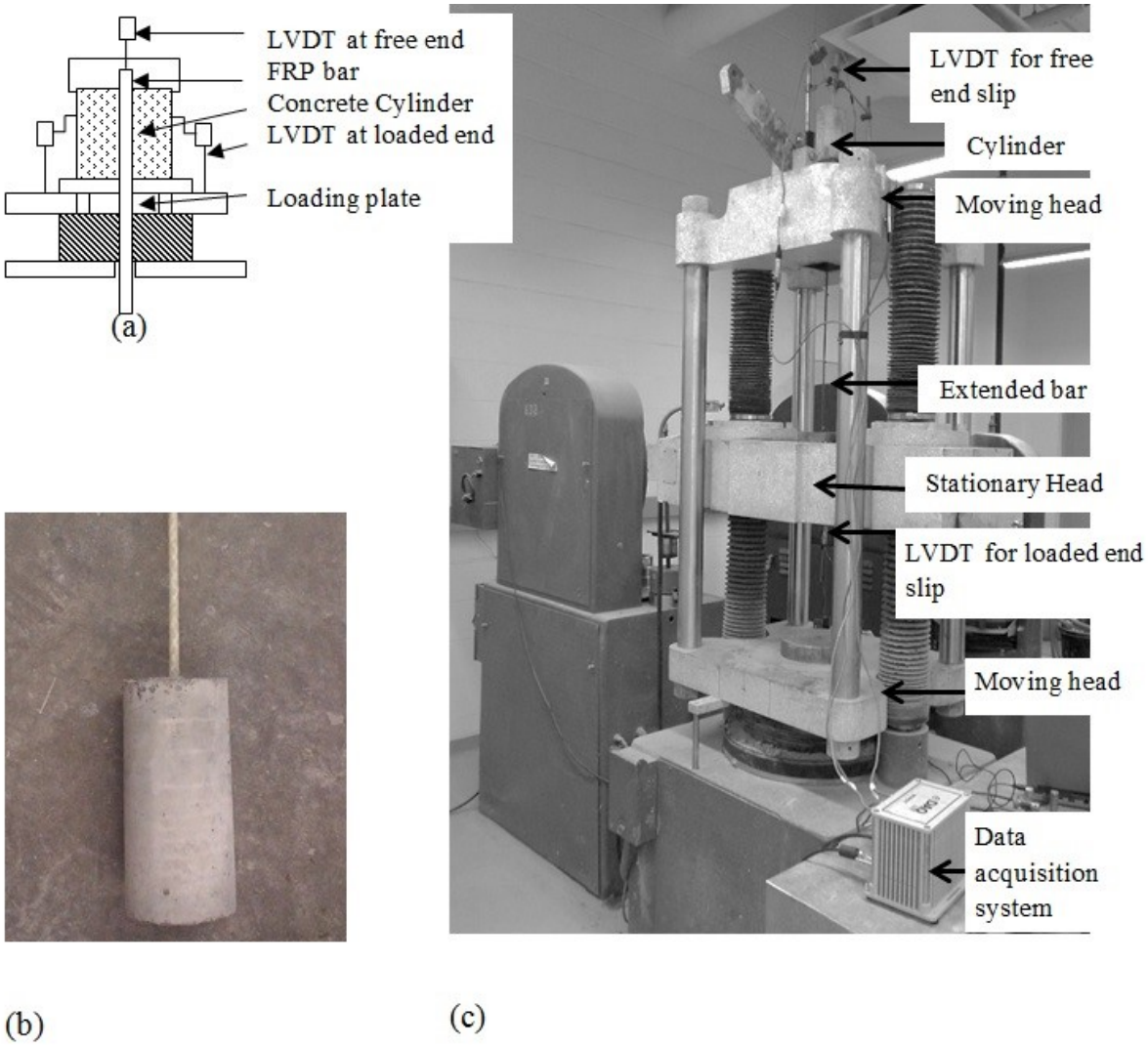

Figure 4-2: Test setup (a) schematic diagram showing instrumentation on pullout test sample, (b) pullout test specimen, (c) pullout test in progress

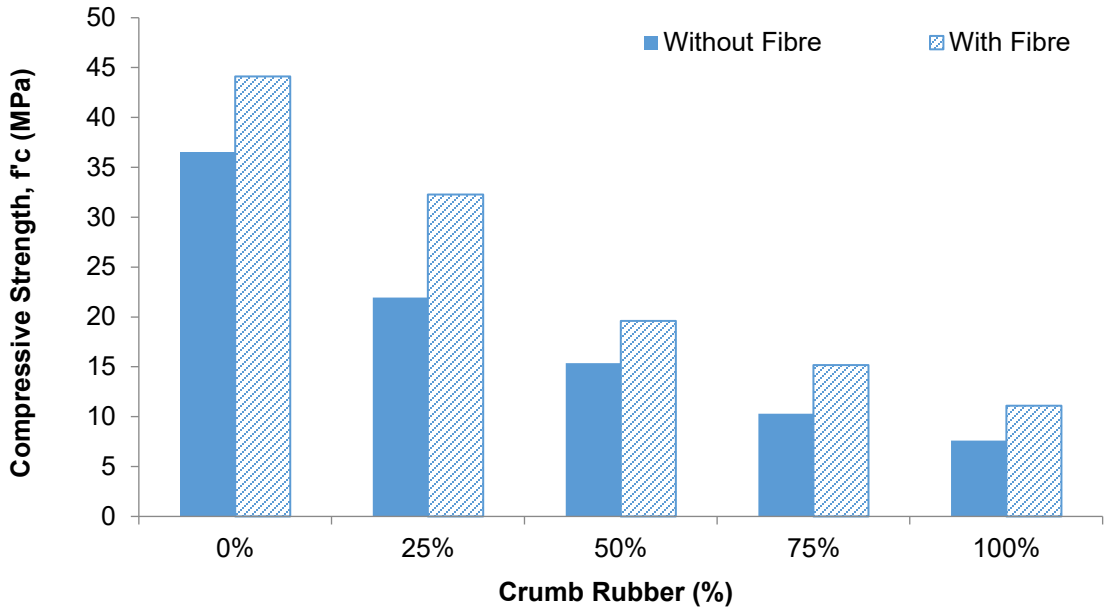

Figure 4-3: Variation in compressive strength with crumb rubber replacement

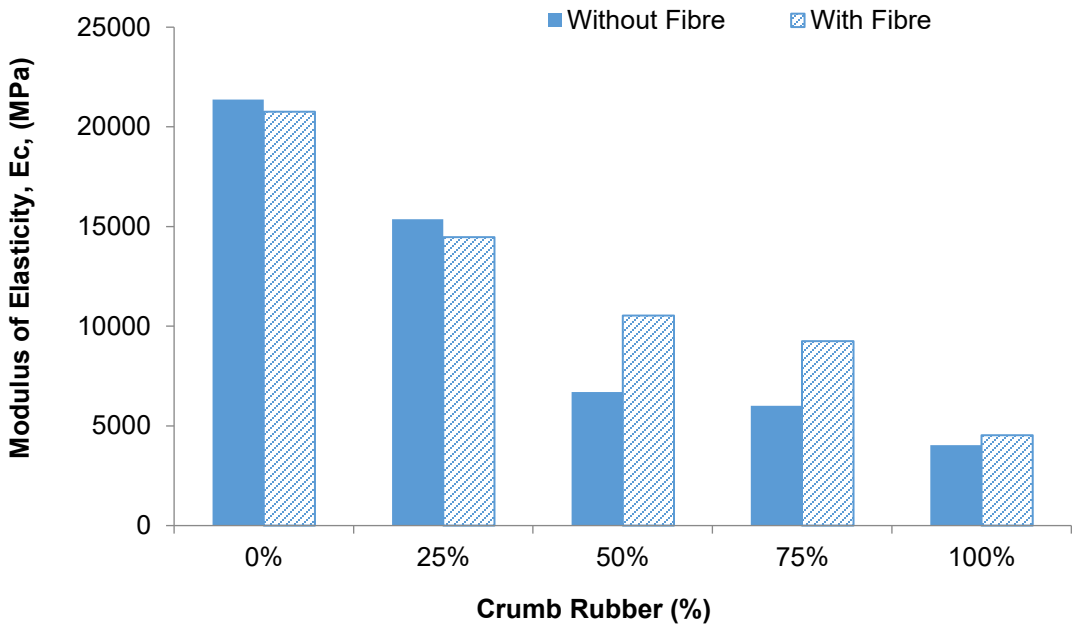

Figure 4-4: Variation of modulus of elasticity with crumb rubber replacement

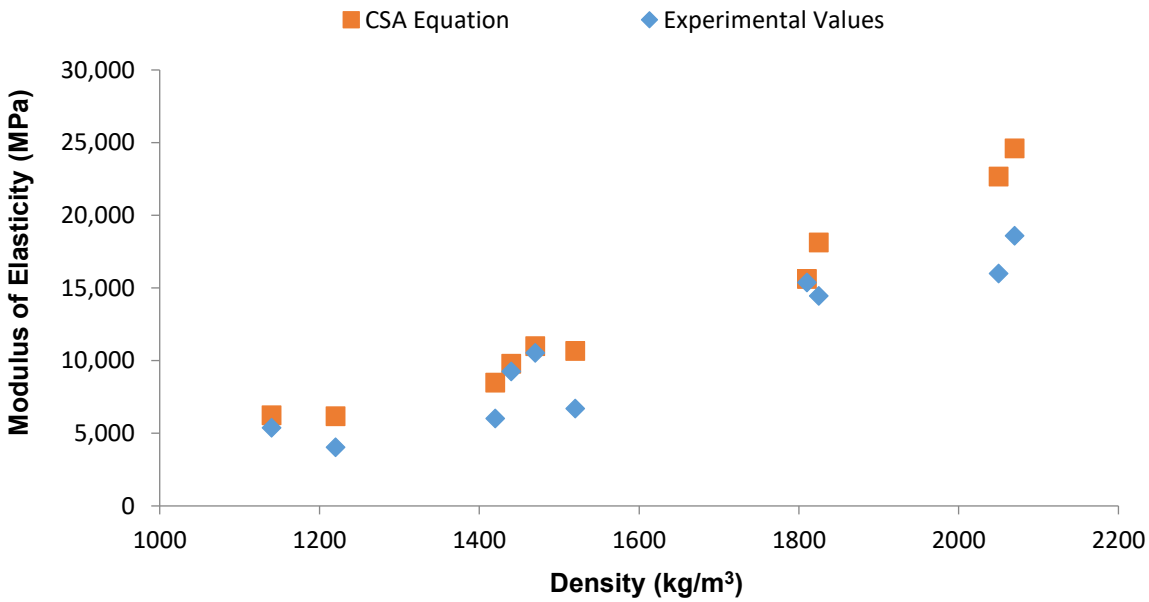

Figure 4-5: Comparison of Modulus of Elasticity with CSA Equation

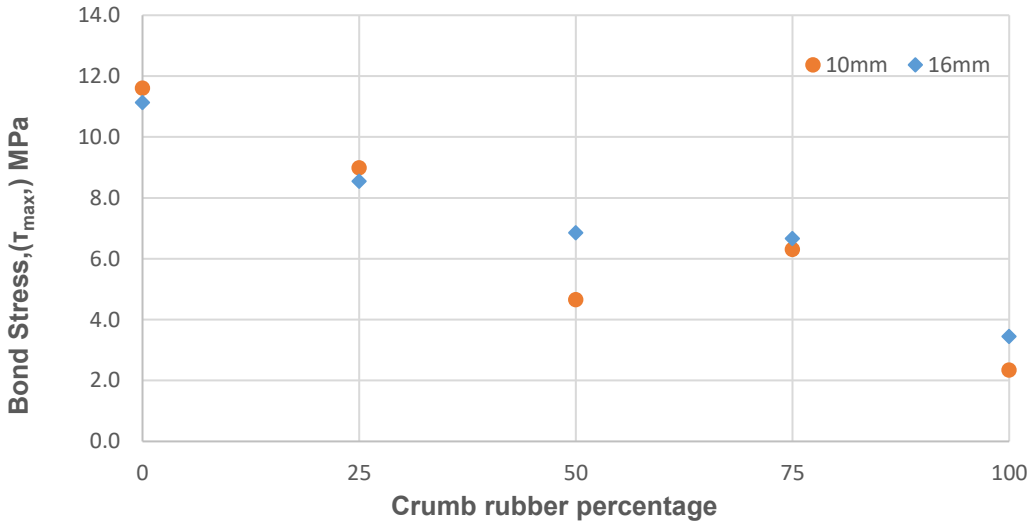

(a)

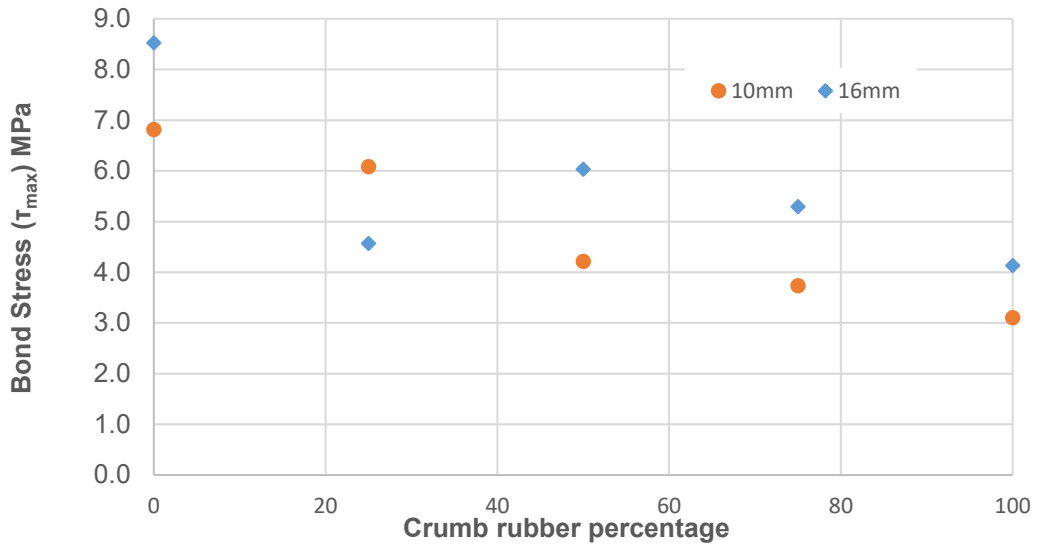

(b)

Figure 4-6: Variation of bond strength for mixes (a) plain concrete; (b) with steel fibre

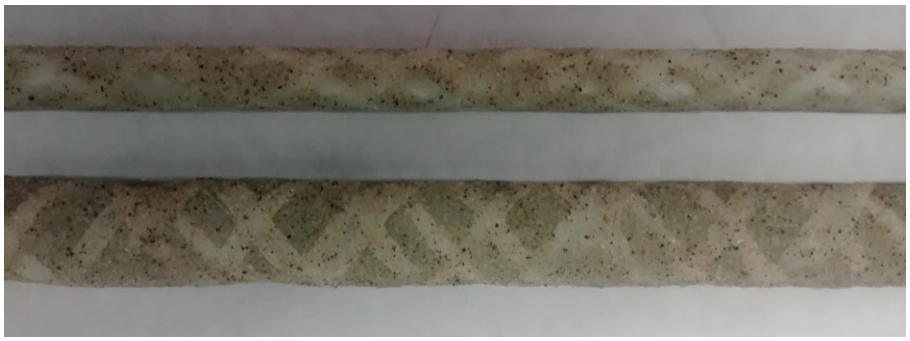

Figure 4-7: Surface condition on bars of different diameter

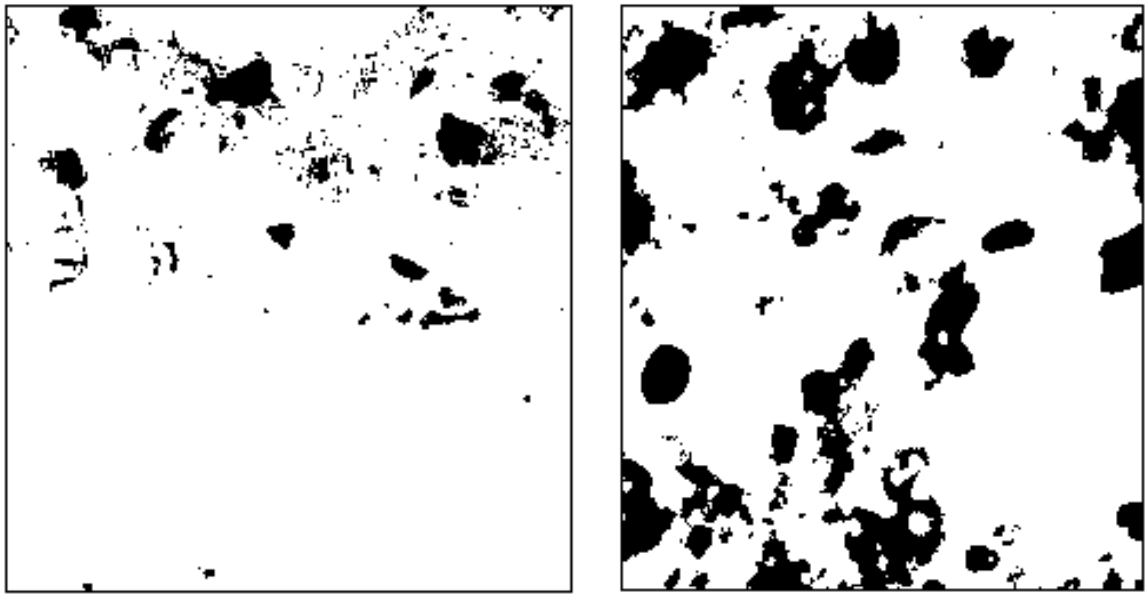

(a) 10 mm diameter bar (b) 16 mm diameter bar

Figure 4-8: Comparative image analysis results for different bar sizes (dark area represents sand particles whereas white area represents the surface of FRP bar)

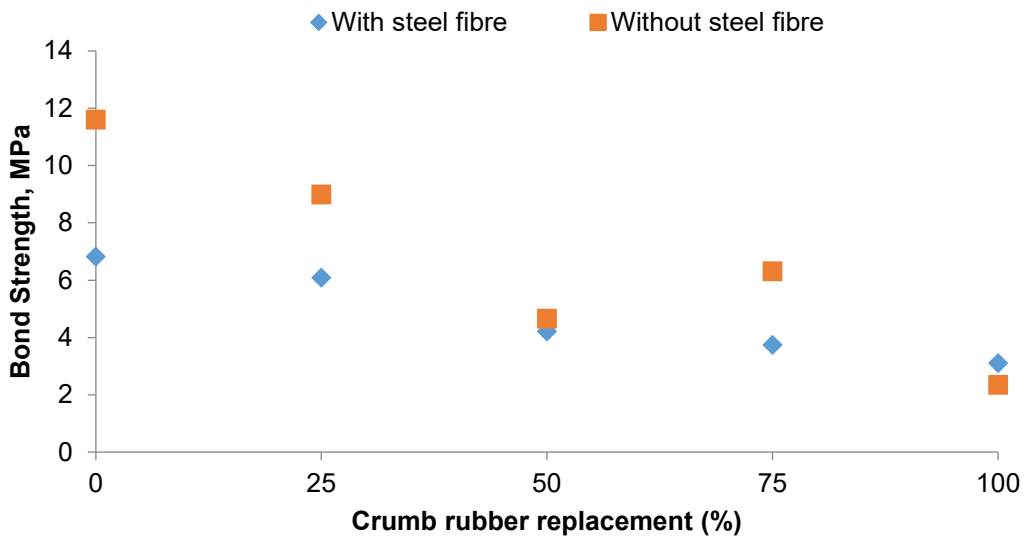

(a)

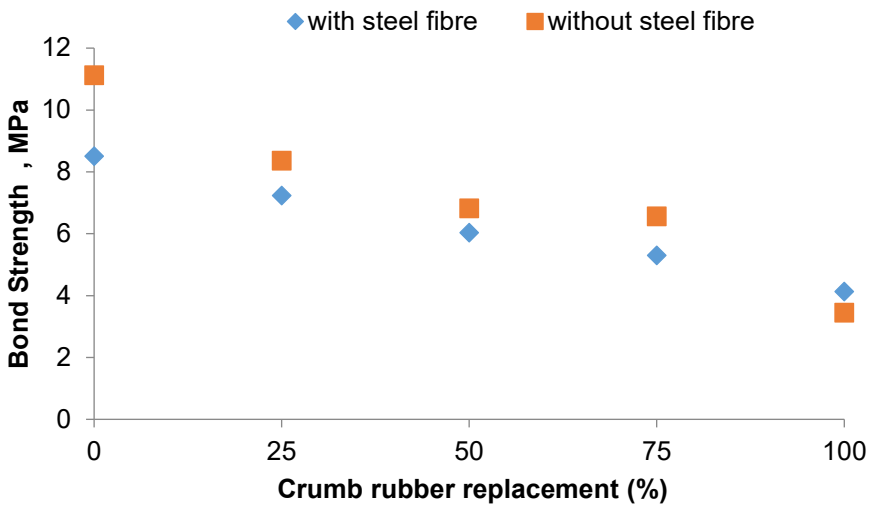

(b)

Figure 4-9: Bond strength variation of (a) 10mm bar; (b) 16mm bar

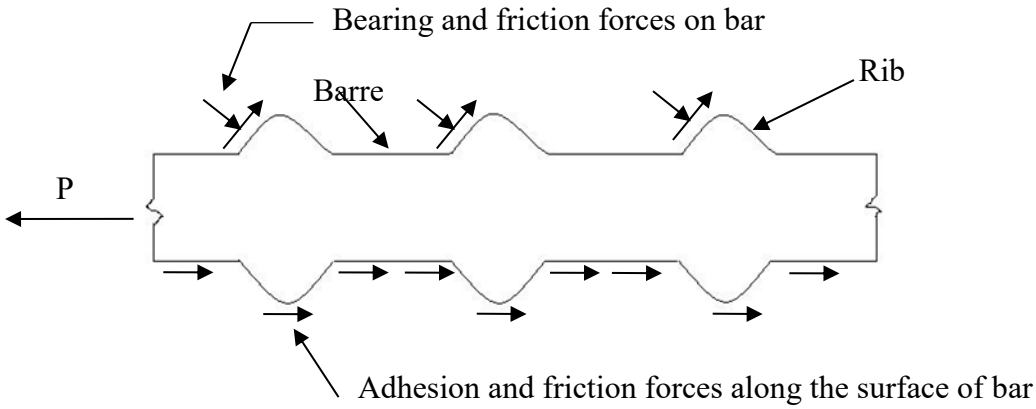

Figure 4-10: Bond mechanism of steel bar in concrete

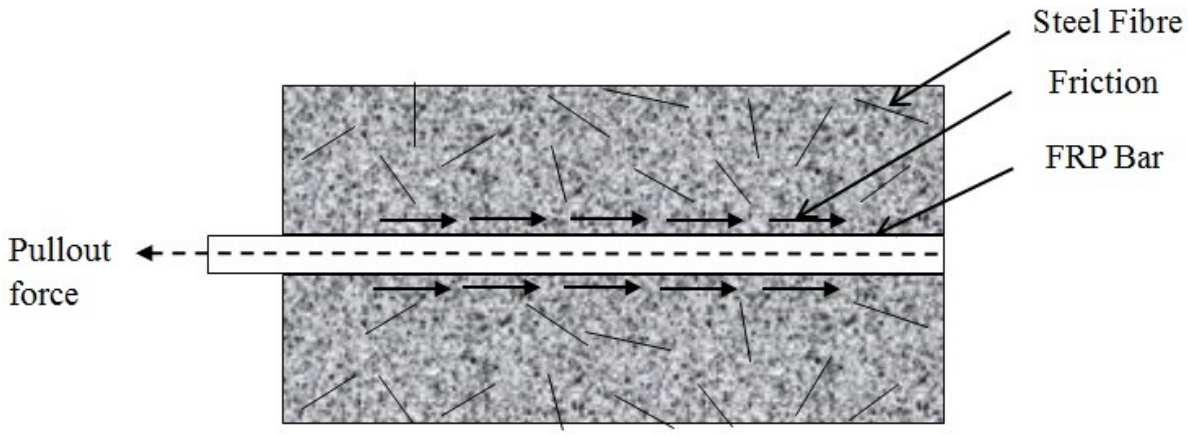

Figure 4-11: Pullout failure pattern of GFRP bar in concrete matrix with steel fibre

References

Achillides, Z., and Pilakoutas, K. (2004). "Bond behavior of fiber reinforced polymer bars under direct pullout conditions." *Journal of Composites for construction*, 8, 173.

Al-Zahrani, M. M., Al-Dulaijan, S. U., Nanni, A., Bakis, C. E., and Boothby, T. E. (1999). "Evaluation of bond using FRP rods with axisymmetric deformations." *Construction and Building Materials*, 13(6), 299–309.

Ametrano, D. (2011). "Bond characteristics of glass fibre reinforced polymer bars embedded in high performance and ultra-high performance concrete." *Ryerson University, Toronto, Ontario, Canada*, 1–132.

Ametrano, D., Hossain, K. M. A., and Lachemi, M. (2011). "Bond characteristics of glass fibre reinforced polymer bars embedded in high strength and ultra-high strength comcrete." *2nd International Engineering Mechanics and Materials Speciality Conference*, Ottawa, Ontario.

ASTM C469. (2010). *Test Method for Static Modulus of Elasticity and Poissons Ratio of Concrete in Compression ASTM C469*. ASTM International, West Conshohocken, PA.

Baena, M., Torres, L., Turon, A., and Barris, C. (2009). "Experimental study of bond behaviour between concrete and FRP bars using a pull-out test." *Composites Part B: Engineering*, 40(8), 784–797.

Baena, M., Turon, A., Torres, L., and Miàs, C. (2011). "Experimental study and code predictions of fibre reinforced polymer reinforced concrete (FRP RC) tensile members." *Composite Structures*, 93(10), 2511–2520.

Balaguru, P. N., and Shah, S. P. (1992). *FIBER-REINFORCED CEMENT COMPOSITES*.

Banthia, N., Yan, C., and Sakai, K. (1998). "Impact resistance of fiber reinforced concrete at subnormal temperatures." *Cement and Concrete Composites*, 20(5), 393–404.

Benmokrane, B., Tighiouart, B., and Chaallal, O. (1996). "Bond strength and load distribution of composite GFRP reinforcing bars in concrete." *ACI Materials Journal*, 93(3).

Bentur, A., and Mindess, S. (2006). *Fibre Reinforced Cementitious Composites, Second Edition*. CRC Press.

Chaallal, O., and Benmokrane, B. (1993). “Pullout and bond of glass-fibre rods embedded in concrete and cement grout.” *Materials and structures*, 26(3), 167–175.

Cosenza, E., Manfredi, G., and Realfonzo, R. (1997). “Behavior and modeling of bond of FRP rebars to concrete.” *Journal of composites for construction*, 1(2), 40–51.

CSA A23.3-04. (2004). “Design of Concrete Structures.” Canadian Standards Association, Mississauga, ON.

CSA A3001. (2009). “Cementitious materials compendium.” Canadian Standards Association, Mississauga, ON.

Delage, P., and Aitcin, P. C. (1983). “Influence of condensed silica fume on the pore-size distribution of concretes.” *Industrial & Engineering Chemistry Product Research and Development*, 22(2), 286–290.

Detwiler, R. J., and Mehta, P. K. (1989). “Chemical and Physical Effects of Silica Fume on the Mechanical Behavior of Concrete.” *Materials Journal*, 86(6), 609–614.

Ding, J.-T., and Li, Z. (2002). “Effects of metakaolin and silica fume on properties of concrete.” *ACI Materials Journal*, 99(4), 393–398.

Ding, Y., Ning, X., Zhang, Y., Pacheco-Torgal, F., and Aguiar, J. B. (2014). “Fibres for enhancing of the bond capacity between GFRP rebar and concrete.” *Construction and Building Materials*, 51, 303–312.

Duval, R., and Kadri, E. H. (1998). “Influence of Silica Fume on the Workability and the Compressive Strength of High-Performance Concretes.” *Cement and Concrete Research*, 28(4), 533–547.

Eldin, N., and Senouci, A. (1993). “Rubber-Tire Particles as Concrete Aggregate.” *Journal of Materials in Civil Engineering*, 5(4), 478–496.

Ezeldin, A. S., and Balaguru, P. N. (1990). “Characterization of bond between fiber concrete and reinforcing bars using nonlinear finite element analysis.” *Computers & Structures*, 37(4), 569–584.

Güneyisi, E., Gesoğlu, M., and Özturan, T. (2004). "Properties of rubberized concretes containing silica fume." *Cement and Concrete Research*, 34(12), 2309–2317.

Hooton, R. D. (1993). "Influence of Silica Fume Replacement of Cement on Physical Properties and Resistance to Sulfate Attack, Freezing and Thawing, and Alkali-Silica Reactivity." *Materials Journal*, 90(2), 143–151.

Hota, S., and Naaman, A. E. (1997). "Bond stress-slip response of reinforcing bars embedded in FRC matrices under monotonic and cyclic loading." *ACI Structural Journal*, 94(5).

Khatib, Z., and Bayomy, F. (2013). "Rubberized Portland Cement Concrete." *Journal of Materials in Civil Engineering*, 11(3), 206–213.

Makitani, E., Irisawa, I., and Nishiura, N. (1993). "Investigation of Bond in Concrete Member With Fiber Reinforced Plastic Bars." *Special Publication*, 138, 315–332.

Malvar, L. J. (1994). *Bond Stress-Slip Characteristics of FRP Rebars.* Office of Naval Research, naval Cailities Engineering Service Center, port Hueneme, California.

Mehta, P. K. (1983). "Pozzolanic and Cementitious Byproducts as Mineral Admixtures for Concrete - A Critical Review." *Special Publication*, 79, 1–46.

Mehta, P. K., and Gjørv, O. E. (1982). "Properties of portland cement concrete containing fly ash and condensed silica-fume." *Cement and Concrete Research*, 12(5), 587–595.

Mufti, A. A., Bentur, A., and Banthia, N. (1998). *Fiber reinforced concrete: present and future*. Canadian Society for Civil Engineering, Montreal.

Najim, K. B., and Hall, M. R. (2012). "Mechanical and dynamic properties of self-compacting crumb rubber modified concrete." *Construction and Building materials*, 27(1), 521–530.

Nanni, A., Al-Zaharani, M. M., Al-Dulaijan, S. U., and Bakis, C. E. (1995). "Bond of FRP reinforcement to concrete - Experimental results." Non-metallic (FRP) reinforcement for concrete structures, L. Taerwe, ed., Spon, 135–145.

Nanni, A., Nenninger, J. S., Ash, K. D., and Liu, J. (1997). "Experimental bond behavior of hybrid rods for concrete reinforcement." *Structural Engineering and Mechanics*, 5(4), 339–354.

Rossetti, V. A., Galeota, D., and Giammatteo, M. M. (1995). "Local bond stress-slip relationships of glass fibre reinforced plastic bars embedded in concrete." *Materials and Structures*, 28(6), 340–344.

Soroushian, P., Mirza, F., and Alhozaimy, A. (1994). "Bond of confined steel fiber reinforced concrete to deformed bars." *ACI Materials Journal*, 91(2).

Tepfers, R. (2006). "Bond clause proposals for FRP bars/rods in concrete based on CEB/FIP Model Code 90. Part 1: Design bond stress for FRP reinforcing bars." *Structural Concrete*, 7(2), 47–55.

Tighiouart, B., Benmokrane, B., and Gao, D. (1998). "Investigation of bond in concrete member with fibre reinforced polymer (FRP) bars." *Construction and Building Materials*, 12(8), 453–462.

Topçu, lker B., and Avcular, N. (1997). "Analysis of rubberized concrete as a composite material." *Cement and Concrete Research*, 27(8), 1135–1139.

Topçu, I. B. (1995). "The properties of rubberized concretes." *Cement and Concrete Research*, 25(2), 304–310.

Yan, C. (1992). "Bond between reinforcing bars and concrete under impact loading." PhD Thesis, University of British Columbia, Vancouver, Canada.

Zheng, L., Huo, X. S., and Yuan, Y. (2008). "Strength, Modulus of Elasticity, and Brittleness Index of Rubberized Concrete." *Journal of Materials in Civil Engineering*, 20(11), 692–699.

Notations

$LVDT$ = Linear variable Displacement Transducer

E_c = Modulus of Elasticity of concrete

f'_c = Compressive strength of concrete

γ_c = Density of concrete

CoV = Coefficient of Variation

P = tensile load in reinforcement bar during pullout test,

d_b = diameter of the bar,

l_b = embedment length

Appendix -IV

Figure IV-1: Sample image analysis of FRP bar surface (16 mm)

(1)

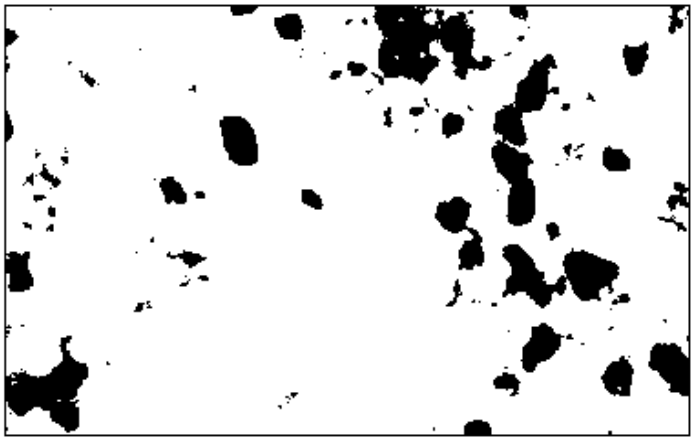

(2)

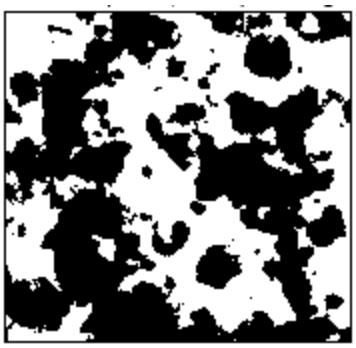

(3)

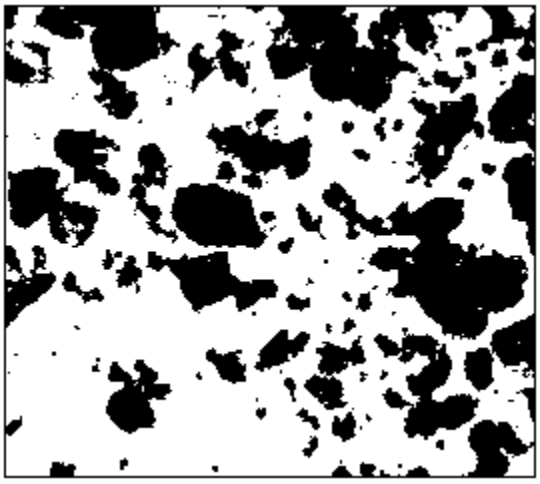

(4)

Figure IV-2: Sample image analysis of FRP bar surface (10 mm)

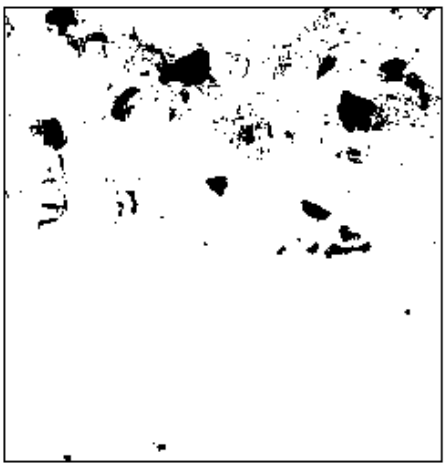

(1)

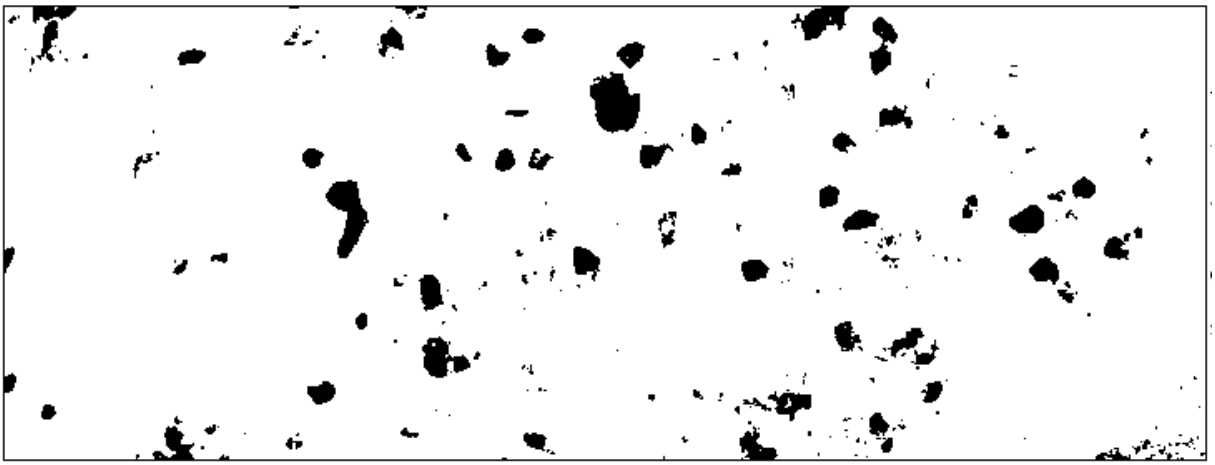

(2)

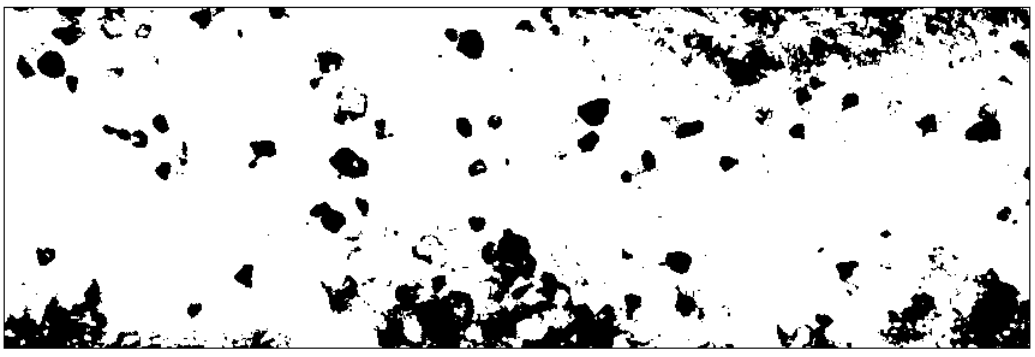

(3)

CHAPTER 5. BOND-SLIP ANALYTICAL MODEL FOR FRP AND CONCRETE WITH CRUMB RUBBER

5.1 Introduction

The use of steel bars as reinforcement for concrete has many advantages but also some disadvantages: in particular the possibility of corrosion which can eventually lead to the total collapse of structures. In some cases the magnetic properties of steel causes malfunctioning to the automatic toll systems and through-way stations. The use of fibre reinforced polymer as reinforcement in concrete structures in considered being a possible alternative to steel in those situations. However, unlike steel, there is no specific guideline about the surface characteristics of FRP bars. Hence, determining the bond characteristics of non-standardized commercial rebars with concrete is a fundamental requirement for their practical use because the bond characteristics influences load transfer mechanism between rebar and concrete.

The mechanics of bond stress transfer between FRP reinforcement and concrete has been investigated by many researchers (Baena et al. 2009; Benmokrane et al. 1996; Chaallal and Benmokrane 1993a; Larralde and Silva-Rodriguez 1993; Makitani et al. 1993; Malvar 1994). The influence of rebar type, embedment length and cross-sectional shape, among others were examined and presented in Achillides and Pilakoutas (2004). From the various researches it was found that the pull-out mechanism of many existing types FRP bar types differed from that of deformed steel bars and was dependent on even more parameters (Chaallal and Benmokrane 1993a; Tepfers 2006). For rebars with a smooth surface, the effect of concrete mechanical properties appeared to be negligible; the bond behavior was therefore solely dependent on the type of discrete fibres and concrete matrix (Nanni et al. 1995). From various studies there is a general trend for larger rebar diameters to have lower bond strengths (Achillides and Pilakoutas 2004; Benmokrane et al. 1996; Cosenza et al. 1995; Nanni et al. 1995; Tighiouart et al. 1998).

Many studies have been conducted to investigate the bond behavior of glass fibre reinforced polymer (GFRP) rebars in plain concrete. The summary of these researches have been

presented by Cosenza (1997) where it was found that FRP smooth rods are inadequate for use in reinforced concrete structures due to very low values of bond strength. Instead, sand-covered continuous fibre rebars show better bond strength compared to smooth bars.

In addition to that, several attempts have been made to establish analytical models to predict the interfacial bond performance of FRP bars in concrete. Malvar (1994) developed a bond model of FRP bar by introducing two empirical constants whose values are dependent on the rebar type. Eligehausen (1982) developed the now well-known Bertero-Popov-Eligehausen (BPE) analytical law for deformed steel and concrete and it was applied for FRP rebars by Cosenza (1995) and Rossetti (1995). Due to lack of softening branch in the model by Eligehausen (1982), Cosenza (1995) proposed an alternative model that modified the softening branch of the BPE model with the introduction of two new parameters. Cosenza (1995) also proposed another fresh model for the ascending branch of bond-slip curve which is now known as the Cosenza-Manfredi-Realfonzo (CMR) model. Note that serviceability is the key issue for most such structures implying that the model is concerned with small value of slip. Some other researchers attempted to calibrate these analytical model for various parameters related to concrete properties, different FRP type and for various positon in casting (Aiello et al. 2007; Baena et al. 2009; Cosenza et al. 1995, 1997; Focacci et al. 2000; Pecce et al. 2001).

5.2 Objective

In this study the bond results of 10 different concrete mixes with two different bar sizes were examined. For each bar size and concrete mix, three samples were prepared. The results of 60 pullout tests are presented with the aim to enhance the experimental database and investigate the bond behavior between lightweight concrete and GFRP bar. The material characterizations of those aforementioned concrete mixes were conducted in Chapter 3. Bond behavior was analyzed for different types of concrete mixes where crumb rubber was used to replace fine aggregate at various percentages, small steel fibres are used in varying dosage, and for different GFRP bar sizes. The pullout tests results and the effect of various parameters were elaborated in Chapter 4. This chapter focused mainly on the empirical calibration of bond performance

between lightweight concrete mixes and sand coated GFRP bars for the Modified Bertero-Popov-Eligehausen- (mBPE) and the Cosenza-Manfredi-Realfonzo (CMR).

5.3 Experimental method

The following parameters were examined to characterize their influence on the bond behavior;

- Effect of density and compressive strength;
- Short discreet fibre effect
- Size effect of reinforcement bars

5.3.1 Materials

5.3.1.1 Concrete mix proportion

The concrete mixes were prepared by the CSA A3001-09 (2009) Type GU ordinary Portland cement (OPC). In addition to that, supplementary cementitious material (silica fume) was incorporated at 10% mass replacement of OPC. A 10mm downgraded expanded shale aggregate was used as coarse aggregate. Locally available river sand were used as fine aggregate. The mix proportions of the concrete mixes with crumb rubber are normally kept the same except for the replacement of fine aggregate with crumb rubber, depending upon the desired crumb rubber percentage. The crumb rubber percentage is defined as the volume ratio of crumb rubber to the total fine aggregate in the concrete mixture and depending upon the selected replacement percentage. The crumb rubber was manufactured from recycled motor vehicle tires and purchased from a local recycling company. Three different size ranges (0.85mm to 3.35mm) of crumb rubber were blended for the mix. The following five combinations of sand and crumb rubber were adopted in this research: 100% sand (CR0), 75% sand + 25% crumb rubber (CR25), 50% sand+50% crumb rubber (CR50), 25% sand + 75% crumb rubber (CR75), 100% crumb rubber (CR100). To evaluate the effect of steel fibre, hooked-end steel fibres of 35 mm in length with aspect ratio of 65 and yield strength of 1100 MPa were employed at 1% volume fraction. This means five mixes of plain concrete and five other mixes have 1% volume fraction of short steel fibre. High range water reducing admixture was incorporated to achieve required workability. The Table 5-1 shows the detail mix

composition used in this study. The concrete for the pullout specimens was prepared in the laboratory. The mean compressive strength of each concrete composition was determined from three control cylindrical samples (100mm x 200mm). The compressive strength, modulus of elasticity, flexural strength and fracture toughness values for all the concrete mixes were determined in Chapter 3.

5.3.1.2 Glass fiber reinforced polymer bar (GFRP Bar)

Nowadays there are various GFRP bar manufacturing companies in the country. For our study TUF-BAR^{TM} GFRP bars were used which were produced by a local manufacturer. The surface of the GFRP bars were sand coated. Properties of GFRP bars are provided in Table 5-2.

5.4 Pullout specimens

The pullout tests were carried out by using cylindrical specimens of 100 mm in diameter and 200 mm in length. Cylindrical pullout specimens are widely used to evaluate the bond performance of various rebar and concrete mix for their ease of fabrication and the simplicity of the test. The stress fields in cylindrical pull out specimens do not realistically simulate the stress condition in actual structural member. However, pullout tests provide a simple means of comparing normalized bond behavior.

The pullout specimens are cast in vertical position using steel moulds. The bars are placed concentrically to the cylindrical moulds. During casting and subsequent compaction the FRP bars were kept straight using specially designed steel fixture. To prevent the rupture of FRP bar and to make sure the pullout failure of the rebar, the embedment length was kept five times the diameter of the bar. Contact between concrete and rebar along the debonded length was disrupted using a coaxially placed soft poly vinyl chloride tube as shown in Figure 5-1.
Concrete was mixed in the laboratory using a drum mixer, poured into moulds and compacted using the vibrating rod. To prevent excessive evaporation the specimens were covered with plastic wrap after casting. The samples were demolded after 24 hours and then stored into a moist room at a temperature of 20±2^{o}c and a humidity of 99% for curing for at least 28 days before testing.

In order to ensure the repeatability of the tests, three specimens were cast for each mix composition investigation. The following protocol was adopted for the specimens ID's: the alphabets "CR" in the first place holder represents crumb rubber and the numeral in the second place holder represents the aggregate replacement percentage, the alphabet in the third place holder stands for short steel fibre and the following numeral represents the percentage volume fraction of fibres in the concrete mix. Typical specimen identification was shown in Figure 5-2.

5.5 Pullout test setup

The pullout tests were performed in a MTS Machine. The schematic illustration of the test setup is shown in Figure 5-3(a) and a typical pullout sample was shown in Figure 5-3(b). The actual test in progress was presented in Figure 5-3(c). During loading the pullout samples were rested on top of the moving head. The FRP bars were extended beyond the stationary head so that the bar can be gripped. During the loading the stationary head gripped the rebar firmly and the moving head is moved upward. As a result the pullout specimen was pressed against the top of moving head. A thin sheet of softwood and hard rubber pad was placed in between pullout samples and the moving head to ensure uniform contact. The load was applied with displacement control at a rate of 2 mm/min. When the moving head moved upward, the rebar was in tension and the resulting pullout force was measured using an electronic data acquisition (eDAQ) system. The loaded end slip was measured with the help of LVDT 1 and the slip at the free/unloaded end was measured with the help of LVDT 2 and 3. All the output of LVDTs was recorded in the eDAQ. The pullout test were terminated when either of the following conditions occurred: (i) pull-through or rupture of the rebar, (ii) splitting of concrete enclosing the rebar

5.6 Results and discussion

The influence of crumb rubber replacement percentage, presence of short steel fibre and bar diameter on the bond performance is described here. In the pull-out test, the average bond

stress at any stage of loading is the recorded pullout load on the bar, P divided by the nominal surface area of the embedment length L. For a circular bar, this is given by

$$\tau = P/\pi \cdot d_b \cdot l_b \quad (5.1)$$

Where P is the tensile load, d_b is the rebar diameter and l_b is the embedment length (which is 5 times diameter of the bar). The relationship between maximum bond stress from the Equation (5.1) and the slip between concrete and FRP bars was used to describe the bond behavior.

The experimental results obtained from the pullout tests and the slip values of loaded and unloaded ends for 10 mm and 16mm bar size were presented in Table 5-3 and 5-4 respectively. In these tables, $f'c$ is the concrete compressive strength of concrete mix, τ_{max} is the bond strength, $s_{m,ue}$ is the unloaded end slip at τ_{max}, $s_{m,le}$ is the loaded end slip at τ_{max}. A normalized bond strength (τ^*_{max}) that accounts for the effect of the concrete strength is defined by

$$\tau^*_{max} = \frac{\tau_{max}}{\sqrt{f'c}} \quad (5.2)$$

The global behavior of bond-slip response in characterized by an initial increase in bond stress with little slippage, followed by softening once the bond stress in reached. After reaching maximum bond stress the bond attributed from the friction between rebar and concrete. Typical measured bond-slip responses for each tested diameters are presented in Figure 5-4 and 5-5.

The bond behavior can be explained by the phases described below. In almost all cases, initially a good bond performance with high bond strength is observed where bond-slip behavior ascends nearly linear upto about 80-90% of the maximum load with relatively small unloaded end slip. Sand coating increases the mechanical bond and adhesion (Chaallal and Benmokrane 1993a; Nanni et al. 1995). The load transfer is provided by friction and chemical adhesion in addition to the confinement action of surround concrete. The initial stiffness of the bond-slip behavior is dependent on the concrete strength for all bar sizes and for all concrete mix types. From the figures it was evident that the initial stiffness was lower with increase in crumb rubber replacement percentage, which implied lower concrete compressive strength.

After reaching the bond strength the softening behavior was initiated. This softening behavior signifies the breakdown of bond strength and development of non-recoverable slip. For all bar sizes and concrete mixes this softening behavior was prominent, though their pattern varies for different bar sizes and concrete mixes. In this descending branch of the bond-slip relationship a continuous decrease in bond resistance with rapid increase of slip was observed followed by a horizontal branch which demonstrated the residual bond strength. The tests were terminated as soon as pullout bond failure took place. No signs of splitting of concrete were observed in any of the pullout specimens.

Most of the bond failure in this investigation was not characterized by complete pullout of the embedded bar from concrete cylinders. Instead, the pullout failure was identified on the basis of the large slip values in the range of 8 to 15mm of loaded end slip.

For both 10mm and 16mm bar and concrete mixes without short steel fibre, there wasn't any sudden bond strength drop, rather it gradually decreased up to certain value and then demonstrated residual bond strength. The concrete mixes with short steel fibres experience sudden drop in bond strength. The detailed discussion on bond characteristics from pullout tests was mentioned in Chapter 4.

5.7 Analytical modeling of bond behavior

To perform numerical analysis of reinforced concrete members and structures, an analytical model of bond-slip constitutive law is necessary. But a general bond-slip law for FRP bar and concrete has not been proposed yet till now due to many factors that influence bond mechanism. FRP bars are relatively new type of reinforcement compared to steel and the bond behavior of FRP bar needs extensive research effort. Some researchers already developed analytical models of the bond-slip relationship by determining its parameters using curve fitting approach. These analytical models are aimed at identifying a general law for various FRP bar types and various concrete mix composition.

5.7.1 Malvar model

The first analytical bond-slip model in case of FRP bar was given Malvar (1994) where he carried out extensive experimental program of GFRP bars with different outer surface. Tests were performed for different confinement pressure and for a fixed tensile strength of the concrete. After analyzing the results, Malvar (1994) proposed an analytical model of the overall bond behavior which depends on the two empirical constants (F & G) which can be determined by using curve fitting approach on experimental bond-slip values.

$$\frac{\tau}{\tau_m} = \frac{F\left(\frac{S}{S_m}\right) + (G-1)(\frac{S}{S_m})^2}{1 + (F-2)\left(\frac{S}{S_m}\right) + G(\frac{S}{S_m})^2} \tag{5.3}$$

where, τ_m, s_m = peak bond stress, slip at peak bond stress and F and G are curve fitting parameters for different bar types.

5.7.2 Eligehausen, Popov and Bertero Model (BPE Model)

A well-known bond-slip analytical model for deformed steel was proposed by Eligehausen (1982), which was successfully applied to FRP bars by (Cosenza et al. 1995; Rossetti et al. 1995). This analytical law express the ascending branch ($s<s_1$) of bond-slip behavior as follows,

$$\frac{\tau}{\tau_1} = (\frac{S}{S_1})^{\alpha} \tag{5.4}$$

where τ_1, s_1 = peak bond stress, slip at peak bond stress and α is the curve fitting parameter, which must not be greater than 1 to be physically meaningful.

BPE model presents a second branch with constant bond up to slip $s = s_2$, a linearly descending branch from s_2, τ_1 to s_3, τ_3 and a horizontal branch for $s > s_3$, as shown in Figure 5-6 (a). Values of s_2, s_3 and t_3 have to be calibrated on the basis of experimental results

5.7.3 Modified BPE model

In their study, Cosenza et al. (1997) proposed an alternative analytical model which is a slight modification of BPE model. When analytical response of FRP bar using original BPE model was compared with the experimental curve it lacked the second branch as described. For that reason the original BPE model doesn't consider for describing bond response between FRP bar and concrete. In the modified BPE model, as shown in Figure 5-6(b), the ascending branch is the same as presented by original BPE model, with a softening branch having a slope of $\rho.\tau_1/s_1$ from (s_1,τ_1) to (s_3,τ_3) which is given by Equation (5.5) and then a horizontal branch for $s>s_3$ to represent the frictional component.

$$\frac{\tau}{\tau_1} = 1 - p\left(\frac{s}{s_1} - 1\right) \qquad (5.5)$$

Therefore, for the case of modified BPE model only three parameters have to be calibrated: parameter α, on which the ascending branch depends; parameter p, on which softening branch depends; and the frictional component, τ_3, of bond resistance.

5.7.4 Cosenza-Manfredi-Realfonzo (CMR) model

As most structural problems are to be dealt with the serviceability state level, a level with very small free end slip in the reinforcing member, a refined model for bond-slip relationship for ascending branch ($s < s_m$) is necessary. Considering this aspect, Cosenza et al.(1995) proposed an analytical model to predict the ascending branch of bond (τ)-slip(s) relationship. This model represents the alternative to BPE model and expressed as follows,

$$\frac{\tau}{\tau_m} = (1 - e^{-\frac{s}{s_r}})^{\beta} \qquad (5.6)$$

where, τ_m = peak bond stress, s_r and β are the parameters based on the curve fitting of the experimental data.

5.7.5 Analytical versus experimental results

Based on the experimental results of the FRP bar and various concrete mix compositions, the parameters of modified BPE model (α, p, τ_3) and CMR model (s_r,β) have been calibrated using

lease square root method. To better estimate relative adequacy of different analytical models, each analytical curve is obtained by using the coefficients derived from its experimental counterpart. The mean values of each parameter were calculated from the experimental results of similar concrete mixtures and bar size and were presented in Table 5-5 and 5-6. These mean values were used to carry out numerical simulations of the experimental results. It can be seen that the numerical prediction using mBPE model correlated well with the experimental data as shown in Figure 5-7 to 5-10. The comparison between experimental data and two models for all mix composition and bar sizes were demonstrated in Appendix – V.

The mBPE model also predicts the softening branch and residual strength more accurately for all bar size and concrete mix compositions.

From the results it can be observed that, for 10mm bar and fibre reinforced concrete mixes the parameter "α" ranged close to unity in most cases. This value was relatively high compared to the values reported by other researchers (Baena et al. 2009, 2011, Cosenza et al. 1995, 1997). This is due to the lightweight mix composition used in this study. The high value of 'α' demonstrate that the initial adhesion between GRP bar and concrete is low compared to steel and other types of FRP bar with various concrete mixes. For the same bar size in plain concrete, this "α" value ranged 0.34 to 0.97, which indicated higher adhesion component in bond strength compare to concrete mixtures with short steel fibre.

The 'τ_3' value represents the frictional component of the bond-slip response. Due to presence of steel fibre in concrete mixes, the surface between concrete and FRP bar was disturbed which resulted in lower τ_3 values for concrete mixes. Again, it was observed that for the bars with larger diameter the residual frictional component is higher. The effect of various factors on these parameters was shown in Figure 5-11.

Similar comparisons were made in Figure 5-12 for the various parameters of CMR model where bond slip responses were calibrated for initial ascending branch. For both bar sizes, a decrease in 'β'was observed with increase in crumb rubber replacement in case of plain

concrete. This value was found almost uniform for the fibre reinforced mixes and both bar sizes.

5.8 Conclusion

In this chapter the interfacial bond behavior between different rebar sizes and concrete mixtures with various levels of fine aggregate replacement with crumb rubber have been analyzed. On the basis of three models defined in the literature the following conclusion can be drawn:

1. Bond behavior between concrete mixtures and FRP bar depends on many factors including concrete compressive strength, rebar diameter and presence of steel fibre. These parameters also influence the characteristics of bond-slip response. Concrete matrices with higher crumb rubber replacement showed lower stiffness. However, for the same percentage of crumb rubber the concrete matrices without steel fibre show higher initial stiffness.
2. There is also a difference in the ascending branch of bond-slip response between steel and GFRP rebar. Steel reinforcement shows higher adhesion and bearing due to the presence of prominent surface deformation, but adhesion and friction are the prominent in case of sand coated GFRP bar and the concrete under consideration, it develops slip from the beginning.
3. The initial branch of experimental bond-slip responses obtained for different bar sizes and various concrete mixes were calibrated for two prominent analytical models, modified BPE and CMR models. In most cases, it was found that mBPE model has better agreement with the experimental responses compared to CMR model.
4. The modified BPE model is also suitable for reproduction of entire curve. Hence, it can be concluded that, mBPE model can be used for satisfactory prediction of the bond-slip response of GFRP bars and concrete with various percentage of fine aggregate replacement with crumb rubber.

5. Also it can be concluded that mBPE model is suitable to predict bond performance of concrete with low compressive strength, low density and fibre reinforced concrete mixtures.

5.8.1 Limitations of this study

This study investigated the bond performance between lightweight concrete mixes with crumb rubber as fine aggregate replacement and sand coated GFRP bar. In addition to that, lightweight expanded shale aggregate was used as coarse aggregate. Use of rubber as coarse aggregate replacement wasn't considered in this study. On the other hand, only silica fume was used as supplementary cementitious material due to its superior durability enhancement characteristics. Fly ash, metakaolin and other supplementary cementitious materials weren't employed here. Again, effect of fibre presence in concrete mixes was performed using steel fibres only. Concrete mixes with high rubber content (75% to 100%) showed low modulus of elasticity, and using low modulus fibres (polypropylene fibres) might be a better alternative of steel fibres in improving bond performance. From reinforcement point of view, only two bar sizes (10 mm and 16 mm) were used for size effect determination. Bond performance with other bar sizes would enrich the current database of bond performance between lightweight concrete and GFRP bars. Moreover, researches can be done on othe types of FRP bars in these lightweight concrete mixes.

Tables

Table 5-1: Proportions of different concrete mixes

Mix[a]	Water-binder ratio	OPC (kg/m^3)	Silica Fume (kg/m^3)	Gravel (Kg/m^3)	Sand (kg/m^3)	Crumb Rubber% (fine aggr. replacement)	Crumb Rubber (kg/m^3)
CR0F0	0.4	495	55	986	640	0	0
CR25F0	0.4	495	55	986	480	25	51
CR50F0	0.4	495	55	986	320	50	102
CR75F0	0.4	495	55	986	160	75	153
CR100F0	0.4	495	55	986	0	100	204
CR0F1	0.4	495	55	986	640	0	0
CR25F1	0.4	495	55	986	480	25	51
CR50F1	0.4	495	55	986	320	50	102
CR75F1	0.4	495	55	986	160	75	153
CR100F1	0.4	495	55	986	0	100	204

Table 5-2: Properties of GFRP bars

US Size	Glass Content, % weight	Nominal Size	Cross Sectional Area	Ultimate tensile strength	Modulus of Elasticity	Ultimate elongation
		mm	mm^2	MPa	GPa	%
#3	78.5	10	75.7	1054	45.4	2.41
#5	78.1	16	212.8	981	44.1	2.45

Table 5-3: Experimental Results for specimens with 10mm GFRP Rebar (for each individual specimen)

Specimen[a]	$f'c$, MPa	$s_{m,ue}$, mm[c]	$s_{m,ue}$[b], mm	$s_{m,le}$, mm[c]	$s_{m,le}$[b],mm	τ_{max} (MPa)[c]	τ_{max}[b] (MPa)	τ^*_{max} ($MPa^{0.5}$)	Failure Mode[d]
CR0F0-1	36.55	0.57	0.68	10.5	8.87	16.38	11.60	2.71	P
CR0F0-2	36.55	0.78		7.16		6.38		1.13	P
CR0F0-3	36.55	-		-		-			
CR25F0-1	21.96	0.6	0.47	11.3	8.54	9.83	8.99	2.10	P
CR25F0-2	21.96	0.33		5.76		8.14		1.74	P
CR25F0-3	21.96	-		-		-			
CR50F0-1	15.36	0.32	0.35	7.32	6.51	5.74	4.65	1.46	P
CR50F0-2	15.36	0.39		5.7		3.56		0.91	P
CR50F0-3	15.36	-		-		-			
CR75F0-1	10.30	0.66	0.46	6.81	6.14	6.43	6.31	2.00	P
CR75F0-2	10.30	0.26		5.46		5.30		1.65	P
CR75F0-3	10.30	-		-		7.20		2.24	P
CR100F0-1	7.60	0.10		3.77		1.97		0.72	P
CR100F0-2	7.60	0.47	0.27	4.20	4.11	2.64	2.34	0.96	P
CR100F0-3	7.60	0.23		4.37		2.42		0.88	P
CR0F1-1	44.12	0.29		14.0		6.65		1.00	P
CR0F1-2	44.12	0.25	0.25	4.60	7.37	7.34	6.82	1.11	P
CR0F1-3	44.12	0.22		3.50		6.46		0.97	P
CR25F1-1	32.27	0.38		9.85		7.24		1.27	P
CR25F1-2	32.27	0.16	0.27	4.17	6.07	4.76	6.08	0.84	P
CR25F1-3	32.27	0.28		4.18		6.24		1.10	P
CR50F1-1	19.60	0.41		9.68		4.12		0.93	P
CR50F1-2	19.60	0.94	0.55	5.84	7.24	4.07	4.21	0.92	P
CR50F1-3	19.60	0.31		6.20		4.45		1.01	P
CR75F1-1	15.17	0.15		5.08		4.57		1.17	P
CR75F1-2	15.17	0.35	0.42	4.62	4.82	3.59	3.74	0.92	P
CR75F1-3	15.17	0.76		4.77		3.05		0.78	P

Specimen[a]	*f'c*, MPa	$s_{m,ue}$, mm[c]	$s_{m,ue}$[b], mm	$s_{m,le}$,mm[c]	$s_{m,le}$[b],mm	τ_{max} (MPa)[c]	τ_{max}[b] (MPa)	τ^*_{max} ($MPa^{0.5}$)	Failure Mode[d]
CR100F1-1	11.11	0.27		3.10		2.81		0.84	P
CR100F1-2	11.11	0.33	0.31	3.75	4.39	2.72	3.10	0.82	P
CR100F1-3	11.11	0.34		6.33		3.77		1.13	P

[a] specimen identification, [b] mean value of similar specimen,

[c] Data not recorded, LVDT measurement blocked

[d] P = Pullout

Table 5-4: Experimental Results for specimens with 16mm GFRP Rebar (for each individual specimen)

Specimen[a]	f'c, MPa	$s_{m,ue}$, mm[c]	$s_{m,ue}$[b], mm	$s_{m,le}$,mm[c]	$s_{m,le}$[b],mm	τ_{max} (MPa)[c]	τ_{max}[b] (MPa)	τ^*_{max} ($MPa^{0.5}$)	Failure Mode[d]
CR0F0-1	36.55	0.65	0.59	9.1	6.54	13.1	11.13	2.17	P
CR0F0-2	36.55	0.53		4		9.15		1.51	P
CR0F0-3	36.55	-		-		-		-	
CR25F0-1	21.96	0.57	0.59	6.30	6.47	8.13	8.54	1.73	P
CR25F0-2	21.96	0.56		6.37		8.60		1.84	P
CR25F0-3	21.96	0.63		6.73		8.90		1.90	P
CR50F0-1	15.36	0.44	0.73	6.73	8.34	5.80	6.85	1.48	P
CR50F0-2	15.36	0.69		10.64		9.00		2.30	P
CR50F0-3	15.36	1.05		7.65		5.75		1.47	P
CR75F0-1	10.30	0.66	0.60	9.16	9.03	6.59	6.67	2.05	P
CR75F0-2	10.30	0.55		8.91		6.74		2.10	P
CR75F0-3	10.30	-		-		-			
CR100F0-1	7.60	083	0.58	10.75	8.95	3.60	3.45	1.31	P
CR100F0-2	7.60	0.5		10.29		4.00		1.45	P
CR100F0-3	7.60	0.4		5.80		2.74		0.99	P

Specimen[a]	f'c, MPa	$s_{m,ue}$, mm[c]	$s_{m,ue}$[b], mm	$s_{m,le}$,mm[c]	$s_{m,le}$[b],mm	τ_{max} (MPa)[c]	τ_{max}[b] (MPa)	τ^*_{max} ($MPa^{0.5}$)	Failure Mode[d]
CR0F1-1	44.12	0.5	0.6	7.10	8.02	7.72	8.52	1.16	P
CR0F1-2	44.12	0.66		8.21		9.00		1.35	P
CR0F1-3	44.12	0.65		8.76		8.85		1.33	P
CR25F1-1	32.27	0.5	0.47	9.86	8.64	4.00	4.57	0.70	P
CR25F1-2	32.27	0.44		7.42		5.13		0.90	P
CR25F1-3	32.27	-		-		-		-	
CR50F1-1	19.60	0.72	0.63	5.67	7.59	4.09	6.03	0.92	P
CR50F1-2	19.60	0.94		9.13		8.04		1.82	P
CR50F1-3	19.60	0.22		7.98		5.97		1.35	P
CR75F1-1	15.17	0.70	0.60	8.41	7.67	5.18	5.29	1.33	P
CR75F1-2	15.17	0.46		7.81		5.65		1.45	P
CR75F1-3	15.17	0.63		6.79		5.05		1.30	P
CR100F1-1	11.11	0.57	0.49	4.48	7.02	3.89	4.13	1.17	P
CR100F1-2	11.11	0.49		10.69		4.15		1.25	P
CR100F1-3	11.11	0.4		5.90		4.35		1.31	P

[a] specimen identification

[b] mean value of similar specimen

[c] Data not recorded, LVDT measurement blocked

[d] P = Pullout

Table 5-5: Mean values of various parameters of mBPE and CMR model for the 10mm GFRP Rebar

Specimen[a]	mBPE Model			CMR Model	
	α	p	τ_3	β	s_r
CR0F0	0.91	0.28	9.81	17.51	0.10
CR25F0	0.34	0.02	7.31	0.49	0.07
CR50F0	0.97	0.08	3.25	4.80	0.08
CR75F0	0.42	0.04	4.01	3.70	0.03
CR100F0	0.45	0.09	1.37	2.85	0.06
CR0F1	0.93	0.40	2.80	6.20	0.06
CR250F1	1.00	0.72	2.71	5.32	0.07
CR50F1	0.57	0.06	2.57	6.75	0.12
CR75F1	1.00	0.28	1.51	3.79	0.21
CR100F1	1.00	0.57	1.61	7.17	0.07

Table 5-6: Mean values of various parameters of mBPE and CMR model for the 16mm GFRP Rebar

Specimen[a]	mBPE Model			CMR Model	
	α	p	τ_3	β	s_r
CR0F0	0.99	1.35	-	10.00	0.12
CR25F0	1.00	-	-	8.93	0.13
CR50F0	0.73	0.10	4.74	2.34	0.19
CR75F0	0.74	0.07	5.66	3.09	0.12
CR100F0	0.74	3.15	2.14	3.62	0.16
CR0F1	1.00	0.70	5.71	4.11	0.17
CR250F1	1.00	0.96	2.51	5.51	0.10
CR50F1	0.66	0.14	3.98	1.99	0.20
CR75F1	0.75	0.07	4.54	6.84	0.11
CR100F1	0.87	1.14	2.54	7.23	0.11

Figures

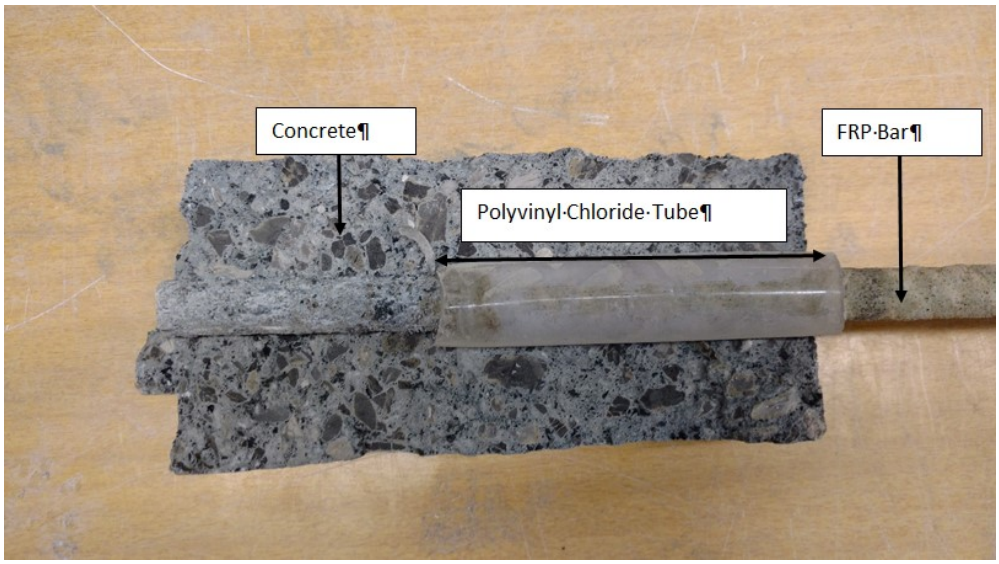

Figure 5-1: A pullout sample after test showing polyvinyl chloride tube for debonding length

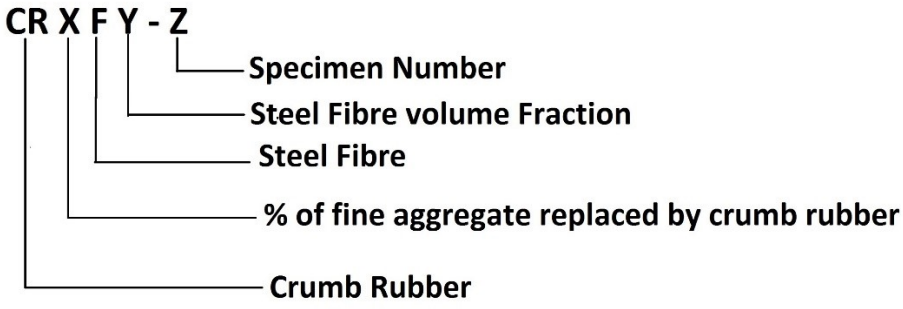

Figure 5-2: Specimen identification description

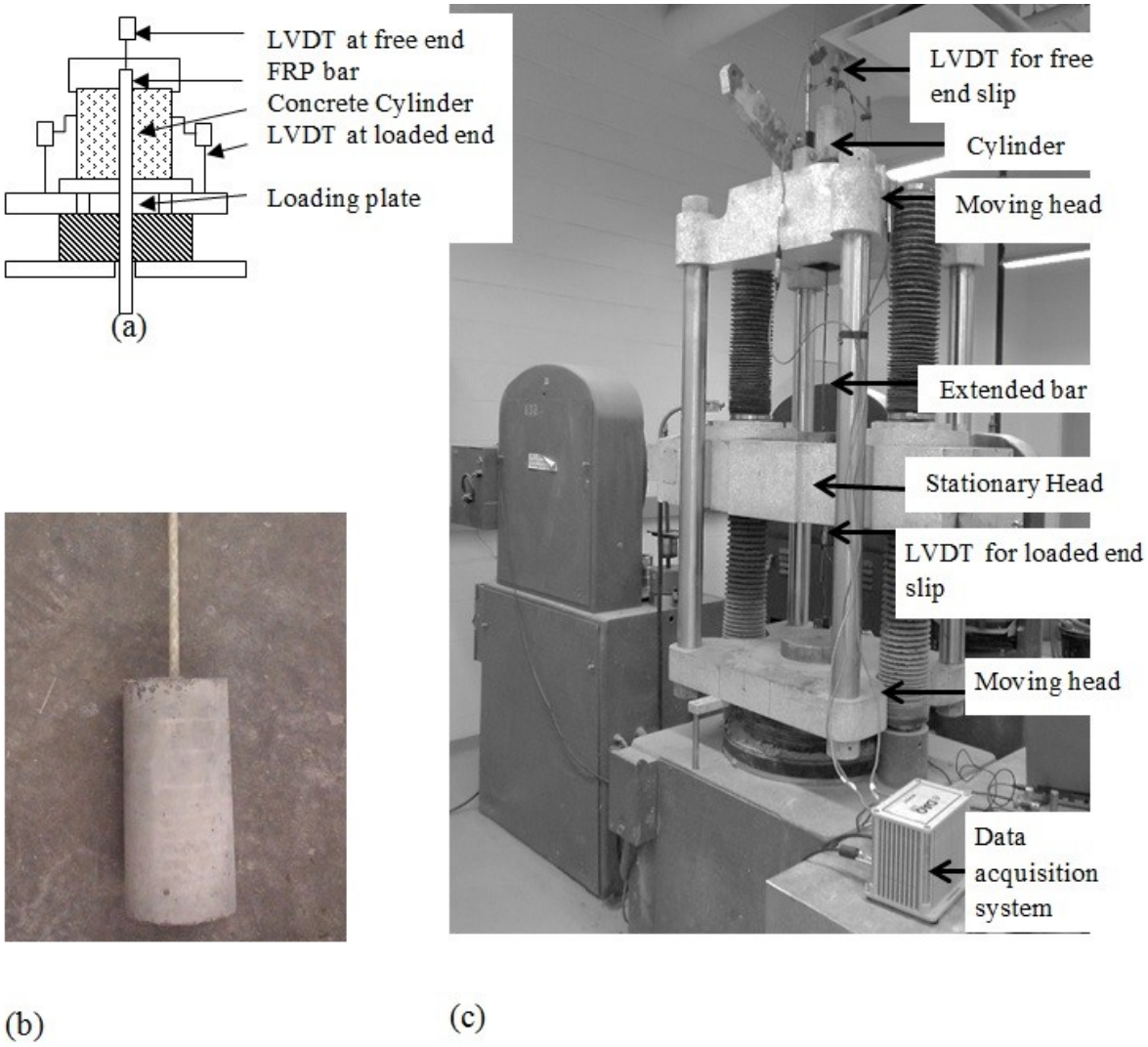

Figure 5-3: Test setup (a) schematic diagram of pullout test setup, (b) pullout test specimen, (c) pullout test in progress

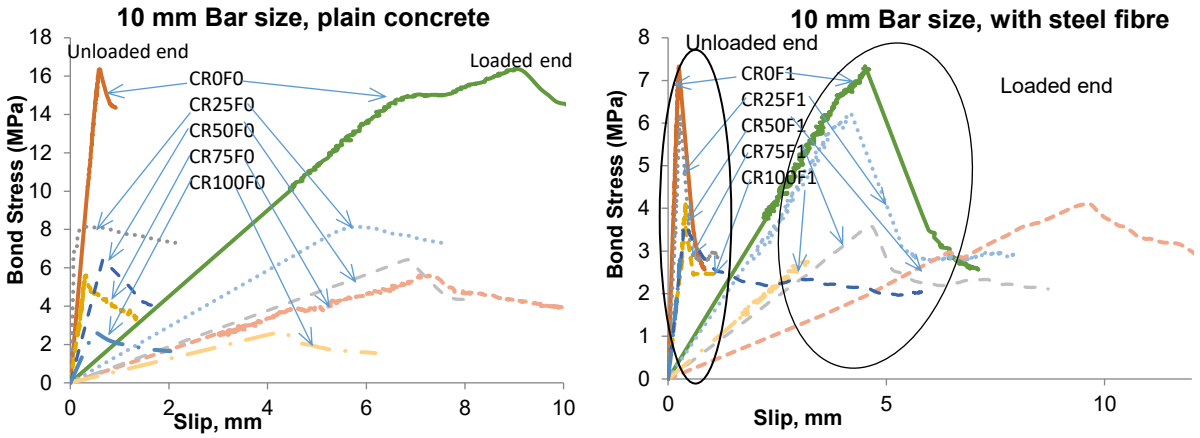

(a) (b)

Figure 5-4: Bond slip response for 10mm bar in (a) plain concrete and (b) fibre reinforced concrete

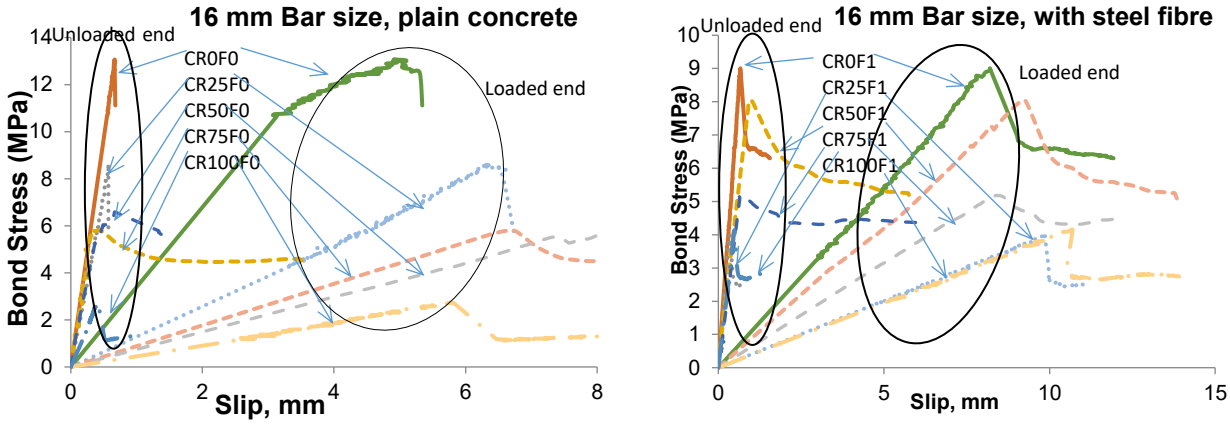

(a) (b)

Figure 5-5: Bond slip response for 16mm bar in (a) plain concrete and (b) fibre reinforced concrete

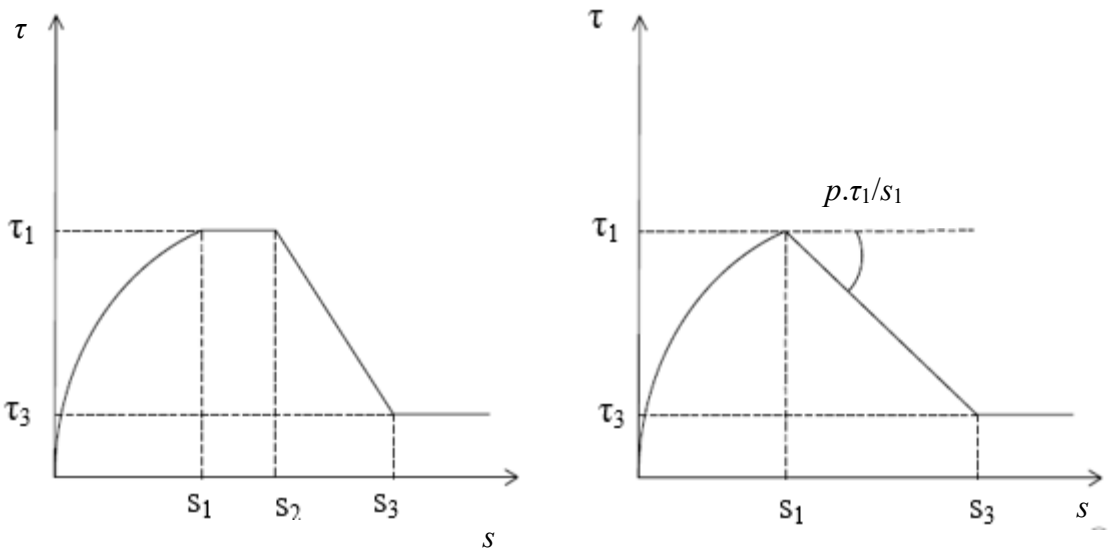

(a) BPE Model (b) Modified BPE Model

Figure 5-6: (a) BPE Model, (b**).** Modified BPE Model

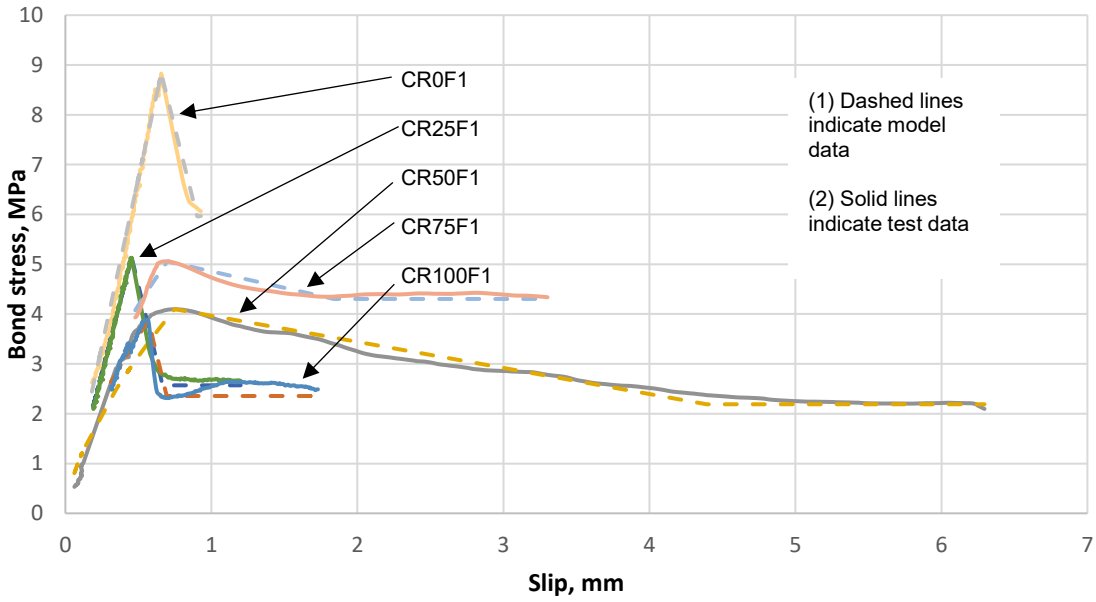

Figure 5-7: Comparison of entire response for samples with 16mm and concrete mixes with steel fibre

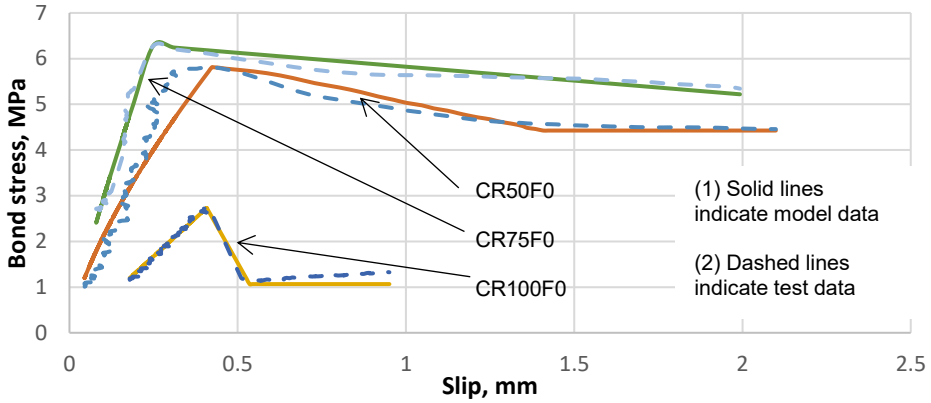

Figure 5-8: Comparison of complete bond-slip responses for samples with 16mm and plain concrete mixes

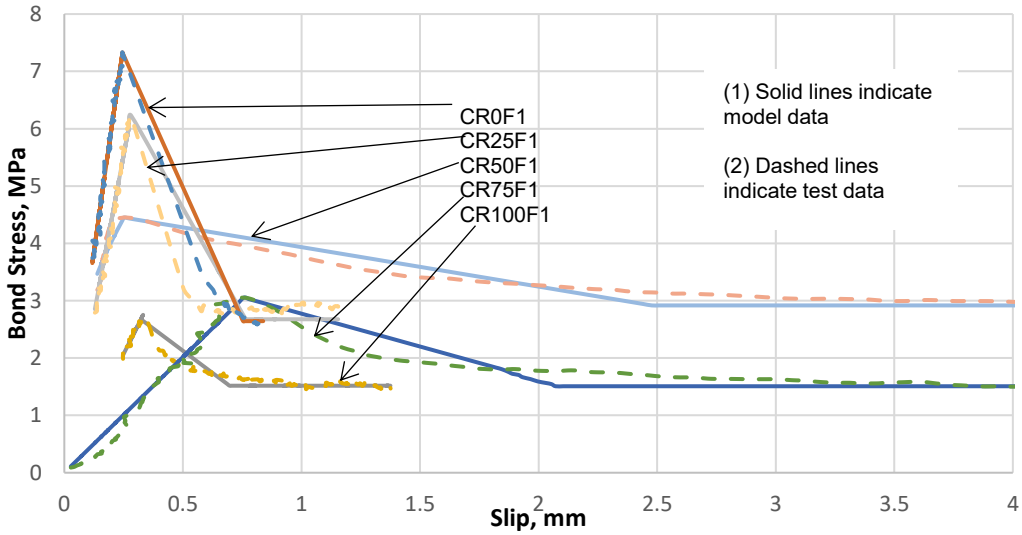

Figure 5-9: Comparison of entire response for samples with 10mm and concrete mixes with steel fibre

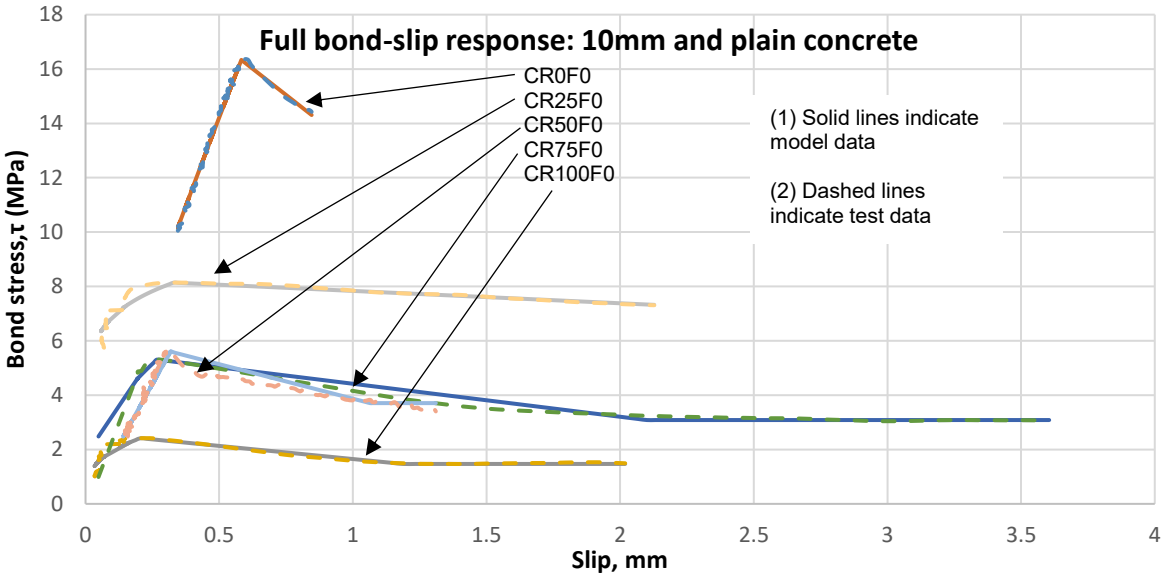

Figure 5-10: Comparison of entire response for samples with 10mm and plain concrete mixes

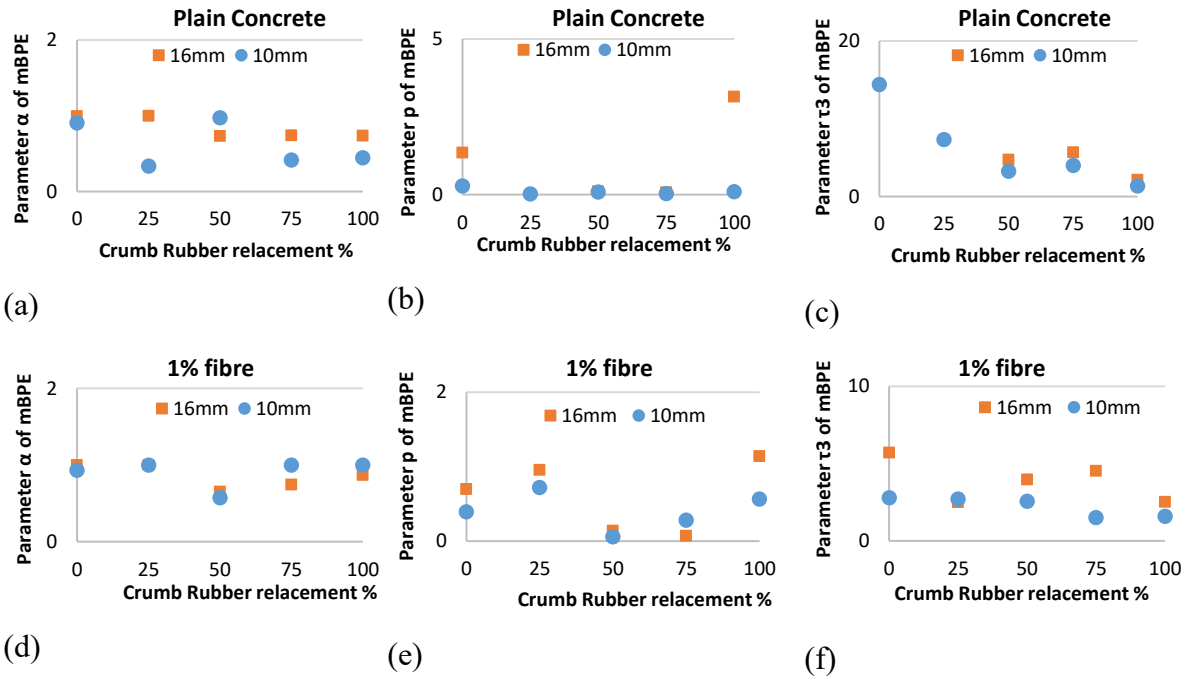

Figure 5-11: Effect of crumb rubber replacement and bar size on various parameters for mBPE model

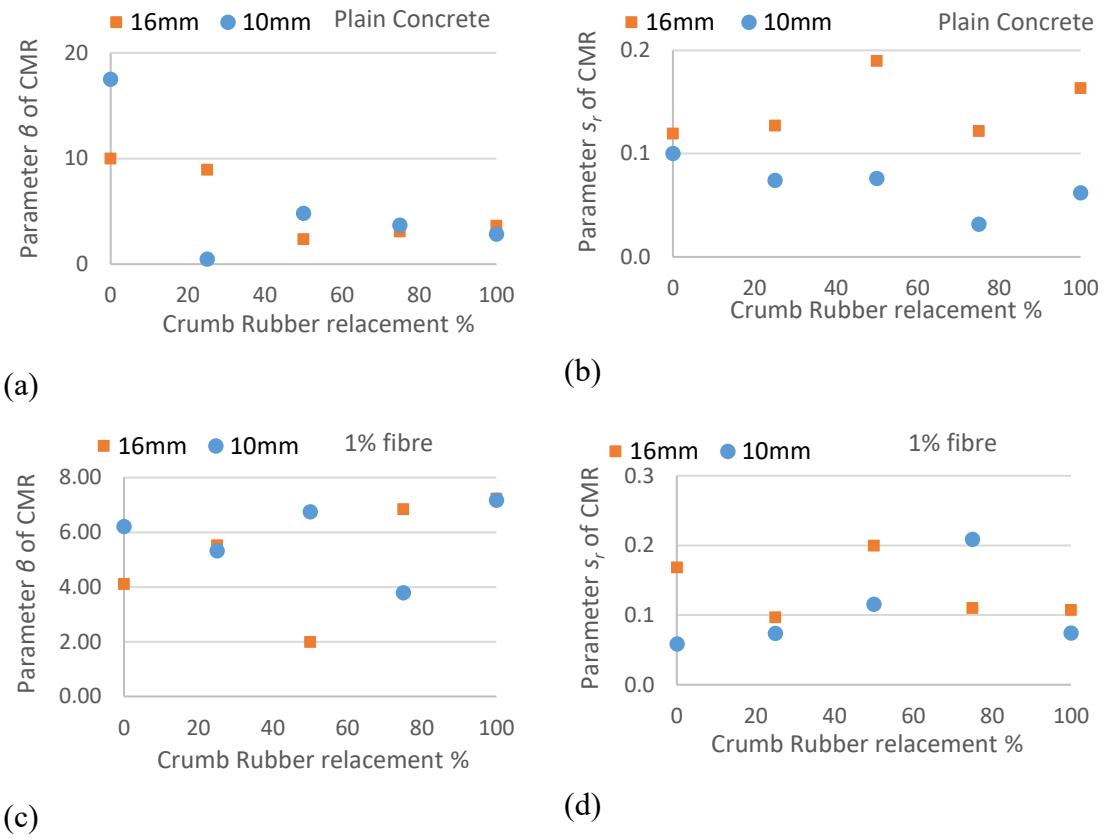

Figure 5-12: Effect of crumb rubber content/fine aggregate content and bar size on various parameters for CMR model

References

Achillides, Z., and Pilakoutas, K. (2004). “Bond behavior of fiber reinforced polymer bars under direct pullout conditions.” *Journal of Composites for construction*, 8, 173.

Aiello, M. A., Leone, M., and Pecce, M. (2007). “Bond Performances of FRP Rebars-Reinforced Concrete.” *Journal of Materials in Civil Engineering*.

Baena, M., Torres, L., Turon, A., and Barris, C. (2009). “Experimental study of bond behaviour between concrete and FRP bars using a pull-out test.” *Composites Part B: Engineering*, 40(8), 784–797.

Baena, M., Turon, A., Torres, L., and Miàs, C. (2011). “Experimental study and code predictions of fibre reinforced polymer reinforced concrete (FRP RC) tensile members.” *Composite Structures*, 93(10), 2511–2520.

Benmokrane, B., Tighiouart, B., and Chaallal, O. (1996). “Bond strength and load distribution of composite GFRP reinforcing bars in concrete.” *ACI Materials Journal*, 93(3).

Chaallal, O., and Benmokrane, B. (1993). “Pullout and bond of glass-fibre rods embedded in concrete and cement grout.” *Materials and structures*, 26(3), 167–175.

Cosenza, E., Manfredi, G., and R, R. (1995). “Analytical modelling of bond between FRP reinforcing bars and concrete.” *ResearchGate*, 164–171.

Cosenza, E., Manfredi, G., and Realfonzo, R. (1997). “Behavior and modeling of bond of FRP rebars to concrete.” *Journal of composites for construction*, 1(2), 40–51.

CSA A3001. (2009). “Cementitious materials compendium.” Canadian Standards Association, Mississauga, ON.

Eligehausen, R., Popov, E. P., and Bertero, V. V. (1982). “Local Bond stress slip relationship of deformed bars under generalized excitations.” *ResearchGate*.

Focacci, F., Nanni, A., and Bakis, C. E. (2000). “Local Bond-Slip Relationship for FRP Reinforcement in Concrete.” *Journal of Composites for Construction*, 4(1), 24–31.

Larralde, J., and Silva-Rodriguez, R. (1993). “Bond and Slip of FRP Rebars in Concrete.” *Journal of Materials in Civil Engineering*, 5(1), 30–40.

Makitani, E., Irisawa, I., and Nishiura, N. (1993). “Investigation of Bond in Concrete Member With Fiber Reinforced Plastic Bars.” *Special Publication*, 138, 315–332.

Malvar, L. J. (1994). *Bond Stress-Slip Characteristics of FRP Rebars.* Office of Naval Research, naval Cailities Engineering Service Center, port Hueneme, California.

Nanni, A., Al-Zaharani, M. M., Al-Dulaijan, S. U., and Bakis, C. E. (1995). “Bond of FRP reinforcement to concrete - Experimental results.” Non-metallic (FRP) reinforcement for concrete structures, L. Taerwe, ed., Spon, 135–145.

Pecce, M., Manfredi, G., Realfonzo, R., and Cosenza, E. (2001). “Experimental and Analytical Evaluation of Bond Properties of GFRP Bars.” *Journal of Materials in Civil Engineering*, 13(4), 282–290.

Rossetti, V. A., Galeota, D., and Giammatteo, M. M. (1995). “Local bond stress-slip relationships of glass fibre reinforced plastic bars embedded in concrete.” *Materials and Structures*, 28(6), 340–344.

Tepfers, R. (2006). “Bond clause proposals for FRP bars/rods in concrete based on CEB/FIP Model Code 90. Part 1: Design bond stress for FRP reinforcing bars.” *Structural Concrete*, 7(2), 47–55.

Tighiouart, B., Benmokrane, B., and Gao, D. (1998). “Investigation of bond in concrete member with fibre reinforced polymer (FRP) bars.” *Construction and Building Materials*, 12(8), 453–462.

Notations

d_b = diameter of the reinforcement bar

F, G = Empirical constant in Malvar Model for each bar type

$f'c$ = compressive strength of concrete

l_b = embedment length

P = the tensile load

p = softening branch slope defining parameter in BPE and mBPE model

s = slip

s_m/s_1 = slip at maximum bond stress

$s_{m,ue}$ = unloaded end slip at maximum bond stress

$s_{m,ue}{}^b$ = average unloaded end slip at maximum bond stress

$s_{m,le}$ = loaded end slip at maximum bond stress

$s_{m,le}{}^b$,= average loaded end slip at maximum bond stress

s_r = curve fitting parameter in Cosenza Manfredi Realfonzo (CMR) model

s_2 = maximum slip at constant maximum bond stress (as per BPE model)

s_3 = slip at the end of softening branch (as per BPE and mBPE model)

α = curve fitting parameter for BPE model and modified BPE model

β = curve fitting parameter in Cosenza Manfredi Realfonzo (CMR) model

τ_m/τ_1 = maximum bond stress

$\tau^*_{\max}$ = maximum normalized bond stress

τ_3 = bond stress at the end of softening branch (as per BPE and mBPE model)

Appendix – V

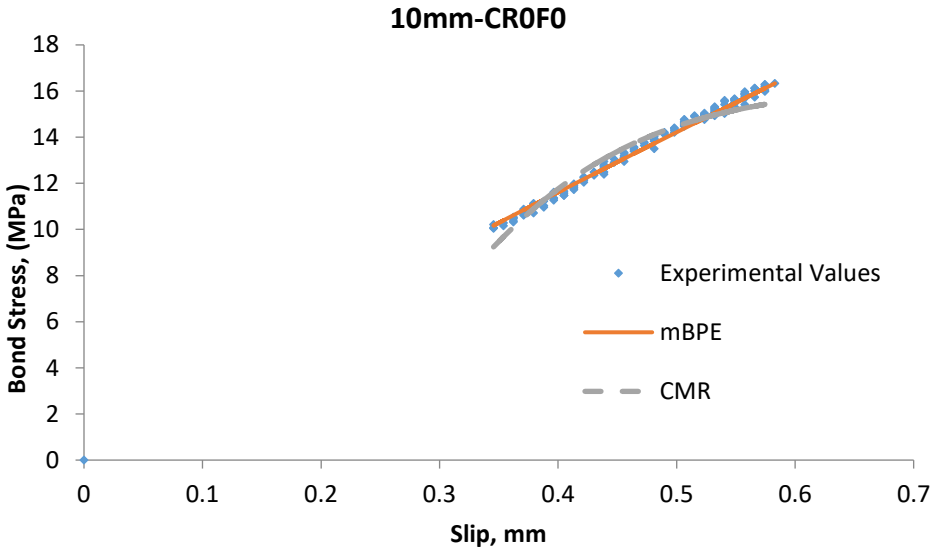

Figure V-1 (a) Comparison for the 10mm bar with 0% rubber without steel fibre

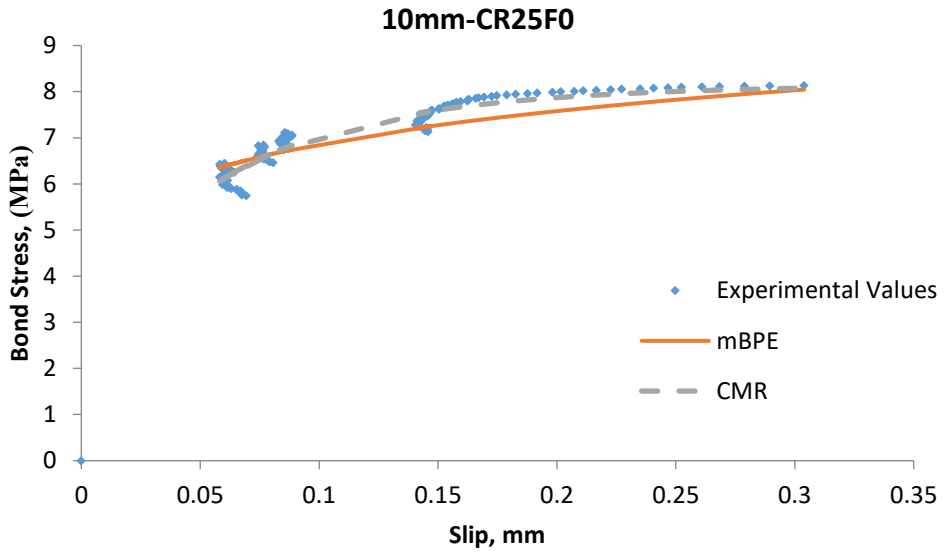

Figure V-1 (b) Comparison for the 10mm bar with 25% rubber without steel fibre

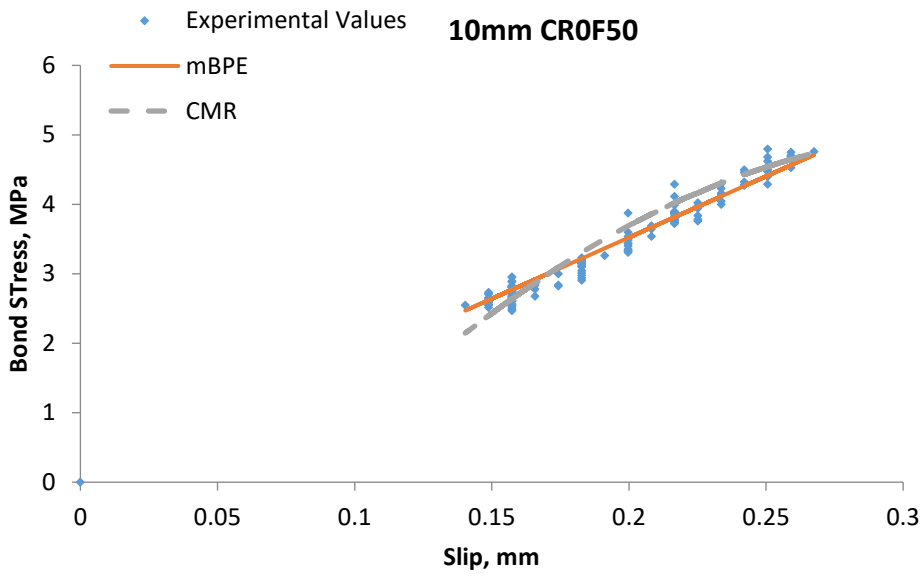

Figure V-1 (c) Comparison for the 10mm bar with 50% rubber without steel fibre

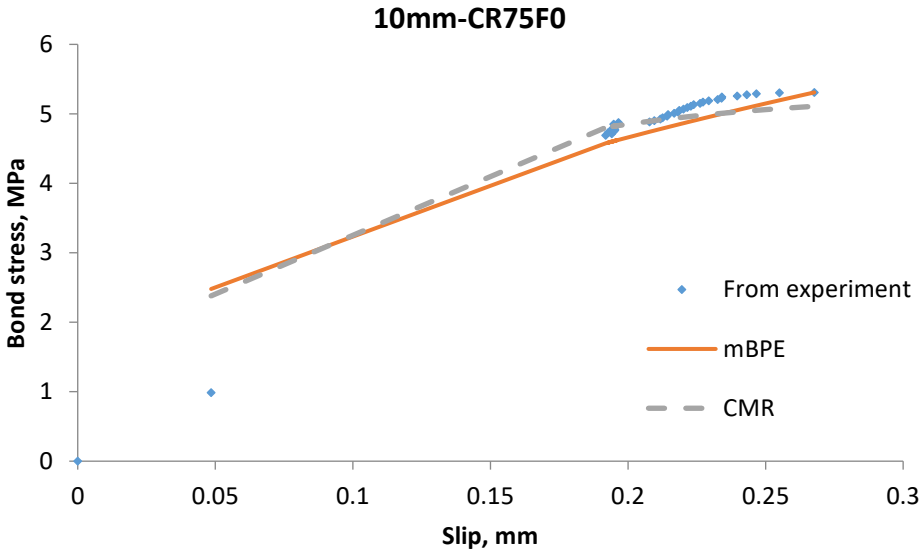

Figure V-1 (d) Comparison for the 10mm bar with 75% rubber without steel fibre

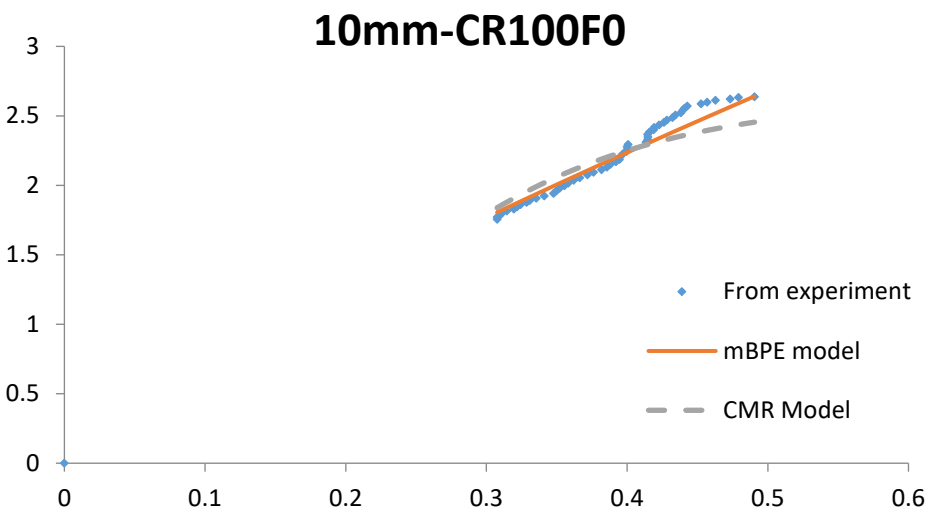

Figure V-1 (e) Comparison for the 10mm bar with 100% rubber without steel fibre

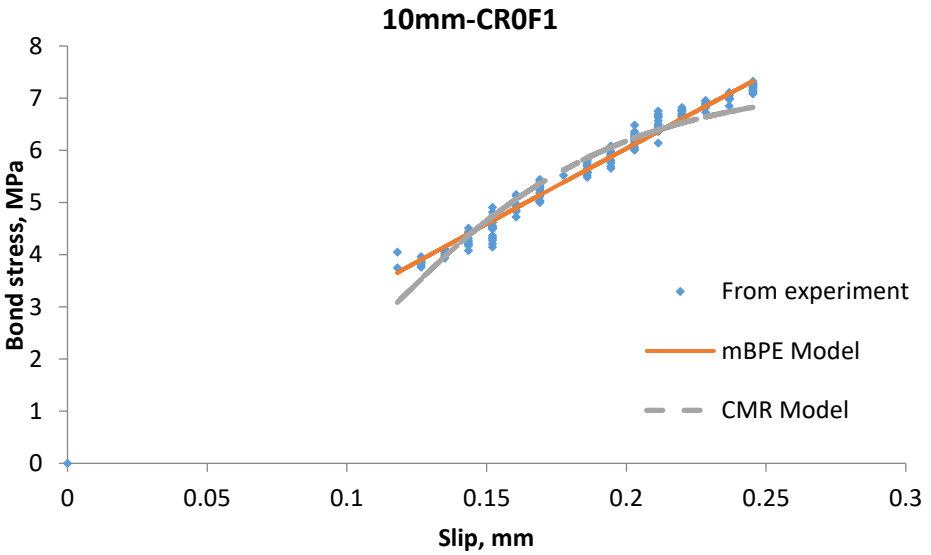

Figure V-2 (a) Comparison for the 10mm bar with 0% rubber with steel fibre

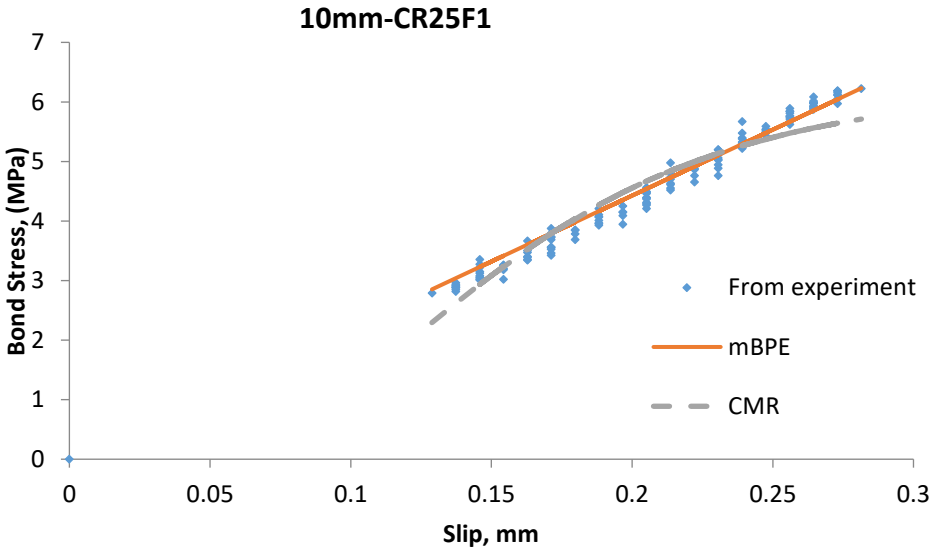

Figure V-2 (b) Comparison for the 10mm bar with 25% rubber with steel fibre

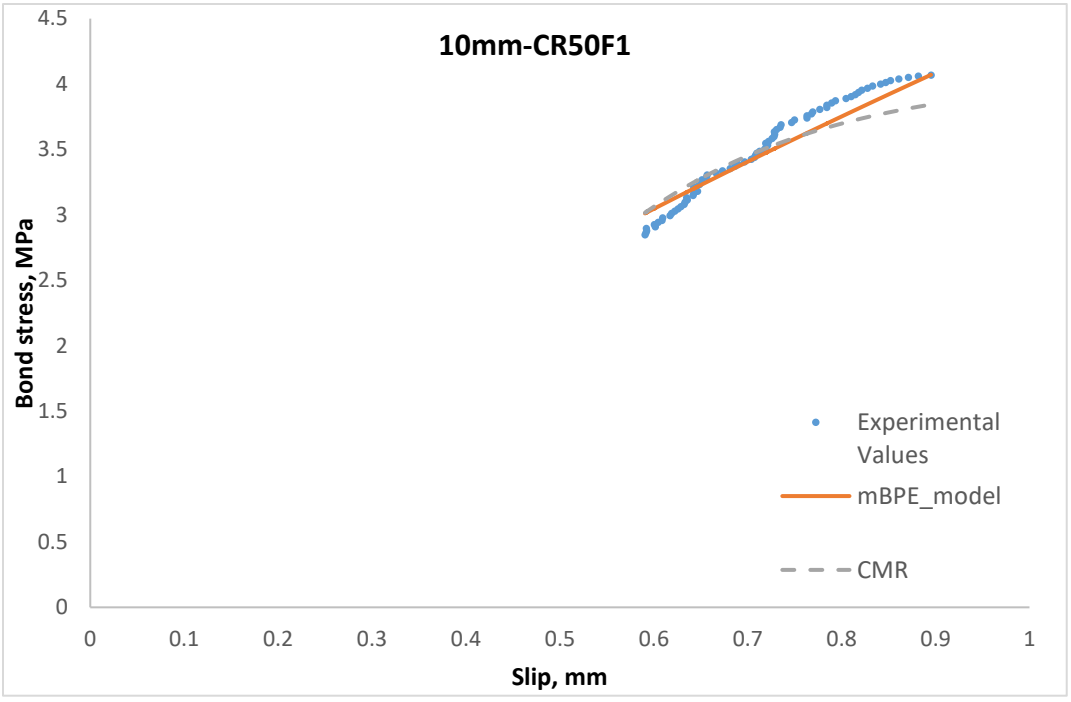

Figure V-2 (c) Comparison for the 10mm bar with 50% rubber with steel fibre

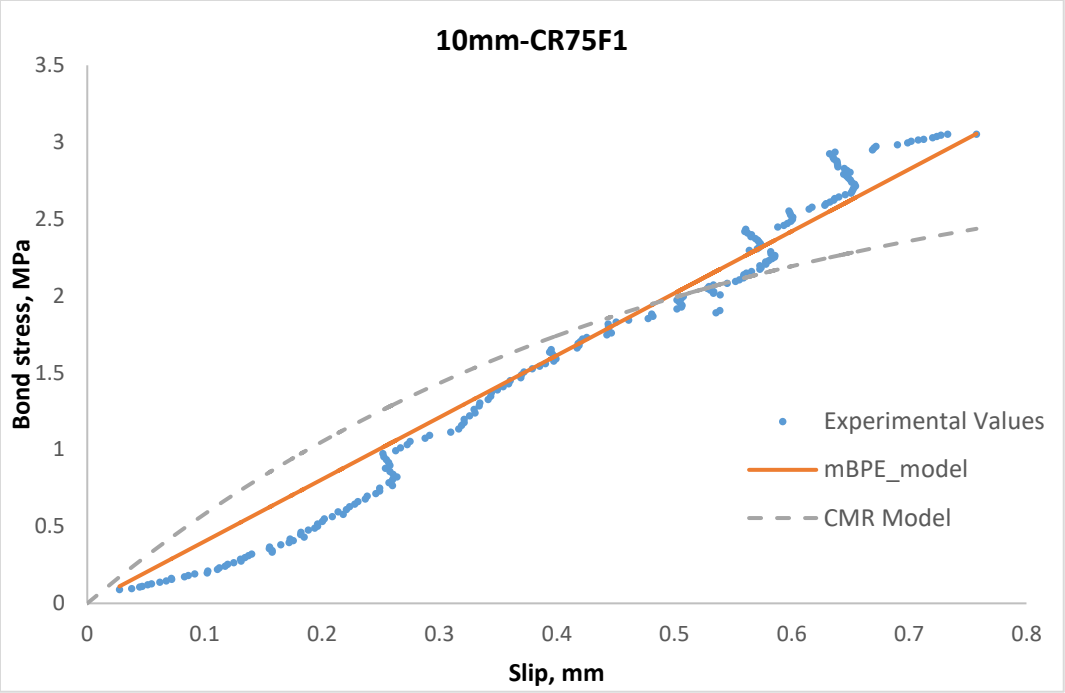

Figure V-2 (d) Comparison for the 10mm bar with 75% rubber with steel fibre

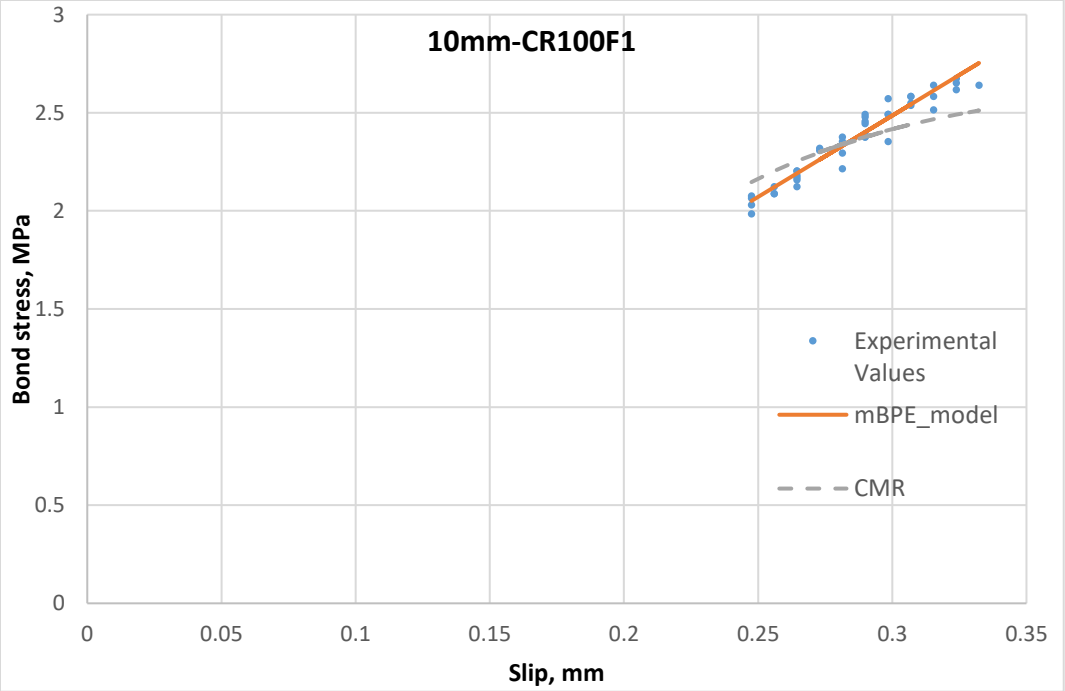

Figure V-2 (e) Comparison for the 10mm bar with 100% rubber with steel fibre

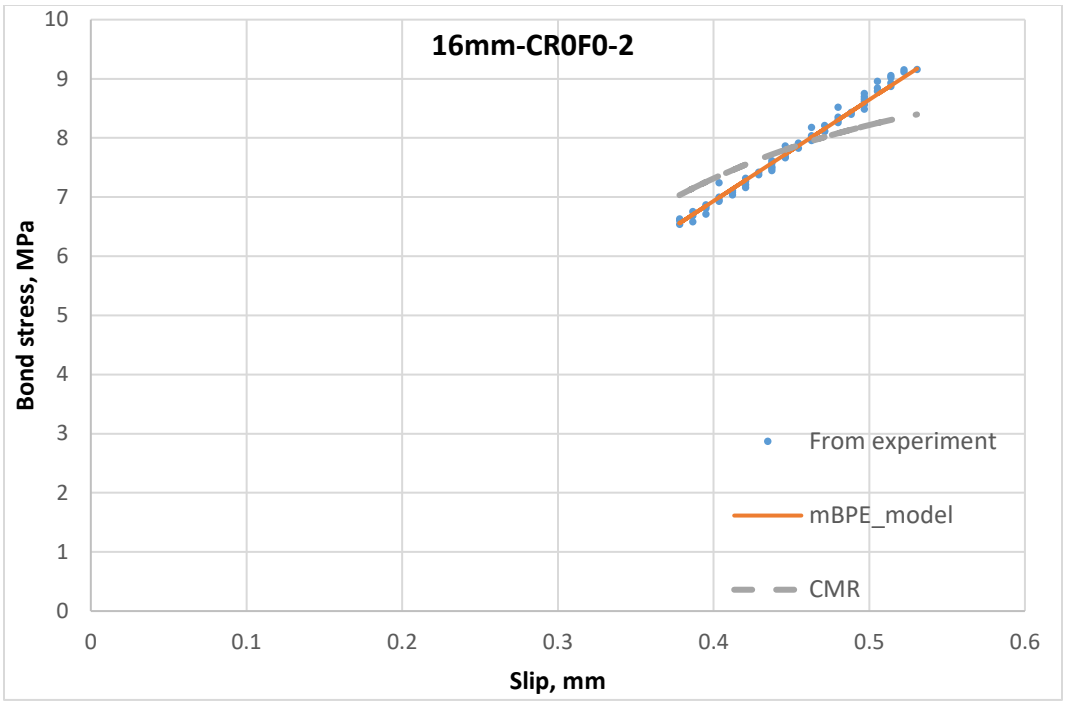

Figure V -3 (a) Comparison for the 16mm bar with 0% rubber without steel fibre

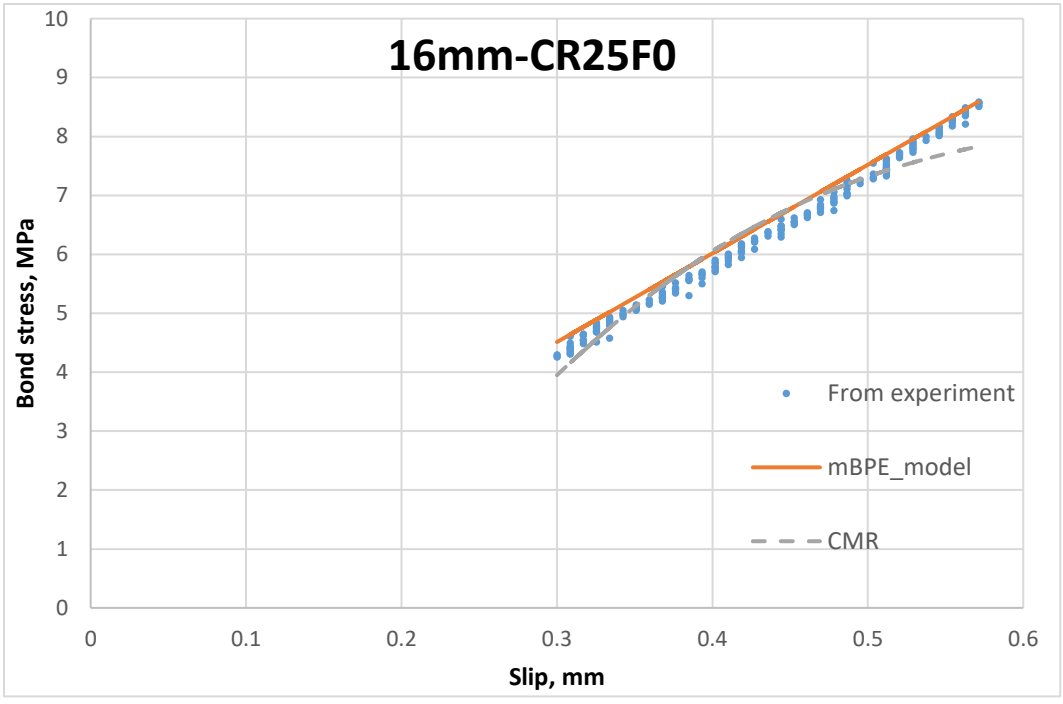

Figure V-3 (b) Comparison for the 16mm bar with 25% rubber without steel fibre

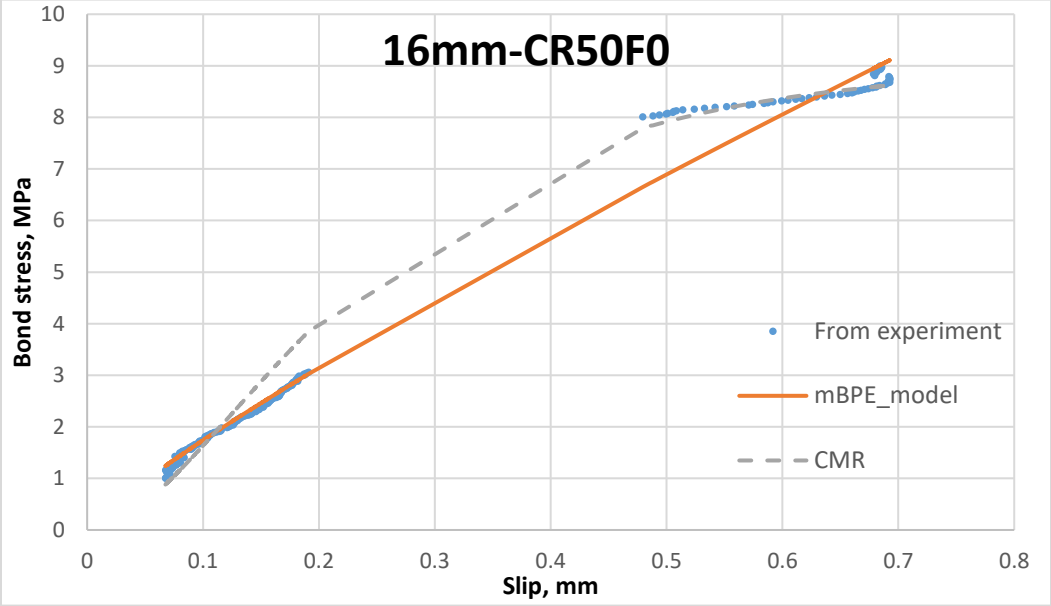

Figure V-3 (c) Comparison for the 16mm bar with 50% rubber without steel fibre

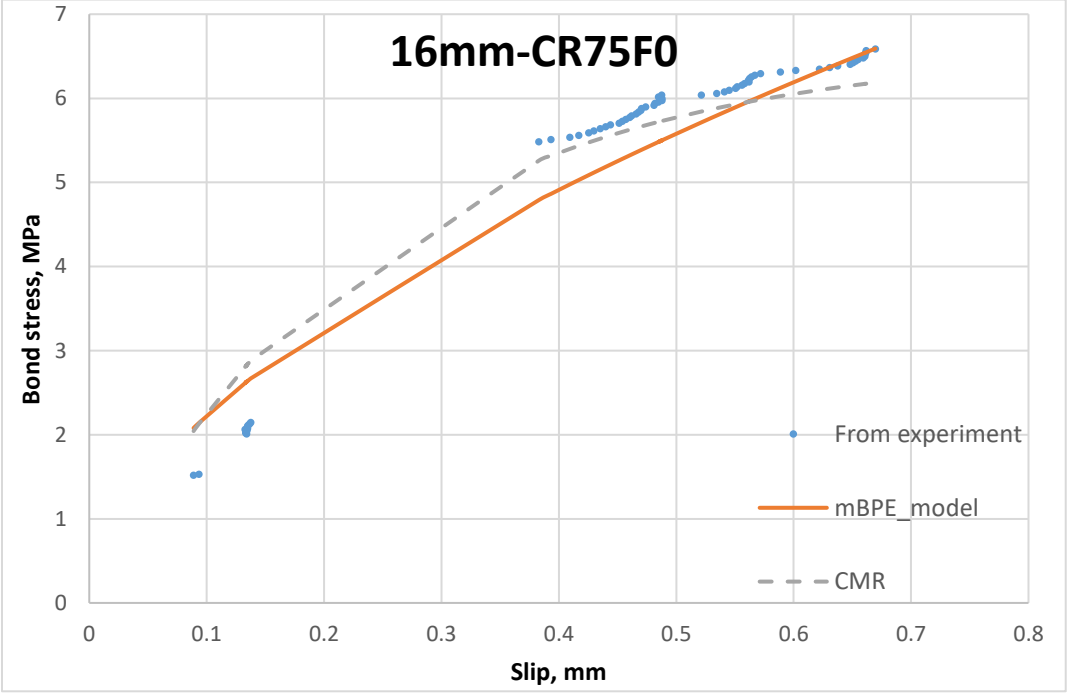

Figure V-3 (d) Comparison for the 16mm bar with 75% rubber without steel fibre

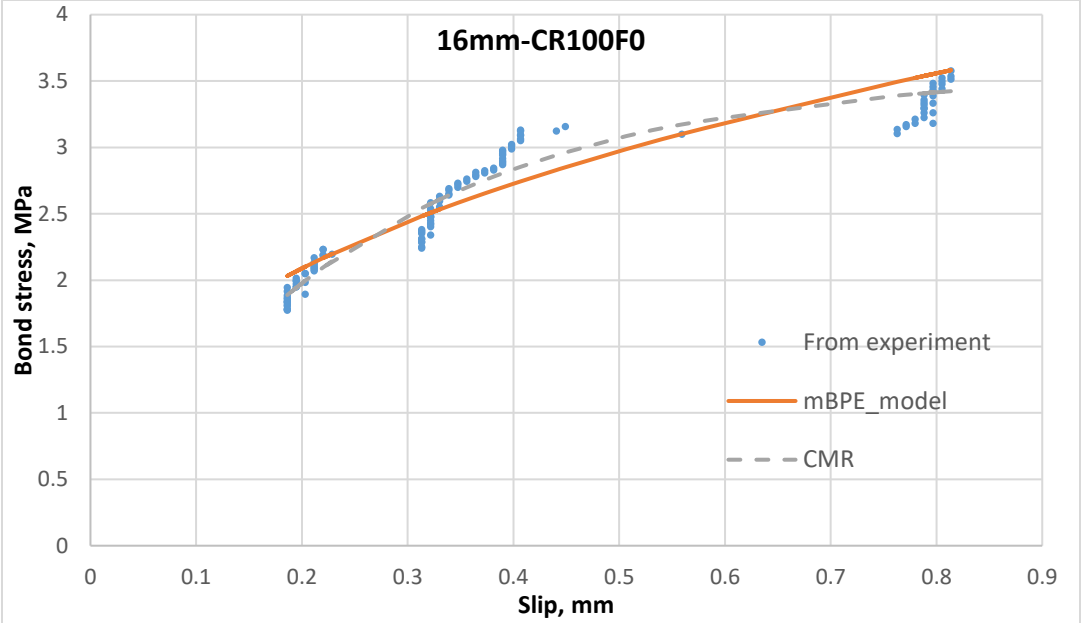

Figure V -3 (e) Comparison for the 16mm bar with 100% rubber without steel fibre

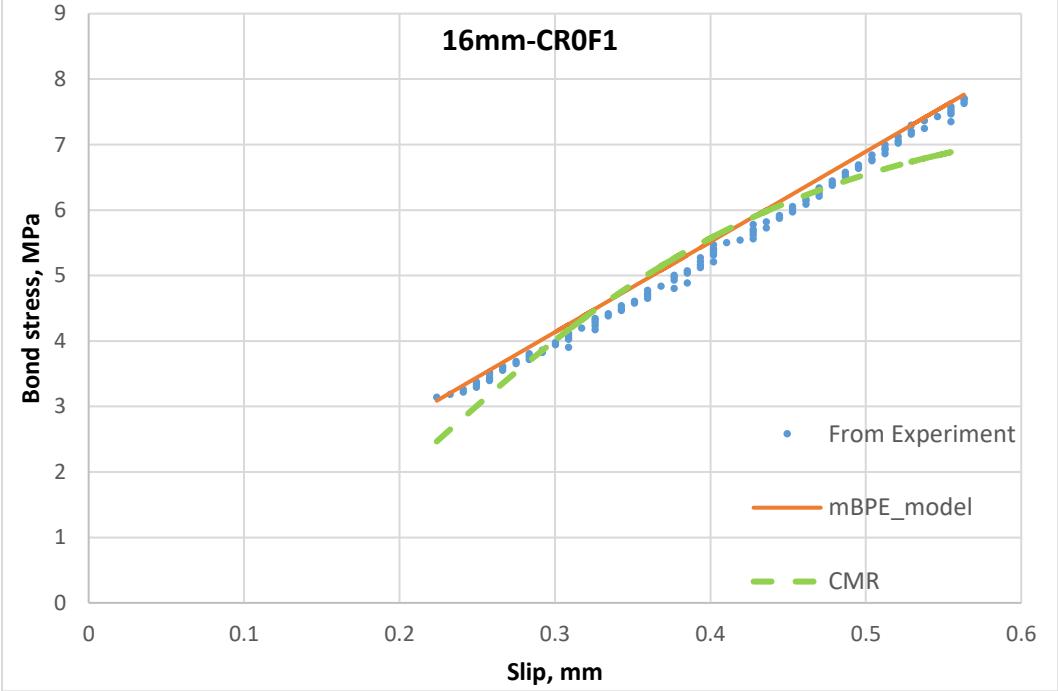

Figure V-4 (a) Comparison for the 16mm bar with 0% rubber with steel fibre

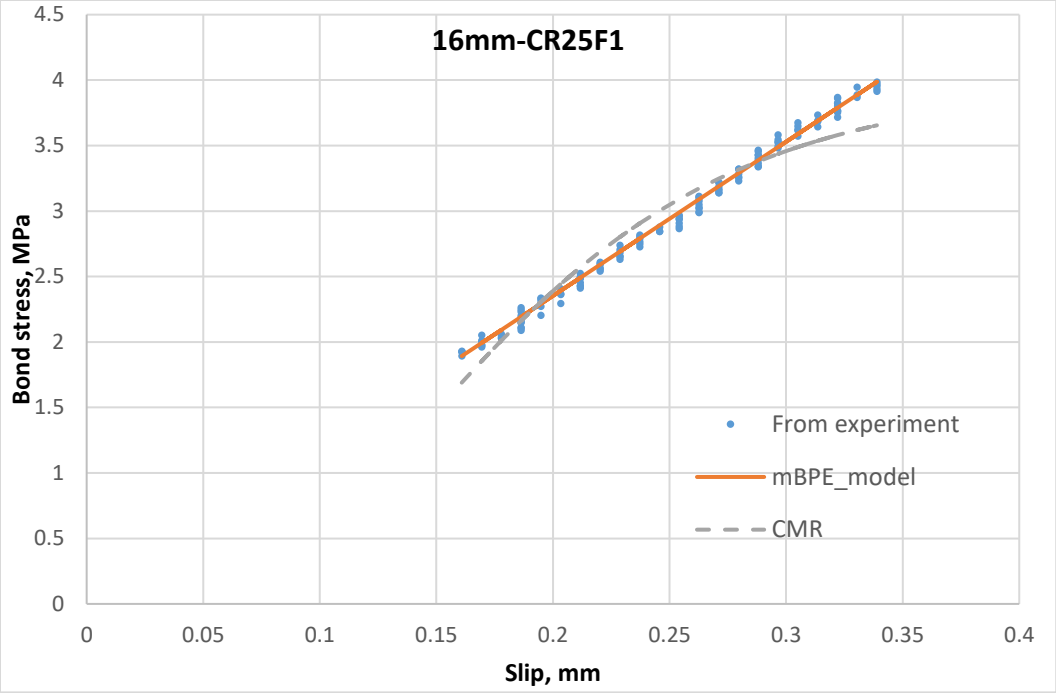

Figure V -4 (b) Comparison for the 16mm bar with 25% rubber with steel fibre

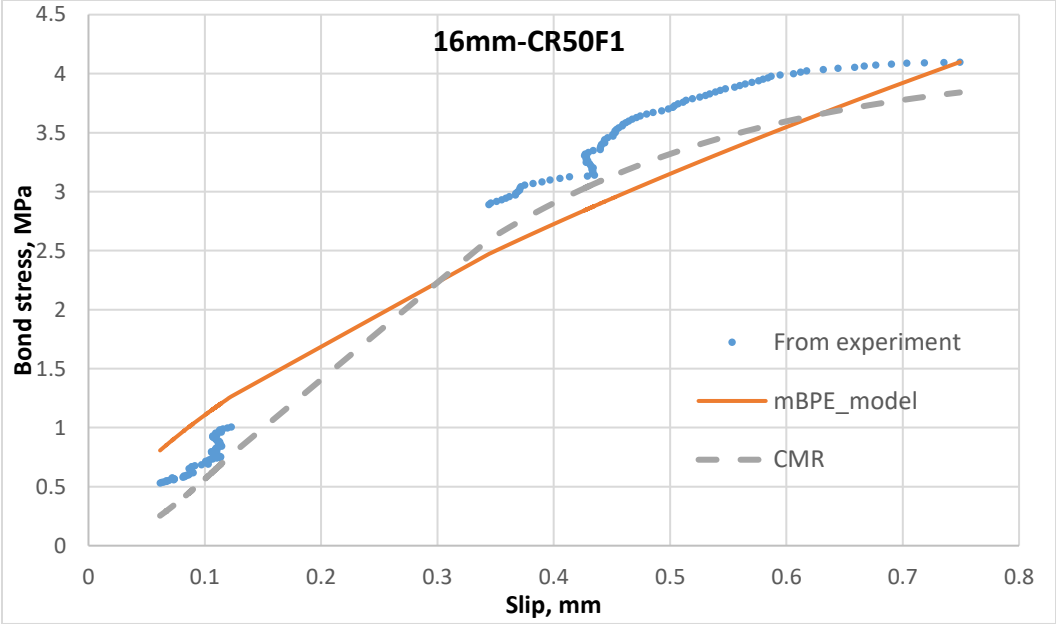

Figure V-4 (c) Comparison for the 16mm bar with 50% rubber with steel fibre

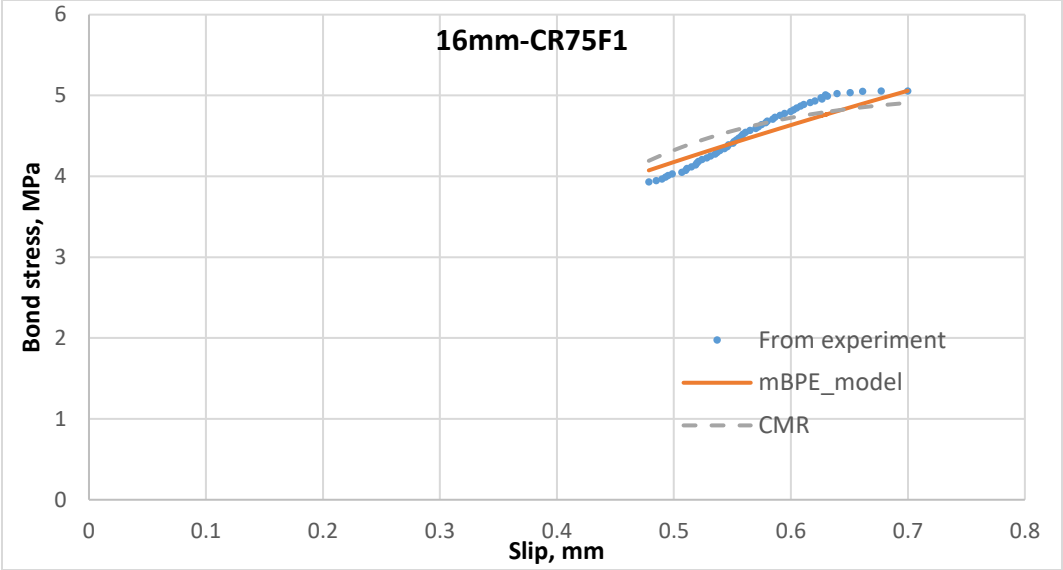

Figure V-4 (d) Comparison for the 16mm bar with 0% rubber with steel fibre

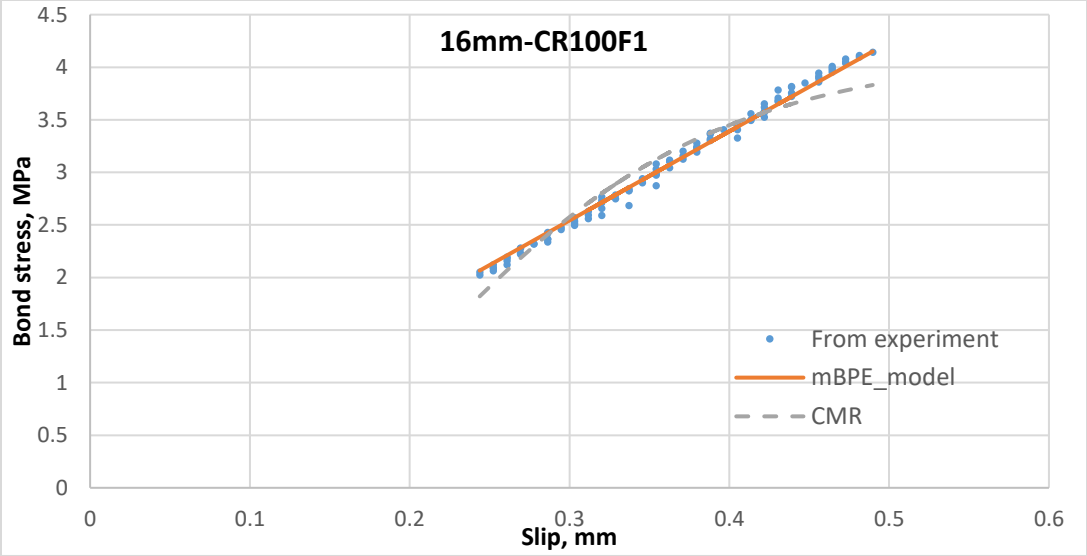

Figure V-4 (e) Comparison for the 16mm bar with 100% rubber with steel fibre

CHAPTER 6. BOND RESPONSE OF FIBRE REINFORCED POLYMER BAR WITH LIGHTWEIGHT CONCRETE: BEAM TEST

6.1 Introduction

Steel reinforcement bars are the most widely used reinforcement in the reinforced concrete structures. Notwithstanding that, the main disadvantage is the corrosion of the steel reinforcement when exposed to corrosive environment which may lead to the deterioration or even complete collapse of the structural elements. In order to prevent the deterioration of reinforced concrete structures, scientist and engineers were looking for alternative reinforcing materials to use instead of steel.

The use of Fibre Reinforced Polymer (FRP) bar as reinforcement in concrete structures is considered to be possible alternative where corrosion is a concern and where design is controlled by durability requirements of the reinforced concrete members. As concrete reinforcement, FRP bars present some favorable characteristics such high tensile strength, low weight, similar thermal expansion to that of concrete, satisfactory behavior in alkaline environment of concrete, small creep deformation, inertial to magnetic and electrical fields. Glass FRP has the relatively low modulus of elasticity and its characteristics stress-strain curve doesn't have well defined yield plateau. As a result the established design framework of reinforced concrete structures, which aims to control the failure mode by rebar yielding, cannot be used directly for the reinforced concrete structures with FRP bar. The composite action of reinforced concrete structures with FRP bar largely depends on the magnitude of bond that may develop at the contact interface between concrete and the bar surface.

Beside the development of alternative reinforcement in the form of FRP bar, efforts were made to prepare concrete using various alternative sources of aggregate. Use of these new materials is not only reduces the environmental effect due to aggregate extraction but also reduce the landfill and recycling cost of those materials, such as use of crumb rubber from scrap tires. Utilization of scrap tires may play a significant role in sustainable development considering the existing stockpile of scrap tires. In the last 20 years the potential use of crumb rubber as

replacement of fine and/or course aggregate was studied by many researchers (Eldin and Senouci 1993; Khatib and Bayomy 2013; Topçu and Avcular 1997; Topçu 1995; Zheng et al. 2008). The rubber aggregates can be loosely classified into four types depending on their particle size, shredded or chipped (the size representing the coarse aggregate), crumb rubber (typically between 4.75mm and 0.425mm), ground tire rubber (passing through No 40 sieve) and fibre rubber aggregate (short fibre typically between 8.5mm and 21.5mm in length) (Najim and Hall 2012) and these are characterized as having negligible water absorption and low density (0.866 kg/m^3). The use of rubber is seen to cause a reduction in both compressive and tensile strength of concrete which is a big challenge to overcome. Use of silica fume in concrete to enhance mechanical properties and durability is widely accepted (Duval and Kadri 1998; Güneyisi et al. 2004). The effect of silica fume on material properties was evaluated and reported in Chapter 4.

6.2 Background

Bond of FRP is different from that of conventional steel reinforcement due to the difference in outer surface characteristics and the material difference in longitudinal and transverse direction. In recent years considerable experimental studies have been conducted in order to evaluate the bond performance of various FRP rebar and concrete (Al-Zahrani et al. 1999; Benmokrane et al. 1996; Chaallal and Benmokrane 1993a; Kanakubu et al. 1993; Larralde and Silva-Rodriguez 1993; Makitani et al. 1993; Malvar 1994; Nanni et al. 1995; Rossetti et al. 1995). Those studies found that in reinforced concrete elements with FRP bar, the transfer of forces between a reinforcing bar and concrete occurs by three mechanisms: (1) chemical adhesion between the bar and the concrete, (2) frictional forces arising from the roughness of the interface, forces transverse to the bar surface, relative slip between the bar and surrounding concrete, and (3) mechanical interlock or bearing arising from the textures or profile of the rebar surface which may be result of hydrostatic pressure of the hardened concrete or expansion of FRP bar due to temperature and moisture change. It was found that the contribution from chemical adhesion is very low in case of FRP bar. Major contribution comes from friction, with mechanical interlock for specific deformed rebar type. To prevent bond failure the rebar

must be embedded deep enough into concrete and should have sufficient confinement provided by the concrete.

There are several factors that affect the bond behavior between FRP rebar and concrete. These factors can be categorized in to three major group; i) bar properties (bar diameter, bar surface condition, fibre type), ii) concrete properties (compressive strength, presence of steel fibres), iii) structural properties (concrete cover, bar spacing, embedment length, bar casting position, transverse reinforcement).

The effect of concrete compressive strength on bond performance of FRP rebar was studied by many researchers (Ametrano 2011; Baena et al. 2009; Chaallal and Benmokrane 1993a; Nanni et al. 1995; Rossetti et al. 1995). Those studies were conducted with the concrete of 30 MPa to 79 MPa in compressive strength and with density range 2380 kg/m^3 to 2580 kg/m^3, and in some case (Ametrano 2011) as high as 175 MPa. Those studies found that bond strength increased with the increase in compressive strength. However, at low compressive strength ($f'c \approx 30$), bond failure mechanism varies with compare to higher compressive strength.

In this study, the bond strength of FRP bar with concrete of low compressive strength (in the range of 7 MPa to 42 MPa) and low density (as low as 1400 kg/m^3) was examined.

6.3 Objective

The objective of this study was to evaluate bond performance of sand coated glass fibre reinforce polymer bars embedded in concrete, where crumb rubber was used as replacement of fine aggregates, using beam tests. Due to stress state in the surrounding concrete, beam tests provide more realistic bond strength. As mentioned in Chapter 3, the variation in crumb rubber replacement produces concrete mixes with different compressive strength. In addition to that, the effect of short steel fibres on bond was observed by incorporating 1% fibre dosage (by volume) in identical mixes. The variable parameters that were used to determine the bond behavior included: compressive strength by varying fine aggregate replacement level with crumb rubber, bar diameter, and the presence of short steel fibres. Three different dosage of

fine aggregate replacement with crumb rubber were identified, which were 0%, 50% and 100%. These three percentages were chosen so that full spectrum of fine aggregate replacement with crumb rubber can be examined. The mechanical properties and other characteristics of these mixes were determined in Chapter 3. Two different bar sizes (10mm and 16mm) were used to observe the effect of bar diameter on the bond performance. Considering plain and short steel fibre concrete, in total 6 concrete mixes were used with two different bar sizes (Table 6-1). In total 12 beam tests were carried out to study the bond behavior of GFRP rebar. Later, the bond performance from beam tests were compared with the results as obtained in pullout tests from Chapter 4.

6.3.1 Beam specimen geometry and configuration

The beam geometry was based on the beam test recommendation established by RILEM/CEB/FIP (1994). In beam tests, the surrounding concrete of rebar is under tensile stress which represents the realistic stress distribution of structural elements (Hamza and Naaman 1991; Larrard et al. 1993). As a result, the bond strength derived from beam tests give more realistic value to actual bond performance of concrete and FRP bar. In their recommendation, two beam types are mentioned which are dependent on the diameter of the rebar. The test beams consisted of two rectangular reinforced concrete blocks joined at the top by a steel hinge and at the bottom by a GFRP reinforcement bar. The beam geometry used in the present research for 10 mm and 16 mm rebars were shown in Figure 6-1. The hinges used in the beam tests are shown in Figure. 6-2. Auxiliary reinforcements were also used to prevent shear failure of the specimen. The auxiliary reinforcements are consisted of plain mild steel bars and their detailing was given in Figure. 6-3. Reinforcing cages were produced using three layers of longitudinal steel reinforcement with five evenly spaced closed stirrups. The longitudinal steel reinforcement was 5/16” (7.94 mm) in diameter and the transverse reinforcement was 1/4” (6.35 mm) in diameter. The beams were cast in the flat position. The concrete was cast and vibrated by means of a vibrating table.

6.3.2 Test setup and procedure

The beam tests were carried out as specified according to the recommendation by RILEM/CEB/FIP (1994). The beams were loaded in bending by two equal forces applied

symmetrically on either side of the steel hinge. The locations of the supports and load applications were placed as indicated in Figure 6-1. The slips at the free ends of reinforcing bars were measured using two LVDTs. The complete test setup is shown in Figure 6-4. A MTS machine has been used for the test purpose. A built-in data acquisition system was used to record data from the two load cells, two linear variable displacement transducers (LVDTs) and frame displacement.

6.4 Results and analysis

Assuming uniform bond stress distribution for each test specimen, the mean bond stress over the embedment length was determined by following Equation (6.1),

$$\tau = \frac{P}{\pi l_e d_b} \tag{6.1}$$

where, τ = average bond stress (MPa); P = axial tensile force in the rebar, le = embedment length of rebar (mm); d_b = rebar diameter (mm).

The bar diameter used in Equation (6.1) was determined by averaging 10 diameter readings measured with a micrometer accurate to 0.001 mm for each GFRP bar. The sand coating was included in the measurement since it affects the concrete surface area in contact with the GFRP bar.

Based on the geometry of the beam specimens, the locations of the applied loads, and supports (Figure 6-1), the tensile load in the GFRP rebar was determined by the following expression:

$$P = 1.25 \cdot F \tag{6.2}$$

Where, P was the tensile load exerted on the FRP rebar, and F was the applied load determined by the load cell. The detailed derivation of the Equation (6.2) was included in Appendix VI.

The friction, adhesion and surface bearing between FRP bar and surrounding concrete are the major contributors to the bond strength between FRP bar and concrete, though surface bearing

in negligible in case of sand grained GFRP bar. Very small free end slip was observed at the peak bond stress which indicates that the FRP bar surface experienced insignificant movement relative to the surrounding concrete. After reaching the peak the bond strength decreases suddenly and significant slip occurs. This indicated that the sand coated GFRP bar exhibited brittle bond failure. After that the bond stress decreased gradually to the residual frictional bond resistance. A constant bond stress plateau was observed in all cases bar sizes and concrete mixes. This flat plateau represents the bond resistance generated from the friction between FRP bar and concrete. All of the beam tests in this study exhibited the pullout mode of failure except the beam with 16mm in the mixes of 0% crumb rubber without fibre. No visual signs of splitting, shear, or moment cracks were observed on any of the beam test specimens.

The effect of crumb rubber, the bar diameter and the short steel fibre on the bond performance was investigated through the beam tests. The bond strength was also expressed with normalizing after compressive strength of the concrete mixes.

The bond strength was significantly affected by the tensile strength of concrete (Baena et al. 2011; Benmokrane et al. 1996; Chaallal and Benmokrane 1993a). This is addressed by various code provisions for determining bond strength where concrete compressive strength is modified to represent the concrete tensile strength. However, in this research the bond test values were compared directly as some of the concrete mixes contain short steel fibre. Steel fibres change the tensile properties of concrete significantly. Hence, comparing bond strength of concrete mixes with and without steel fibre based on normalized value won't eliminate the effect of compressive strength.

The summary of the results are presented in Table 6-2. The values are the average of two sets of data derived from each side of the beam.

6.4.1 Effect of rubber content on the bond strength

From the reported results in Table 6-2 it was observed that bond strength decreases with increase in crumb rubber replacement for all bar sizes and steel fibre volume. For the mixes without steel fibre, this reduction is 73% and 90% for 10mm bar whereas for 16mm bar this

reduction is 56% and 78% for 50% and 100% replacement with rubber. For the mixes with steel fibre the reductions are 30% and 53% for 10mm bar, 29% and 61% for 16mm bar for crumb rubber replacement of 50% and 100% respectively. This strength loss is due to the lower density of the concrete mixes with increase in crumb rubber replacement. The crumb rubber is much lighter with compare to sand. Hence, more sand replaced by crumb rubber results lesser density mixes. The lower density mixes exert lower resistance against the adhesion and friction between rebar and concrete mixes which yields lower bond strength. Also due to the difference in their stiffness crumb rubber particles deform more than the surrounding cement paste under the load. This results in micro-crack formation which causes weak bond between rubber and cement paste. The complete bond-slip responses for various concrete mixes with different bar sizes are presented in Figure 6-5 to 6-8.

6.4.2 Effect of bar diameter on the bond strength

Many studies were done to evaluate the effect of bar sizes on the bond strength of GFRP bar in concrete mixes with different ranges of compressive strength (Achillides and Pilakoutas 2004; Benmokrane et al. 1996; Cosenza et al. 1997; Nanni et al. 1995; Tepfers 2006; Tighiouart et al. 1998). Among all the studies there was a general trend for larger rebar diameter to have lower bond strength. Similar observations were recorded in this study. The bond strength of two bar diameters without steel fibre are shown in Figure 6-9 to 6-11 while that with steel fibre reinforced concrete mixes are shown in Figure 6-12 to 6-14. It was observed that the bond strength decreases with an increase in bar size for all concrete mixes both with and without steel fibres.

For mixes without steel fibres, 16mm bar showed 55%, 25% and 4% decrease in bond strength with compare to 10mm bar, for 0%, 50% and 100% rubber respectively. This was due to the greater amount of bleed water, which became trapped beneath larger diameter bars producing voids, reducing the contact area between the concrete and the rebar thus lowering its bond capacity. For the mixes with lower crumb rubber the amount of bleed water is higher which in turns affect the bond strength.

Again, for mixes with steel fibre, 16mm bar showed 11%, 10% and 27% reduction in bond strength when compared with 10mm bar, for 0%, 50% and 100% rubber content respectively. The reduction is less prominent for the plain concrete. This is due to the fact that steel fibre itself disturb the contact surface between FRP bar and concrete and the amount of trapped bleed water underneath the larger bar size doesn't depends on the crumb rubber replacement level.

6.4.3 Effect of short steel fibre

To evaluate the effect of short steel fibre the results for mixes without steel fibre are compared with the similar mixes where 1% volume fraction of steel fibres were added. The variation of bond-slip performance with and without steel fibre for different bar sizes and crumb rubber percentages are presented in Figure 6-15 to 6-20.

In case of 10mm bar, the presence of steel fibres has a negative impact on the bond strength for 0% and 50% rubber content mixes. For the mix with no rubber replacement, addition of steel fibre reduced the bond strength by 67%, whereas this reduction is 13% for mixes with 50% crumb rubber. For 100% rubber replacement an increase in bond was observed with the addition to steel fibre.

For the specimens with 16mm bar, 35% reduction in bond strength for mix with no rubber, 4.5% increase in bond strength for mix with 50% rubber content and 17% increase in bond strength with 100% crumb rubber replacement was observed.

Whereas in case of steel rebars, it is well known that steel fibres in the concrete will enhance the bond performance, in the present study, it was found that steel fibres led to a drop in the bond strength at lower rubber content. Once again, noting that the predominant stress-transfer mechanism was through friction, the drop in case of steel fibre reinforced concrete maybe attributed to the interference in the surrounding matrix caused by the presence of fibres. This interference is likely more dramatic in case of a smaller bar diameter. Also, for higher strength concrete, this disruption is more prominent and hence a decrease in bond strength occurs. The presence of steel fibre may incorporate voids at the FRP bar-concrete interface. Hence proper

bonding can't be developed which caused lower adhesion and lower friction and thus generate lower bond strength.

6.4.4 Comparison with pullout test results

In the previous Chapter 4, bond tests were performed using pullout tests. In the pullout tests the concrete surrounding the reinforcing bar is under compression. Hence, the possibility of cracking is reduced and thus there is an increase in the bond strength (Benmokrane et al. 1996); whereas, in beam tests the concrete surrounding the reinforcement bars is under flexural tensile stress. This causes cracks in the concrete at low stresses and hence reducing bond strength even though it has transverse reinforcement.

The comparison of the bond strength for pullout tests and beam tests were shown in Figure 6-21 to 6-24. For 10 mm bar in fibre reinforced concrete and 16 mm bar in both plain and fibre reinforced concrete showed lower bond strength in beam tests. In the case of 10 mm bar in fibre reinforced concrete, 6% to 10% reductions were observed. However, much larger reduction (24% to 48%) was found in case of 16 mm bar in plain and fibre reinforced concrete. In their study Benmokrane et al. (1996) also found similar results where they obtained 5 to 82% higher bond strength in pullout tests with compare to beam tests depending on the reinforcing bar diameter. This bond strength reduction in beam test was also observed for steel reinforcement in normal weight concrete. Soretz (1972) found that the maximum bond strength from beam tests was approximately 63 to 96 percent of that from pullout tests depending on steel reinforcement bar diameter.

The bond strength reduction for beam tests in case of 16 mm was found to be more prominent compared to 10 mm bar. In the pullout tests for bond, it was observed that in general, the free end slips at maximum bond stress were higher for 16 m bar specimens with compare to 10 mm bar specimen for almost all rubber content in the study. The comparison of free end slip at maximum bond stress for plain and fibre reinforced concrete were shown in Figure 6-25 and 6-26 respectively. This trend of higher slip values for 16 mm bar diameter was one of the reasons for having lower bond stress in beam specimens. Typically it was observed that the

pullout specimen with smaller bar sizes experienced higher bond stress for a given slip value less than the corresponding slip at maximum bond stress for smaller bar specimen Figure 6-27 and 6-28. In other word, at relatively small slip, specimen with 10 mm bar sizes demonstrated higher bond stress with compared to the specimens with 16 mm bar. In the beam specimen for bond tests, maximum bond stress was reached at relatively short slip. Hence, smaller bar sizes have greater bond with compare to larger bar sizes when beam specimens were considered. Moreover, in the beam specimen for bond tests, flexural cracks developed at very low stress. As a result the frictional component of bond strength was affected. Due to larger contact area with surrounding concrete, 16 mm bar diameter experienced significant bond strength reduction with compare to 10 mm bar diameter. In addition to that, in beam specimen substantial amount of bleed water trapped beneath the reinforcement, which generates voids and reduce contact area between the concrete and reinforcement (Tighiouart et al. 1998). For larger bar diameter this interference is more prominent with compare to smaller bar, hence significant bond strength reduction for beam tests with 16 mm bar was observed.

6.5 Conclusion

In this chapter the interfacial bond between FRP and different kinds of concrete mixes were analyzed from the results obtained through beam tests. The following conclusion can be drawn:

1. Adhesion and friction are the major contributor for the bond between FRP bar and concrete. After the loss of adhesion, the friction between FRP bar and concrete provides the residual bond strength.
2. In the presence of crumb rubber, the bond strength between FRP bar and concrete decrease with an increase in the crumb rubber replacement. This is due to lower compressive strength and lowered unit weight of the mixtures with higher crumb rubber replacement. Lower density mixtures exert lower resistance to adhesion and friction between FRP rebar which yields lower bond resistance.
3. The presence of short steel fibres has a negative impact on the bond strength between lightweight concrete and FRP bar at lower rubber content mixes. This is likely due to the

fibres interfering with the surrounding matrix and thus adversely affecting the friction between the bar and concrete.

4. The bond strength in case of larger bar diameter was lower than that for the smaller diameter. The presence of flexural cracks and presence of bleed water affect the contact surface between concrete and GFRP bar and yield lower bond strength.

6.5.1 Limitations of the study

This study was focused on the bond between concrete mixes with crumb rubber as fine aggregate replacement and sand coated GFRP bars. Concrete mixes with rubber as coarse aggregate replacement wasn't evaluated in this study. Bar size effect on bond strength was done with only two different bar sizes (10 mm and 16 mm). In addition to that, this study examined the effect of short fibres on the bond performance. This was done by using only steel fibres in the mixes, no other fibre types were considered in this study. Concrete mixes with low modulus fibres i.e. polypropylene fibres, may be used for bond performance evaluation. Again, only one dosage of fibre volume was applied in the mixes.

Tables

Table 6-1: Proportions of different concrete mixes

GFRP Rebar	Diameter Including Sand Coating
10mm	10.226mm
16mm	16.744mm

Table 6-2: Experimental results

Specimen	Bar Diameter	τ_{max} (MPa)	Failure Type
CR0F0	10mm	18.74	P
CR50F0		5	P
CR100F0		1.88	P
CR0F1		6.16	P
CR50F1		4.32	P
CR100F1		2.89	P
CR0F0	16mm	8.44	-
CR50F0		3.71	P
CR100F0		1.794	P
CR0F1		5.46	P
CR50F1		3.88	P
CR100F1		2.11	P

τ_{max}= Bond strength, P = Pullout Failure

Figure

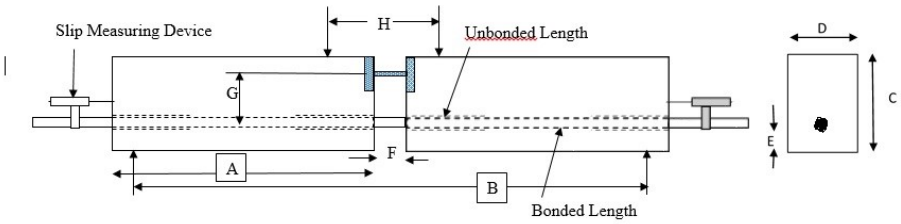

Figure 6-1: Beam geometry

A = 375mm

B = 650mm

C = 180mm

D = 100mm

E = 50mm

F = 50mm

G = 100mm

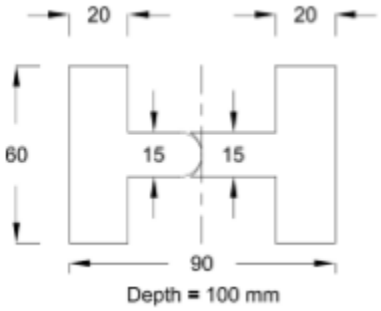

Figure 6-2: Dimension of steel hinges used in the beam

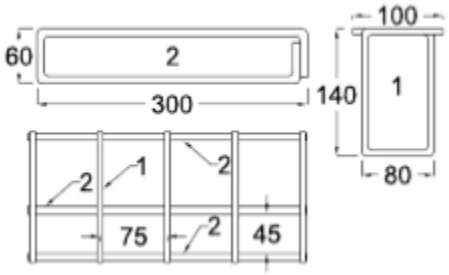

Figure 6-3: Details of reinforcement used in the beams

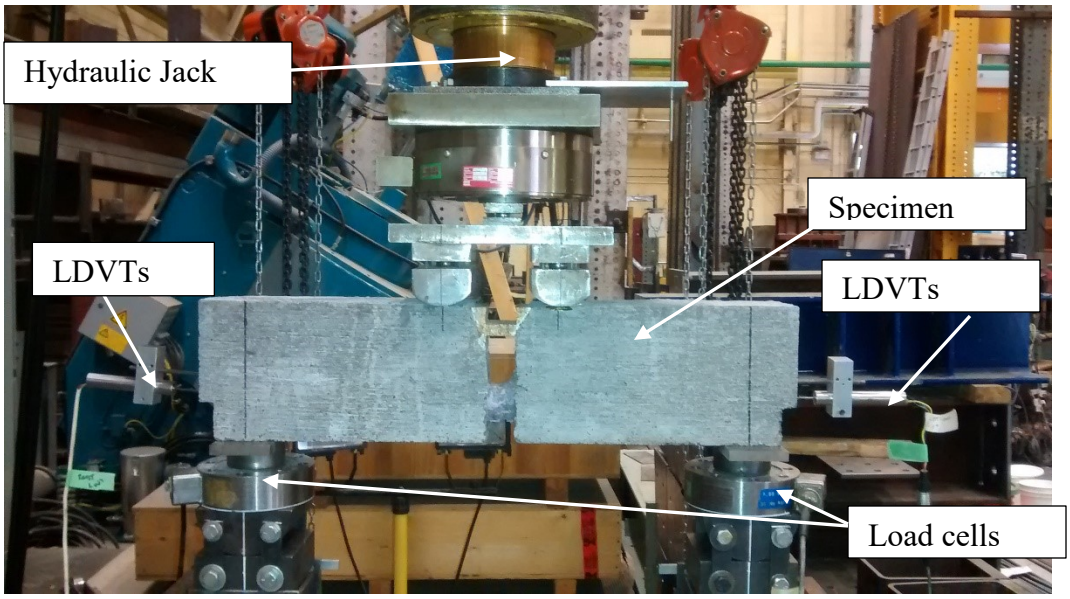

Figure 6-4: Test setup for beam test

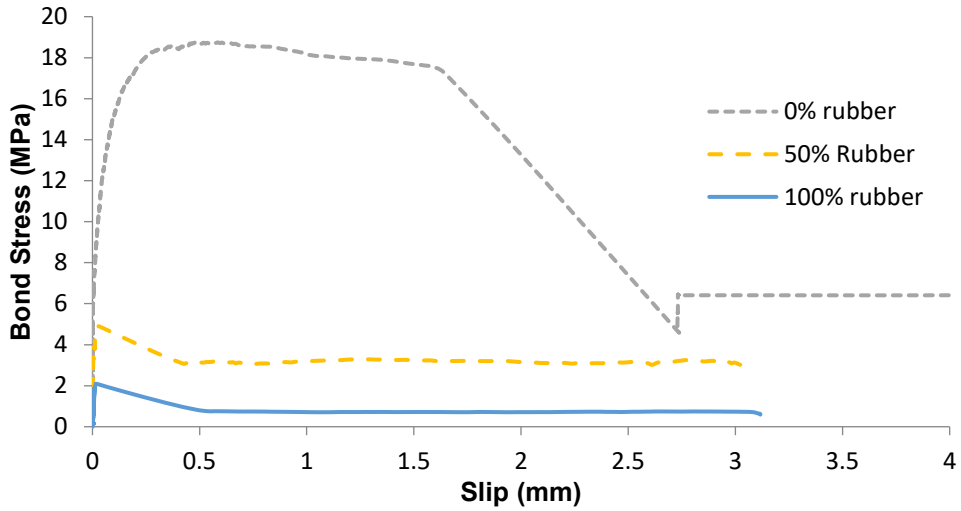

Figure 6-5: Bond slip response of 10mm bar with 0% fibre

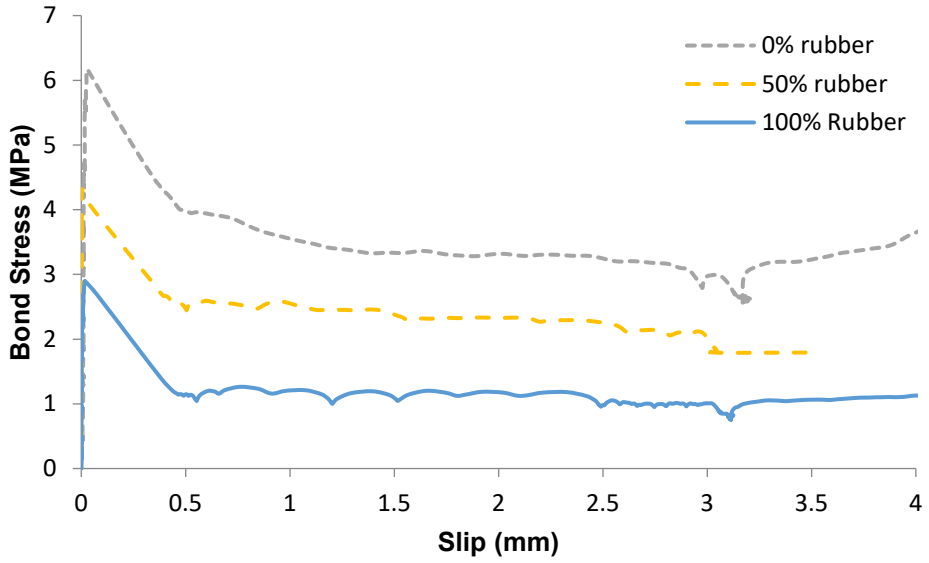

Figure 6-6: Bond slip response of 10mm bar with 1% fibre

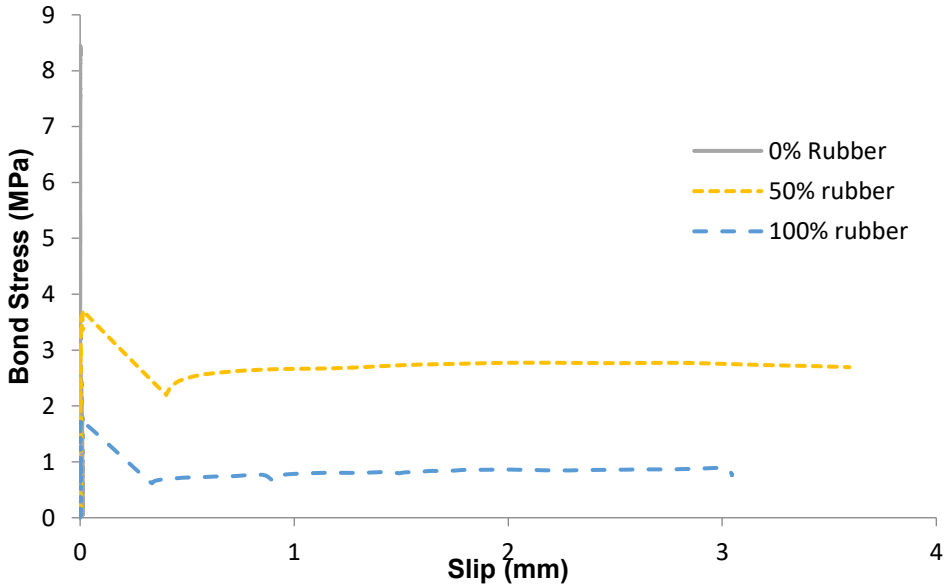

Figure 6-7: Bond slip response of 16mm bar with 0% fibre

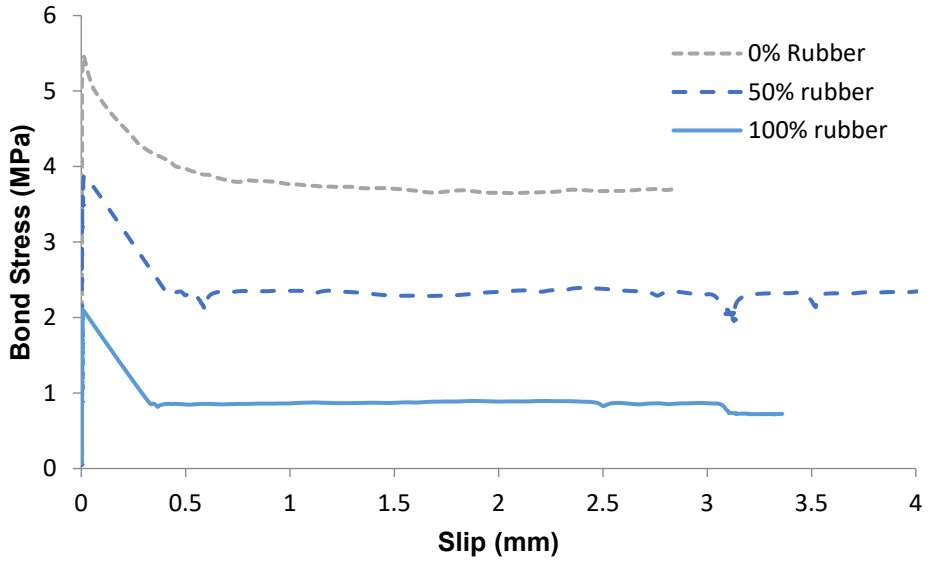

Figure 6-8: Bond slip response of 16mm bar with 1% fibre

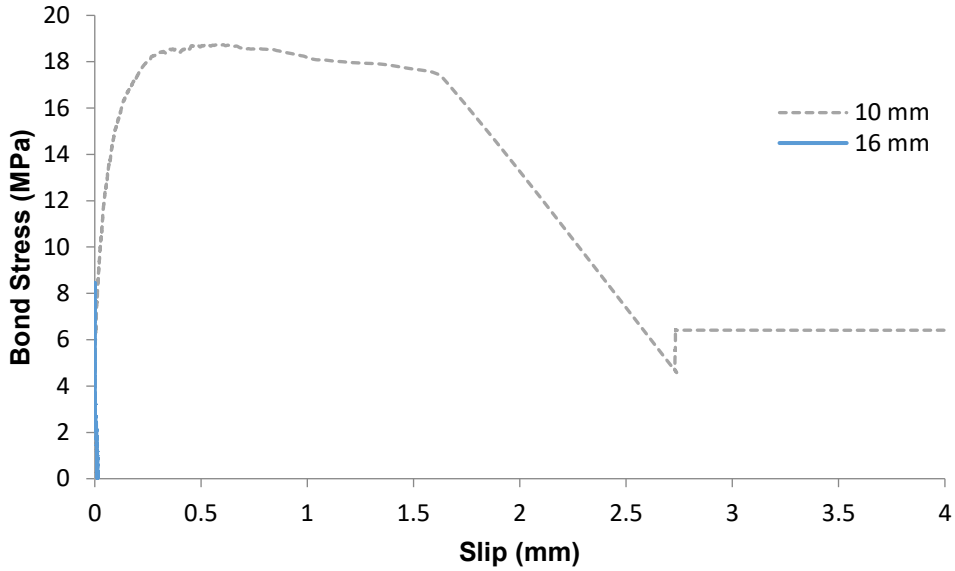

Figure 6-9: Comparison of Bond slip response of various bar sizes for plain concrete with 0% crumb rubber replacement

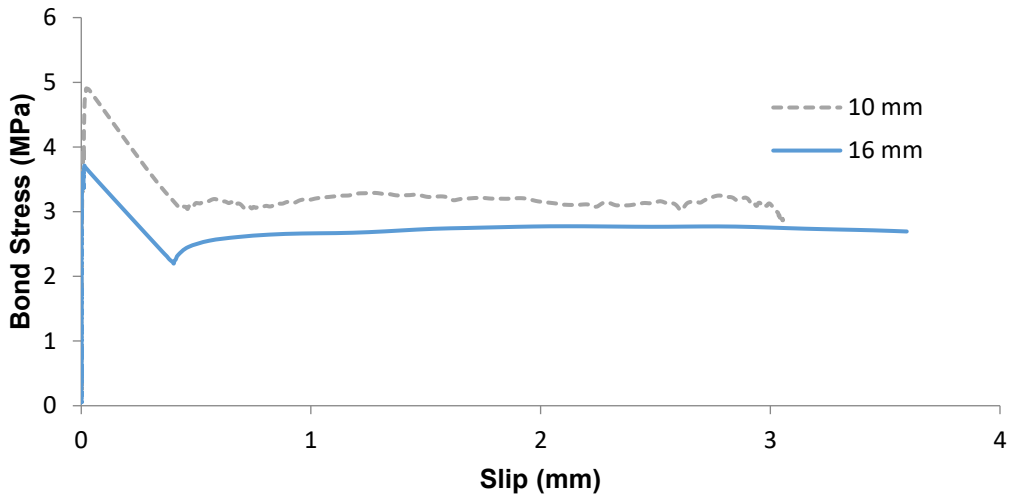

Figure 6-10: Comparison of Bond slip response of various bar sizes for plain concrete mixes with 50% crumb rubber replacement

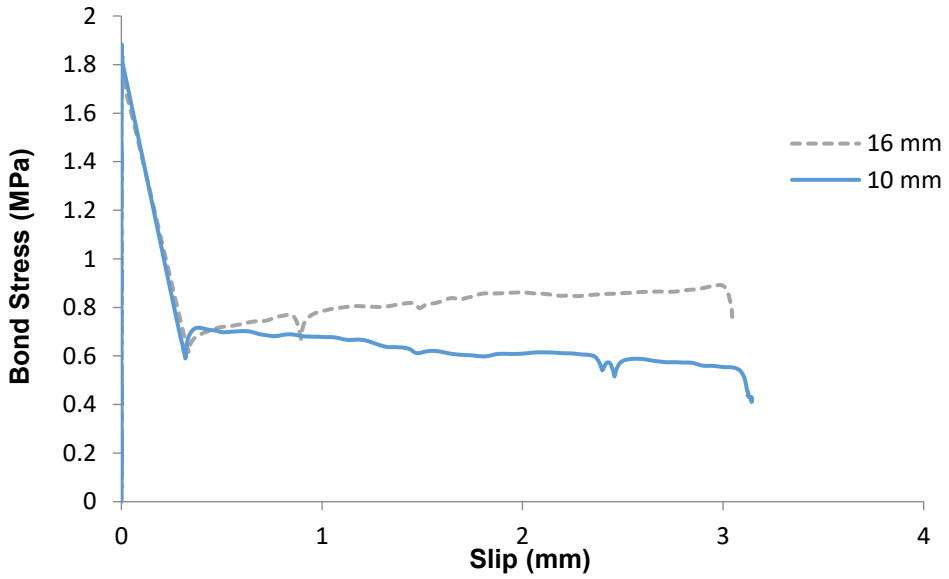

Figure 6-11: Comparison of Bond slip response of various bar sizes for plain concrete mixes with 100% crumb rubber replacement

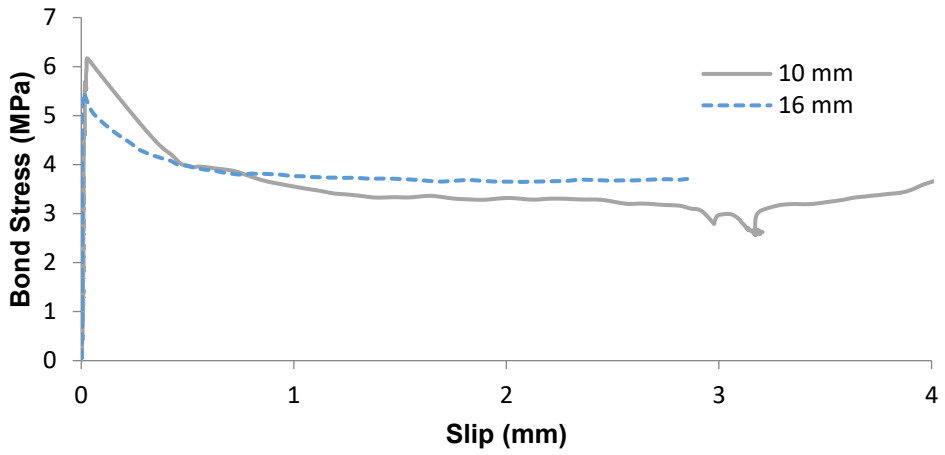

Figure 6-12: Comparison of Bond slip response of various bar sizes for concrete mixes with 1% fibre and with 0% crumb rubber replacement

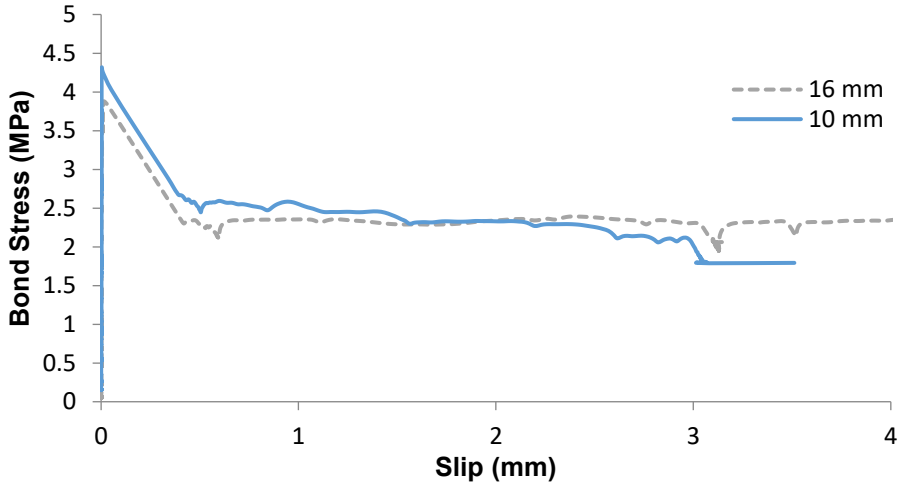

Figure 6-13: Comparison of Bond slip response of various bar sizes for concrete mixes with 1% fibre and 50% crumb rubber replacement

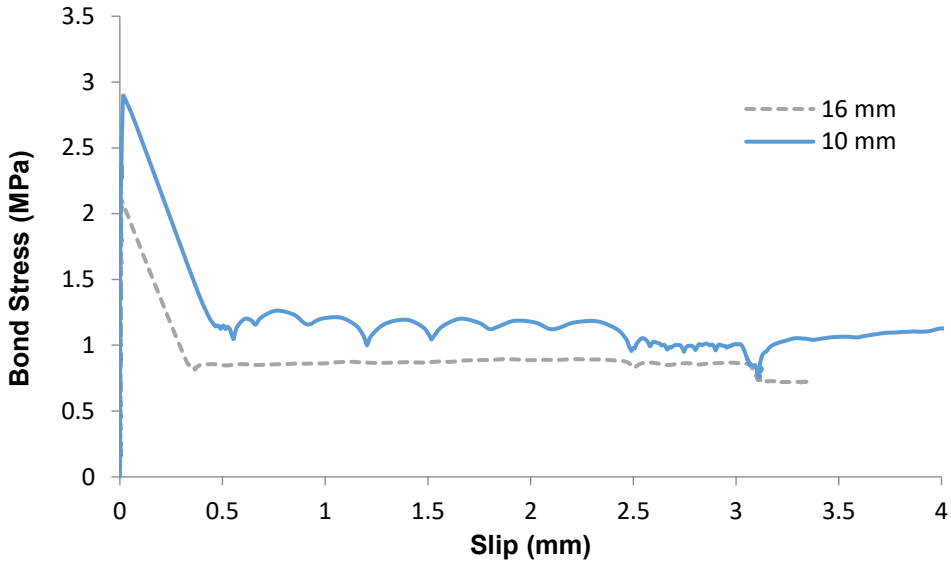

Figure 6-14: Comparison of Bond slip response of various bar sizes for concrete mixes with 1% fibre and 100% crumb rubber replacement

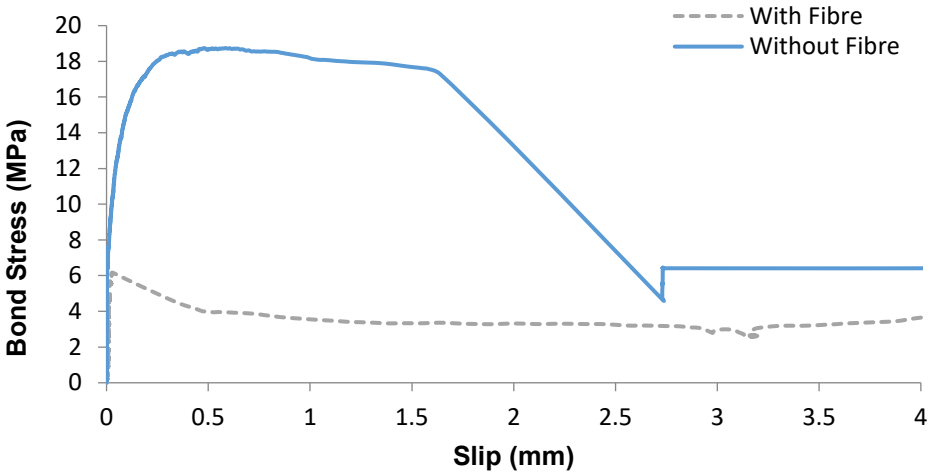

Figure 6-15 Comparison of Bond slip response of mixes of different fibre contents with 10mm bar and 0% crumb rubber replacement

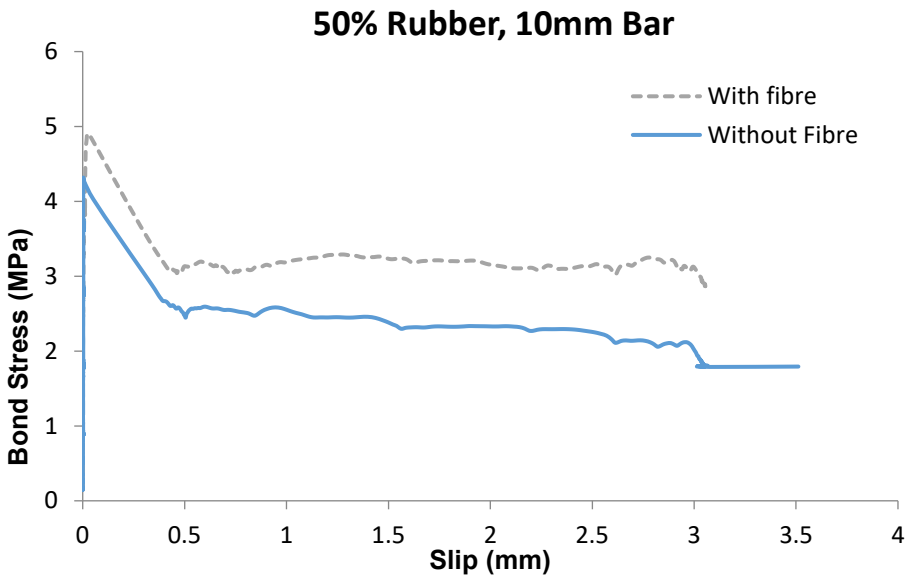

Figure 6-16 Comparison of Bond slip response of mixes of different fibre contents with 10mm bar and 50% crumb rubber replacement

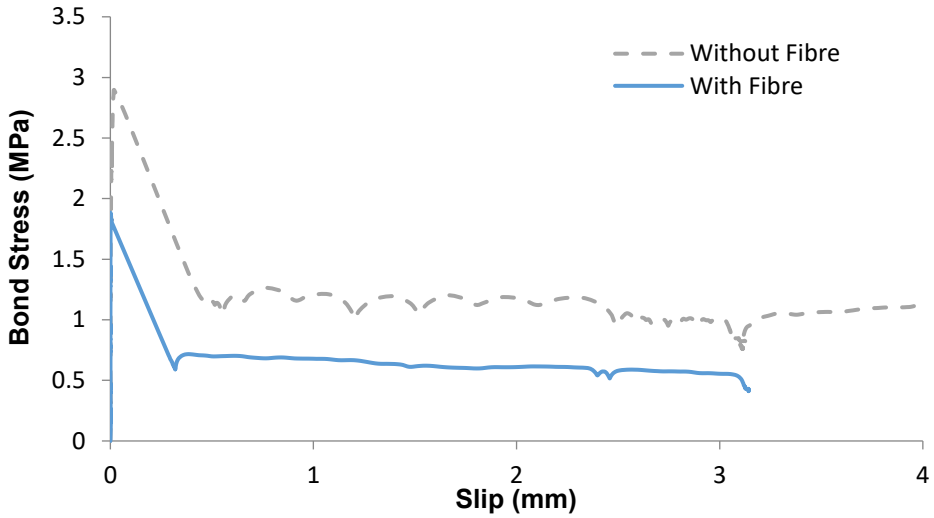

Figure 6-17 Comparison of Bond slip response of mixes of different fibre contents with 10mm bar and 100% crumb rubber replacement

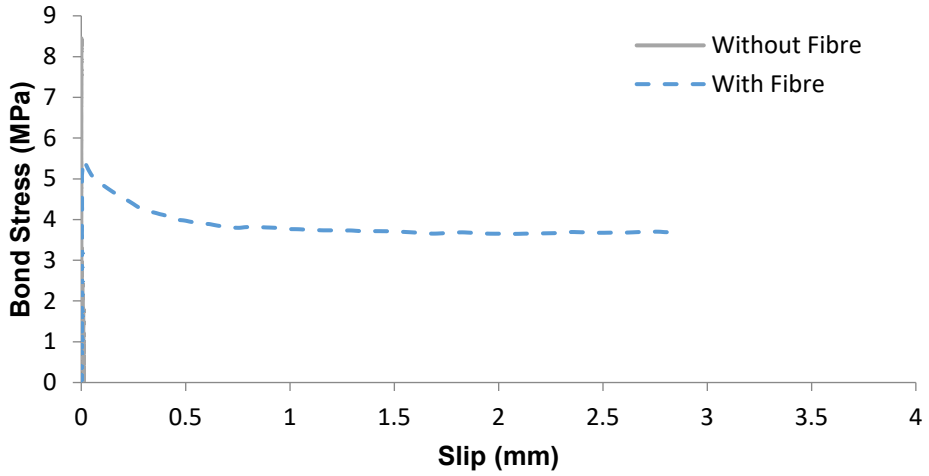

Figure 6-18 Comparison of Bond slip response of mixes of different fibre contents with 16mm bar and 0% crumb rubber replacement

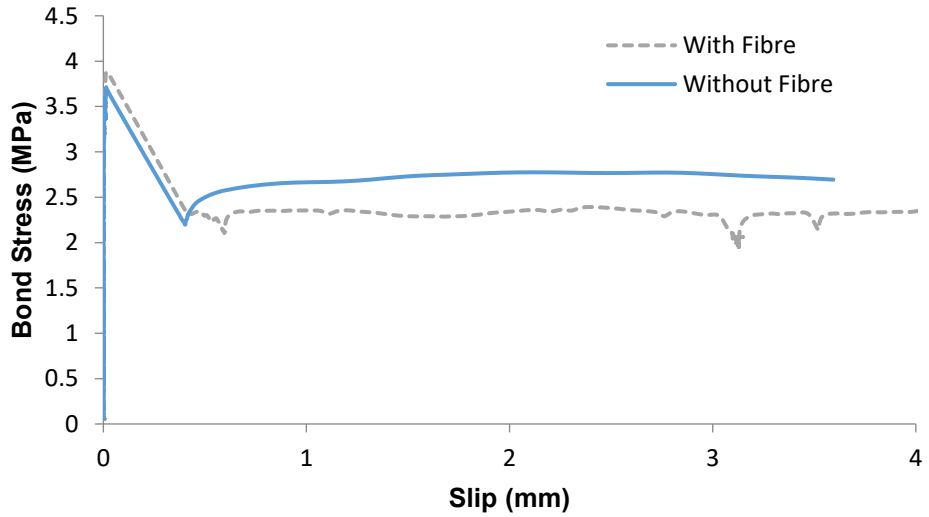

Figure 6-19 Comparison of Bond slip response of mixes of different fibre contents with 16mm bar and 50% crumb rubber replacement

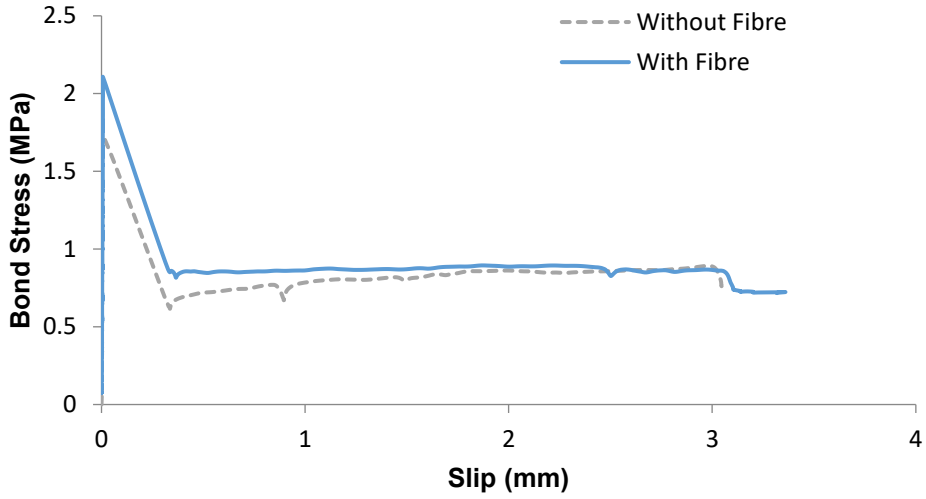

Figure 6-20 Comparison of Bond slip response of mixes of different fibre contents with 16mm bar and 100% crumb rubber replacement

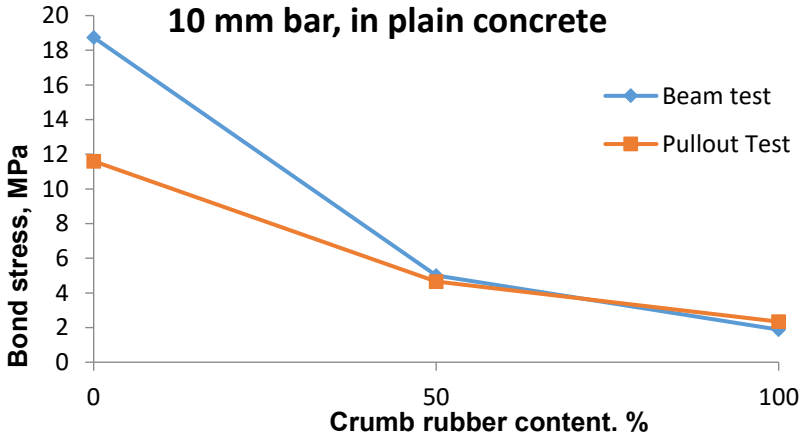

Figure 6-21 Comparison of beam test and pullout test results for 10 mm bar in plain concrete

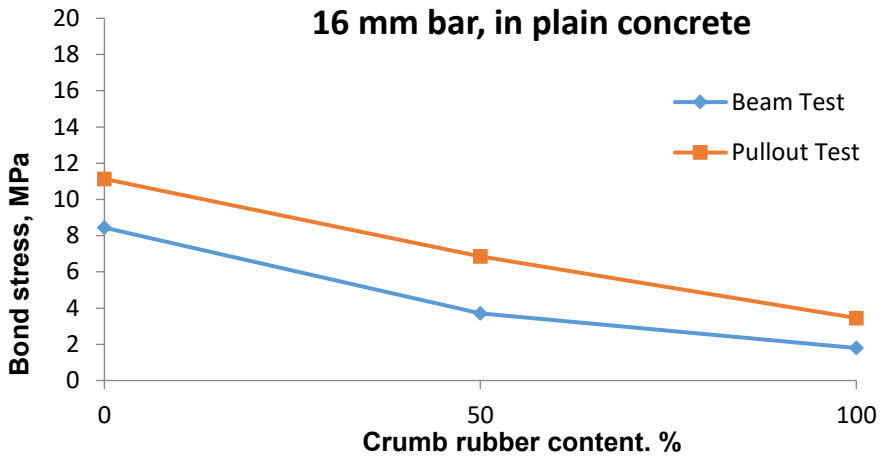

Figure 6-22 Comparison of beam test and pullout test results for 16 mm bar in plain concrete

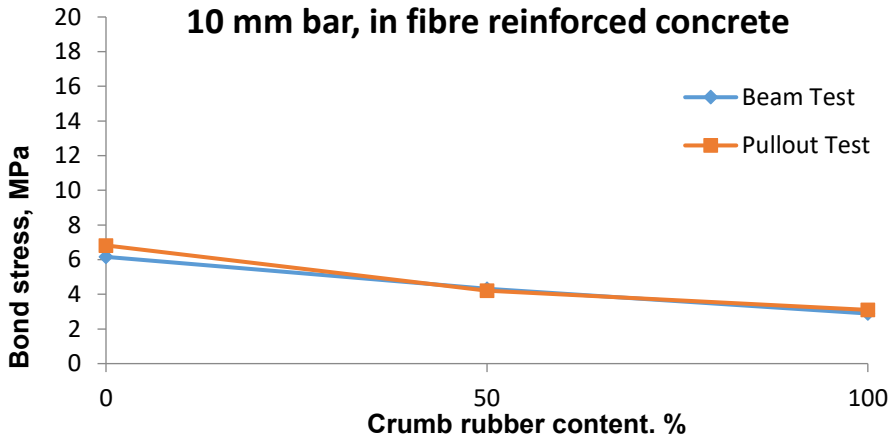

Figure 6-23 Comparison of beam test and pullout test results for 10 mm bar in reinforced concrete

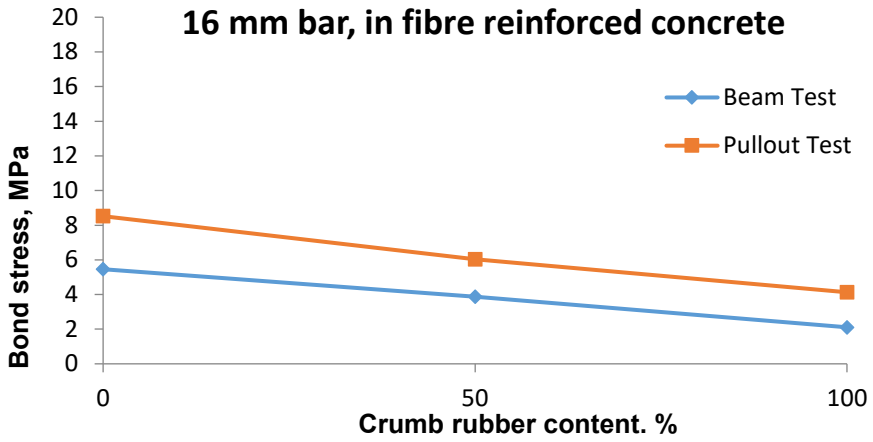

Figure 6-24 Comparison of beam test and pullout test results for 16 mm bar in fibre reinforced concrete

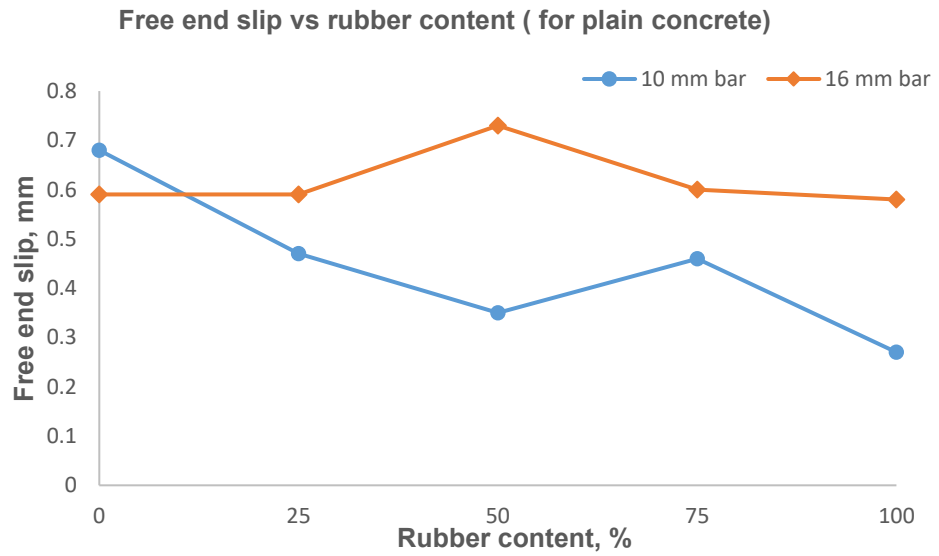

Figure 6-25 Comparison of free end slips for plain concrete

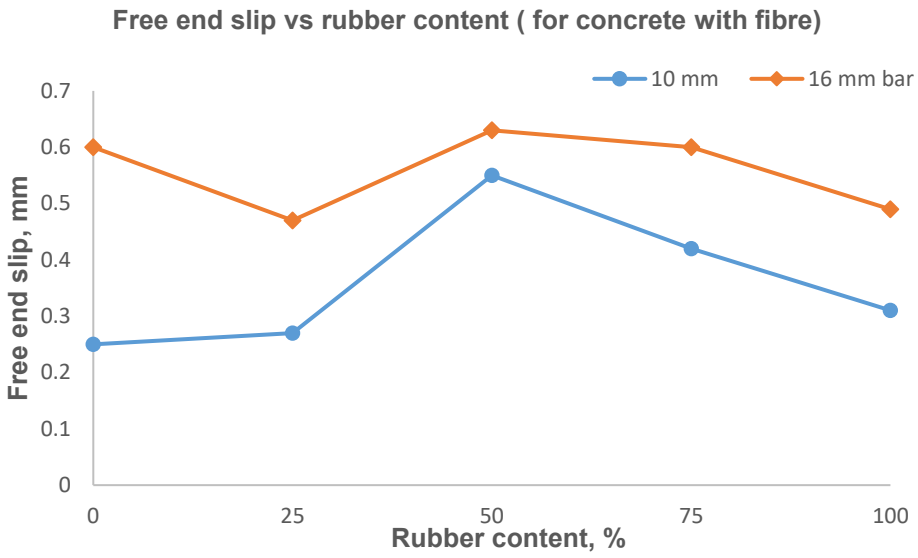

Figure 6-26 Comparison of free end slip for fibre reinforced concrete

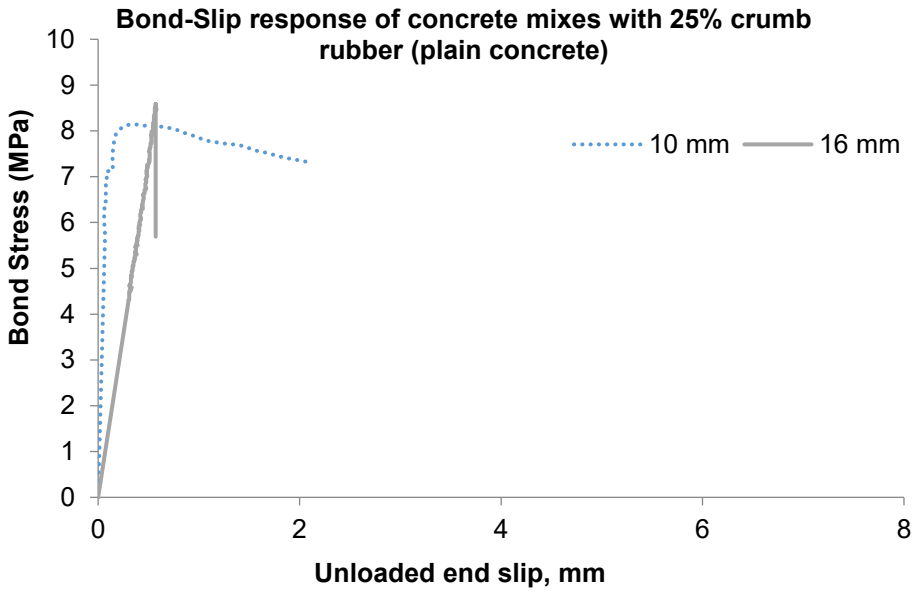

Figure 6-27 Comparison of bond-slip response of concrete mixes with 25% crumb rubber (plain concrete)

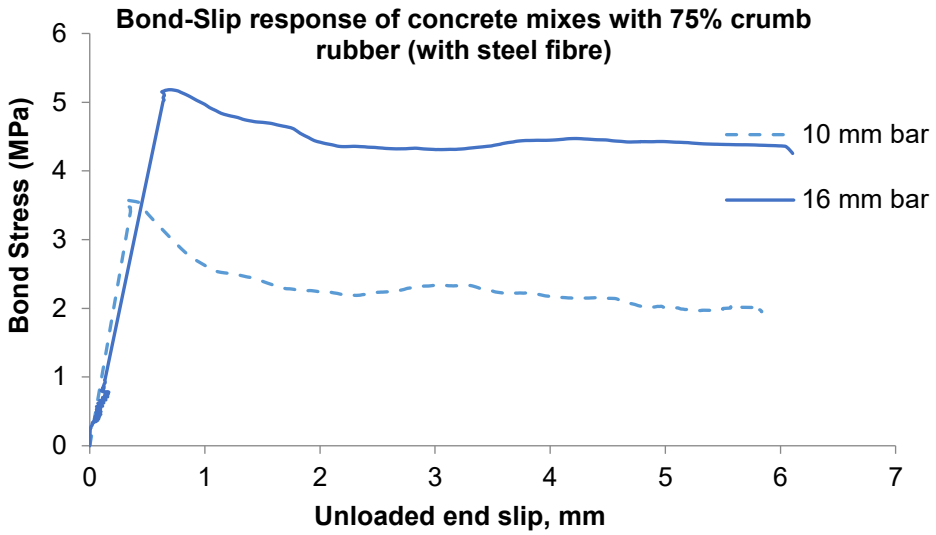

Figure 6-28 Bond-slip response of concrete mixes with 75% crumb rubber (fibre reinforced concrete)

References

Achillides, Z., and Pilakoutas, K. (2004). "Bond behavior of fiber reinforced polymer bars under direct pullout conditions." *Journal of Composites for construction*, 8, 173.

Al-Zahrani, M. M., Al-Dulaijan, S. U., Nanni, A., Bakis, C. E., and Boothby, T. E. (1999). "Evaluation of bond using FRP rods with axisymmetric deformations." *Construction and Building Materials*, 13(6), 299–309.

Ametrano, D. (2011). "Bond characteristics of glass fibre reinforced polymer bars embedded in high performance and ultra-high performance concrete." *Ryerson University, Toronto, Ontario, Canada*, 1–132.

Baena, M., Torres, L., Turon, A., and Barris, C. (2009). "Experimental study of bond behaviour between concrete and FRP bars using a pull-out test." *Composites Part B: Engineering*, 40(8), 784–797.

Baena, M., Turon, A., Torres, L., and Miàs, C. (2011). "Experimental study and code predictions of fibre reinforced polymer reinforced concrete (FRP RC) tensile members." *Composite Structures*, 93(10), 2511–2520.

Benmokrane, B., Tighiouart, B., and Chaallal, O. (1996). "Bond strength and load distribution of composite GFRP reinforcing bars in concrete." *ACI Materials Journal*, 93(3).

CEB-FIP. (1994). *Test of the Bond Strength of Reinforcement of Concrete: Test by Bending.* RILEM Recommendations for the Testing and use of Constructions Materials,.

Chaallal, O., and Benmokrane, B. (1993). "Pullout and bond of glass-fibre rods embedded in concrete and cement grout." *Materials and structures*, 26(3), 167–175.

Cosenza, E., Manfredi, G., and Realfonzo, R. (1997). "Behavior and modeling of bond of FRP rebars to concrete." *Journal of composites for construction*, 1(2), 40–51.

Duval, R., and Kadri, E. H. (1998). "Influence of Silica Fume on the Workability and the Compressive Strength of High-Performance Concretes." *Cement and Concrete Research*, 28(4), 533–547.

Eldin, N., and Senouci, A. (1993). "Rubber-Tire Particles as Concrete Aggregate." *Journal of Materials in Civil Engineering*, 5(4), 478–496.

Güneyisi, E., Gesoğlu, M., and Özturan, T. (2004). "Properties of rubberized concretes containing silica fume." *Cement and Concrete Research*, 34(12), 2309–2317.

Hamza, A. M., and Naaman, A. E. (1991). "Bond Strength of Reinforcing Bars in SIFCON." ASCE, 1071–1075.

Kanakubu, T., Yonemaru, K., Fukuyama, H., Fujisawa, M., and Sonobe, Y. (1993). "Bond Performance of Concrete Members Reinforced With FRP Bars." *Special Publication*, 138, 767–788.

Khatib, Z., and Bayomy, F. (2013). "Rubberized Portland Cement Concrete." *Journal of Materials in Civil Engineering*, 11(3), 206–213.

Larralde, J., and Silva-Rodriguez, R. (1993). "Bond and Slip of FRP Rebars in Concrete." *Journal of Materials in Civil Engineering*, 5(1), 30–40.

Larrard, F. D., Shaller, I., and Fuchs, J. (1993). "Effect of the Bar Diameter on the Bond Strength of Passive Reinforcement in High-Performance Concrete." *Materials Journal*, 90(4), 333–339.

Makitani, E., Irisawa, I., and Nishiura, N. (1993). "Investigation of Bond in Concrete Member With Fiber Reinforced Plastic Bars." *Special Publication*, 138, 315–332.

Malvar, L. J. (1994). *Bond Stress-Slip Characteristics of FRP Rebars.* Office of Naval Research, naval Cailities Engineering Service Center, port Hueneme, California.

Najim, K. B., and Hall, M. R. (2012). "Mechanical and dynamic properties of self-compacting crumb rubber modified concrete." *Construction and Building materials*, 27(1), 521–530.

Nanni, A., Al-Zaharani, M. M., Al-Dulaijan, S. U., and Bakis, C. E. (1995). "Bond of FRP reinforcement to concrete - Experimental results." Non-metallic (FRP) reinforcement for concrete structures, L. Taerwe, ed., Spon, 135–145.

Rossetti, V. A., Galeota, D., and Giammatteo, M. M. (1995). "Local bond stress-slip relationships of glass fibre reinforced plastic bars embedded in concrete." *Materials and Structures*, 28(6), 340–344.

Soretz, S. (1972). “A comparison of beam tests and pull-out tests.” *Matériaux et Constructions*, 5(4), 261–264.

Tepfers, R. (2006). “Bond clause proposals for FRP bars/rods in concrete based on CEB/FIP Model Code 90. Part 1: Design bond stress for FRP reinforcing bars.” *Structural Concrete*, 7(2), 47–55.

Tighiouart, B., Benmokrane, B., and Gao, D. (1998). “Investigation of bond in concrete member with fibre reinforced polymer (FRP) bars.” *Construction and Building Materials*, 12(8), 453–462.

Topçu, lker B., and Avcular, N. (1997). “Analysis of rubberized concrete as a composite material.” *Cement and Concrete Research*, 27(8), 1135–1139.

Topçu, I. B. (1995). “The properties of rubberized concretes.” *Cement and Concrete Research*, 25(2), 304–310.

Zheng, L., Huo, X. S., and Yuan, Y. (2008). “Strength, Modulus of Elasticity, and Brittleness Index of Rubberized Concrete.” *Journal of Materials in Civil Engineering*, 20(11), 692–699.

Notations

τ = average bond stress (MPa);

P = axial tensile force in the rebar,

l_e = embedment length of rebar (mm);

d_b = rebar diameter (mm).

F = Applied load on the beam during testing

Appendix – VI

F = Total applied load on the beam

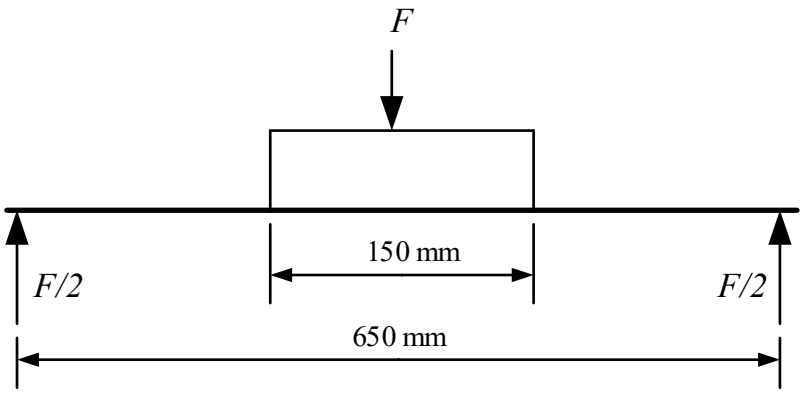

Reaction at each support = $F/2$ (due to loading symmetry)

Maximum Moment = $F/2 \times 250 = 125 \cdot F$

This moment is resisted by the couple between tensile force in the rebar T and compressive force, C. This tensile force is equal to the pullout force exerted in the bar, P

Resisting moment = T × moment arm = $100 \cdot P$

Hence, $100 \cdot P = 125 \cdot F$

$P = 1.25 \cdot F$

CHAPTER 7. STRESS RATE SENSITIVITY OF STEEL FIBRE REINFORCED LIGHTWEIGHT CONCRETE WITH CRUMB RUBBER

7.1 Introduction

Concrete is the most widely used building materials in the world, which has been used in a variety of structural elements. In addition to that, concrete has been used in some specialized applications where it experiences high loading rate including military and strategic structures as sacrificial component, rock bursting during mining operation, earthquake loads, impact loads during pile driving, air craft landing tarmacs, crash cushioning barriers in the roads etc. Typical strain rates occurring in various dynamic events are summarized in Table 7-1. Concrete used for crash cushioning barriers is one of the most important applications. Improving its crash cushioning capacity can play a major role in minimizing the loss of human life and economic resources resulting from a motor accident. Concrete crash cushioning road barriers have been in popular use over several decades. However, much remains to be improved including its impact resistance and energy absorption. At the same time, a key consideration in their manufacture and transport is their performance-to-weight ratio. In this chapter, the strain rate effect on the lightweight concrete mix that developed in Chapter 4 was presented. The purpose was two-fold namely, to achieve efficient material composition for shock absorption and at the same time to promote the disposal and reuse of scrap tires across Canada.

The potential use of crumb rubber as replacement of fine and/or course aggregate was studied by many researchers (Eldin and Senouci 1993; Khatib and Bayomy 1999; Topçu and Avcular 1997; Topçu 1995; Wong and Ting 2009; Zheng et al. 2008). The rubber aggregates can be loosely classified into four types depending on their particle size, shredded or chipped (the size representing the coarse aggregate), crumb rubber (typically between 4.75mm and 0.425mm), ground tire rubber (passing through No 40 sieve) and fibre rubber aggregate (short fibre typically between 8.5mm and 21.5mm in length as mentioned by (Najim and Hall 2012) and these are characterized as having negligible water absorption and low density (0.866 kg/m^3). All these studies were carried out on the concrete with normal weight aggregate. The use of rubber is seen to cause a reduction in both compressive and tensile strength of concrete (Eldin

and Senouci 1993; Khatib and Bayomy 1999) which is a big challenge to overcome to be able to incorporate rubber as a concrete constituent for wide range of application.

In order to overcome this strength loss, supplementary cementitious materials have been used with rubber aggregates in concrete with notable improvement due to silica fume and ground granulated blast furnace slag (Güneyisi et al. 2004; Wong and Ting 2009). Use of supplementary cementitious material is widely used method to improve various physical and mechanical properties of concrete. Previous studies (Detwiler and Mehta 1989; Ding and Li 2002; Hooton 1993; Mehta 1983; Mehta and Gjørv 1982) showed that silica fume as supplementary cementitious material improve mechanical properties by acting as filler and with pozzolanic reaction. Silica fume reduced bleed in fresh concrete and thus improved the density of transition zone between cement and coarse aggregate particle. Silica Fume also found to reduce pore sizes in concrete (Delage and Aitcin 1983; Mehta and Gjørv 1982) and completely eliminate 500 and 0.5 microns in sizes. The reduction of pore sizes reduces permeability and increase long term durability. Similar effect of metakaolin on the mechanical properties of concrete (Qian and Li 2001; Wild et al. 1996) and durability can be observed (Gruber et al. 2001).

On the other hand, crumb rubber in concrete was evaluated to examine their impact resistance. Few studies (Eldin and Senouci 1993; Khatib and Bayomy 1999) demonstrated that the failure mode of concrete containing rubber was more quasi-brittle as opposed to conventional concrete. Other studies (Eldin and Senouci 1993; Topçu and Avcular 1997; Topçu 1995) also found that the impact resistance of concrete increased when rubber aggregates were introduced into the concrete mixtures. Topçu (1995) found that the use of rubber as aggregate in concrete leads to higher impact resistance under both compressive and tensile loading. This increase in impact resistance was generated from the enhanced ability of the rubberized composite to absorb energy.

Concrete is usually described as quasi brittle material, but crack nucleation in concrete occurs without much effort and the lack of crack tip plasticity leads to a brittle failure that does not necessitate much energy. Application of fibre reinforcement in concrete was found to improve

many properties of concrete including crack control in the plastic state, serviceability and structural integrity, compressive and flexural toughness, with substantial improvement to resistance to impact, blast or explosive loading (Balaguru and Shah 1992; Banthia et al. 1998; Bentur and Mindess 2006; Mufti et al. 1998). Fibres in concrete usually develop more efficient toughening and strengthening mechanism in their vicinity with compare to aggregate particles and cement paste because of their aspect ratios, large surface areas and elastic properties. Since all cement matrices are brittle, they reach failure strain before the fibres. Once the crack formed, fibres bridge the matrix cracks and act as stress transfer bridges. As a result, fibres help to maintain the material integrity and the section demonstrates post cracking tensile strength unlike plain concrete.

There are many types of fibres are in use in concrete industry; steel fibres, glass fibres, asbestos fibres, synthetic fibres as well as some natural fibres. Among all these types of fibres, use of steel fibre is gaining popularity for their effectiveness in improving post peak behavior in concrete. After the crack formation in cement matrices, steel fibre bridges the crack and provides stress transfer mechanism. At higher deformation, fibre pullout process initiates which provides toughening or energy absorption mechanisms. The fibre pullout processes are the fundamental micro mechanisms that decide concrete composite toughness or post peak behavior. The factors affecting post peak behavior includes fibre shape, fibre geometry and fibre amount. Straight fibres, hooked fibres and enlarged-end fibres are the most commonly used steel fibres and hooked and enlarged-end fibres are found to have superior pullout behavior which in turn aid in better toughening process when used in concrete. The dynamic strength of concrete reinforced with various types of fibres subjected to dynamic flexural, tensile and compressive strength is 3 to 10 times greater than that for plain concrete (Suaris and Shah 1984). The impact strength was derived from the higher energy required to pullout the fibre from the concrete matrices (Wedding et al. 1981). It was also observed that the energy absorbed by steel fibre reinforced beams, subjected to impact loading and instrumented drop height and charpy-type systems, can be as much as 40 to 100 times that for unreinforced beams (Gopalaratnam et al. 1984; Gopalaratnam and Shah 1986; Naaman and Gopalaratnam 1983; Suaris and Shah 1983). Steel fibres were found effective in crack bridging and mechanical properties improvement with normal to high strength concrete due to comparable modulus of

elasticity of concrete mixes and steel fibre. However, for the low strength and low modulus concrete mixes, polypropylene fibres might work more effectively in crack bridging and toughening mechanism.

This study illustrates the response of steel fibre reinforced concrete containing manufactured and recycled lightweight aggregates under quasi-static and impact loading. The mixes were characterized first in quasi-static compression followed by a dynamic crack growth analysis in flexure. The dynamic responses were compared with existing CEB-FIP models (CEB-FIP 1990) to assess their stress rate sensitivity.

7.2 Research significance

Response of concrete under dynamic loading is a key parameter regarding its performance as impact resistance structure. Achieving higher performance to weight ratio for this type of concrete is very crucial. This chapter describes the responses of some concrete mixes where crumb rubber is used as partial replacement of fine aggregate and lightweight expanded shale aggregates were used as coarse aggregate. In addition, hooked short steel fibers and supplementary cementitious materials were also incorporated. The dynamic responses of these concrete mixes will provide new insights into to effect of crumb rubber and supplementary cementitious material on the performance of concrete. Another aspect of this study is the possible recycling of the rubber tire into road barrier as crumb rubber is generally derived from the scrap tire. Incorporating crumb rubber as fine aggregate replacements may also save valuable natural resources and will make the concrete sustainable.

7.3 Objectives

The objectives of this study were as follows;

- Effect of higher stress rate on flexural properties
- Effect of stress rate on fracture toughness
- Effect of crumb rubber content on various mechanical properties at higher stress rate

- Effect of supplementary cementitious material at higher stress rate

7.4 Experimental program

The following parameters were examined to characterize their influence on the dynamic response of concrete:

- Crumb rubber as aggregate replacement: varied at 0%, 25% and 75% by volume of total fine aggregates;
- Supplementary cementitious materials: silica fume (SF) or metakaolin (MK) included at 0% or 10% by mass of the cementitious material;
- Rate of loading: quasi-static loading and impact from drop-height of 250 mm, 500 mm & 750 mm.

7.4.1 Materials

The cement used was a (CSA A3001 2009) Type GU ordinary Portland cement (OPC). In addition to OPC, silica fume and metakaolin were incorporated as a supplementary cementitious material at 0 and 10% by mass of the binder. A 10mm downgraded expanded shale aggregate was used as the coarse aggregate. A locally available river sand and crumb rubber were used as the fine aggregate. The crumb rubber aggregate were obtained in 3 size ranges (0.85 mm to 3.35 mm) available market. These three sizes were blended to achieve a distribution as shown in Figure 7-1. This blended aggregate was used at 25% and 75% volume replacement of total fine aggregates. The crumb rubber was manufactured from recycled motor vehicle tires and purchased from a local recycling company. Hooked-end steel fibres, 35 mm in length, with aspect ratio of 70 and yield strength of 1100 MPa were employed at 1% volume fraction in all the mixes.

The mix proportions were derived as per ACI (1991) for the concrete mix composition for 28 days compressive strength of 35 MPa with. This range of compressive strength is suitable for different structural as well as non-structural concrete application. In order to achieve a lower density concrete, the present study used a lightweight expanded shale aggregate. The water-cementitious material ratio (w/cm) was 0.40 for all mixes. Use of silica fume and steel fibres

were found to reduce the workability of concrete. Hence, a high range water reducing admixture was used to achieve adequate workability (50mm to 150mm slump). The detail mix proportions for the resulting 9 (nine) mixes are given in Table 7-2. The quasi static test results (compressive strength, modulus of elasticity, flexural strength) of these mixes were discussed elaborately in Chapter 3.

7.4.2 Specimen preparation

All specimens were prepared in accordance with ASTM C192 (ASTM C192 2012) using a drum mixer of 75 litre capacity. From each mix, twelve 400 mm × 100 mm × 100 mm prisms were prepared to be tested in flexure. Three cylinders, 100 mm diameter and 200 mm height were also produced to be tested in compression. The specimens were demolded 24 hours after casting and then cured in a moist room under controlled humidity (>99%) and temperature (22 ^{o}C) until testing. A 4-mm wide notch was sawn into each flexural specimen to a height of approximately 10 mm. This notch was intended to facilitate crack growth analysis under Mode-I fracture.

7.4.3 Test setup

7.4.3.1 Compression test

The compression tests were performed in accordance with ASTM C469 (2010a) to evaluate the modulus of elasticity and establish the compressive stress-strain response. A displacement-controlled servo-hydraulic Materials Testing System with 2600 kN capacity was used to test the cylinders. Three longitudinal Linear Variable Displacement Transducers (LVDT) were placed at 120^{o} separation about the longitudinal axis together with two LVDTs in the transverse direction to measure axial and radial displacements respectively. The test arrangement is shown in Figure 7-2. The data was collected through a continuous-record data acquisition system at 10Hz. The cross-arm displacement rate was set to 1.25 mm/min as recommended by ASTM C469 (2010a).

7.4.3.2 Flexural test

7.4.3.2.1 Quasi-static test

For quasi static flexural test, three prisms were tested in third-point bending according to ASTM C1609 (2010b) from each mixes. A Material Testing System of 1000 kN capacity was used for this purpose. The load was applied by setting the cross-arm displacement rate to 0.15 mm/min which conformed to ASTM C1609 (2010b). As shown in Figure 7-3, a yoke was installed around the specimens to attach two LVDTs, one on either side. This yoke ensured that the displacement measured was that of the neutral axis and eliminated any errors due to support settlement. The LVDTs were used to measure the mid-span deflection of the beam. All the loads and displacement readings were sampled at 10 Hz.

7.4.3.3 Impact tests

In order to evaluate impact responses, drop weight impact tests were conducted in an instrumented drop weight impact machine shown in Figure 7-4. A 62 kg hammer was released from three different drop heights of 250 mm, 500 mm and 750 mm to achieve increasing strain rates in the samples. Three prisms were tested from each drop height. A piezoelectric accelerometer was attached underneath the test specimen next to the notch at mid span in order to capture the acceleration time history. The total impacting load (including the inertial load) was recorded by using a bridge loading device (tup) attached to the striking knife edge. Two high speed cameras were also installed to obtain a stereoscopic record of the impact test. The accelerometer and load cell recorded data at 100,000 Hz while the two cameras captured images at a frequency of 10,000 frames per second. A trigger mechanism was installed so that all four sets of data (i.e. from the accelerometer, the load cell and the two high speed cameras) were synchronized to the same time-stamp. Later, the images were analyzed using image processing software to measure the crack mouth opening displacement (CMOD) and vertical displacement for each individual specimen. From the image analysis, the values of mid span deflection and CMOD were plotted and a best fit straight line passing through the origin is drawn to get a linear relationship between them. The relationship between CMOD and displacement was used to determine the stress intensity factor of the specimen based on the formulation by Guinea et al.(1998). This relationship was used to calculate the crack growth

resistance curve and fracture toughness. The inertial component of the applied load was accounted for as described by (Banthia et al. 1989). Assuming a linear acceleration distribution along the span and using the virtual work principle, the generalized inertial load can be calculated using Equation (7.1).

$$P_i\,(t) \;= A\,\ddot{u}\,(t)\rho\,\left(\frac{S}{3}+\frac{8l^3}{3S^2}\right) \qquad (7.1)$$

where, $S =$ Span; $l =$ overhang; $A =$ cross sectional area; $\rho =$ mass density; $\ddot{u}\,(t)$ = acceleration at mid span at any time *t*.

The effective bending load was computed by subtracting the inertial load from the recorded total load captured by the bridge loading tup.

Analyses were carried out to compute the displacement time history, $\Delta_0(t)$, from the acceleration time history, $\ddot{u}$ (t), at the location of accelerometer. Equation (7.2) was used to compute the displacement time history with the consideration of zero velocity and zero displacement at t = 0.

$$\Delta_0(t) = \iint \ddot{u}\,(\mathrm{t})\,.\,\mathrm{dt}\,.\,\mathrm{dt} \qquad (7.2)$$

7.5 Results and discussion

7.5.1 Compressive response

The stress-strain responses of all mixes under compression were shown in Figure 7-5. The compressive strength values were summarized in Table 7-3. In addition to compressive strength the modulus of elasticity for each mixes were calculated as per ASTM C469 (2010a). The variation of compressive strength and modulus of elasticity with crumb rubber replacement (replacement of fine aggregate with crumb rubber) are shown in Figure 7-6.

7.5.1.1 Effect of rubber content on compressive response

From the results it is observed that an increase in crumb rubber replacement from 25% to 75% by volume replacement of sand caused a drop in the compressive strength. For mixes with only OPC this drop in compressive strength was 69% whereas for mixes with silica fume and

metakaolin this drop was 53% and 38% respectively. When the results of concrete mixtures with 25% and 75% crumb rubber replacement were compared with concrete mixtures of 0% crumb rubber content, it was found that 13% and 73% strength reduction took place for mixtures with only OPC, 27% and 66% strength reduction happened for mixtures with OPC and silica fume and 38% and 62% strength reduction was observed for concrete mixtures with OPC and metakaolin.

The reduction of compressive strength of concrete containing crumb rubber as aggregate can be attributed to three main reasons. First, due to high deformability of rubber particles compared with the surrounding cement paste, cracks are initiated around the rubber particles in the mix. This accelerates the failure in rubber-cement matrix (Eldin and Senouci 1993; Khatib and Bayomy 1999; Lee et al. 1998; Taha et al. 2008). Secondly due to the lack of proper adhesion or bond between rubber particle and cement paste, soft rubber particles may be considered as voids in the concrete mix (Chung and Hong 1999; Eldin and Senouci 1993; Taha et al. 2008) and thus responsible for lower strength. The density of concrete matrix depends greatly on the density, size and hardness of the aggregate and the third possible reason of strength reduction is due to the possible reduction of density of the concrete with crumb rubber. The deformability of soft rubber particles has more prominent effect on the compressive strength reduction of concrete mixes. When the concrete mixes with crumb rubber is subjected to a compressive stress state, the crumb rubber particles act as soft aggregate and tensile stress developed at the rubber particle surface and in the cement paste vicinity. This type of tensile stresses result in premature cracking in the cement matrix.

The significant strength loss also attributed to the low bond between rubber particles and the cement paste. All the crumb rubber particles were untreated in this study which yields low bond between crumb rubber particles and cement paste. Some researchers showed that surface treatment of rubber particles enhanced bond strength between rubber particle and cement paste (Chung and Hong 1999; Lee et al. 1998; Raghavan et al. 1998b; Taha et al. 2008). Treating rubber particle using Sodium Hydroxide (NaOH) and Calcium Hydroxide ($Ca(OH_2)$) demonstrated enhanced bond and thus increased compressive and flexural properties (Chung and Hong 1999; Raghavan et al. 1998b; Segre and Joekes 2000).

7.5.1.2 Effect of supplementary cementitious material

At lower crumb rubber replacement, supplementary cementitious materials do not improve compressive strength of concrete. Though, in comparison between silica fume and metakaolin, concrete mixes with silica fume showed higher compressive strength at 25% crumb rubber replacement. On the other hand, the mixtures with 75% crumb rubber replcement and with silica fume and metakaolin showed an improvement in compressive strength by 25% and 33% respectively. Supplementary cementitious material acted as filler and filled the voids due to higher crumb rubber volume percentage. Also, pozzolanic reaction improved interface between cement paste and crumb rubber aggregate which contributed to this improved compressive strength.

7.5.2 Flexural response

7.5.2.1 Quasi-static response

The load-deflection responses of all the mixes under third-point bending were shown in Figure 7-7. Since a notch was introduced, the modulus of rupture, f_r was calculated using the effective cross sectional dimensions after accounting for the notch. The post peak energy dissipation was evaluated as per ASTM C1609 (2010) for fibre reinforced concrete. This method introduces an equivalent flexural strength ratio ($R^D_{T,150}$) as calculated by using Equation (7.3).

$$R^D_{T,150} = 150 \cdot T^D_{150}/(f_1 \cdot b \cdot d^2) \quad (7.3)$$

where, T^D_{150}= toughness up to a net deflection of $L/150$,

f_1 = first Peak Strength,

b = average width of the specimen at fracture,

d = average depth of the specimen at fracture.

A summary of the quasi-static flexural properties was provided in Table 7-4.

7.5.2.2 Effect of supplementary cementitious material

The concrete mixes with only OPC and the one with a blend of OPC and metakaolin showed relatively large drop in f_r (34% and 24% respectively) whilst in case of concrete with silica fume this drop was only 9% with the increase in rubber content from 25% to 75%. Moreover,

at 75% crumb rubber content, the concrete mixes with silica fume had better flexural strength with compared to other mixes. Due to its fineness silica fume acts as filler in addition to its pozzolanic activity. Hence concrete mixes with silica fume demonstrated better strength at higher crumb rubber replacement.

7.5.2.3 Effect of crumb rubber content

Again, under application of load, the rubber aggregate can undergo large deformation before failure. Hence, a tension crack that develops in cement paste or at a mineral aggregate propagates until it reaches a piece of rubber particle. Rubber does not fail in tensile stress as easily as the surrounding matrix. Moreover, reduction in flexural strength is due to the weak bond between cement past and rubber particles. The strength reduction can be attributed both to a reduction of the solid load carrying material in the concrete mixes.

7.5.3 Dynamic response

The results from the impact tests were analyzed to derive the load-deflection responses. Here, load data from tup-loads were accounted for inertial load as per Equation 7.1. Deflections were calculated from acceleration data measured from accelerometer. For deflection calculation, Equation 7.2 was employed with boundary conditions of $v_{(t=0)} = 0$ and $u_{(t=0)} = 0$. The load-deflections results for different loading rate and various crumb rubber content are shown in Figure 7-8. The loading range varies from 10 kPa/s to 63400x10^3 kPa/s. From these plots, the equivalent flexural strength ratio and modulus of rupture were calculated and are summarized in Table 7-4. It was possible to derive acceleration data from loads (Force = mass*acceleration) and from camera data. However, the acceleration data from accelerometer and from loads were shown in Appendix VII for comparison purpose.

7.5.3.1 Effect of loading rate

From the results it was observed that, flexural strength increased with higher drop height, and higher drop height generates higher loading rate. Mixes with OPC and various rubber contents showed 3 to 6 times increase in flexural strength. This increase is more prominent in mixes with supplementary cementitious material. Concrete mixes with OPC and silica fume showed

3.5 time to 8 times increase from static load and 4 to 6 times increase in flexural strength was observed in mixes with OPC and metakaolin.

7.5.3.2 Effect of supplementary cementitious material

From the results it was found that at lower rubber content, concrete mixes with silica fume are showed significant strength increase 5 to 8 times more strength from static strength. Concrete mixes with metakolin showed moderate strength gain at higher loading rate. At higher crumb rubber content, concrete mixes didn't show any significant difference in terms of strength gain. Nevertheless, it was found that concrete mixes with silica fume showed better strength at higher stress rate

7.5.3.3 Fracture toughness

For the quasi static flexural load, Armelin and Banthia (1997) has proposed that, the mid span deflection of the beam, Δ and CMOD are related according to the following Equation (7.4),

$$\Delta = 0.75 \cdot CMOD \tag{7.4}$$

Δ is the vertical displacement of the neutral axis at mid span of the beam. Using this relation, the stress intensity factor was calculated from the load-deflection response as propose by prior researchers (Broek 1986; Guinea et al. 1998).

However, for higher loading rate, Δ-*CMOD* relationship may vary. The flexural strength using images from the stereoscopic high speed imaging system, the CMOD and corresponding mid span deflection were recorded. A best fit straight line similar to Equation (7.5) was drawn for those recorded values.

$$\Delta = m \cdot CMOD \tag{7.5}$$

where, Δ = mid span deflection;

m = slope of the straight line;

CMOD = crack mouth opening displacement.

The slopes for all types of mixes and all drop heights have been shown in Table 7-5 except for the mix with OPC and 25% rubber due to unavailability of camera data. From those tabulated values it has been observed that for 500 mm and 750 mm drop height the relationship is almost similar (±10%) to that derived by (Armelin and Banthia 1997). But for 250 mm drop height this relationship varies quite significantly and for some cases the difference is as high as 70%. From the relationships the crack growth resistance curves (shown in Figure 7-9) for the specimens were obtained in a manner similar to the quasi-static analysis (Broek 1986; Guinea et al. 1998). The fracture toughness values for both static as well as impact loadings were shown in Table 7-6. From the results, increase fracture toughness was observed with increase in loading rate. For mixes with no rubber content, only 50% to 150% increase in fracture toughness was observed depending on various supplementary cementitious materials. At higher rubber content 5 to 10 times increase in fracture toughness was recorded. It was also noted that concrete mixes with only OPC experienced least increase, whereas concrete mixes with silica fume demonstrated most increase in fracture toughness value with higher loading rate. The densification and improved interfacial transition zone due to pozzolanic effect were the main contributors for this fracture toughness increase for mixes with silica fume.

Fracture toughness for lightweight concrete mixes with steel fibre has not been examined prior to this study. However, Kramar and Bindiganavile (2013) studied the impact response of lightweight mortar with expanded perlite reinforced with polypropylene fibre. The mortars in that study had density of 1400 kg/m^3 to 1900 kg/m^3 and compressive strength of 20 MPa to 40 MPa. They found that for 100 mm x 100 mm specimen, the fracture toughness values ranges from 0.24 to 0.31 MPa*√m which is significantly lower than the value obtained in this study (3.5 to 9 MPa*√m). This difference was due to difference in fibre type used in the mix. In the current study it was found that the fracture toughness values were corresponded to the CMOD and deflection in the post peak zone. It is well-known that the hooked end steel fibres are more effective in crack bridging and toughening of the matrix due to their pullout behavior. For that reason, fracture toughness values were higher in the current mixes.

7.5.3.4 Stress rate sensitivity

The stress rate sensitivity of flexural strength is shown in Figure 7-10. The results show that in general the CEB-FIP model uniformly underestimates the stress-rate sensitivity of mixes containing crumb rubber. To describe the stress rate sensitivity, Nadeau et al. (1982) has also proposed the following Equation (7.6),

$$\ln \sigma_f = \frac{1}{N+1} \ln B\, \dot{\sigma} + \frac{1}{N+1} \ln(\sigma_i^{N-2} - \sigma_f^{N-2}) \quad (7.6)$$

where,

σ_f = stress at final condition, σ_i = stress at initial condition

B, N = constant, $\dot{\sigma}$= stress rate

According to the Equation (7.6), a plot of log strength versus log stress rate yields a line with a slope of $1/(N + 1)$. The parameter N is dependent on material strength and stress-rate and a lower N-value denotes higher stress rate sensitivity.

7.5.3.4.1 Stress rate sensitivity of flexural strength

The N-values of flexural strength evaluated for each types of mix and for different loading rates have been presented in Table 7-7. It has been observed that at higher stress rate flexural strength value is more sensitive than lower stress rate. Again, the N-values for the concrete mixes with OPC and silica fume with 0%, 25% and 75% rubber content were 1.39, 0.64 and 0.28 respectively. The lower N-values of concrete mixes with higher rubber content indicated higher stress rate sensitivity. For the concrete mixes with OPC and metakaolin, the N values were 2.73, 0.73, -0.66 for 0%, 25% and 75% rubber content respectively. This indicated higher stress rate sensitivity with higher rubber content mixes. Moreover, concrete mix with higher crumb rubber replacement and with silica fume and metakaolin appears to be more sensitive to stress rate.

7.5.3.4.2 Stress rate sensitivity of fracture toughness

The stress rate sensitivity of fracture toughness was shown in Figure 7-11 and the associated N-values were presented in Table 7-8. Currently no model is available to predict the stress rate

sensitivity for fracture toughness values. However, from the results shown in Figure 7-11, it was evident that fracture toughness is also sensitive to stress rate irrespective of rubber content and supplementary cementitious material. At higher stress rate, the concrete mixes with only OPC and 25% and 75% rubber content had the N values of -0.08 and 0.2. In case of concrete mixes with OPC and silica fume, the N values were -0.35 and -0.48; whereas for concrete mixes with OPC and metakaolin, the N values were -0.44 and -0.8. For all combinations of cementitious material, it was evident that fracture toughness of concrete mixes with higher rubber content was sensitive to stress rate.

As mentioned earlier, prior to the current study no other researcher has examined the stress rate sensitivity of lightweight concrete mixes. However, stress rate sensitivity of flexural strength of lightweight cement paste (density 475 – 1200 kg/m^3) was examined by Mamun (2010). It was found that flexural strength of lighter matrices was more sensitive to stress rate. On the other hand, Kramar and Bindiganavile (2013) investigated the effect of stress rate on flexural strength and fracture toughness of lightweight mortar (density 960 – 1460 kg/m^3) with expanded perlite. They also found that flexural strength and fracture toughness of lighter mixes were more sensitive to stress rate. The stress rate sensitivity results from both lightweight cement paste and mortar were aligned to the stress rate sensitivity results found in this study.

7.6 Concluding remarks

The introduction of higher amount of rubber as volume replacement of fine aggregates significantly reduces the compressive strength and modulus of elasticity. The other findings are described below.

1) The modulus of rupture decreases with an increase in crumb rubber replacement but level of crumb rubber replacement does not have any significant effect on equivalent flexural strength ratios. Modulus of rupture also increases for increased loading rates but the equivalent flexural strength ratio was lower for impact loading compared to quasi-static loading.

2) The fracture toughness was similar regardless of the crumb rubber replacement but the presence of supplementary cementitious material improves the fracture toughness value.
3) At higher crumb rubber replacement, addition of supplementary cementitious material improves the compressive strength, modulus of elasticity and modulus of rupture.
4) At higher crumb rubber replacement along with supplementary cementitious material like silica fume and metakaolin, concrete flexural strength and fracture toughness demonstrated more sensitivity towards stress rate.
5) Existing stress rate sensitivity model for tensile strength of concrete (CEB-FIP) underestimate the dynamic impact factor of the flexural strength of concrete containing crumb rubber.

7.6.1 Limitations of the study

This study was focused on the stress rate sensitivity of flexural strength and fracture toughness of concrete mixes with various crumb rubber content and different supplementary cementitious material. All of the mixes contained 1% volume of hooked end steel fibre. No other fibre types were used to compare results with steel fibre. Also, there were no mixes with plain concrete to compare the effect of steel fibre on mechanical properties, although effectiveness of steel fibre is well established. The gradation of crumb rubber was intended to match with fine aggregate, though it wasn't possible due to unavailability of different crumb rubber sizes in the market. All flexural and impact tests were performed on 100 mm x 100 mm x 400 mm prisms. Size effect on the flexural strength and fracture toughness wasn't evaluated in this study.

Tables

Table 7-1: Typical Strain-Rates for various types of loading

Type of loading	**Strain Rate (s^{-1})**
Traffic	10^{-6} to 10^{-4}
Gas Explosion	$5x10^{-5}$ to $5x10^{-4}$
Earthquake	$5x10^{-3}$ to $5x10^{-1}$
Pile Driving	10^{-2} to 10^{0}
Air Craft Impact	$5x10^{-2}$ to $2x10^{0}$
Hard Impact	10^{0} to $5x10^{1}$
Hypervelocity Impact	10^{2} to 10^{6}

Table 7-2: Mix Proportions (Water-binder ratio = 0.4, Steel fibre = 1% by volume)

Mix[1]	OPC kg/m^3	SF kg/m^3	MK kg/m^3	Sand kg/m^3	Crumb Rubber[2] %	Crumb Rubber (kg/m^3)	Hardened Density (kg/m^3)
OPC, 0% Rubber	550	0	0	641	0	0	2132
OPC+SF, 0% Rubber	495	55	0	641	0	0	2018
OPC+MK, 0% Rubber	495	0	55	641	0	0	2089
OPC, 25% Rubber	550	0	0	481	25	51	2018
OPC+SF, 25% Rubber	495	55	0	481	25	51	1908
OPC+MK, 25% Rubber	495	0	55	481	25	51	1881
OPC, 75% Rubber	550	0	0	160	75	153	1766
OPC+SF, 75% Rubber	495	55	0	160	75	153	1748
OPC+MK, 75% Rubber	495	0	55	160	75	153	1788

[1] Gravel content 986 kg/m^3
[2] Fine aggregate replacement

Table 7-3: Summary of compression response

Mix Description	f'_c (MPa)	CoV	E_C (MPa)	CoV
OPC, 0% Rubber	45	0.11	17100	0.09
OPC & SF,0% Rubber	44	0.02	18590	0.10
OPC &MK,0% Rubber	42	0.04	23460	0.18
OPC, 25% Rubber	39	0.05	15300	0.44
OPC & SF,25% Rubber	32	0.03	14600	0.34
OPC &MK,25% Rubber	26	0.16	12390	0.17
OPC, 75% Rubber	12	0.07	7800	0.43
OPC & SF,75% Rubber	15	0.02	9250	0.84
OPC & MK,75% Rubber	16	0.02	7240	0.29

Table 7-4: Summary of quasi-static flexural response for mixes with various supplementary cementitious materials

	Quasi Static		*Drop height 250mm*		*Drop Height 500mm*		*Drop Height 750mm*	
Mix Description	f_r (MPa)	$R^D_{T,150,}$ %	f_r (MPa)	$R^D_{T,150}$ %	f_r (MPa)	$R^D_{T,150}$ %	f_r (MPa)	$R^D_{T,150}$ %
OPC, 0% Rubber	9.7	76.5	27.5	31.9	32.5	31.6	35.1	37.0
OPC & SF,0% Rubber	5.17	83.2	27.9	30.7	38.1	31.9	40.0	35.5
OPC &MK,0% Rubber	7.9	82.1	30.9	35.2	34.5	25.8	37.9	34.5
OPC, 25% Rubber	7.0	84	23.7	40.0	28.6	41.0	42.1	37.0
OPC & SF,25% Rubber	5.6	78	22.0	44.5	33.4	40.5	43.0	40
OPC &MK,25% Rubber	6.6	76	23.6	47.0	32.0	41.5	34.8	44.0
OPC, 75% Rubber	4.6	73.5	13.1	45	21.0	48.0	26.5	50.0
OPC & SF,75% Rubber	5.1	75.5	17.8	41	25.0	46	25.0	50.0
OPC & MK,75% Rubber	5.0	78.0	20.1	43.0	22.7	49.0	29.3	46

Table 7-5: Slope of Δ-*CMOD* curve

Mix Description	Drop Height		
	250 mm	500 mm	750 mm
OPC, 0% Rubber	0.92	0.77	0.74
OPC & SF, 0% Rubber	1.05	0.78	0.85
OPC & MK, 0% Rubber	0.83	0.8	0.83
OPC, 25% Rubber	-	0.686	0.731
OPC & SF, 25% Rubber	1	0.796	0.793
OPC & MK, 25% Rubber	1	0.795	0.75
OPC, 75% Rubber	1.22	0.771	0.79
OPC & SF, 75% Rubber	1.28	0.754	0.761
OPC & MK, 75% Rubber	0.885	0.829	0.793

Table 7-6: Fracture toughness, K_{IC} (MPa.√m)

Mix Description	K_{IC} (Quasi Static)	K_{IC} (Drop Height 250 mm)	K_{IC} (Drop Height 500 mm)	K_{IC} (Drop Height 750 mm)
OPC, 0% Rubber	9.0	8.3	10.2	13.0
OPC & SF, 0% Rubber	8.7	10.4	13.8	23.1
OPC & MK, 0% Rubber	9.0	8.6	12.1	13.9
OPC, 25% Rubber	6.4	-	10.9	17.5
OPC & SF, 25% Rubber	5.2	17.4	34.2	37.5
OPC & MK, 25% Rubber	4.7	11.7	30.8	27.9
OPC, 75% Rubber	3.4	5.3	9.8	19.3
OPC & SF, 75% Rubber	4	13.8	21.4	28.9
OPC & MK, 75% Rubber	3.9	18.1	33.2	28.8

Table 7-7: *N*-values for flexural strength, f_r

Mix	Stress Rate Range (kPa/sec)	N value
OPC, 0% Rubber	9 - $24653x10^3$	16.1
	$24653x10^3$ – $42700x10^3$	1.55
OPC & SF, 0% Rubber	10 - $28261x10^3$	8.57
	$28261x10^3$ - $63392x10^3$	1.39
OPC & MK, 0% Rubber	12 - $18201x10^3$	10.18
	$18201x10^3$ – $57400x10^3$	2.73
OPC, 25% Rubber	8 – $10611x10^3$	12.5
	$10611x10^3$ – $53737x10^3$	0.55
OPC & SF, 25% Rubber	9 – $8218x10^3$	11
	$8218x10^3$ – $56406x10^3$	0.64
OPC & MK, 25% Rubber	14 – $4000x10^3$	10.3
	$4000x10^3$ – $19390x10^3$	0.73
OPC, 75% Rubber	9 – $4410x10^3$	8.3
	$4410x10^3$ – $24320x10^3$	0.97
OPC & SF, 75% Rubber	10 – $6182x10^3$	10.5
	$6182x10^3$ – $25210x10^3$	0.28
OPC & MK, 75% Rubber	11 – $13012x10^3$	7.8
	$13012x10^3$ – $26045x10^3$	-0.66

Table 7-8: *N*-values for fracture toughness, K_{IC}

Mix	Stress Rate Range (kPa/s)	*N* value
OPC, 25% Rubber	$8 – 10611 \times 10^3$	16.2
	$10611 \times 10^3 – 53737 \times 10^3$	0.08
OPC & SF, 25% Rubber	$9 – 8218 \times 10^3$	10.1
	$8218 \times 10^3 – 56406 \times 10^3$	-0.35
OPC & MK, 25% Rubber	$14 – 4000 \times 10^3$	10.5
	$4000 \times 10^3 – 19390 \times 10^3$	-0.44
OPC, 75% Rubber	$9 – 4410 \times 10^3$	28.2
	$4410 \times 10^3 – 24320 \times 10^3$	-0.2
OPC & SF, 75% Rubber	$10 – 6182 \times 10^3$	7.01
	$6182 \times 10^3 – 25210 \times 10^3$	-0.48
OPC & MK, 75% Rubber	$11 – 13012 \times 10^3$	7.95
	$13012 \times 10^3 – 26045 \times 10^3$	-0.81

Figures

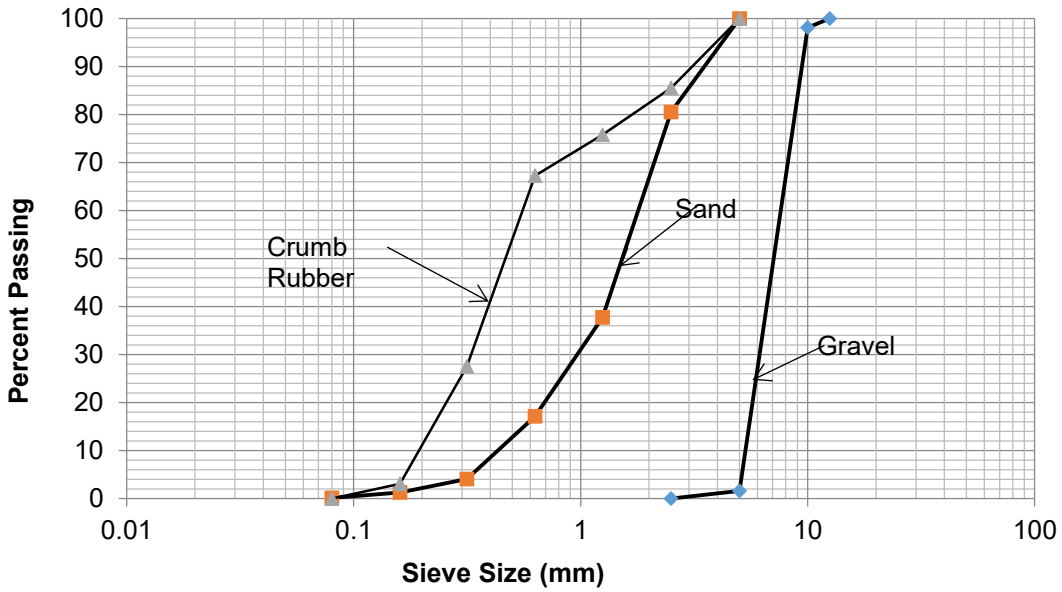

Figure 7-1: Grain size distribution of coarse aggregate, fine aggregate and crumb rubber

Figure 7-2: Compression test setup

Figure 7-3: Quasi static flexural test setup

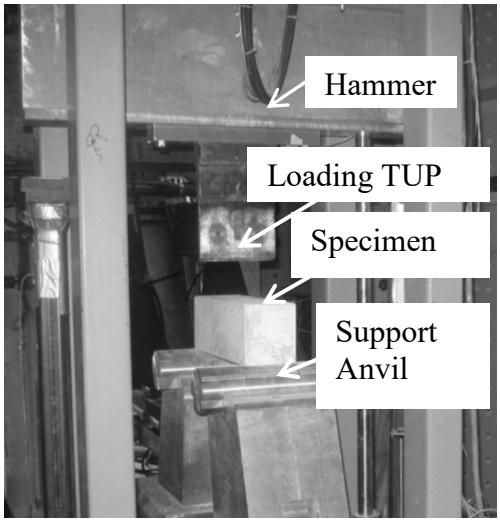

a) Drop weight impact machine

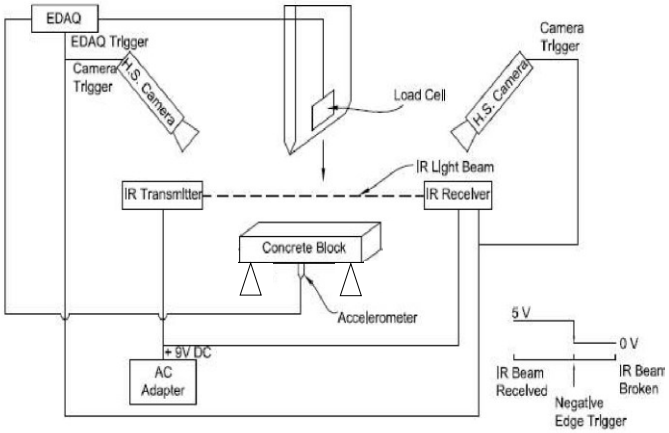

b) Schematic diagram of trigger mechanism to activate high-speed data collection

Figure 7-4: Drop weight impact test setup

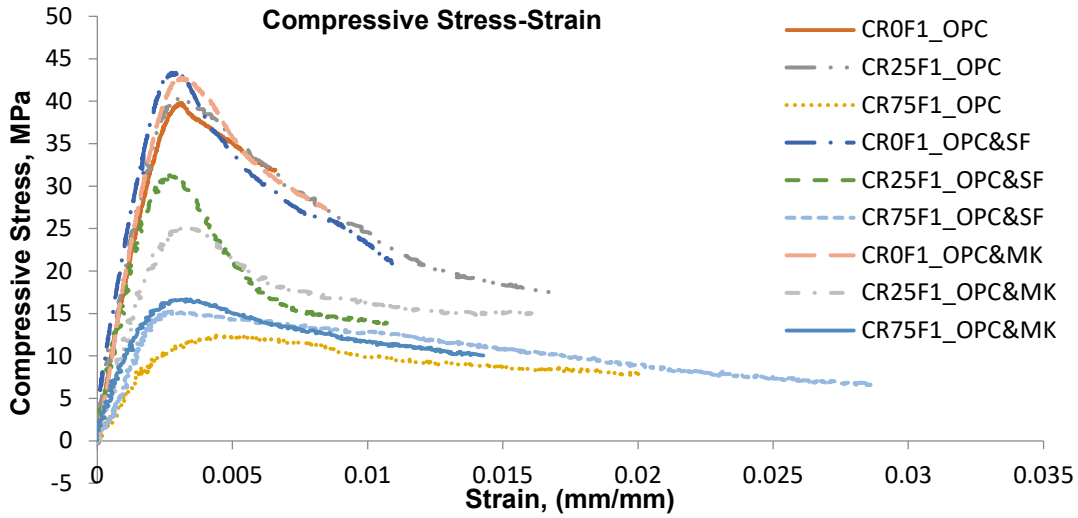

Figure 7-5: Compressive stress-strain response

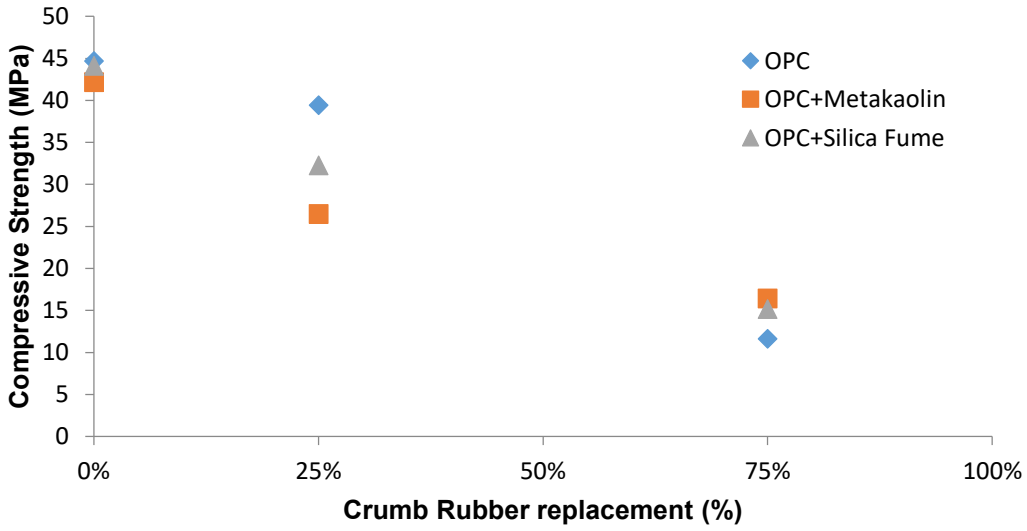

(a)

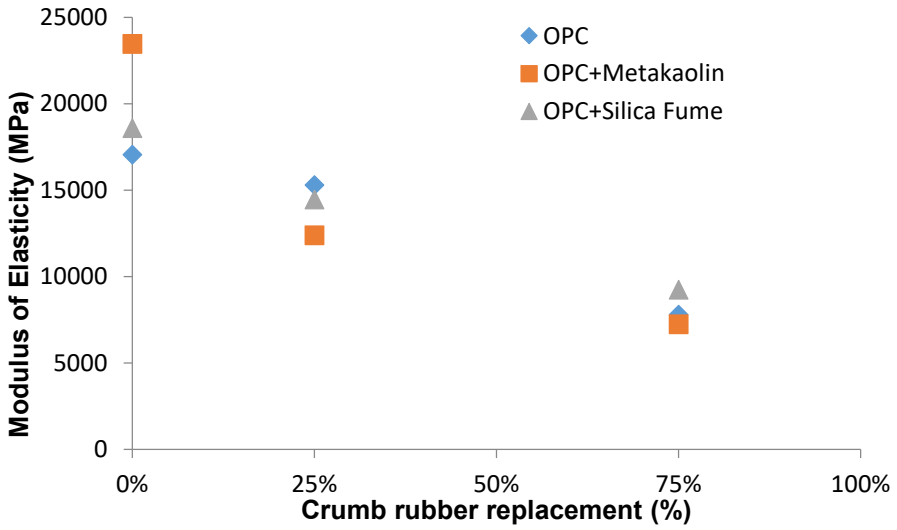

(b)

Figure 7-6: Effect of crumb rubber on (a) compressive strength, (b) modulus of elasticity

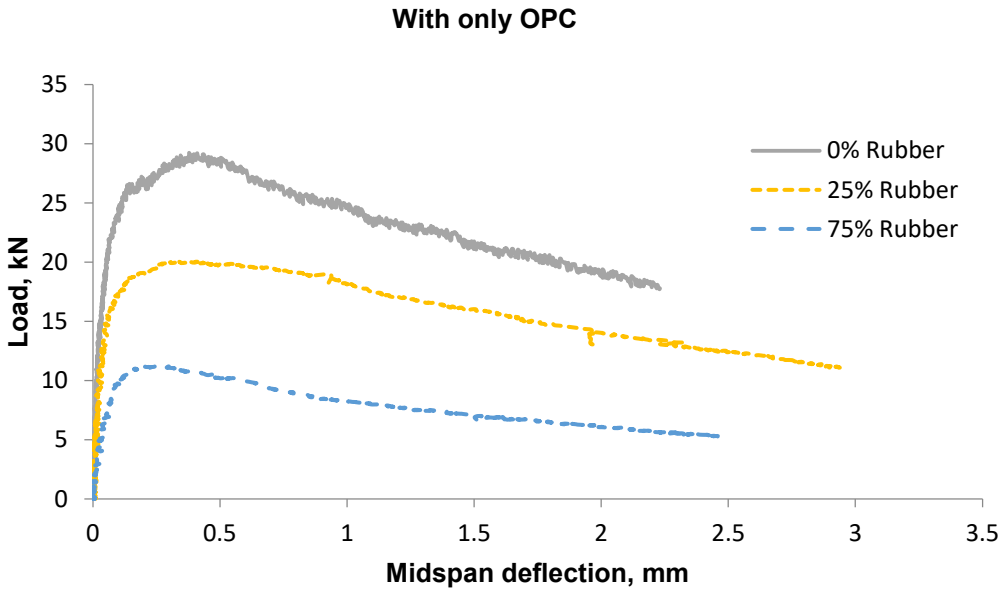

(a)

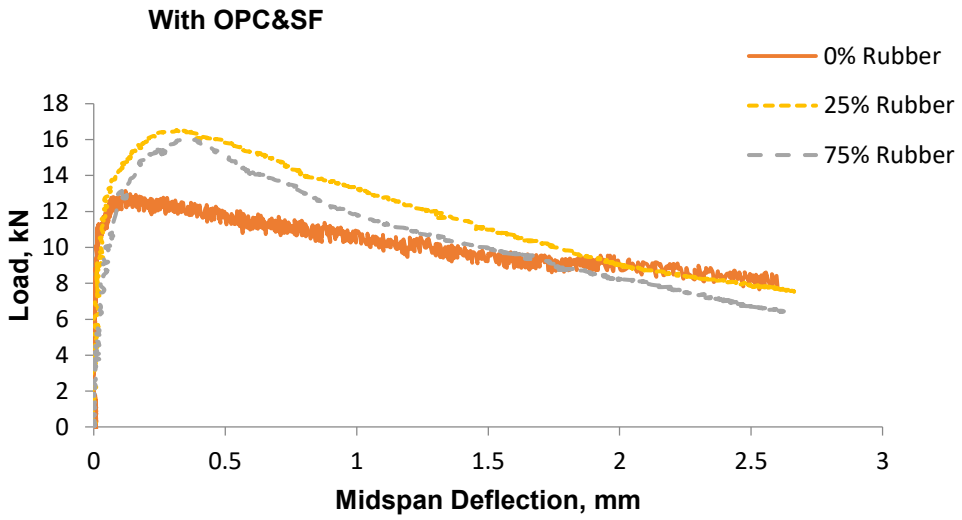

(b)

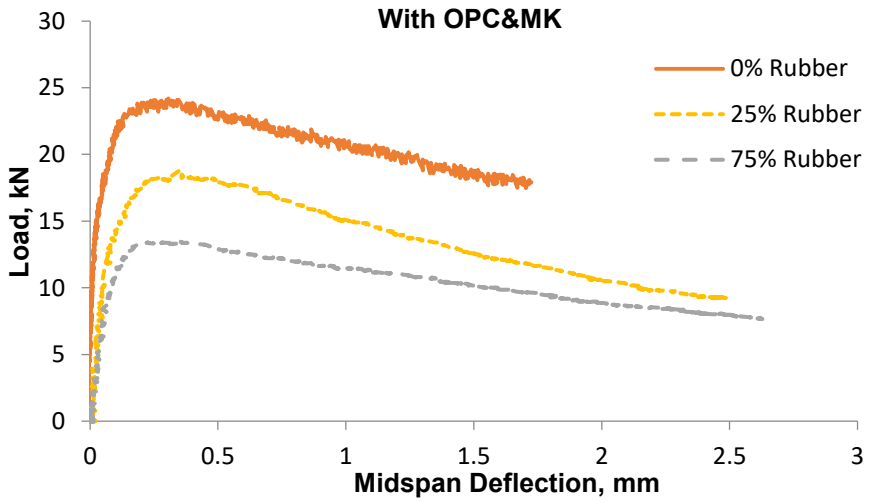

(c)

Figure 7-7: Load-Deflection response for concrete mixes with various supplementary cementitious material (a) With only OPC, (b) With OPC and SF, (c) With OPC and MK

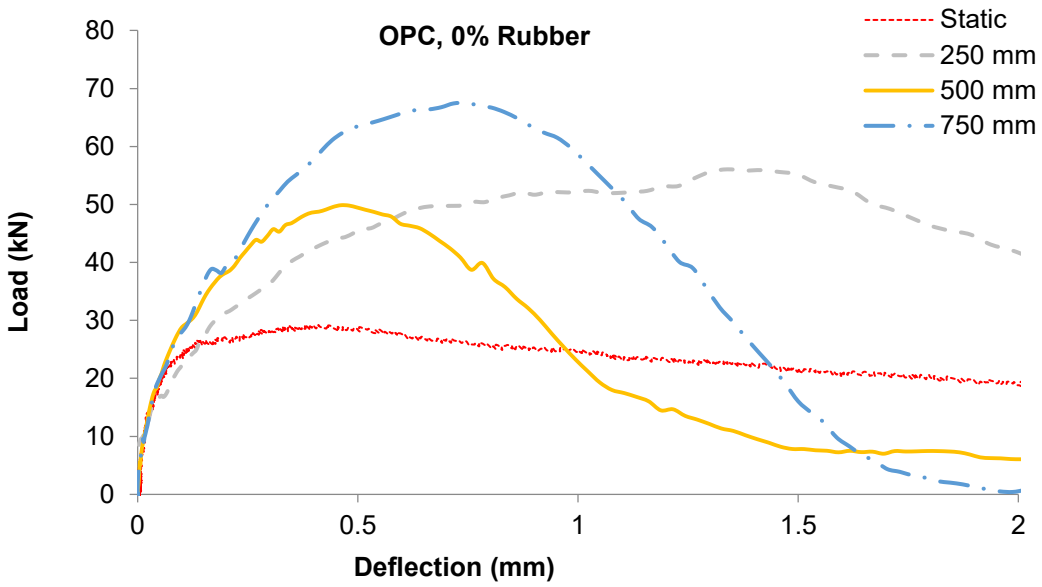
OPC, 0% Rubber
Static
250 mm
500 mm
750 mm
Load (kN)
Deflection (mm)
0
10
20
30
40
50
60
70
80
0
0.5
1
1.5
2

(a)

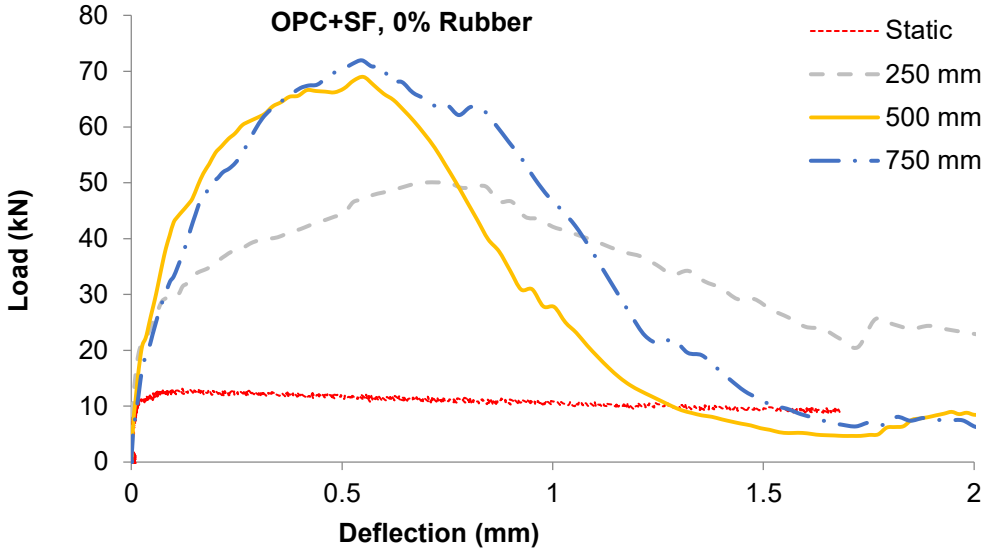
OPC+SF, 0% Rubber
Static
250 mm
500 mm
750 mm
Load (kN)
Deflection (mm)
0
10
20
30
40
50
60
70
80
0
0.5
1
1.5
2

(b)

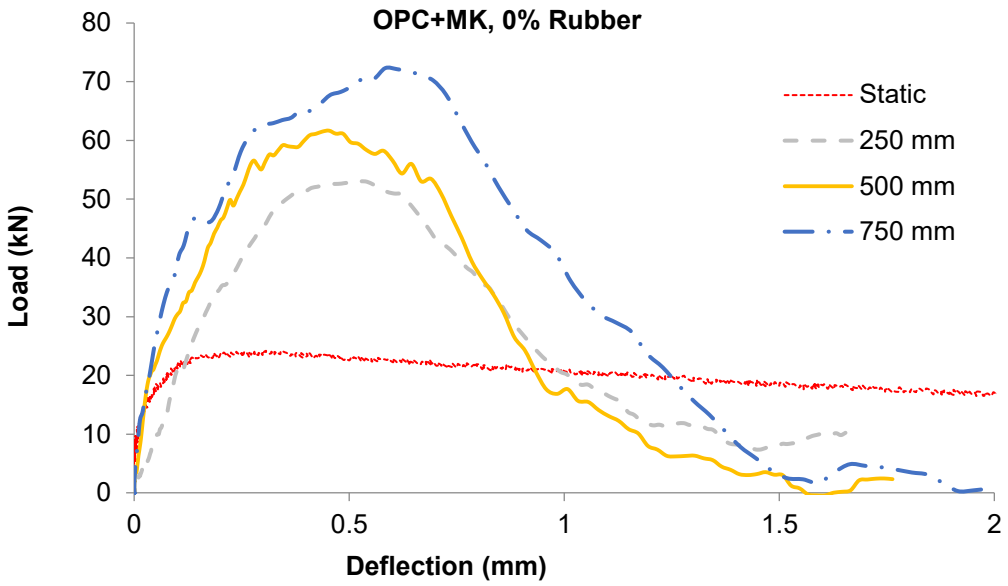
OPC+MK, 0% Rubber
Load (kN)
Deflection (mm)
Static
250 mm
500 mm
750 mm
0
10
20
30
40
50
60
70
80
0
0.5
1
1.5
2

(c)

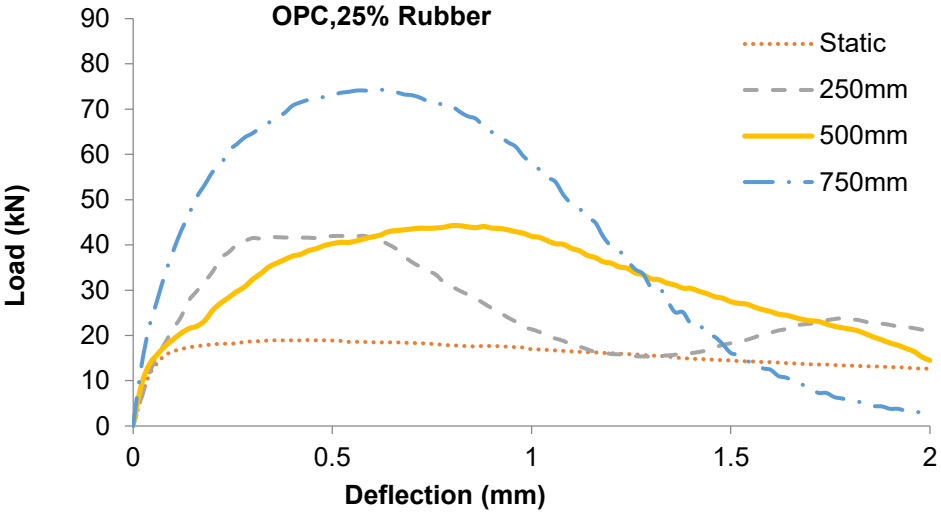
OPC,25% Rubber
Load (kN)
Deflection (mm)
Static
250mm
500mm
750mm
0
10
20
30
40
50
60
70
80
90
0
0.5
1
1.5
2

(d)

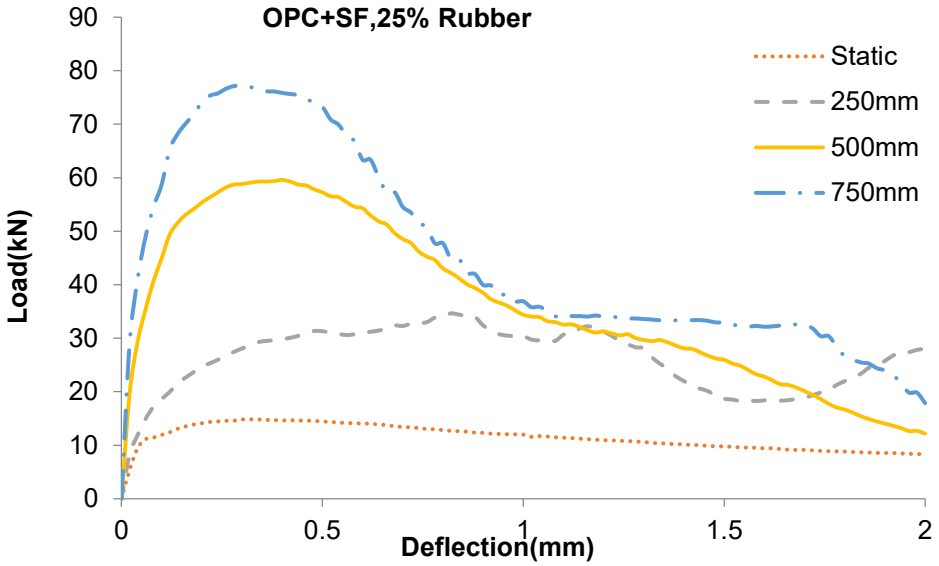
OPC+SF,25% Rubber
Static
250mm
500mm
750mm
Load(kN)
Deflection(mm)
0
10
20
30
40
50
60
70
80
90
0
0.5
1
1.5
2

(e)

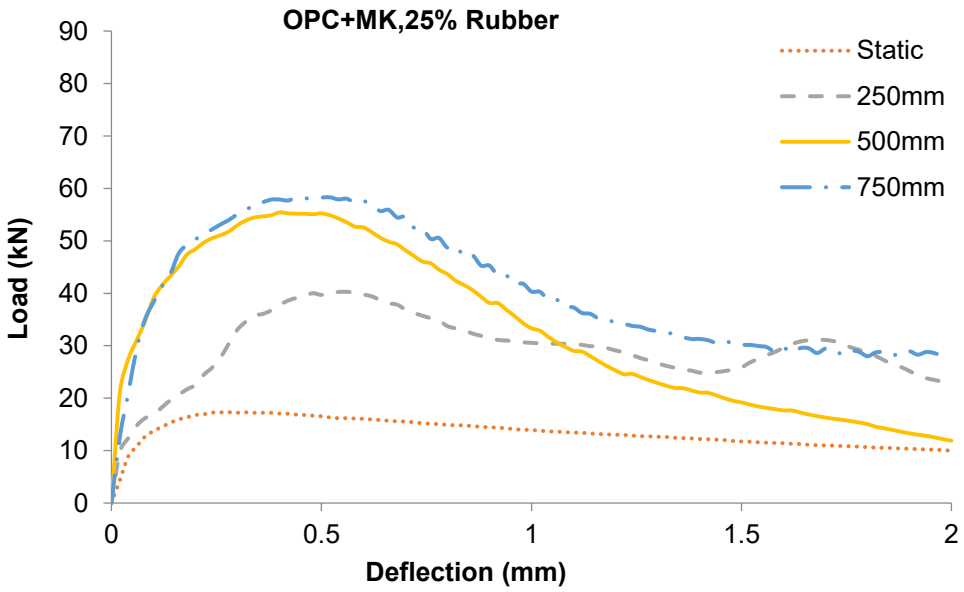
OPC+MK,25% Rubber
Static
250mm
500mm
750mm
Load (kN)
Deflection (mm)
0
10
20
30
40
50
60
70
80
90
0
0.5
1
1.5
2

(f)

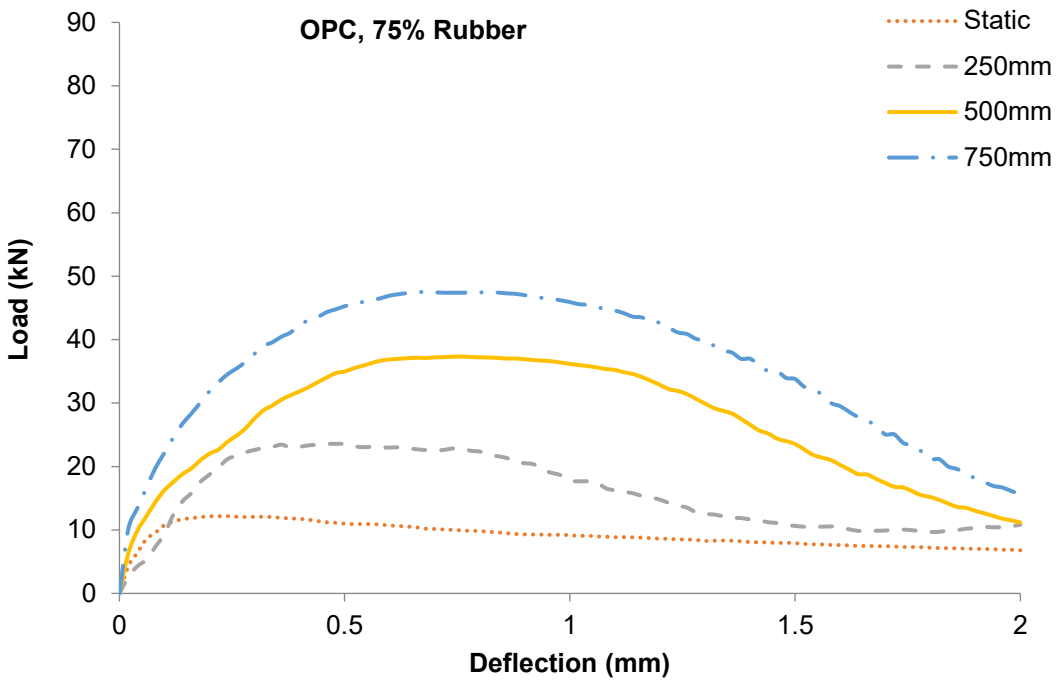
OPC, 75% Rubber
Static
250mm
500mm
750mm
Load (kN)
Deflection (mm)
0
10
20
30
40
50
60
70
80
90
0
0.5
1
1.5
2

(g)

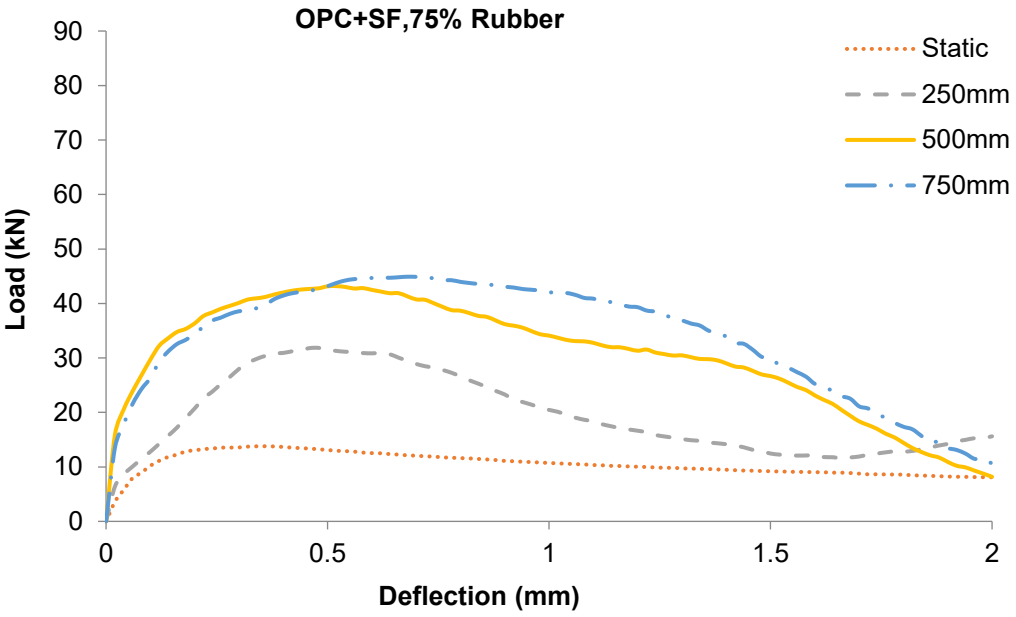
OPC+SF,75% Rubber
Static
250mm
500mm
750mm
Load (kN)
Deflection (mm)
0
10
20
30
40
50
60
70
80
90
0
0.5
1
1.5
2

(h)

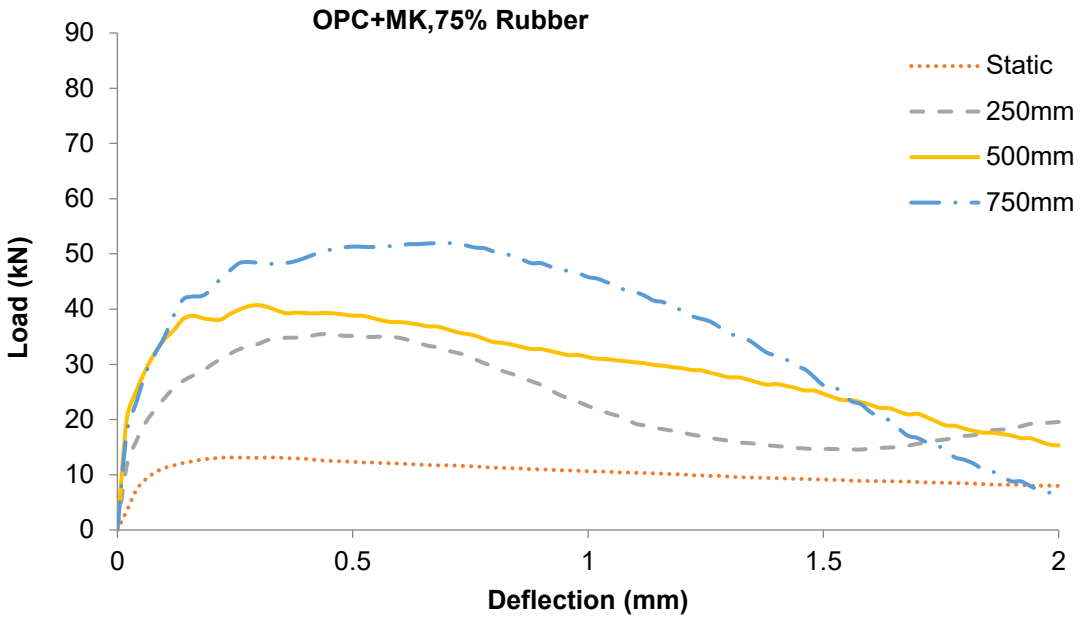

(i)

Figure 7-8: Flexural response under quasi-static and impact load

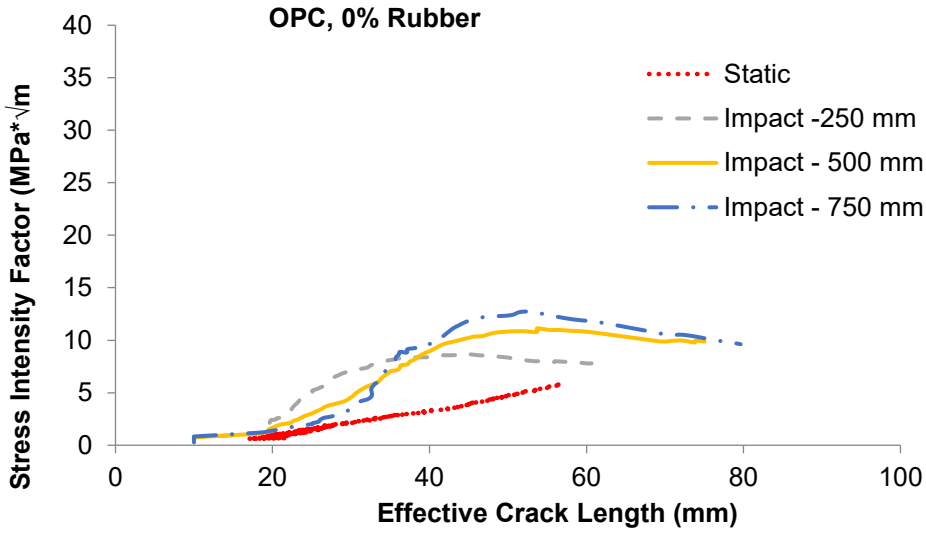

(a)

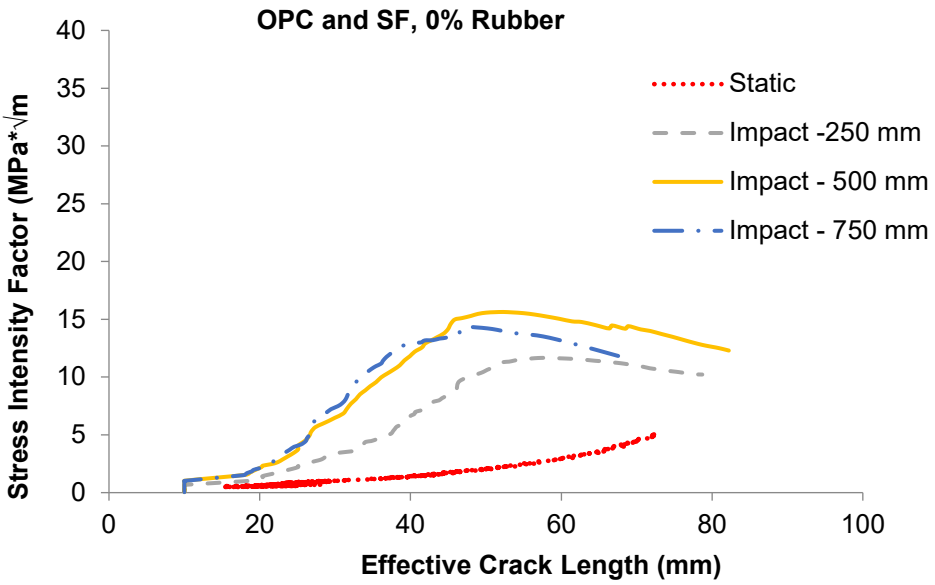
OPC and SF, 0% Rubber
Stress Intensity Factor (MPa*√m
Effective Crack Length (mm)
Static
Impact -250 mm
Impact - 500 mm
Impact - 750 mm
0
5
10
15
20
25
30
35
40
0
20
40
60
80
100

(b)

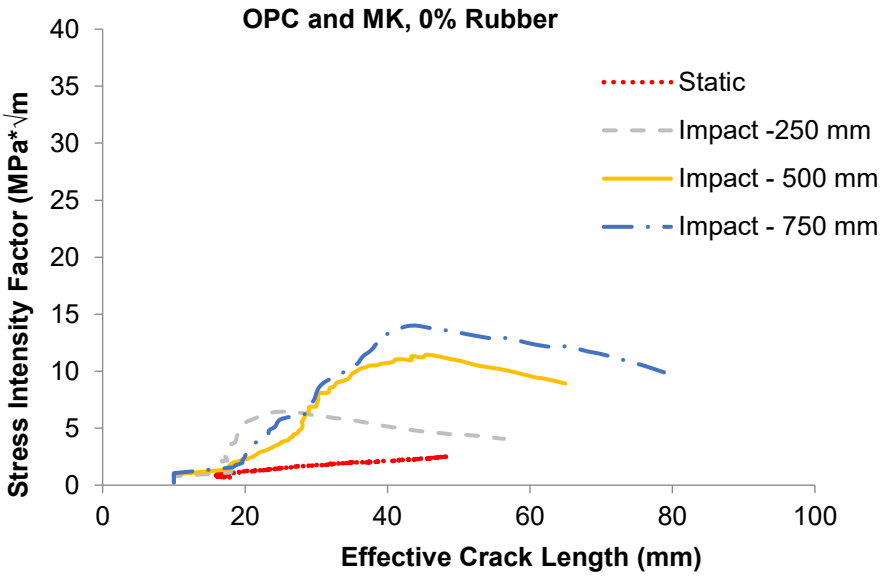
OPC and MK, 0% Rubber
Stress Intensity Factor (MPa*√m
Effective Crack Length (mm)
Static
Impact -250 mm
Impact - 500 mm
Impact - 750 mm
0
5
10
15
20
25
30
35
40
0
20
40
60
80
100

(c)

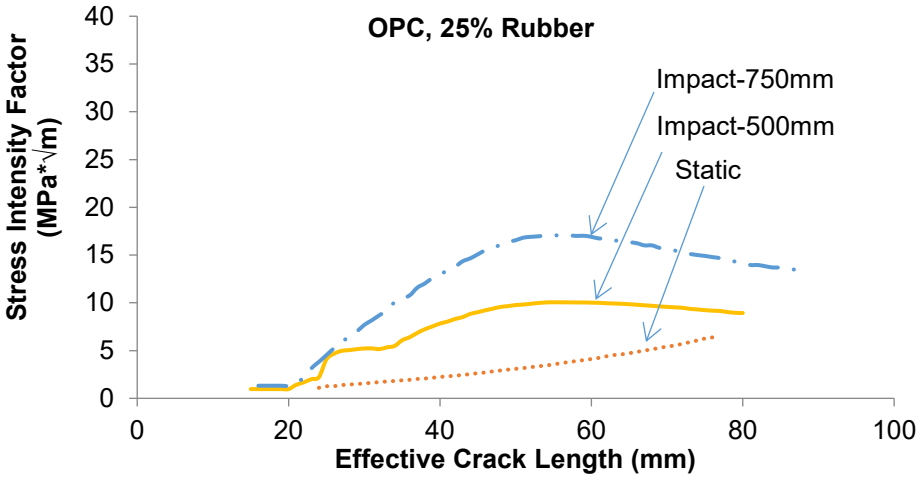
OPC, 25% Rubber
Impact-750mm
Impact-500mm
Static
Stress Intensity Factor (MPa*√m)
Effective Crack Length (mm)
0
5
10
15
20
25
30
35
40
0
20
40
60
80
100

(d)

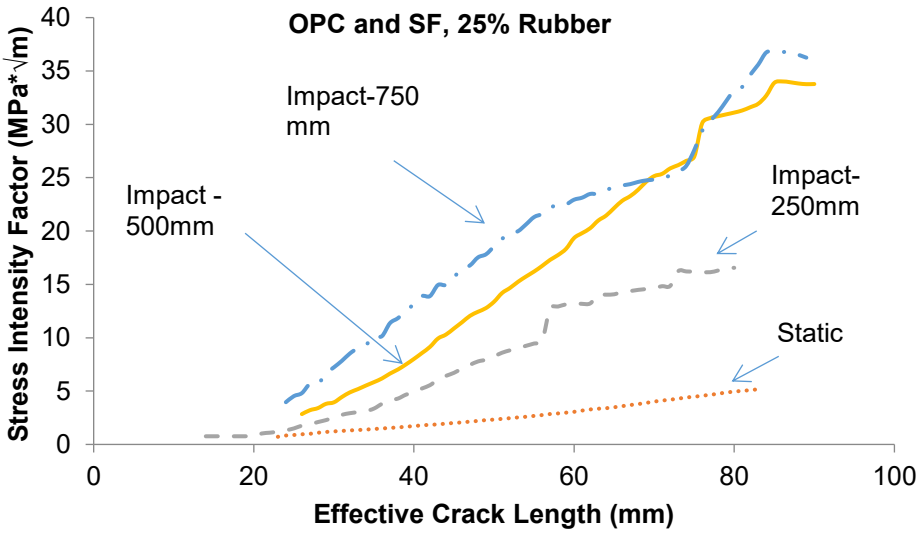
OPC and SF, 25% Rubber
Impact-750 mm
Impact - 500mm
Impact-250mm
Static
Stress Intensity Factor (MPa*√m)
Effective Crack Length (mm)
0
5
10
15
20
25
30
35
40
0
20
40
60
80
100

(e)

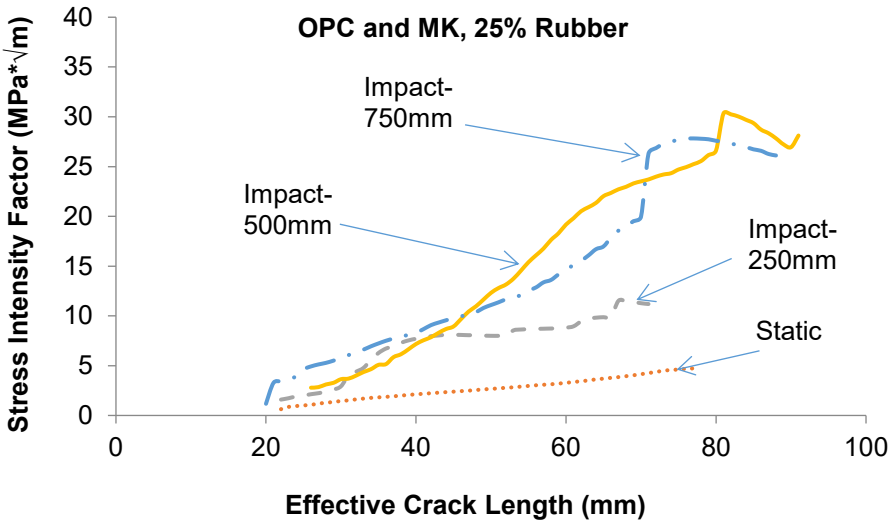
OPC and MK, 25% Rubber
Impact-750mm
Impact-500mm
Impact-250mm
Static
Stress Intensity Factor (MPa*√m)
Effective Crack Length (mm)
0
5
10
15
20
25
30
35
40
0
20
40
60
80
100

(f)

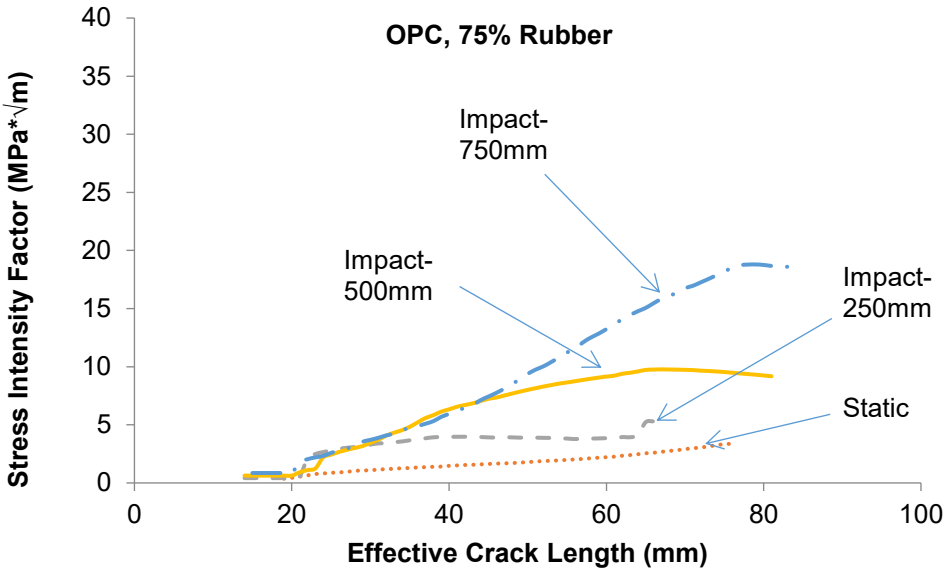
OPC, 75% Rubber
Impact-750mm
Impact-500mm
Impact-250mm
Static
Stress Intensity Factor (MPa*√m)
Effective Crack Length (mm)
0
5
10
15
20
25
30
35
40
0
20
40
60
80
100

(g)

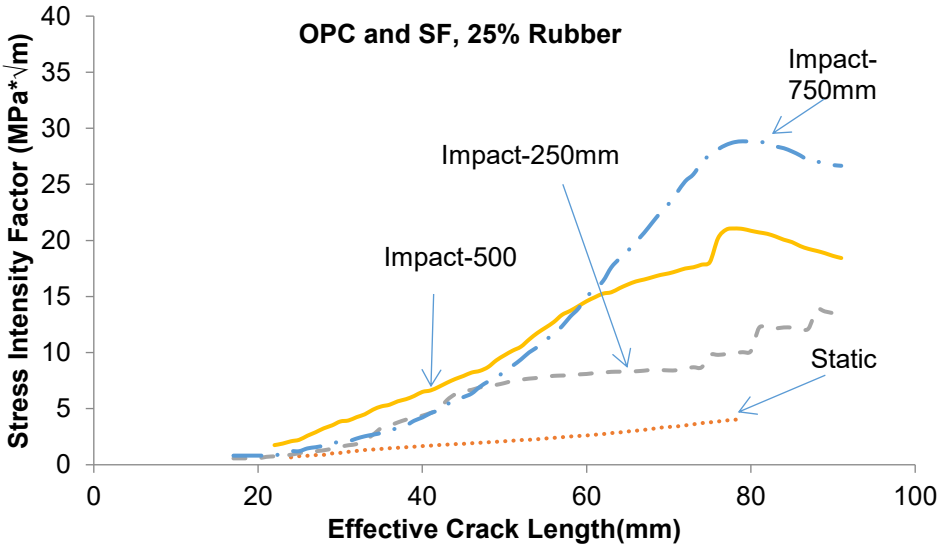

(h)

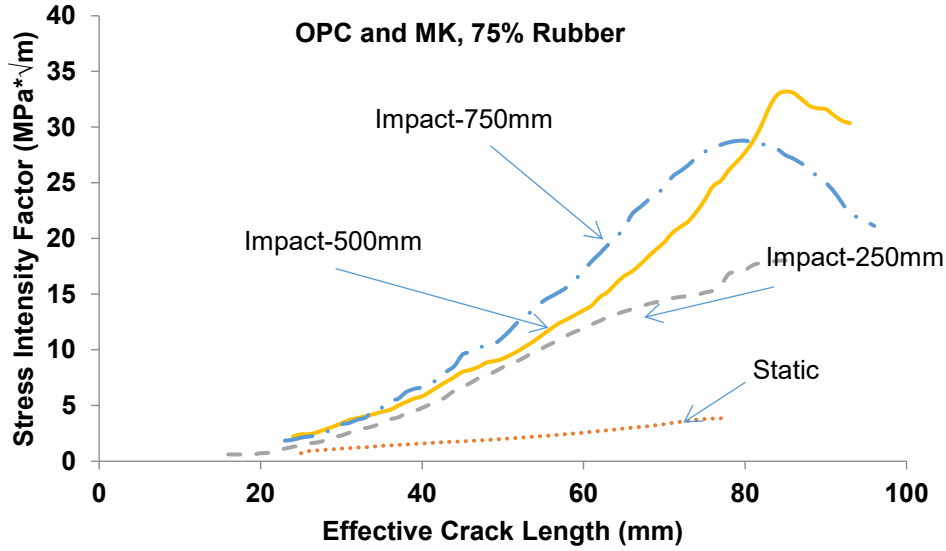

(i)

Figure 7-9: Crack growth resistance curves for various mixes

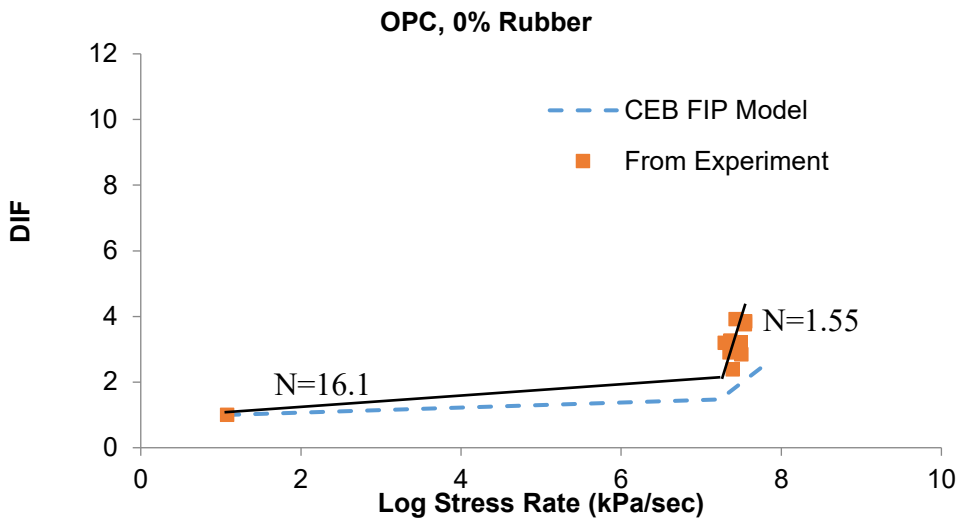
OPC, 0% Rubber
CEB FIP Model
From Experiment
DIF
Log Stress Rate (kPa/sec)
N=16.1
N=1.55
0
2
4
6
8
10
12

(a)

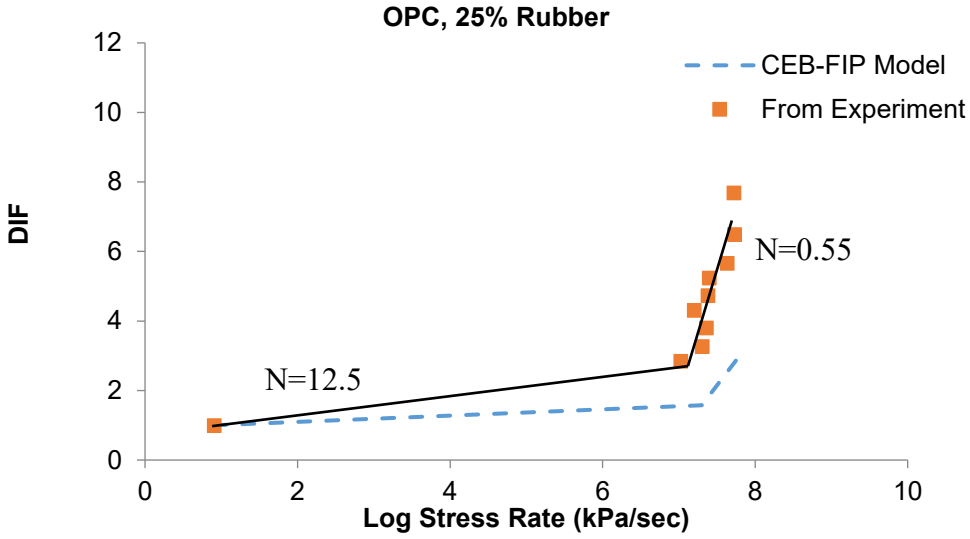
OPC, 25% Rubber
CEB-FIP Model
From Experiment
DIF
Log Stress Rate (kPa/sec)
N=12.5
N=0.55
0
2
4
6
8
10
12

(b)

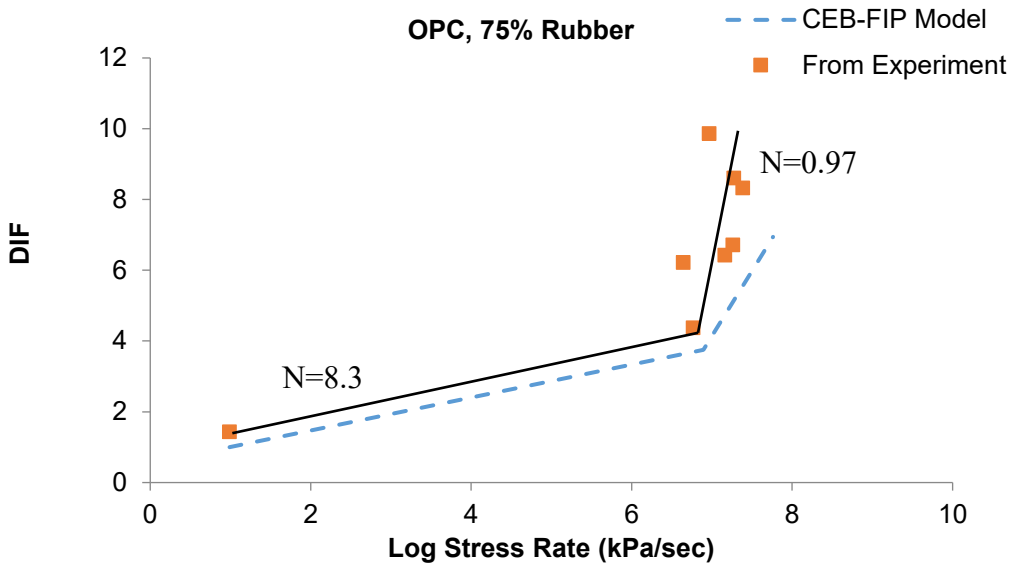
OPC, 75% Rubber
CEB-FIP Model
From Experiment
N=0.97
N=8.3
DIF
Log Stress Rate (kPa/sec)
0
2
4
6
8
10
12

(c)

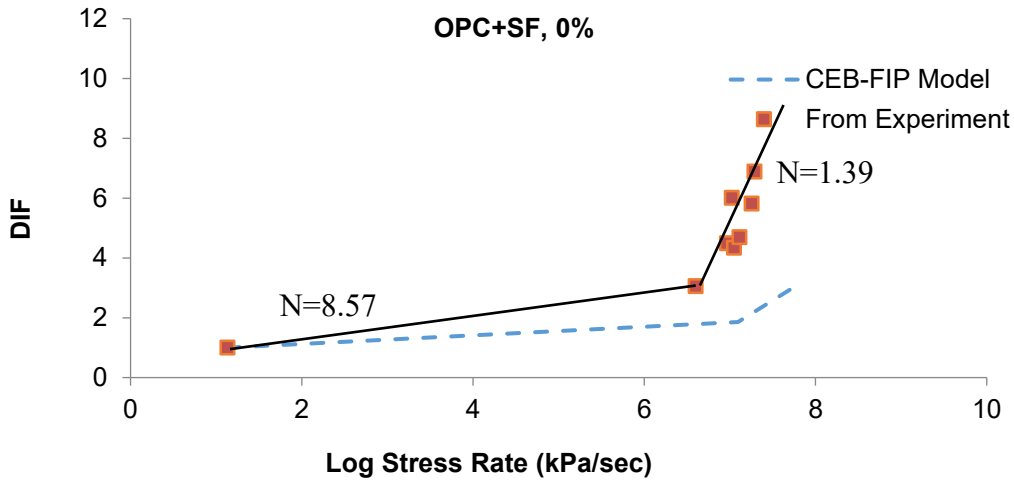
OPC+SF, 0%
CEB-FIP Model
From Experiment
N=1.39
N=8.57
DIF
Log Stress Rate (kPa/sec)
0
2
4
6
8
10
12

(d)

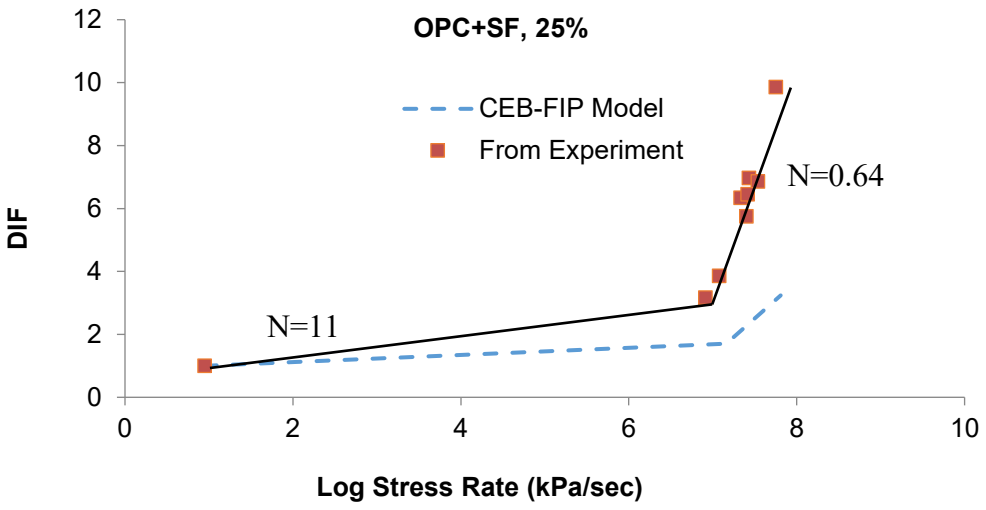
OPC+SF, 25%
CEB-FIP Model
From Experiment
N=0.64
N=11
DIF
Log Stress Rate (kPa/sec)
0
2
4
6
8
10
12

(e)

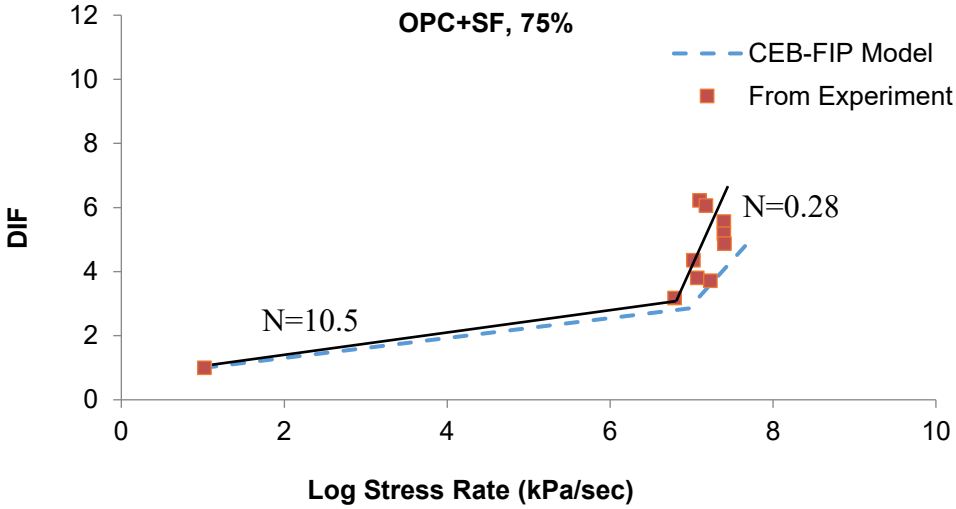
OPC+SF, 75%
CEB-FIP Model
From Experiment
N=0.28
N=10.5
DIF
Log Stress Rate (kPa/sec)
0
2
4
6
8
10
12

(f)

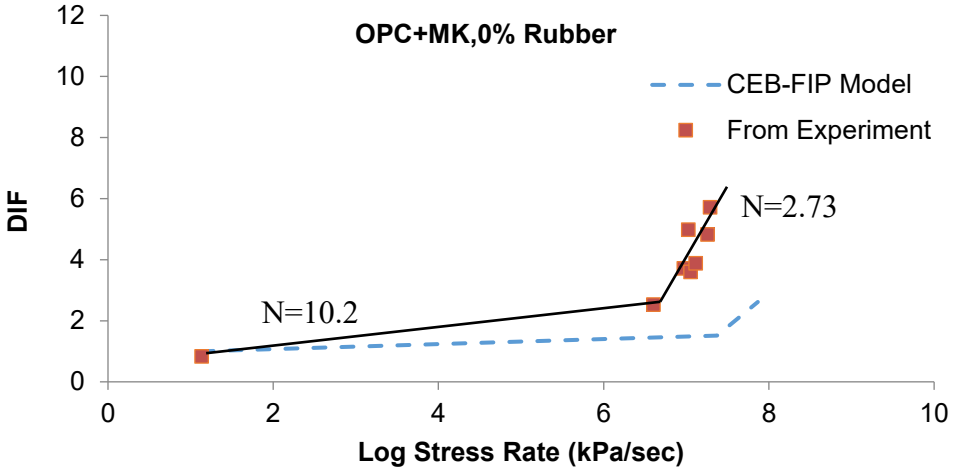
OPC+MK,0% Rubber
CEB-FIP Model
From Experiment
N=2.73
N=10.2
DIF
Log Stress Rate (kPa/sec)
0
2
4
6
8
10
12

(g)

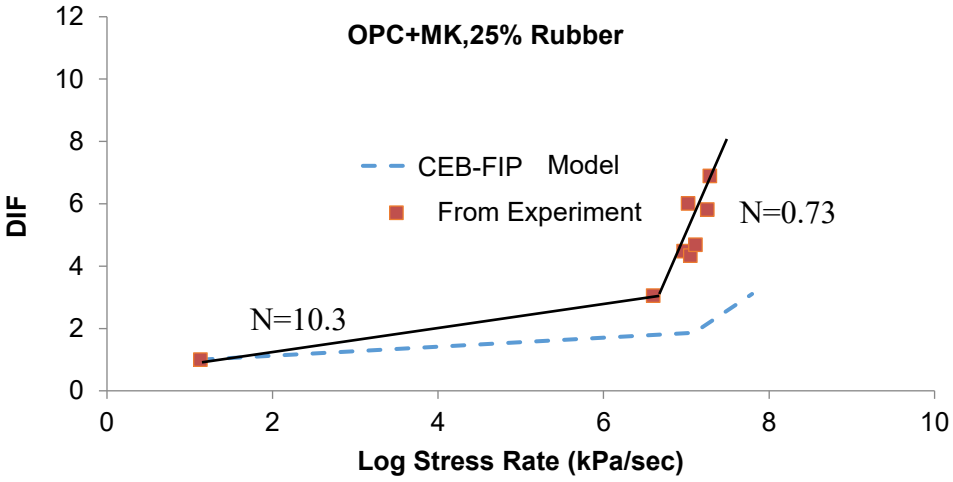
OPC+MK,25% Rubber
CEB-FIP Model
From Experiment
N=0.73
N=10.3
DIF
Log Stress Rate (kPa/sec)
0
2
4
6
8
10
12

(h)

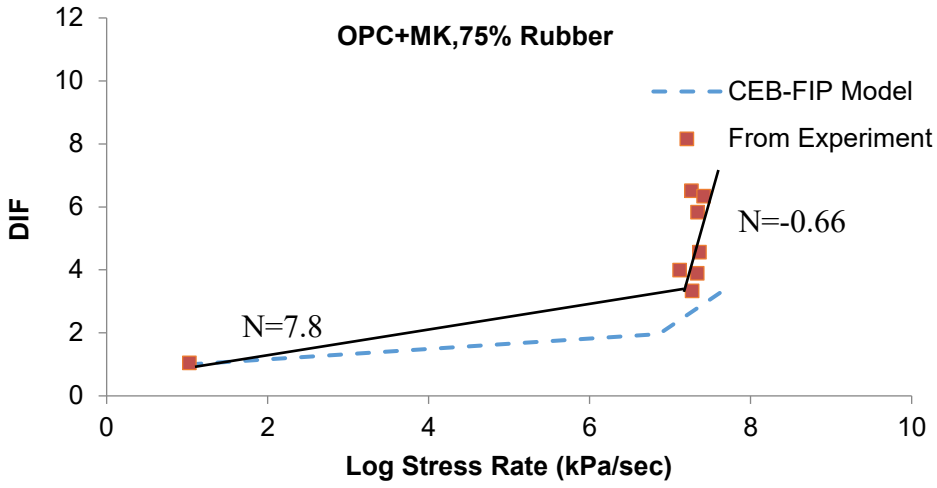

(i)

Figure 7-10: Stress rate sensitivity on flexural strength of various mixes

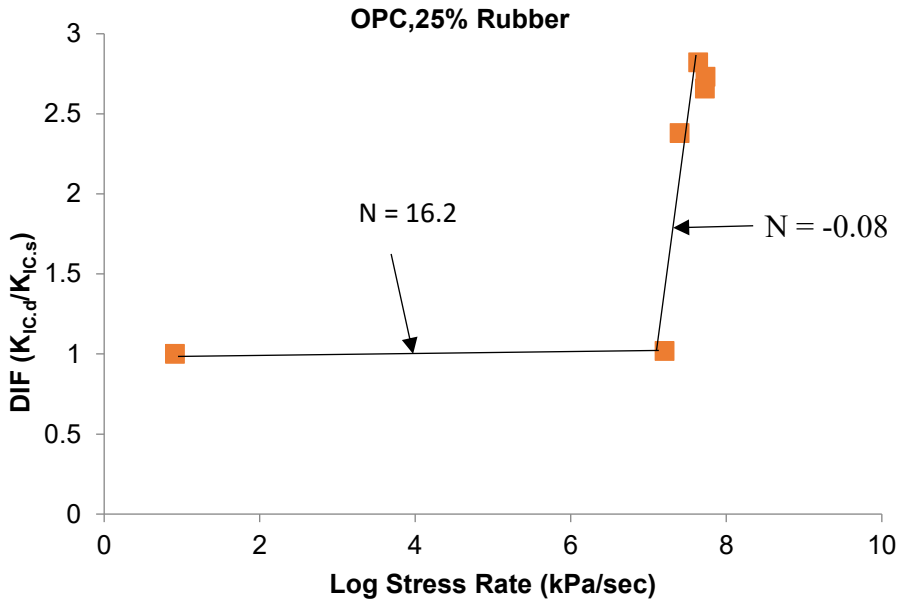

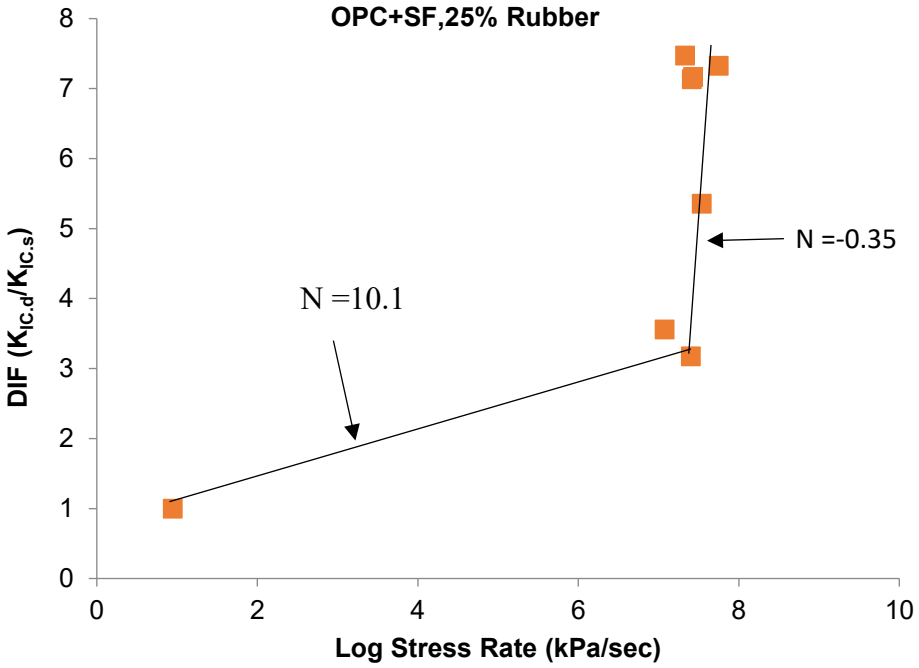
OPC+SF,25% Rubber
DIF ($K_{IC.d}/K_{IC.s}$)
Log Stress Rate (kPa/sec)
N =10.1
N =-0.35
0
1
2
3
4
5
6
7
8
0
2
4
6
8
10

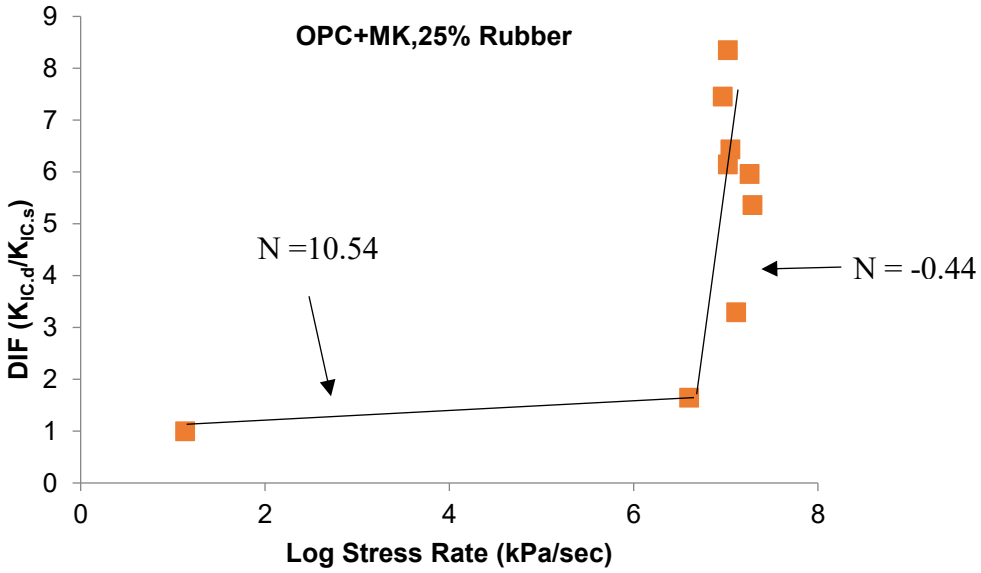
OPC+MK,25% Rubber
DIF ($K_{IC.d}/K_{IC.s}$)
Log Stress Rate (kPa/sec)
N =10.54
N = -0.44
0
1
2
3
4
5
6
7
8
9
0
2
4
6
8

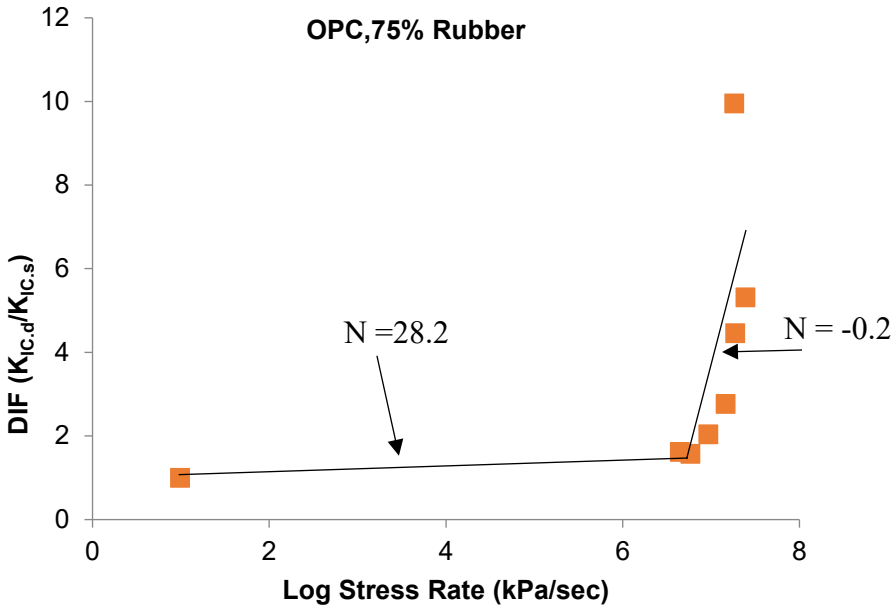
OPC,75% Rubber
DIF ($K_{IC.d}/K_{IC.s}$)
Log Stress Rate (kPa/sec)
N =28.2
N = -0.2
0
2
4
6
8
10
12

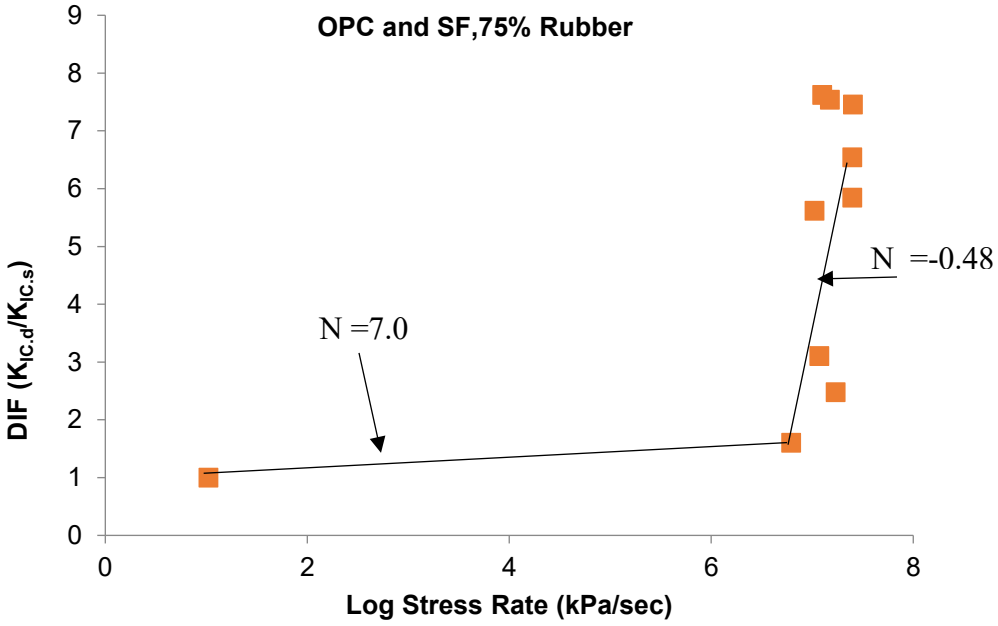
OPC and SF,75% Rubber
DIF ($K_{IC.d}/K_{IC.s}$)
Log Stress Rate (kPa/sec)
N =7.0
N =-0.48
0
1
2
3
4
5
6
7
8
9

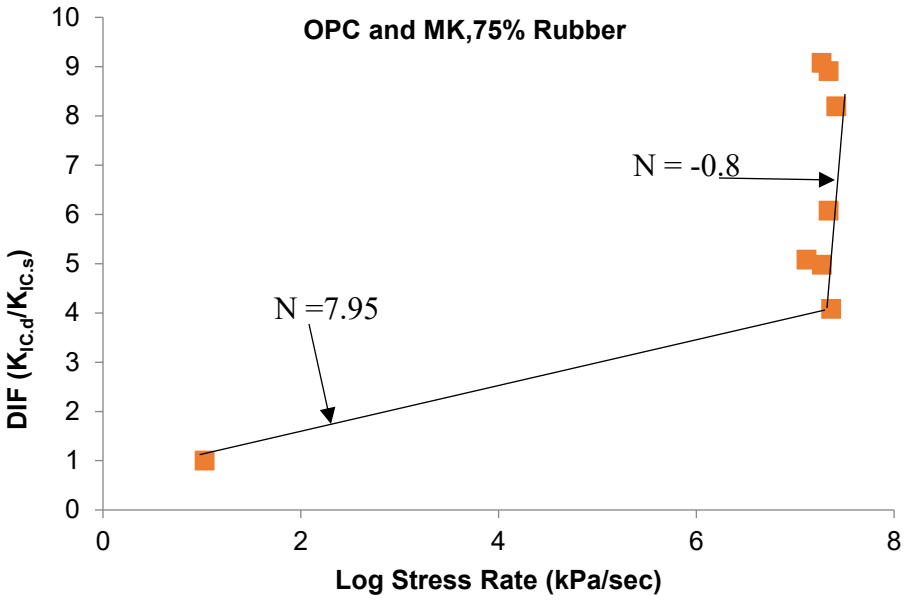

Figure 7-11: Effect of stress rate on fracture toughness, K_{IC}

References

ACI Committee 211.1. (1991). "Standard Practice for Selecting Proportions for Normal, Heavyweight, and Mass Concrete ACI 211.1 (Reapproved 2009)."

Armelin, H. S., and Banthia, N. (1997). "Predicting the flexural postcracking performance of steel fiber reinforced concrete from the pullout of single fibers." *ACI materials Journal*, 94(1).

ASTM C192. (2012). *Practice for Making and Curing Concrete Test Specimens in the Laboratory (ASTM C192)*. ASTM International, West Conshohocken, PA.

ASTM C469. (2010a). *Test Method for Static Modulus of Elasticity and Poissons Ratio of Concrete in Compression ASTM C469*. ASTM International, West Conshohocken, PA.

ASTM C1609. (2010b). *Test Method for Flexural Performance of Fiber-Reinforced Concrete (Using Beam With Third-Point Loading) ASTM C1609*. ASTM International, West Conshohocken, PA.

Balaguru, P. N., and Shah, S. P. (1992). *FIBER-REINFORCED CEMENT COMPOSITES*.

Banthia, N., Mindess, S., Bentur, A., and Pigeon, M. (1989). "Impact testing of concrete using a drop-weight impact machine." *Experimental Mechanics*, 29(1), 63–69.

Banthia, N., Yan, C., and Sakai, K. (1998). "Impact resistance of fiber reinforced concrete at subnormal temperatures." *Cement and Concrete Composites*, 20(5), 393–404.

Bentur, A., and Mindess, S. (2006). *Fibre Reinforced Cementitious Composites, Second Edition*. CRC Press.

Broek, D. (1986). *Elementary Engineering Fracture Mechanics*. Springer.

CEB-FIP. (1990). "CEB-FIP Model Code 90, Comite Euro-International du Beton –Federation Internationale de la Precontrainte."

Chung, K.-H., and Hong, Y.-K. (1999). "Introductory Behavior of Rubber Concrete." *JOURNAL OF APPLIED POLYMER SCIENCE*, 72(1), 35–40.

CSA A3001. (2009). "Cementitious materials compendium." Canadian Standards Association, Mississauga, ON.

Delage, P., and Aitcin, P. C. (1983). “Influence of condensed silica fume on the pore-size distribution of concretes.” *Industrial & Engineering Chemistry Product Research and Development*, 22(2), 286–290.

Detwiler, R. J., and Mehta, P. K. (1989). “Chemical and Physical Effects of Silica Fume on the Mechanical Behavior of Concrete.” *Materials Journal*, 86(6), 609–614.

Ding, J.-T., and Li, Z. (2002). “Effects of metakaolin and silica fume on properties of concrete.” *ACI Materials Journal*, 99(4), 393–398.

Eldin, N., and Senouci, A. (1993). “Rubber-Tire Particles as Concrete Aggregate.” *Journal of Materials in Civil Engineering*, 5(4), 478–496.

Gopalaratnam, V. S., and Shah, S. P. (1986). “Properties of steel fiber reinforced concrete subjected to impact loading.” *ACI Journal Proceedings*.

Gopalaratnam, V. S., Shah, S. P., and John, R. (1984). “A modified instrumented charpy test for cement-based composites.” *Experimental Mechanics*, 24(2), 102–111.

Gruber, K. A., Ramlochan, T., Boddy, A., Hooton, R. D., and Thomas, M. D. A. (2001). “Increasing concrete durability with high-reactivity metakaolin.” *Cement and Concrete Composites*, 23(6), 479–484.

Guinea, G. V., Pastor, J. Y., Planas, J., and Elices, M. (1998). “Stress Intensity factor, compliance and CMOD for a General Three-Point-Bend Beam.” *International Journal of Fracture*, 89(2), 103–116.

Güneyisi, E., Gesoğlu, M., and Özturan, T. (2004). “Properties of rubberized concretes containing silica fume.” *Cement and Concrete Research*, 34(12), 2309–2317.

Hooton, R. D. (1993). “Influence of Silica Fume Replacement of Cement on Physical Properties and Resistance to Sulfate Attack, Freezing and Thawing, and Alkali-Silica Reactivity.” *Materials Journal*, 90(2), 143–151.

Khatib, Z. K., and Bayomy, F. M. (1999). “Rubberized Portland Cement Concrete.” *Journal of Materials in Civil Engineering*, 11(3), 206–213.

Kramar, D., and Bindiganavile, V. (2013). “Impact response of lightweight mortars containing expanded perlite.” *Cement and Concrete Composites*, 37, 205–214.

Lee, H. S., Lee, H., Moon, J. S., and Jung, H. W. (1998). “Development of tire-added latex concrete.” *ACI Materials Journal*, 95(4), 356–364.

Mehta, P. K. (1983). “Pozzolanic and Cementitious Byproducts as Mineral Admixtures for Concrete - A Critical Review.” *Special Publication*, 79, 1–46.

Mehta, P. K., and Gjørv, O. E. (1982). “Properties of portland cement concrete containing fly ash and condensed silica-fume.” *Cement and Concrete Research*, 12(5), 587–595.

Mufti, A. A., Bentur, A., and Banthia, N. (1998). *Fiber reinforced concrete: present and future*. Canadian Society for Civil Engineering, Montreal.

Muhammad Mamun. (2010). “Loading Rate Effects and Sulphate Resistance of Fibre Reinforced Cement-based Foams.” Master’s Thesis, University of Alberta.

Naaman, A. E., and Gopalaratnam, V. S. (1983). “Impact properties of steel fibre reinforced concrete in bending.” *International Journal of Cement Composites and Lightweight Concrete*, 5(4), 225–233.

Nadeau, J. S., Bennett, R., and Fuller Jr, E. R. (1982). “An explanation for the rate-of-loading and the duration-of-load effects in wood in terms of fracture mechanics.” *Journal of Materials Science*, 17(10), 2831–2840.

Najim, K. B., and Hall, M. R. (2012). “Mechanical and dynamic properties of self-compacting crumb rubber modified concrete.” *Construction and Building materials*, 27(1), 521–530.

Qian, X., and Li, Z. (2001). “The relationships between stress and strain for high-performance concrete with metakaolin.” *Cement and Concrete Research*, 31(11), 1607–1611.

Raghavan, D., Huynh, H., and Raghavan, D. (1998). “Workability, mechanical properties, and chemical stability of a recycled tyre rubber-filled cementitious composite.” *Journal of Materials Science*, 33(7), 1745–1752.

Segre, N., and Joekes, I. (2000). “Use of tire rubber particles as addition to cement paste.” *Cement and Concrete Research*, 30(9), 1421–1425.

Suaris, W., and Shah, S. P. (1983). “Properties of Concrete Subjected to Impact.” *Journal of Structural Engineering*, 109(7), 1727–1741.

Suaris, W., and Shah, S. P. (1984). “Test Methods for Impact Resistance of Fiber Reinforced Concrete.” *Special Publication*, 81, 247–266.

Taha, M. M. R., El-Dieb, A. S., El-Wahab, M. A. A., and Abdel-Hameed, M. E. (2008). “Mechanical, fracture, and microstructural investigations of rubber concrete.” *Journal of Materials in Civil Engineering*, 20(10), 640–649.

Topçu, lker B., and Avcular, N. (1997). “Analysis of rubberized concrete as a composite material.” *Cement and Concrete Research*, 27(8), 1135–1139.

Topçu, I. B. (1995). “The properties of rubberized concretes.” *Cement and Concrete Research*, 25(2), 304–310.

Wedding, P., Suaris, W., and Shah, S. (1981). “Inertial Effects in the Instrumented Impact Testing of Cementitious Composites.” *Cement, Concrete and Aggregates*, 3(2), 77.

Wild, S., Khatib, J. M., and Jones, A. (1996). “Relative strength, pozzolanic activity and cement hydration in superplasticised metakaolin concrete.” *Cement and Concrete Research*, 26(10), 1537–1544.

Wong, S.-F., and Ting, S.-K. (2009). “Use of recycled rubber tires in normal and high-strength concretes.” *ACI Materials Journal*, 106(4).

Zheng, L., Huo, X. S., and Yuan, Y. (2008). “Strength, Modulus of Elasticity, and Brittleness Index of Rubberized Concrete.” *Journal of Materials in Civil Engineering*, 20(11), 692–699.

Notations

$S =$ Span

l = overhang span

A = cross sectional area

$\rho =$ mass density

$\ddot{u}(t)$ = acceleration at mid span at any time t

Δ_0 = deflection history

$R^D_{T,150}$ = Equivalent flexural strength ratio

T^D_{150}= toughness up to a net deflection of $L/150$,

L = Span of the beam specimen

f_1 = first Peak Strength

b = average width of the specimen at fracture

d = average depth of the specimen at fracture

f'_c = Compressive Strength of concrete

E_c = Modulus of Elasticity of concrete

f_r= Modulus of rupture

Δ = deflection at midspan

$CMOD$ = crack mouth opening displacement

m = slope of deflection-CMOD line

K_{IC} = Fracture Toughness

σ_f = stress at final condition

σ_i = stress at initial condition

B = constant in stress rate sensitivity Equation (7.7) proposed by Nadeau et al.(1982)

N = constant in stress rate sensitivity Equation (7.7) proposed by Nadeau et al.(1982), which particularly related to stress rate sensitivity of parameters

$\dot{\sigma}$= stress rate

Appendix – VII

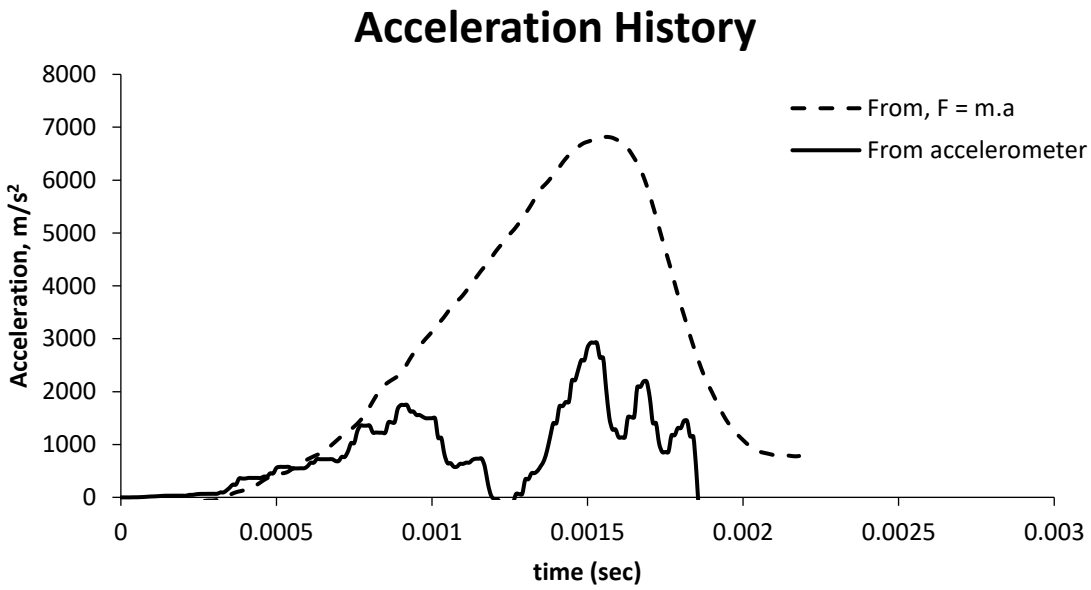

CR0F1- Only OPC –Drop Height 250 mm

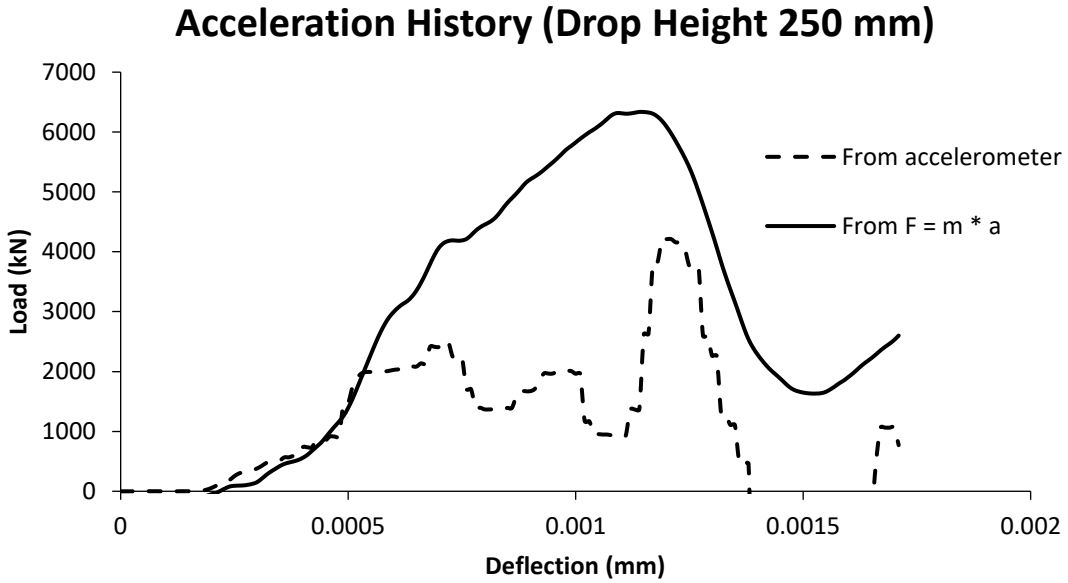

CR0F1 OPC and Silica Fume, Drop Height 250 mm

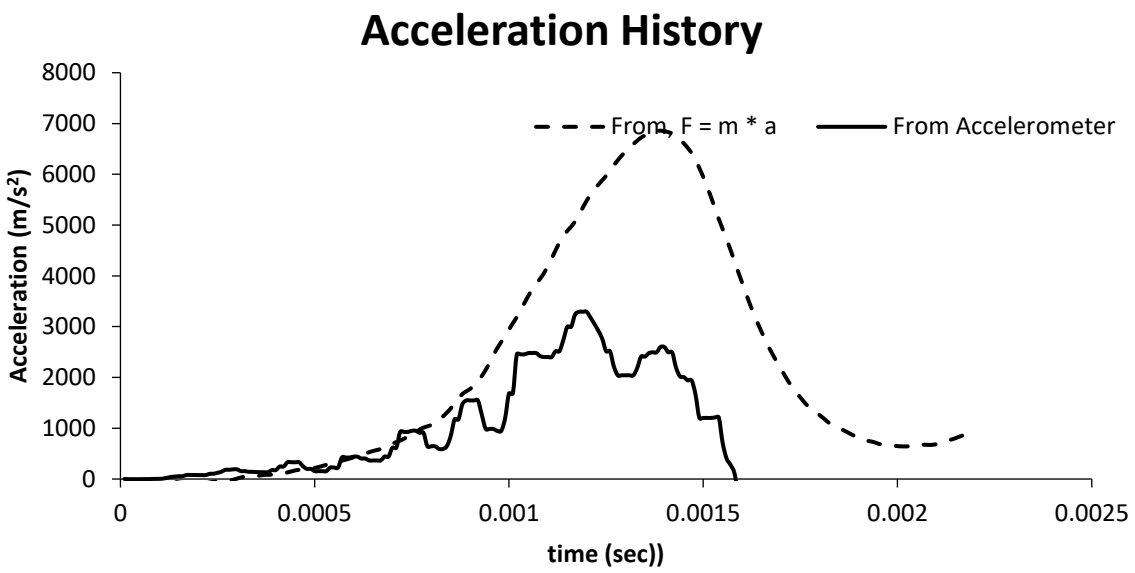

CR0F1OPC and Metakaolin, Drop Height 250 mm

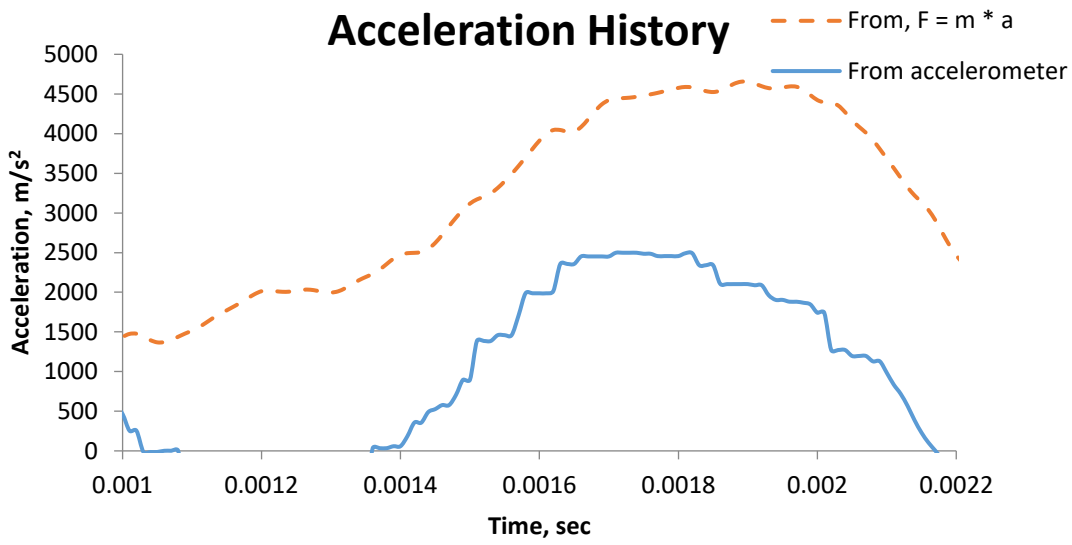

CR25F1 Only OPC, Drop Height 250 mm

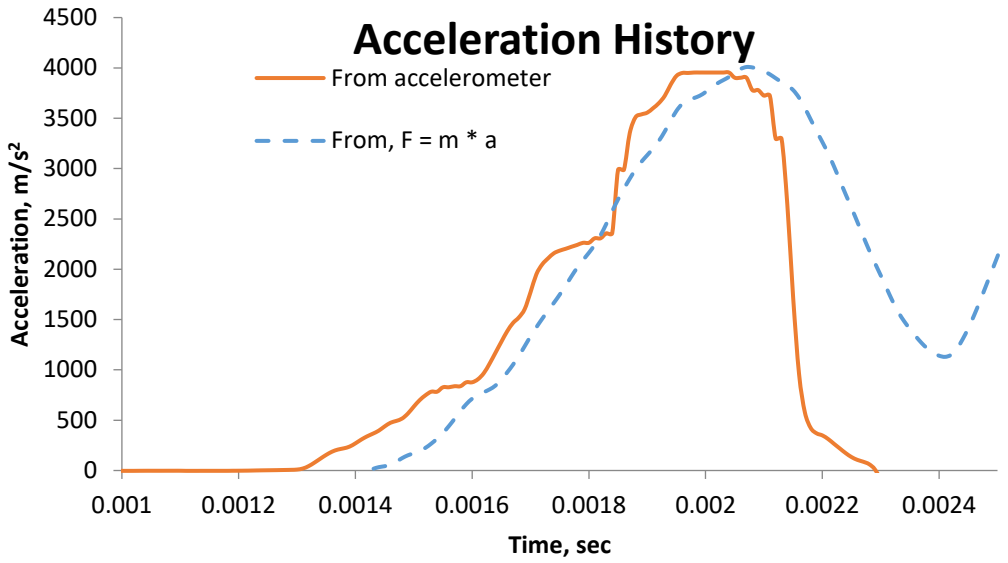

CR25F1 OPC and Silica Fume, Drop Height 250 mm

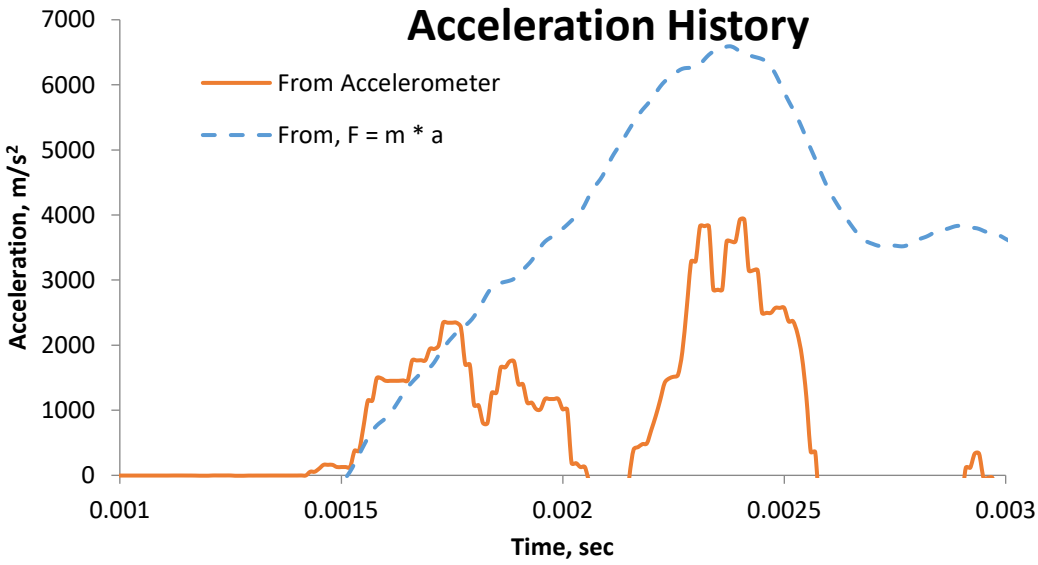

CR25F1 OPC and Metakaolin, Drop Height 250 mm

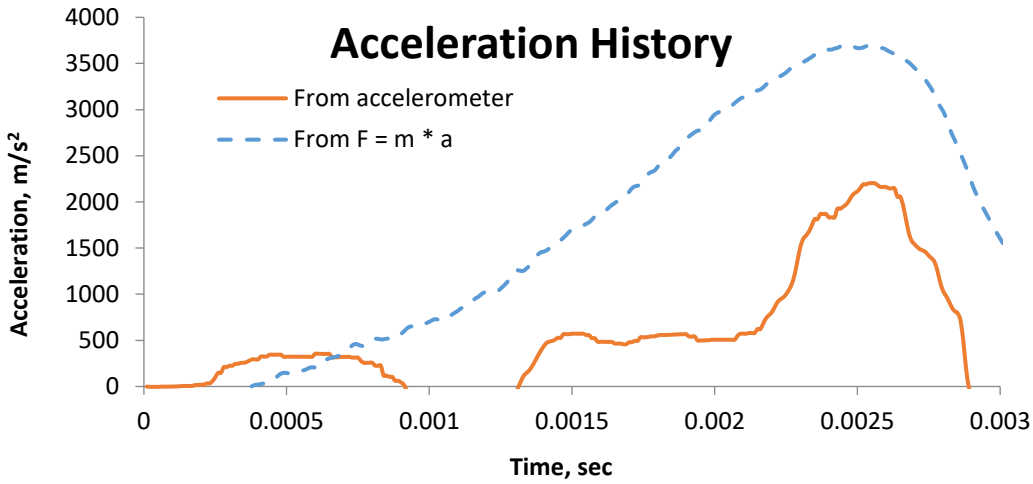

CR75F1 Only OPC, Drop Height 250 mm

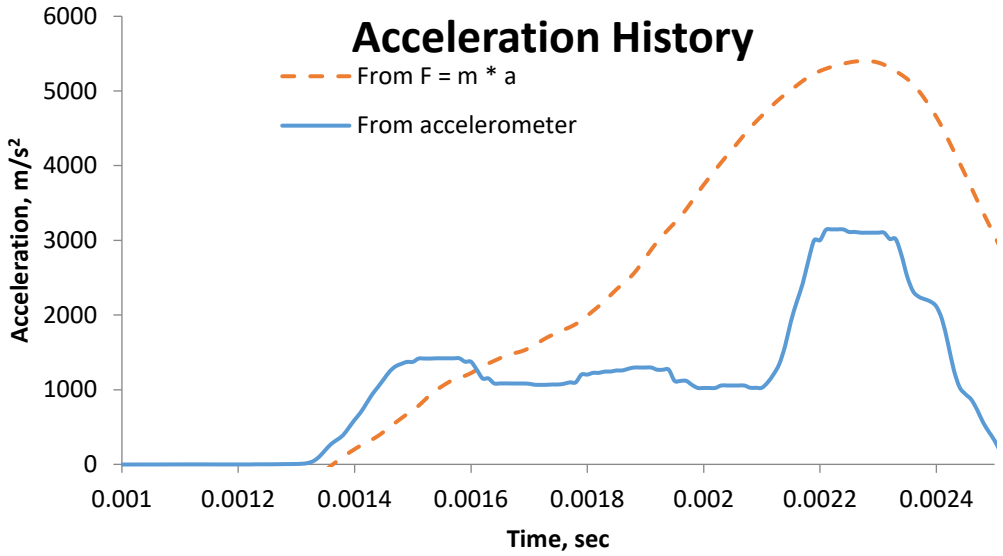

CR75F1 OPC and Silica Fume, Drop Height 250 mm

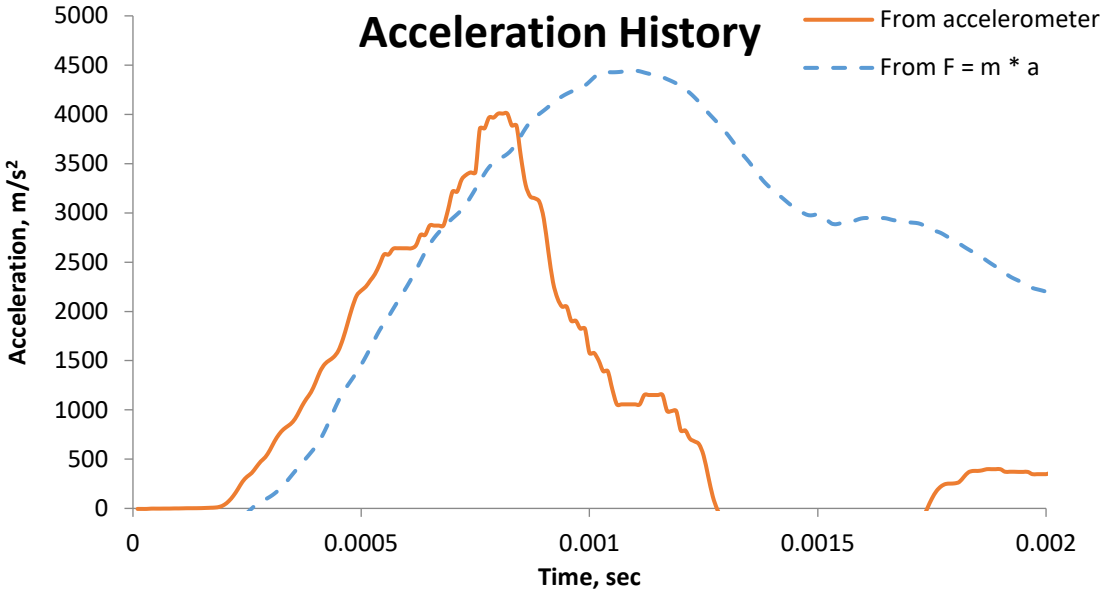

CR75F1 OPC and Metakaolin, Drop Height 250 mm

CHAPTER 8. CONCLUSION

8.1 Research summary

This research has the overall goal of developing a sustainable concrete mixtures where crumb rubber from scrap tires have been used and then evaluating bond-slip performances of those concrete mixtures with FRP bar.

For the sustainable concrete mix developments; first, concrete mixtures were prepared using various percentage of crumb rubber as replacement of fine aggregate and using various supplementary cementitious materials for evaluation of preliminary physical and mechanical properties, as described in Chapter 3. After completing the comparative analysis of the results, further concrete mixtures were developed using 0%, 25%, 50%, 75% and 100% replacement of fine aggregate with crumb rubber and with silica fume as supplementary cementitious material and by evaluating their mechanical and physical properties as shown in Chapter 4.

For establishing bond-slip analytical models, first, pullout specimens were prepared and bond tests were performed on different concrete mixtures and different bar sizes. Those results were presented in Chapter 5. In Chapter 6, the bond-slip responses derived in Chapter 5 were evaluated with existing analytical models and necessary parameters were derived for various mix composition and bar sizes. Later those models were verified with experimental results. In Chapter 7 the bond-slip analysis were done on beam specimens to evaluate the effect of different stress condition in surrounding concrete on the bond performance.

8.2 Conclusions

Detailed conclusions can be found in each Chapter from Chapter 3 to Chapter 7. The more generalized conclusions are summarized as follows.

1) In Chapter 3, the compressive strength, modulus of elasticity and modulus of rupture decreases with an increase in crumb rubber replacement. At higher crumb rubber replacement addition of supplementary cementitious material improves the

compressive strength, modulus of elasticity and modulus of rupture. For mixes with steel fibre, at 50% crumb rubber replacement level, the modulus of rupture is the maximum with compare to other mixes with different crumb rubber replacement level.

2) In Chapter 4 it was found that, in the presence of crumb rubber, the bond strength between FRP bar and concrete decreases with an increase in the crumb rubber replacement. In the plain concrete, larger diameter rebar yields lower bond strength at lower crumb rubber replacement. However, at higher crumb rubber replacement larger bar diameter rebar yields better bond strength. The presence of short steel fibre reduces the bond strength at lower crumb rubber replacement.
3) In Chapter 5, bond-slip responses between various concrete mixes and bar sizes were evaluated and compared with existing analytical bond-slip models. Among other models, mBPE model was found to have reliable prediction of the bond-slip responses between FRP and concrete mixes of this study.
4) In Chapter 6, bond-slip responses were studied in beam samples. Decrease in bond strength was observed with increase in crumb rubber replacement. Larger diameter bar yields lower bond strength. Presence of steel fibre were found to have negative impact on bond strength.
5) In Chapter 7, various concrete mixes with different crumb rubber replacement and supplementary cementitious material (silica fume and metakaolin) were tested under various loading rates. At higher crumb rubber replacement, concrete mixes with silica fume and metakaolin showed higher stress rate sensitivity for flexural strength.

8.3 Contributions

This research mainly has two areas of contributions, namely, the development of sustainable concrete matrices and the development of analytical bond model to predict the bond-slip performances between FRP bar and developed concrete matrices.

In the area of sustainable concrete mixtures development, lightweight concrete has been developed. This concrete has lower density, comparable concrete compressive strength, flexural strength and better ductility or higher energy absorption.

In the area of analytical model development, all the parameters for various analytical models were determined. Careful comparison was made to determine the applicability of those models. One analytical model (mBPE) was found to represent bond-slip responses more closely with compare to others.

This research mainly targets on the problems of lightweight shock absorbing concrete mixes by incorporating crumb rubber as replacement of fine aggregate and their bond performance with FRP bar. But it is not limited to this application. Concrete with crumb rubber can be used as foundation pad for machinery or trench filling, paving slabs where high compressive strength concrete isn't significant.

8.4 Recommendations for future research

In the areas of sustainable lightweight concrete mixtures development and analytical bond-slip model development, some recommendations for future research based on the author's knowledge are listed as follows,

1. Concrete mixtures with all ranges of crumb rubber percentages can be developed using other available supplementary cementitious material i.e. fly Ash and blast-furnace slag.
2. The effect of specimen sizes on various mechanical properties can be evaluated for all the matrices.
3. Bond performance of GFRP bar and concrete mixes with tire chips as coarse aggregate replacement can be evaluated, which would consume a significant amount of tire waste.
4. Exploring the influence of other steel fibre dosages as well as other fibre types to the mechanical and fresh concrete properties of the concrete mixes. Varying dosage of steel fibre and polypropylene fibre can also be used to determine their effect on bond strength.

   Different bar sizes (other than 10mm and 16m) may be incorporated to analysis the effect of bar diameter on the bond strength in lightweight concrete. In addition to that, the bond strength of FRP bars with different surface condition can be evaluated.

BIBLIOGRAPHY

Achillides, Z., and Pilakoutas, K. (2004). "Bond behavior of fiber reinforced polymer bars under direct pullout conditions." *Journal of Composites for construction*, 8, 173.

ACI 318. (2014). *Building Code Requirements for Structural Concrete and Commentary*. American Concrete Institute, Farmington Hills, MI.

ACI 408R-03. (2012). *Bond and Development of Straight Reinforcing Bars in Tension*. American Concrete Institute, Farmington Hills, MI.

ACI Committee 211.1. (1991). "Standard Practice for Selecting Proportions for Normal, Heavyweight, and Mass Concrete ACI 211.1 (Reapproved 2009)."

Aiello, M. A., Leone, M., and Pecce, M. (2007). "Bond Performances of FRP Rebars-Reinforced Concrete." *Journal of Materials in Civil Engineering*.

Alexander, M., and Mindess, S. (2005). *Aggregates in Concrete*. Taylor and Francis, 270 Madison Ave, New York, NY.

Altowaiji, W. A. K., Darwin, D., and Donahey, R. C. (1986). "Bond of Reinforcement to Revibrated Concrete." *Journal Proceedings*, 83(6), 1035–1042.

Al-Zahrani, M. M., Al-Dulaijan, S. U., Nanni, A., Bakis, C. E., and Boothby, T. E. (1999). "Evaluation of bond using FRP rods with axisymmetric deformations." *Construction and Building Materials*, 13(6), 299–309.

Ametrano, D. (2011). "Bond characteristics of glass fibre reinforced polymer bars embedded in high performance and ultra-high performance concrete." *Ryerson University, Toronto, Ontario, Canada*, 1–132.

Ametrano, D., Hossain, K. M. A., and Lachemi, M. (2011). "Bond characteristics of glass fibre reinforced polymer bars embedded in high strength and ultra-high strength comcrete." *2nd International Engineering Mechanics and Materials Speciality Conference*, Ottawa, Ontario.

Armelin, H. S., and Banthia, N. (1997). "Predicting the flexural postcracking performance of steel fiber reinforced concrete from the pullout of single fibers." *ACI materials Journal*, 94(1).

ASTM C192. (2012). *Practice for Making and Curing Concrete Test Specimens in the Laboratory (ASTM C192)*. ASTM International, West Conshohocken, PA.

ASTM C469. (2010a). *Test Method for Static Modulus of Elasticity and Poissons Ratio of Concrete in Compression ASTM C469*. ASTM International, West Conshohocken, PA.

ASTM C1609. (2010b). *Test Method for Flexural Performance of Fiber-Reinforced Concrete (Using Beam With Third-Point Loading) ASTM C1609*. ASTM International, West Conshohocken, PA.

ASTM D6114. (2009). *Standard Specification for Asphalt-Rubber Binder, ASTM D6114/D6114M*. ASTM International, West Conshohocken, PA.

ASTM D6270. (2009). *Standard practice for use of scrap tires in civil engineering applications. ASTM D6270*. West Conshohocken, PA.

Azizinamini, A., Chisala, M., and Ghosh, S. K. (1995). "Tension development length of reinforcing bars embedded in high-strength concrete." *Engineering structures*, 17(7), 512–522.

Azizinamini, A., Stark, M., Roller, J. J., and Ghosh, S. (1993). "Bond performance of reinforcing bars embedded in high-strength concrete." *ACI Structural Journal*, 90(5), 554–561.

Baena, M., Torres, L., Turon, A., and Barris, C. (2009). "Experimental study of bond behaviour between concrete and FRP bars using a pull-out test." *Composites Part B: Engineering*, 40(8), 784–797.

Baena, M., Turon, A., Torres, L., and Miàs, C. (2011). "Experimental study and code predictions of fibre reinforced polymer reinforced concrete (FRP RC) tensile members." *Composite Structures*, 93(10), 2511–2520.

Balaguru, P. N., and Shah, S. P. (1992). *FIBER-REINFORCED CEMENT COMPOSITES*.

Banthia, N., and Dubey, A. (1999). “Measurement of Flexural Toughness of Fiber-Reinforced Concrete Using a Novel Technique—Part 1: Assessment and Calibration.” *Materials Journal*, 96(6), 651–656.

Banthia, N., and Dubey, A. (2000). “Measurement of Flexural Toughness of Fiber-Reinforced Concrete Using a Novel Technique—Part 2: Performance of Various Composites.” *Materials Journal*, 97(1), 3–11.

Banthia, N., Mindess, S., Bentur, A., and Pigeon, M. (1989). “Impact testing of concrete using a drop-weight impact machine.” *Experimental Mechanics*, 29(1), 63–69.

Banthia, N. P., Mindess, S., and Bentur, A. (1987). “Impact behaviour of concrete beams.” *Materials and Structures*, 20(4), 293–302.

Banthia, N., Yan, C., and Sakai, K. (1998). “Impact resistance of fiber reinforced concrete at subnormal temperatures.” *Cement and Concrete Composites*, 20(5), 393–404.

Barr, B., and Newman, P. D. (1985). “Toughness of polypropylene fibre-reinforced concrete.” *Composites*, 16(1), 48–53.

Benmokrane, B., Tighiouart, B., and Chaallal, O. (1996). “Bond strength and load distribution of composite GFRP reinforcing bars in concrete.” *ACI Materials Journal*, 93(3).

Bentur, A., and Mindess, S. (2006). *Fibre Reinforced Cementitious Composites, Second Edition*. CRC Press.

Bertollo, S. (2004). *Mechanical properties of asphalt mixtures using recycled tyre rubber produced in Brazil – a laboratory evaluation*. 83rd TRB Annual Meeting, Washington.

Biel, T., and Lee, H. (1996). “Magnesium Oxychloride Cement Concrete with Recycled Tire Rubber.” *Transportation Research Record: Journal of the Transportation Research Board*, 1561, 6–12.

Brettmann, B. B., Darwin, D., and Donahey, R. C. (1986). “Bond of Reinforcement to Superplasticized Concrete.” *ACI Journal Proceedings*, 83(1), 98–107.

Broek, D. (1986). *Elementary Engineering Fracture Mechanics*. Springer.

Caltrans. (2006). *Caltrans. Asphalt Rubber Usage Guide*. State of California Department of Transportation, Materials Engineering and Testing Services.

CEB-FIP. (1990). "CEB-FIP Model Code 90, Comite Euro-International du Beton –Federation Internationale de la Precontrainte."

CEB-FIP. (1994). *Test of the Bond Strength of Reinforcement of Concrete: Test by Bending.* RILEM Recommendations for the Testing and use of Constructions Materials,.

Chaallal, O., and Benmokrane, B. (1993a). "Pullout and bond of glass-fibre rods embedded in concrete and cement grout." *Materials and structures*, 26(3), 167–175.

Chaallal, O., and Benmokrane, B. (1993b). "Physical and mechanical performance of an innovative glass-fiber-reinforced plastic rod for concrete and grouted anchorages." *Canadian Journal of Civil Engineering*, 20(2), 254–268.

Chung, K.-H., and Hong, Y.-K. (1999). "Introductory Behavior of Rubber Concrete." *JOURNAL OF APPLIED POLYMER SCIENCE*, 72(1), 35–40.

Cosenza, E., Manfredi, G., and R, R. (1995). "Analytical modelling of bond between FRP reinforcing bars and concrete." *ResearchGate*, 164–171.

Cosenza, E., Manfredi, G., and Realfonzo, R. (1997). "Behavior and modeling of bond of FRP rebars to concrete." *Journal of composites for construction*, 1(2), 40–51.

CSA A23.3-04. (2004). "Design of Concrete Structures." Canadian Standards Association, Mississauga, ON.

CSA A3001. (2009). "Cementitious materials compendium." Canadian Standards Association, Mississauga, ON.

CSA S806-12. (2012). "Design and construction of building structures with fibre-reinforced polymers." Canadian Standards Association, Mississauga, ON.

Darwin, D., and Graham, E. K. (1993). "Effect of Deformation Height and Spacing on Bond Strength of Reinforcing Bars." *Structural Journal*, 90(6), 646–657.

Darwin, D., McCabe, S. L., Idun, E. K., and Schoenekase, S. P. (1992). "Development Length Criteria: Bars Not Confined by Transverse Reinforcement." *Structural Journal*, 89(6), 709–720.

Darwin, D., Tholen, M. L., Idun, E. K., and Zuo, J. (1996). "Splice Strength of High Relative Rib Area Reinforcing Bars." *Structural Journal*, 93(1), 95–107.

Delage, P., and Aitcin, P. C. (1983). "Influence of condensed silica fume on the pore-size distribution of concretes." *Industrial & Engineering Chemistry Product Research and Development*, 22(2), 286–290.

Detwiler, R. J., and Mehta, P. K. (1989). "Chemical and Physical Effects of Silica Fume on the Mechanical Behavior of Concrete." *Materials Journal*, 86(6), 609–614.

Dhir, R. K., Dyer, T. D., and Halliday, J. E. (Eds.). (2002a). *Challenges of Concrete Construction: Volume 5, Sustainable Concrete Construction: Proceedings of the International Conference held at the University of Dundee, Scotland, UK on 9–11 September 2002*. Thomas Telford Publishing.

Dhir, R. K., McCarthy, M. J., and Newlands, M. D. (Eds.). (2002b). *Challenges of Concrete Construction: Volume 6, Concrete for Extreme Conditions: Proceedings of the International Conference held at the University of Dundee, Scotland, UK on 9–11 September 2002*. Thomas Telford Publishing.

Ding, J.-T., and Li, Z. (2002). "Effects of metakaolin and silica fume on properties of concrete." *ACI Materials Journal*, 99(4), 393–398.

Ding, Y., Ning, X., Zhang, Y., Pacheco-Torgal, F., and Aguiar, J. B. (2014). "Fibres for enhancing of the bond capacity between GFRP rebar and concrete." *Construction and Building Materials*, 51, 303–312.

Drescher, A., and Newcomb, D. E. (1994). *Development of design guidelines for use of shredded tires as a lightweight fill in road subgrade and retaining walls*. Report, Minnesota Department of Transportation.

Duval, R., and Kadri, E. H. (1998). “Influence of Silica Fume on the Workability and the Compressive Strength of High-Performance Concretes.” *Cement and Concrete Research*, 28(4), 533–547.

Ehsani, M., Saadatmanesh, H., and Tao, S. (1996). “Design recommendations for bond of GFRP rebars to concrete.” *Journal of Structural Engineering*, 122(3), 247–254.

Ehsani, M., Saadatmanesh, H., and Tao, S. (1997). “Bond behavior of deformed GFRP rebars.” *Journal of Composite Materials*, 31(14), 1413–1430.

Eldin, N., and Senouci, A. (1993). “Rubber-Tire Particles as Concrete Aggregate.” *Journal of Materials in Civil Engineering*, 5(4), 478–496.

Eligehausen, R., Popov, E. P., and Bertero, V. V. (1982). “Local Bond stress slip relationship of deformed bars under generalized excitations.” *ResearchGate*.

Epps, J. A. (1994). “USES OF RECYCLED RUBBER TIRES IN HIGHWAYS.” *NCHRP Synthesis of Highway Practice*, (198).

Esfahani, M. R., Kianoush, M. R., and Lachemi, M. (2005). “Bond strength of glass fibre reinforced polymer reinforcing bars in normal and self-consolidating concrete.” *Canadian Journal of Civil Engineering*, 32(3), 553–560.

Esfahani, M. R., and Rangan, B. V. (1998). “Bond between Normal Strength and High-Strength Concrete (HSC) and Reinforcing Bars in Splices in Beams.” *Structural Journal*, 95(3), 272–280.

Ezeldin, A. S., and Balaguru, P. N. (1990). “Characterization of bond between fiber concrete and reinforcing bars using nonlinear finite element analysis.” *Computers & Structures*, 37(4), 569–584.

Fattuhi, N. I., and Clark, L. A. (1996). “Cement-based materials containing shredded scrap truck tyre rubber.” *Construction and Building Materials*, 10(4), 229–236.

Fedroff, D., Ahmad, S., and Savas, B. (1996). “Mechanical Properties of Concrete with Ground Waste Tire Rubber.” *Transportation Research Record: Journal of the Transportation Research Board*, 1532, 66–72.

Focacci, F., Nanni, A., and Bakis, C. E. (2000). “Local Bond-Slip Relationship for FRP Reinforcement in Concrete.” *Journal of Composites for Construction*, 4(1), 24–31.

Gonçalves, M. C., and Margarido, F. (Eds.). (2015). *Materials for Construction and Civil Engineering*. Springer International Publishing, Cham.

Gopalaratnam, V. S., and Shah, S. P. (1986). “Properties of steel fiber reinforced concrete subjected to impact loading.” *ACI Journal Proceedings*.

Gopalaratnam, V. S., Shah, S. P., and John, R. (1984). “A modified instrumented charpy test for cement-based composites.” *Experimental Mechanics*, 24(2), 102–111.

Gruber, K. A., Ramlochan, T., Boddy, A., Hooton, R. D., and Thomas, M. D. A. (2001). “Increasing concrete durability with high-reactivity metakaolin.” *Cement and Concrete Composites*, 23(6), 479–484.

Guinea, G. V., Pastor, J. Y., Planas, J., and Elices, M. (1998). “Stress Intensity factor, compliance and CMOD for a General Three-Point-Bend Beam.” *International Journal of Fracture*, 89(2), 103–116.

Guneyisi, E. (2010). “Fresh properties of self-compacting rubberized concrete incorporated with fly ash.” *Materials and Structures/Materiaux et Constructions*, 43(8), 1037–1048.

Güneyisi, E., Gesoğlu, M., and Özturan, T. (2004). “Properties of rubberized concretes containing silica fume.” *Cement and Concrete Research*, 34(12), 2309–2317.

Hamza, A. M., and Naaman, A. E. (1991). “Bond Strength of Reinforcing Bars in SIFCON.” ASCE, 1071–1075.

Hasaba, S., Kawamura, M., Koizumi, T., and Takemoto, K. (1984). “Resistibility Against Impact Load and Deformation Characteristics Under Bending Load in Polymer and Hybrid (Polymer and Steel) Fiber Reinforced Concrete.” *Special Publication*, 81, 187–196.

Hooton, R. D. (1993). “Influence of Silica Fume Replacement of Cement on Physical Properties and Resistance to Sulfate Attack, Freezing and Thawing, and Alkali-Silica Reactivity.” *Materials Journal*, 90(2), 143–151.

Hooton, R., Nehdi, M., and Khan, A. (2001). "Cementitious Composites Containing Recycled Tire Rubber: An Overview of Engineering Properties and Potential Applications." *Cement, Concrete and Aggregates*, 23(1), 3.

Hoppe, E. (1998). "Field Study of Shredded-Tire Embankment." *Transportation Research Record: Journal of the Transportation Research Board*, 1619, 47–54.

Hota, S., and Naaman, A. E. (1997). "Bond stress-slip response of reinforcing bars embedded in FRC matrices under monotonic and cyclic loading." *ACI Structural Journal*, 94(5).

Huang, B., Li, G., Pang, S.-S., and Eggers, J. (2004). "Investigation into Waste Tire Rubber-Filled Concrete." *Journal of Materials in Civil Engineering*, 16(3), 187–194.

Humphrey, D. N. (2008). *Civil engineering application of tire derived aggregate.* Alberta Recycling Management Authority, Edmonton.

Humphrey, D. N., Whetten, N., Weaver, J., Recker, K., and Cosgrove, T. A. (1998). "TDA as lightweight fill for embankments and retaining walls." *Conf. on Recycled Materials in Geotechnical Applications*, Arlington, VA.

Jung, J., Kaloush, K., and Way, G. (2003). *Life cycle cost analysis: conventional versus asphalt rubber pavements.* Rubber Pavement Association.

Kaloush, K., Witczak, M., Sotil, A., and Way, G. (2003). *Laboratory evaluation of asphalt rubber mixtures using the dynamic modulus (E∗) Test.* Washington.

Kanakubu, T., Yonemaru, K., Fukuyama, H., Fujisawa, M., and Sonobe, Y. (1993). "Bond Performance of Concrete Members Reinforced With FRP Bars." *Special Publication*, 138, 767–788.

Khatib, Z., and Bayomy, F. (2013). "Rubberized Portland Cement Concrete." *Journal of Materials in Civil Engineering*, 11(3), 206–213.

Khatib, Z. K., and Bayomy, F. M. (1999). "Rubberized Portland Cement Concrete." *Journal of Materials in Civil Engineering*, 11(3), 206–213.

Kramar, D., and Bindiganavile, V. (2013). "Impact response of lightweight mortars containing expanded perlite." *Cement and Concrete Composites*, 37, 205–214.

Larralde, J., and Silva-Rodriguez, R. (1993). “Bond and Slip of FRP Rebars in Concrete.” *Journal of Materials in Civil Engineering*, 5(1), 30–40.

Larrard, F. D., Shaller, I., and Fuchs, J. (1993). “Effect of the Bar Diameter on the Bond Strength of Passive Reinforcement in High-Performance Concrete.” *Materials Journal*, 90(4), 333–339.

Lee, H. S., Lee, H., Moon, J. S., and Jung, H. W. (1998). “Development of tire-added latex concrete.” *ACI Materials Journal*, 95(4), 356–364.

Leung, F., Tighe, S., Macdonald, G., and Penton, S. (2006). “Noise Reducing Asphalt Pavements: A Canadian Case Study.”

Lo Presti, D. (2013). “Recycled Tyre Rubber Modified Bitumens for road asphalt mixtures: A literature review.” *Construction and Building Materials*, 49, 863–881.

Makitani, E., Irisawa, I., and Nishiura, N. (1993). “Investigation of Bond in Concrete Member With Fiber Reinforced Plastic Bars.” *Special Publication*, 138, 315–332.

Malvar, L. J. (1994). *Bond Stress-Slip Characteristics of FRP Rebars.* Office of Naval Research, naval Cailities Engineering Service Center, port Hueneme, California.

Md Toihidul Islam. (2010). “Static and Dynamic Response of Sandstone Masonry Units Bound with Fibre Reinforced Mortars.” Master’s Thesis, University of Alberta.

Mehta, P. K. (1983). “Pozzolanic and Cementitious Byproducts as Mineral Admixtures for Concrete - A Critical Review.” *Special Publication*, 79, 1–46.

Mehta, P. K., and Gjørv, O. E. (1982). “Properties of portland cement concrete containing fly ash and condensed silica-fume.” *Cement and Concrete Research*, 12(5), 587–595.

Mehta, P. K., and Monteiro, P. J. M. (2014). *Concrete. Structure, properties and materials*. New York, McGraw-Hill Professional.

Mills, B., and McGinn, J. (2010). “Design, Construction, and Performance of a Highway Embankment Failure Repaired with Tire-Derived Aggregate.” *Transportation Research Record: Journal of the Transportation Research Board*, 2170, 90–99.

Mindess, S., Banthia, N., and Bentur, A. (1986). “The response of reinforced concrete beams with a fibre concrete matrix to impact loading.” *International Journal of Cement Composites and Lightweight Concrete*, 8(3), 165–170.

Mindness, S., Bentur, A., Yan, C., and Vondran, G. (1989). “Impact Resistance of Concrete Containing Both Conventional Steel Reinforcement and Fibrillated Polypropylene Fibers.” *Materials Journal*, 86(6), 545–549.

Mor, A. (1993). “Steel-Concrete Bond in High-Strength Lightweight Concrete.” *Materials Journal*, 89(1), 76–82.

Mufti, A. A., Bentur, A., and Banthia, N. (1998). *Fiber reinforced concrete: present and future*. Canadian Society for Civil Engineering, Montreal.

Muhammad Mamun. (2010). “Loading Rate Effects and Sulphate Resistance of Fibre Reinforced Cement-based Foams.” Master’s Thesis, University of Alberta.

Naaman, A. E., and Gopalaratnam, V. S. (1983). “Impact properties of steel fibre reinforced concrete in bending.” *International Journal of Cement Composites and Lightweight Concrete*, 5(4), 225–233.

Nadeau, J. S., Bennett, R., and Fuller Jr, E. R. (1982). “An explanation for the rate-of-loading and the duration-of-load effects in wood in terms of fracture mechanics.” *Journal of Materials Science*, 17(10), 2831–2840.

Najim, K. B., and Hall, M. R. (2012). “Mechanical and dynamic properties of self-compacting crumb rubber modified concrete.” *Construction and Building materials*, 27(1), 521–530.

Nanni, A., Al-Zaharani, M. M., Al-Dulaijan, S. U., and Bakis, C. E. (1995). “Bond of FRP reinforcement to concrete - Experimental results.” Non-metallic (FRP) reinforcement for concrete structures, L. Taerwe, ed., Spon, 135–145.

Nanni, A., Nenninger, J. S., Ash, K. D., and Liu, J. (1997). “Experimental bond behavior of hybrid rods for concrete reinforcement.” *Structural Engineering and Mechanics*, 5(4), 339–354.

Nelson, B. E. (2009). “Using tire chips for roadway embankment fill.” Centre for Integrated Waste management, Buffalo, NY.

NRMCA. (2012). *National Ready Mixed Concrete Association Concrete CO2 Fact Sheet*.

Pecce, M., Manfredi, G., Realfonzo, R., and Cosenza, E. (2001). “Experimental and Analytical Evaluation of Bond Properties of GFRP Bars.” *Journal of Materials in Civil Engineering*, 13(4), 282–290.

Qian, X., and Li, Z. (2001). “The relationships between stress and strain for high-performance concrete with metakaolin.” *Cement and Concrete Research*, 31(11), 1607–1611.

Raghavan, D., Huynh, H., and Ferraris, C. (1998a). “Workability, mechanical properties, and chemical stability of a recycled tyre rubber-filled cementitious composite.” *Journal of Materials Science*, 33(7), 1745–1752.

Raghavan, D., Huynh, H., and Raghavan, D. (1998b). “Workability, mechanical properties, and chemical stability of a recycled tyre rubber-filled cementitious composite.” *Journal of Materials Science*, 33(7), 1745–1752.

Reid, R. A., Soupir, S. P., and Schaefer, V. R. (1998). “Mitigation of Void Development under Bridge Approach Slabs Using Rubber Tire Chips.” ASCE, 37–50.

Rossetti, V. A., Galeota, D., and Giammatteo, M. M. (1995). “Local bond stress-slip relationships of glass fibre reinforced plastic bars embedded in concrete.” *Materials and Structures*, 28(6), 340–344.

Sabir, B. B. (1997). “Mechanical properties and frost resistance of silica fume concrete.” *Cement and Concrete Composites*, 19(4), 285–294.

Savas, B., Ahmad, S., and Fedroff, D. (1997). “Freeze-Thaw Durability of Concrete with Ground Waste Tire Rubber.” *Transportation Research Record: Journal of the Transportation Research Board*, 1574, 80–88.

Segre, N., and Joekes, I. (2000). “Use of tire rubber particles as addition to cement paste.” *Cement and Concrete Research*, 30(9), 1421–1425.

Siddique, R., and Naik, T. R. (2004). “Properties of concrete containing scrap-tire rubber - An overview.” *Waste Management*, 24(6), 563–569.

Soretz, S. (1972). “A comparison of beam tests and pull-out tests.” *Matériaux et Constructions*, 5(4), 261–264.

Soroushian, P., Mirza, F., and Alhozaimy, A. (1994). “Bond of confined steel fiber reinforced concrete to deformed bars.” *ACI Materials Journal*, 91(2).

Suaris, W., and Shah, S. P. (1983). “Properties of Concrete Subjected to Impact.” *Journal of Structural Engineering*, 109(7), 1727–1741.

Suaris, W., and Shah, S. P. (1984). “Test Methods for Impact Resistance of Fiber Reinforced Concrete.” *Special Publication*, 81, 247–266.

Taha, M. M. R., El-Dieb, A. S., El-Wahab, M. A. A., and Abdel-Hameed, M. E. (2008). “Mechanical, fracture, and microstructural investigations of rubber concrete.” *Journal of Materials in Civil Engineering*, 20(10), 640–649.

Tatlisoz, N., Edil, T. B., and Benson, C. H. (1998). “Interaction between Reinforcing Geosynthetics and Soil-Tire Chip Mixtures.” *Journal of Geotechnical and Geoenvironmental Engineering*, 124(11), 1109–1119.

Tepfers, R. (1979). “Cracking of concrete cover along anchored deformed reinforcing bars.” *Magazine of concrete research*, 31(106), 3–12.

Tepfers, R. (2006). “Bond clause proposals for FRP bars/rods in concrete based on CEB/FIP Model Code 90. Part 1: Design bond stress for FRP reinforcing bars.” *Structural Concrete*, 7(2), 47–55.

Terrel, R., and Walter, J. (1986). “Modified asphalt materials – the European Experience.” *AAPT*, 482–518.

Tighiouart, B., Benmokrane, B., and Gao, D. (1998). “Investigation of bond in concrete member with fibre reinforced polymer (FRP) bars.” *Construction and Building Materials*, 12(8), 453–462.

Topçu, lker B., and Avcular, N. (1997). “Analysis of rubberized concrete as a composite material.” *Cement and Concrete Research*, 27(8), 1135–1139.

Topçu, I. B. (1995). “The properties of rubberized concretes.” *Cement and Concrete Research*, 25(2), 304–310.

Toutanji, H. A. (1996). “The use of rubber tire particles in concrete to replace mineral aggregates.” *Cement and Concrete Composites*, 18(2), 135–139.

Tweedie, J., Humphrey, D., and Sandford, T. (1998a). “Full-Scale Field Trials of Tire Shreds as Lightweight Retaining Wall Backfill Under At-Rest Conditions.” *Transportation Research Record: Journal of the Transportation Research Board*, 1619, 64–71.

Tweedie, J. J., Humphrey, D. N., and Sandford, T. C. (1998b). “Tire Shreds as Lightweight Retaining Wall Backfill: Active Conditions.” *Journal of Geotechnical and Geoenvironmental Engineering*, 124(11), 1061–1070.

“U.S. Scrap Tire Market.” (2003). *Rubber Manufacturer Association*.

Wartman, J., Natale, M. F., and Strenk, P. M. (2007). “Immediate and Time-Dependent Compression of Tire Derived Aggregate.” *Journal of Geotechnical and Geoenvironmental Engineering*, 133(3), 245–256.

Wedding, P., Suaris, W., and Shah, S. (1981). “Inertial Effects in the Instrumented Impact Testing of Cementitious Composites.” *Cement, Concrete and Aggregates*, 3(2), 77.

Whetten, N., Weaver, J., Humphrey, D., and Sandford, T. (1997). “RUBBER MEETS THE ROAD IN MAINE.” *Civil Engineering*, 67(9).

Wild, S., Khatib, J. M., and Jones, A. (1996). “Relative strength, pozzolanic activity and cement hydration in superplasticised metakaolin concrete.” *Cement and Concrete Research*, 26(10), 1537–1544.

Wong, S.-F., and Ting, S.-K. (2009). “Use of recycled rubber tires in normal and high-strength concretes.” *ACI Materials Journal*, 106(4).

Yan, C. (1992a). “Bond between reinforcing bars and concrete under impact loading.” University of British Columbia.

Yan, C. (1992b). “Bond between reinforcing bars and concrete under impact loading.” PhD Thesis, University of British Columbia, Vancouver, Canada.

Zheng, L., Huo, X. S., and Yuan, Y. (2008). “Strength, Modulus of Elasticity, and Brittleness Index of Rubberized Concrete.” *Journal of Materials in Civil Engineering*, 20(11), 692–699.

Zollo, R. F. (1984). “Collated Fibrillated Polypropylene Fibers in FRC.” *Special Publication*, 81, 397–410.

Zuo, J., and Darwin, D. (2000). “Bond Slip of High Relative Rib Area Bars under Cyclic Loading.” *Structural Journal*, 97(2), 331–334.

APPENDIX

Appendix - A

Figure A-1: Sample image analysis of FRP bar surface (16 mm)

(1)

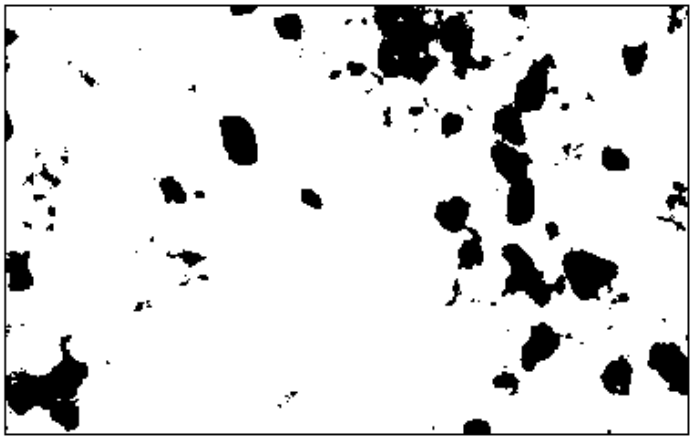

(2)

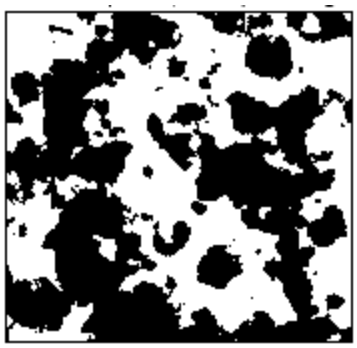

(3)

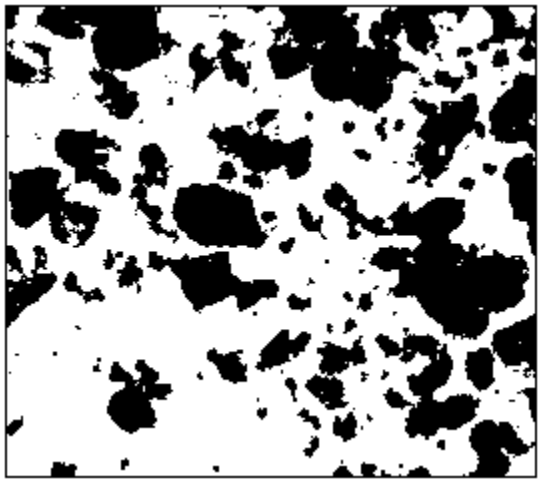

(4)

Figure A-2: Sample image analysis of FRP bar surface (10 mm)

(1)

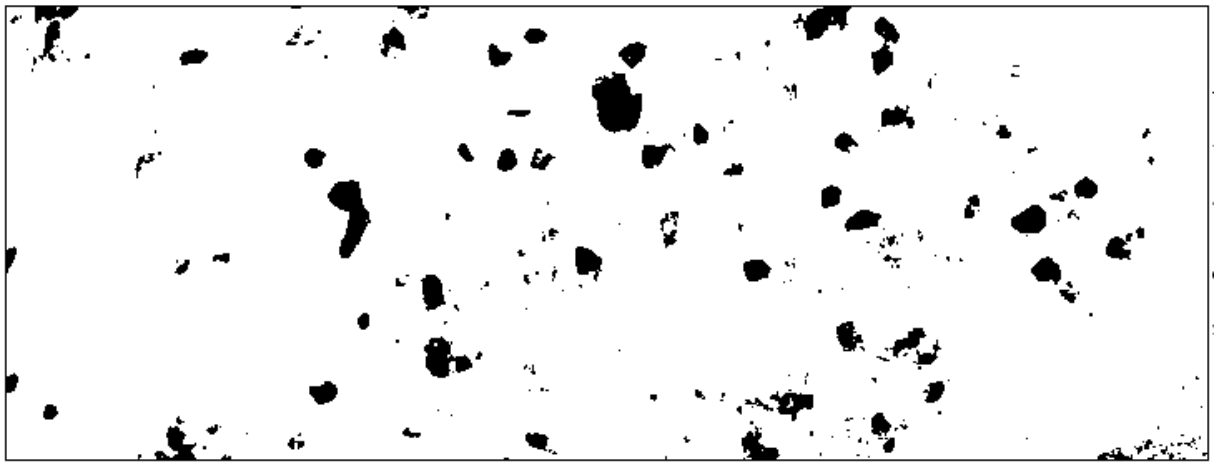

(2)

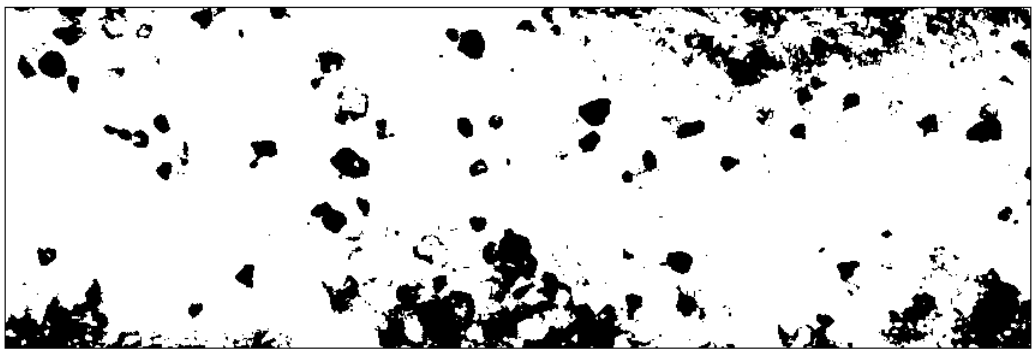

(3)

Appendix – B

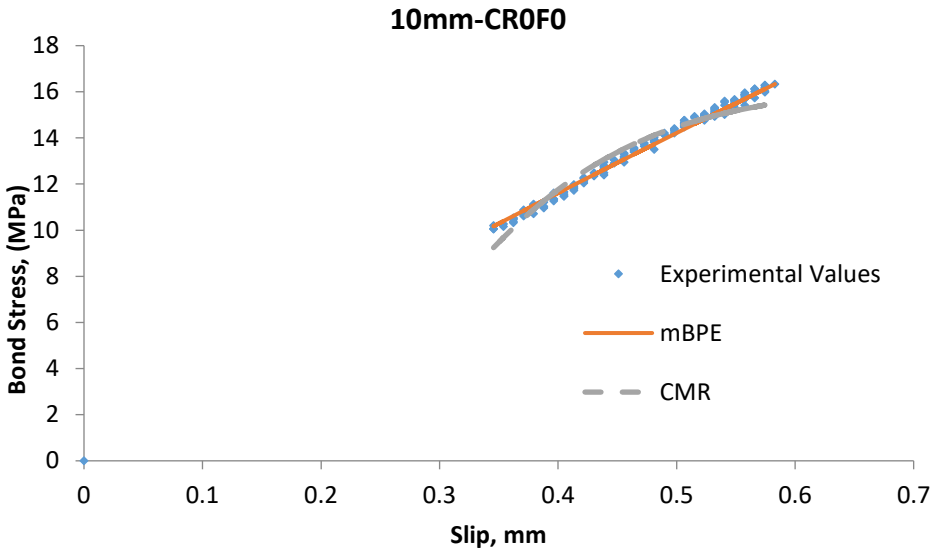

Figure B-1 (a) Comparison for the 10mm bar with 0% rubber without steel fibre

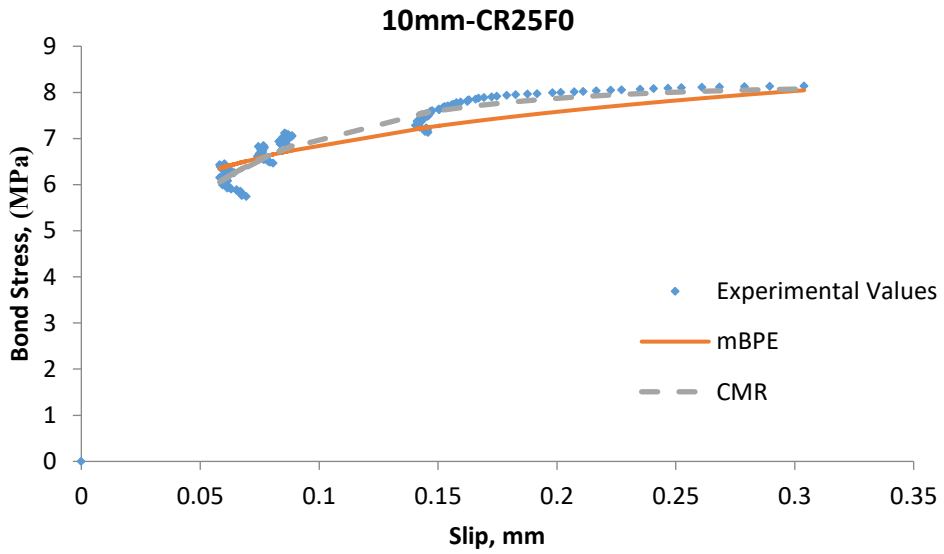

Figure B-1 (b) Comparison for the 10mm bar with 25% rubber without steel fibre

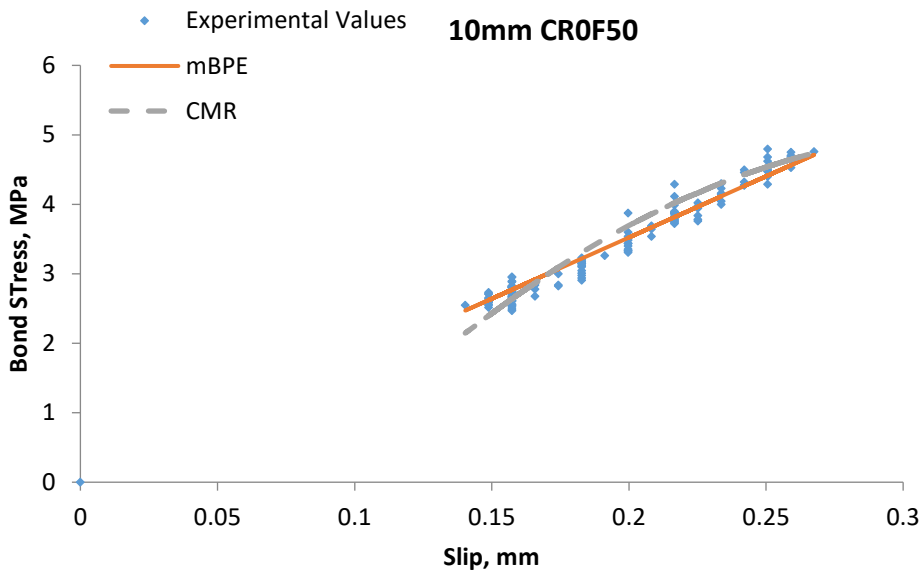

Figure B-1 (c) Comparison for the 10mm bar with 50% rubber without steel fibre

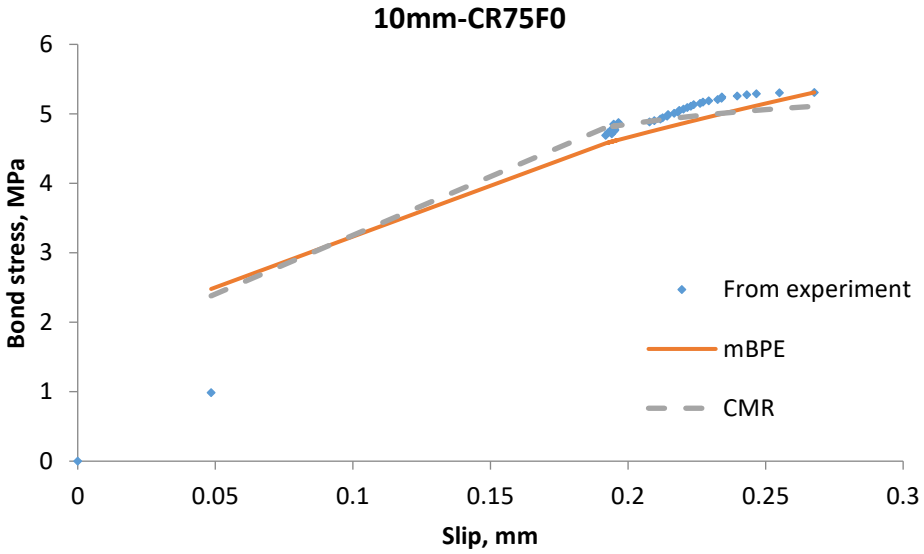

Figure B-1 (d) Comparison for the 10mm bar with 75% rubber without steel fibre

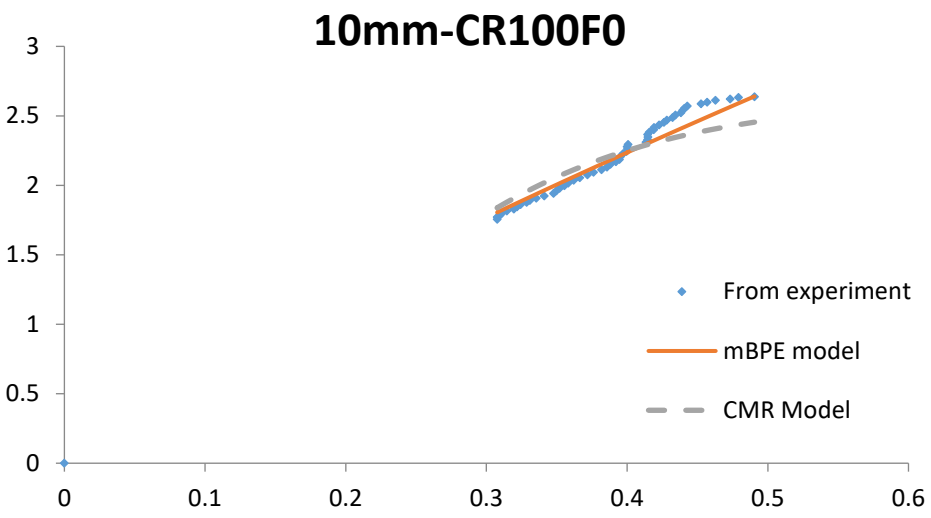

Figure B-1 (e) Comparison for the 10mm bar with 100% rubber without steel fibre

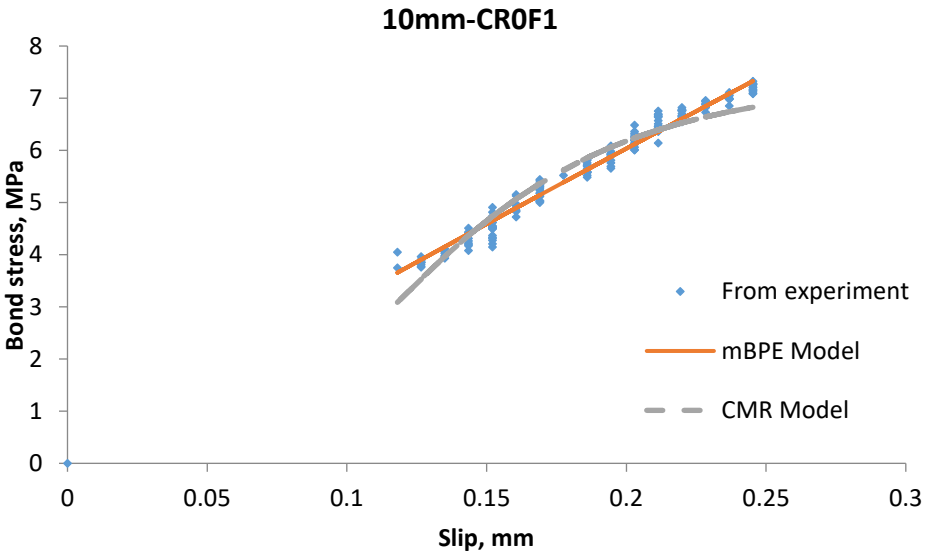

Figure B-2 (a) Comparison for the 10mm bar with 0% rubber with steel fibre

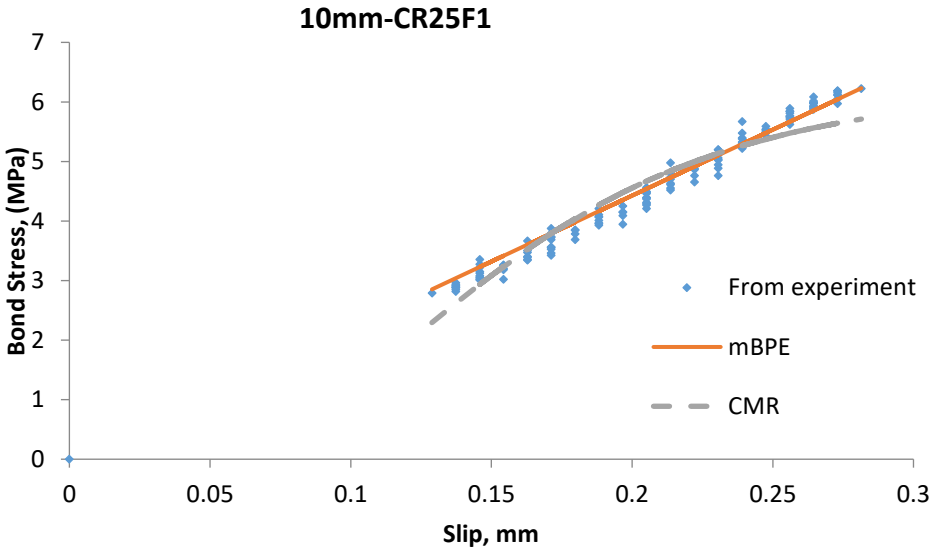

Figure B-2 (b) Comparison for the 10mm bar with 25% rubber with steel fibre

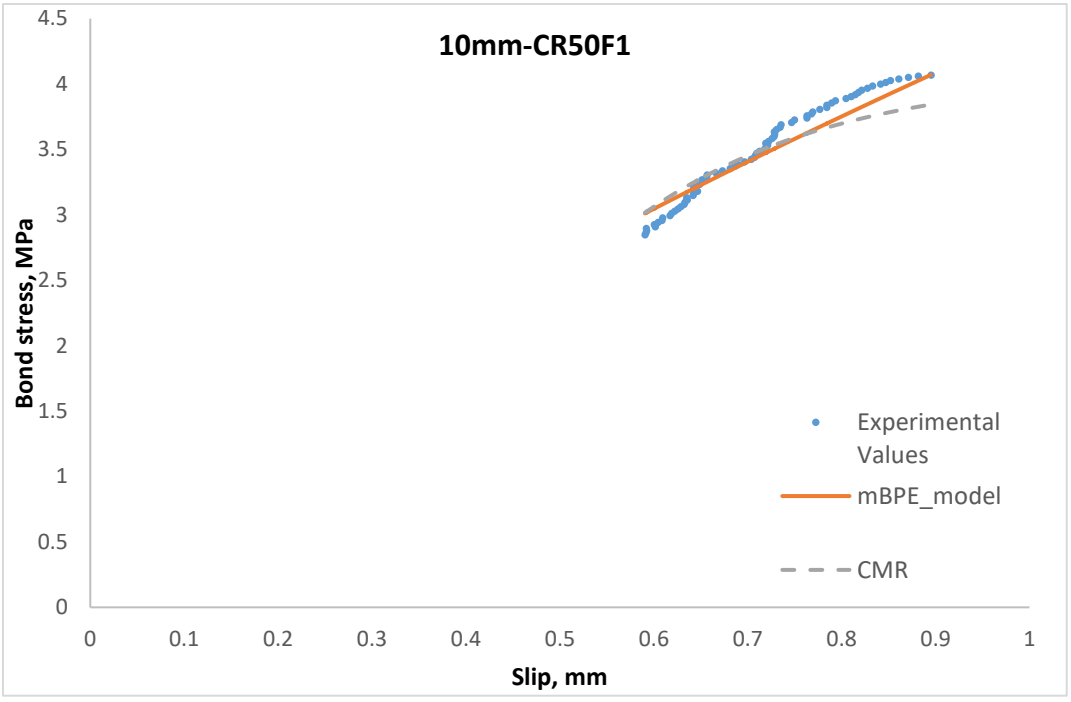

Figure B-2 (c) Comparison for the 10mm bar with 50% rubber with steel fibre

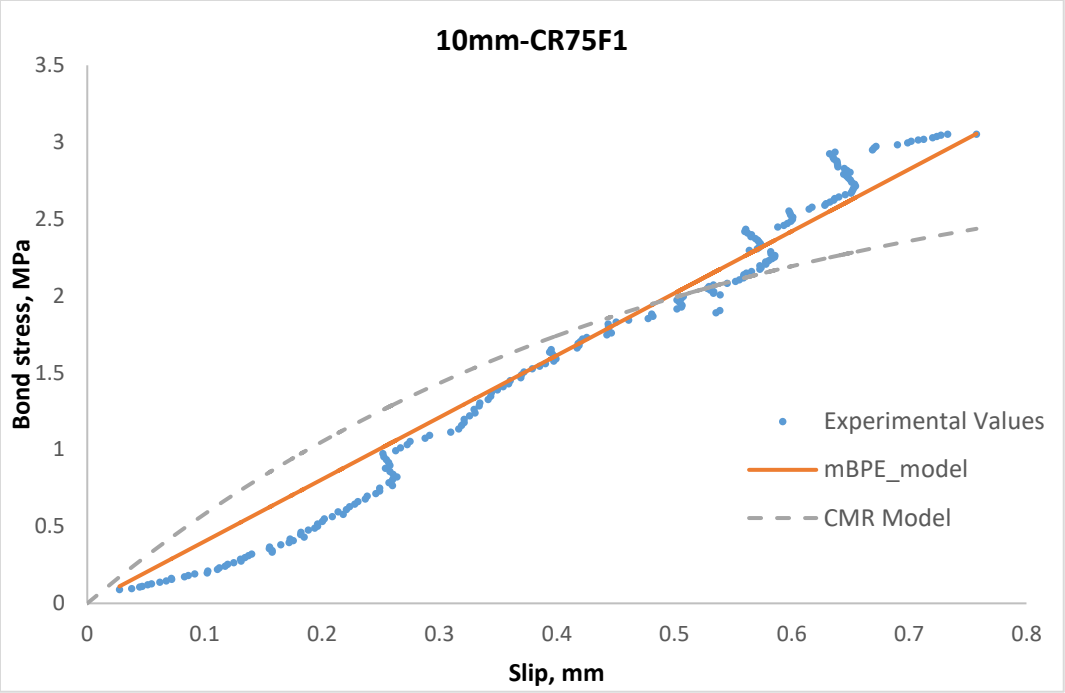

Figure B-2 (d) Comparison for the 10mm bar with 75% rubber with steel fibre

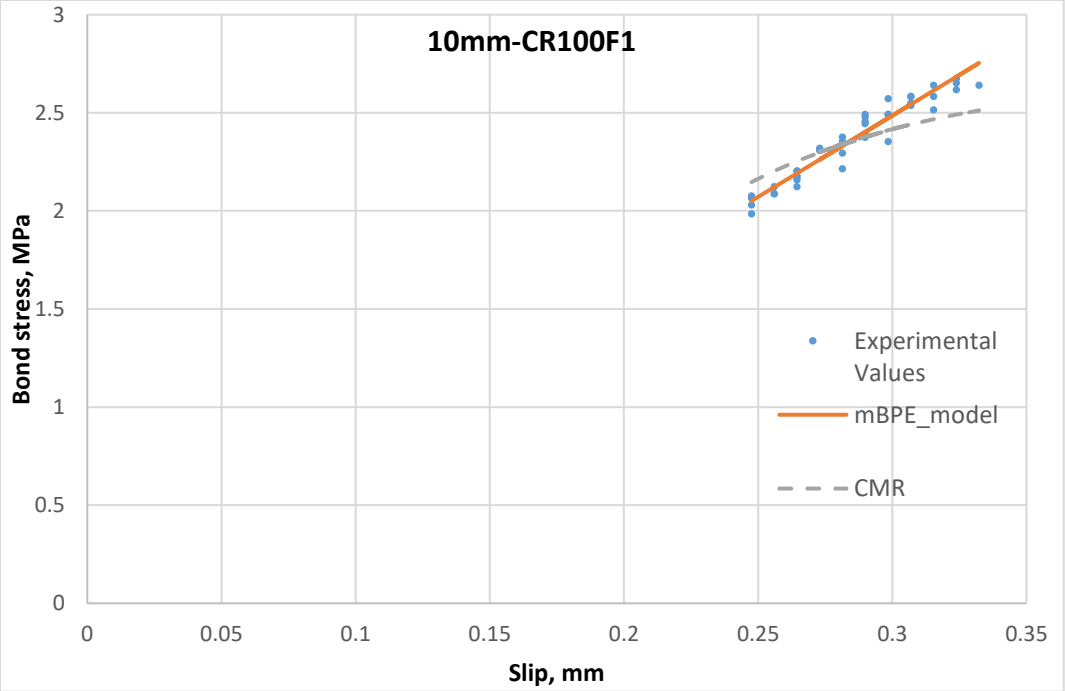

Figure B-2 (e) Comparison for the 10mm bar with 100% rubber with steel fibre

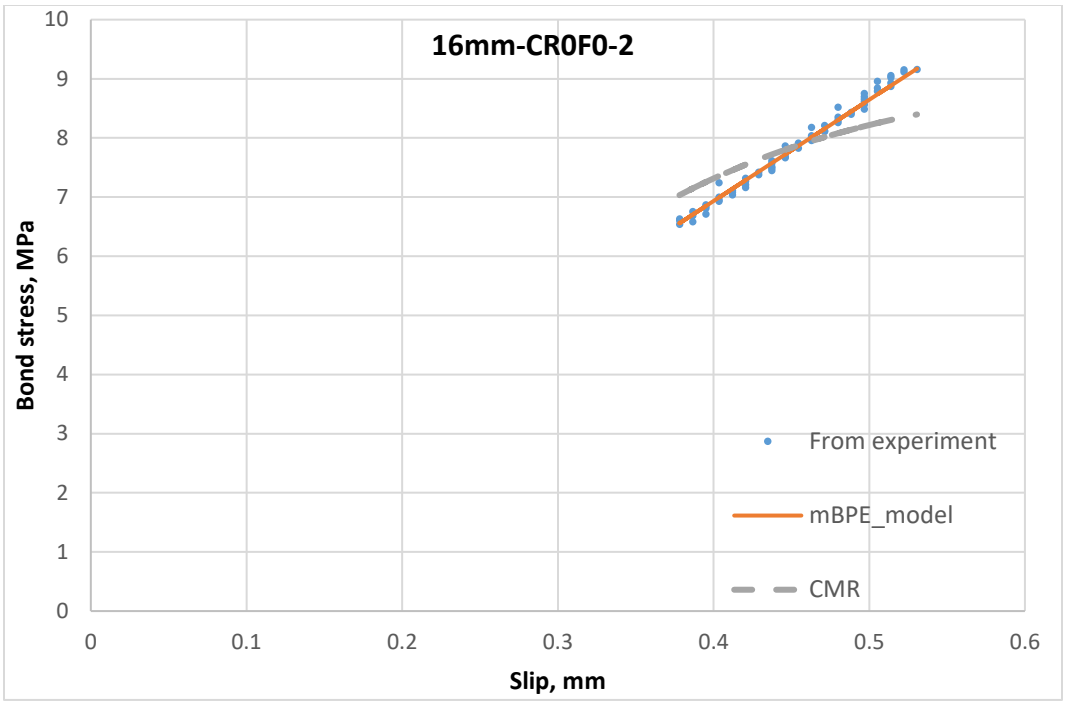

Figure B -3 (a) Comparison for the 16mm bar with 0% rubber without steel fibre

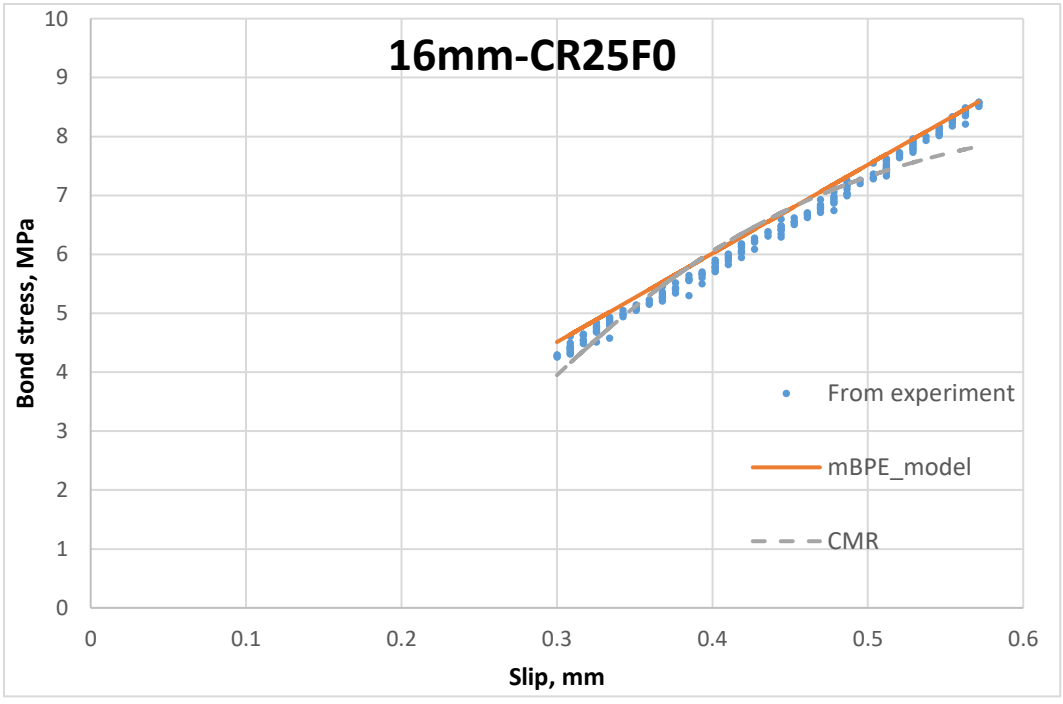

Figure B-3 (b) Comparison for the 16mm bar with 25% rubber without steel fibre

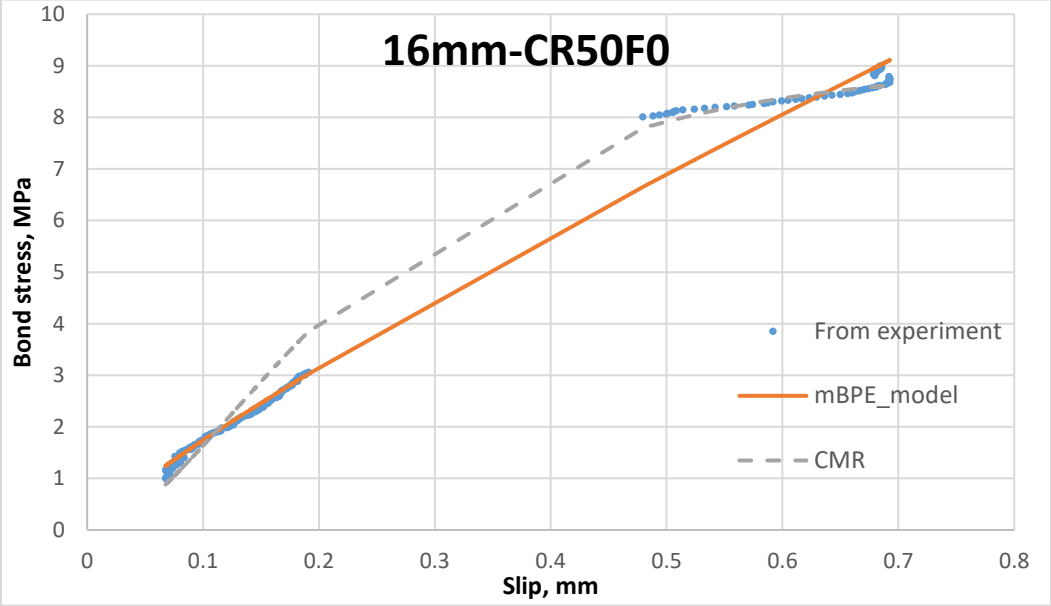

Figure B-3 (c) Comparison for the 16mm bar with 50% rubber without steel fibre

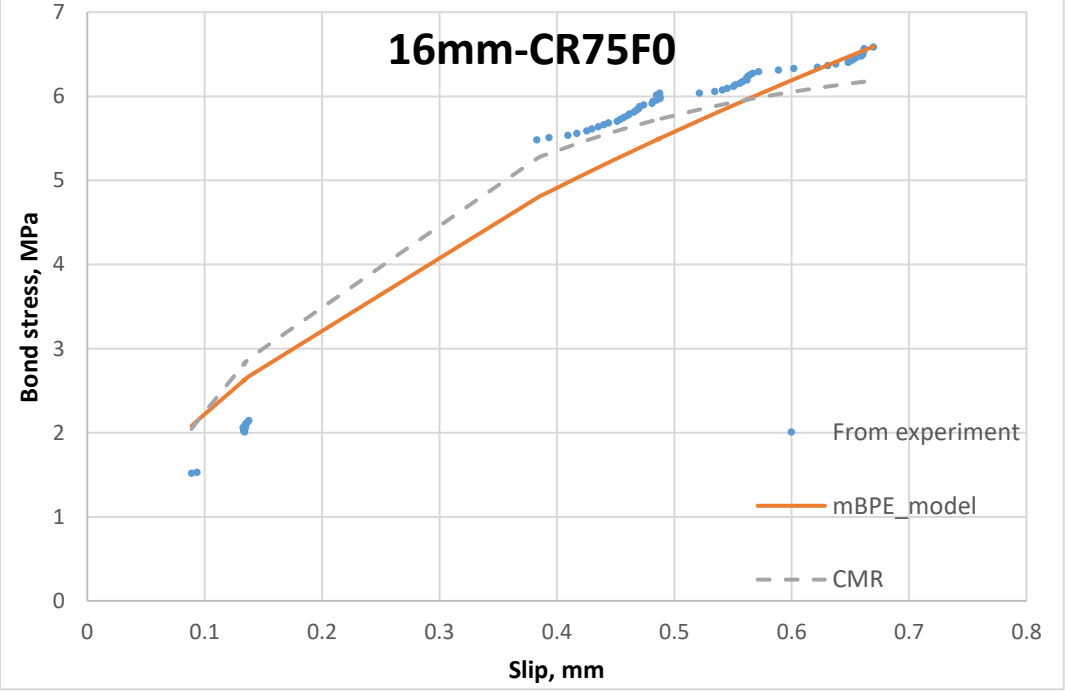

Figure B-3 (d) Comparison for the 16mm bar with 75% rubber without steel fibre

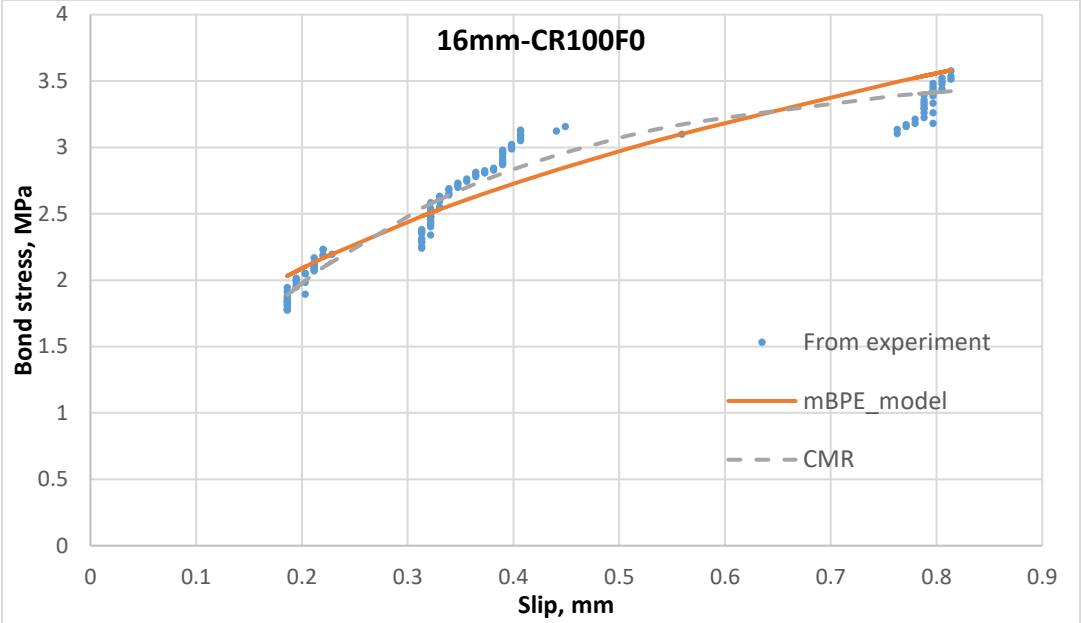

Figure B -3 (e) Comparison for the 16mm bar with 100% rubber without steel fibre

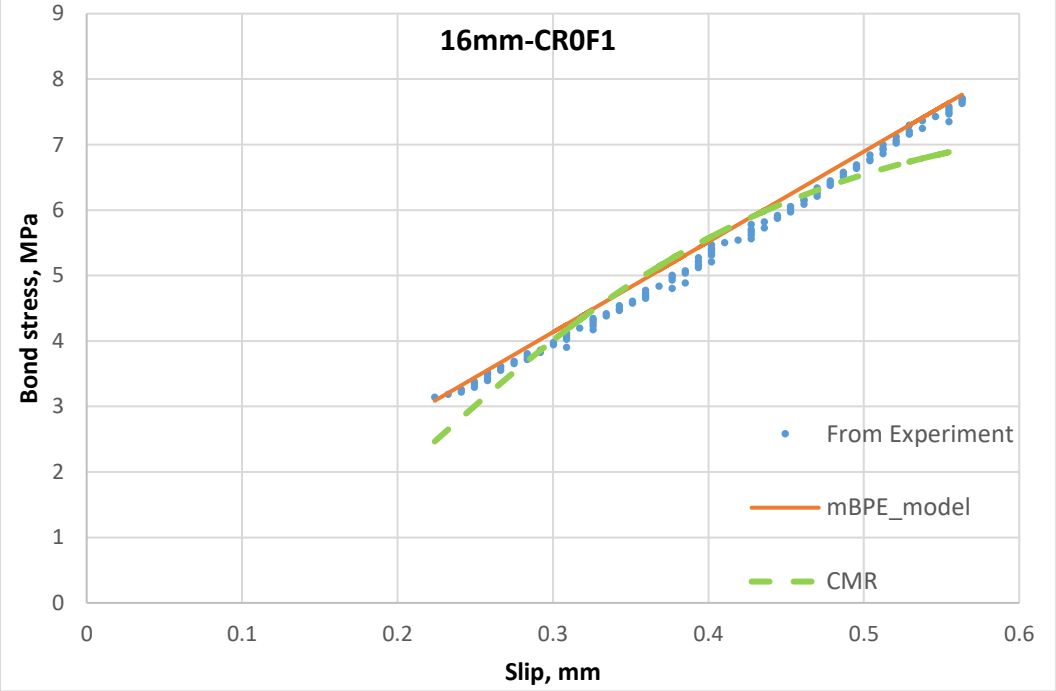

Figure B-4 (a) Comparison for the 16mm bar with 0% rubber with steel fibre

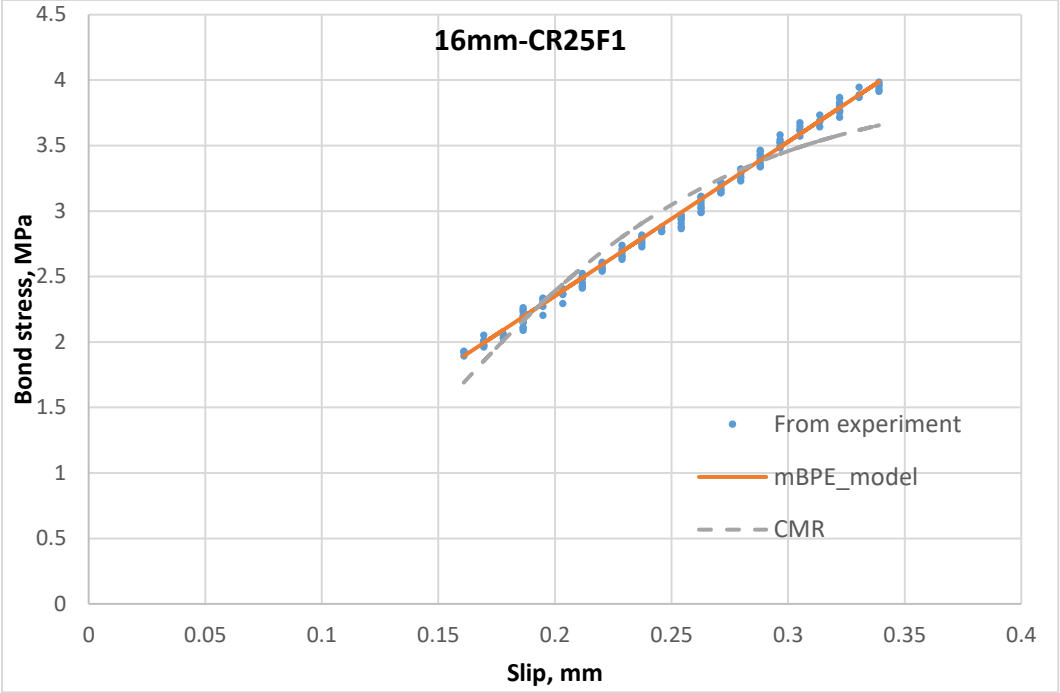

Figure B -4 (b) Comparison for the 16mm bar with 25% rubber with steel fibre

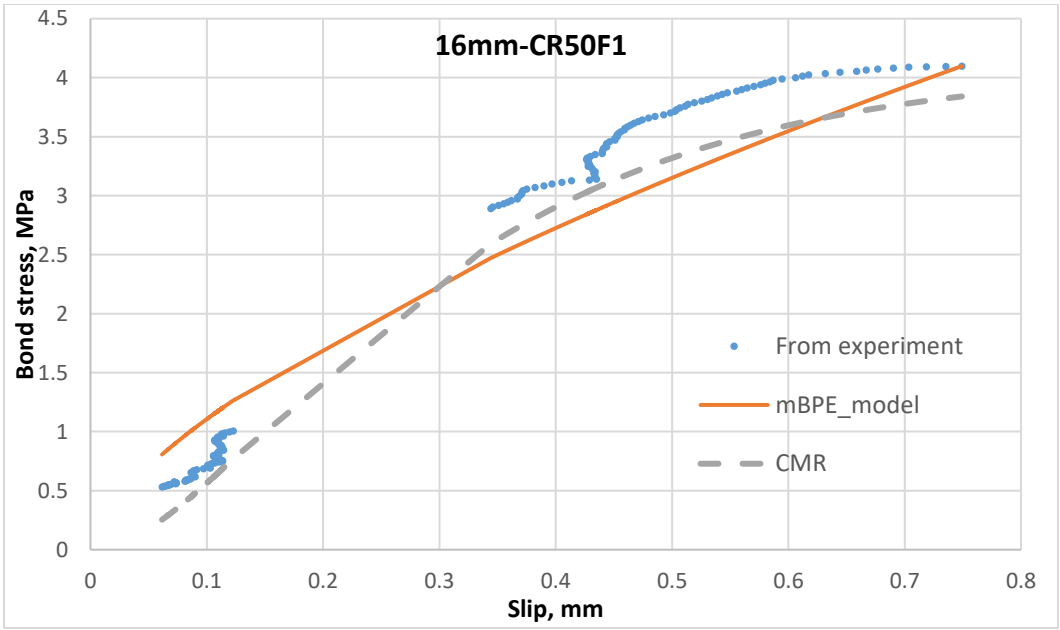

Figure B-4 (c) Comparison for the 16mm bar with 50% rubber with steel fibre

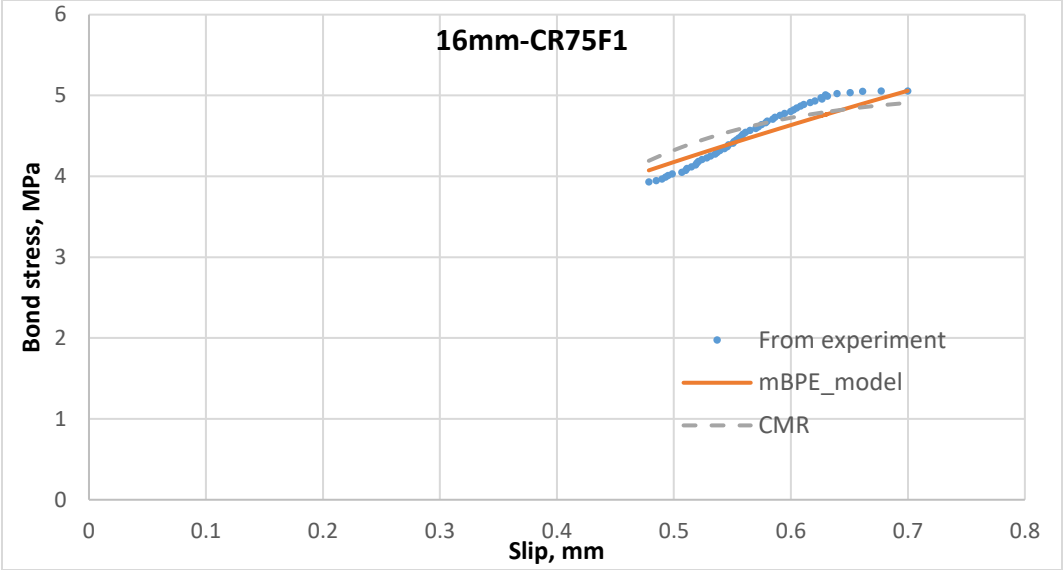

Figure B-4 (d) Comparison for the 16mm bar with 0% rubber with steel fibre

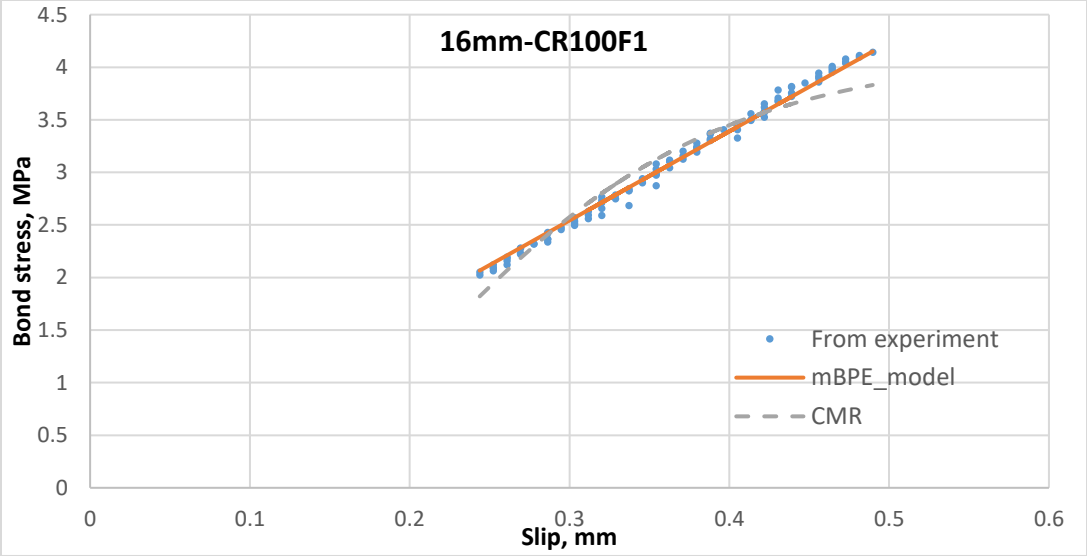

Figure B-4 (e) Comparison for the 16mm bar with 100% rubber with steel fibre

Appendix – C

F = Total applied load on the beam

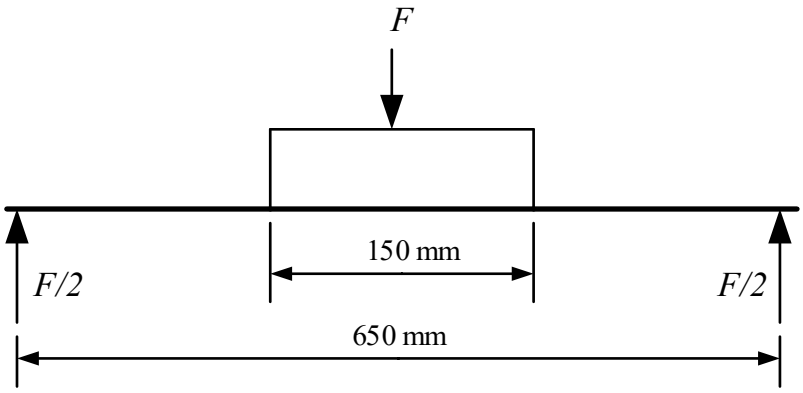

Reaction at each support = $F/2$ (due to loading symmetry)

Maximum Moment = $F/2 \times 250 = 125 \cdot F$

This moment is resisted by the couple between tensile force in the rebar T and compressive force, C. This tensile force is equal to the pullout force exerted in the bar, P

Resisting moment = T × moment arm = $100 \cdot P$

Hence, $100 \cdot P = 125 \cdot F$

$P = 1.25 \cdot F$

Appendix – D

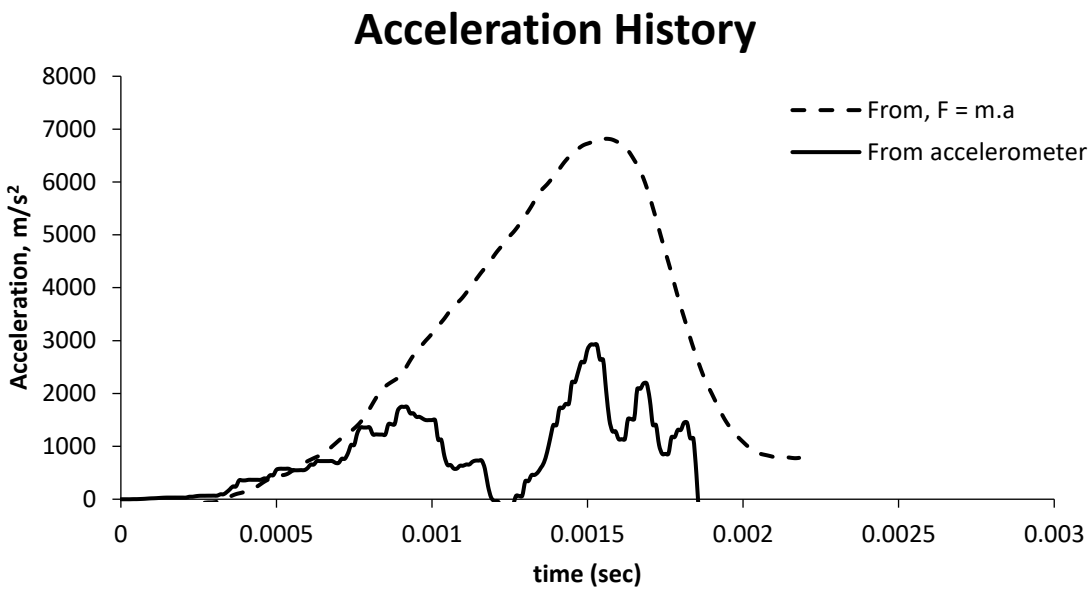

CR0F1- Only OPC –Drop Height 250 mm

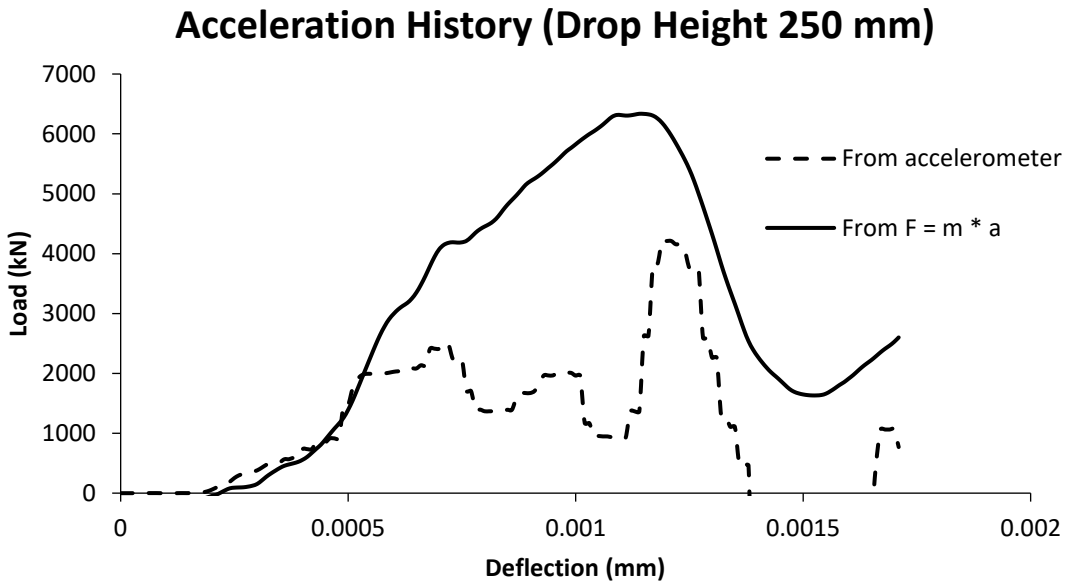

CR0F1 OPC and Silica Fume, Drop Height 250 mm

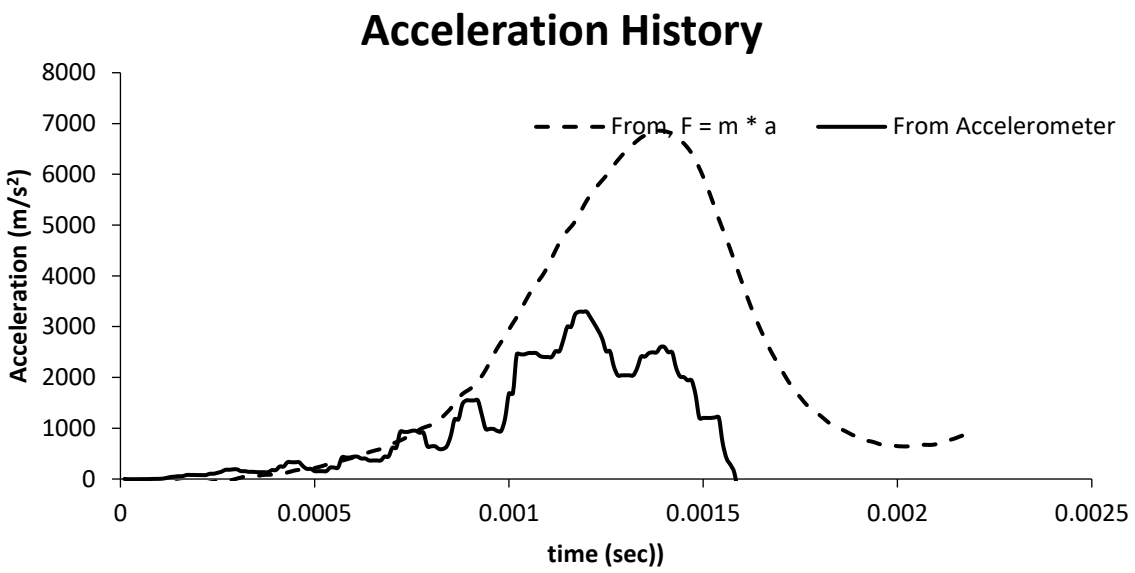

CR0F1OPC and Metakaolin, Drop Height 250 mm

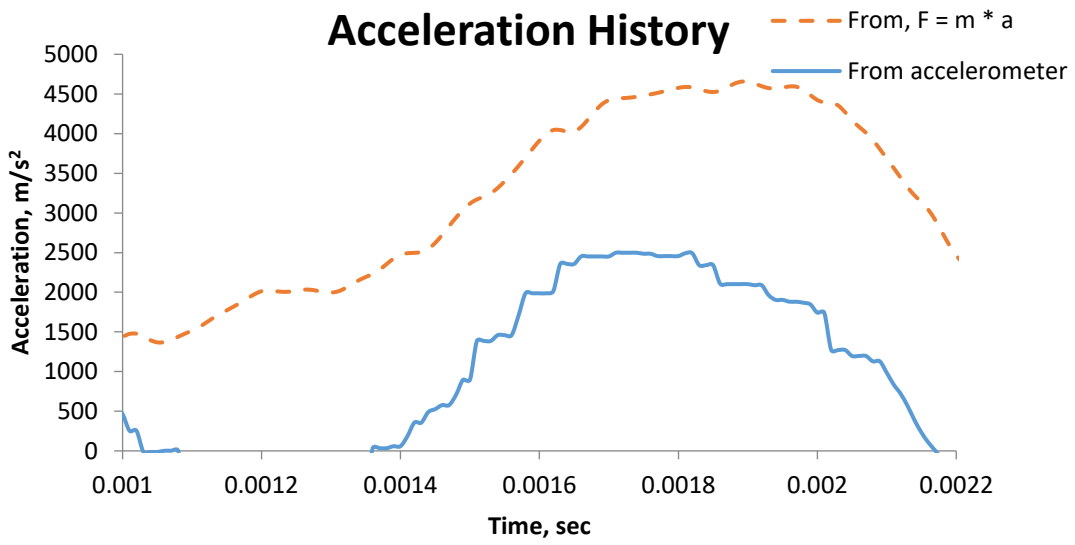

CR25F1 Only OPC, Drop Height 250 mm

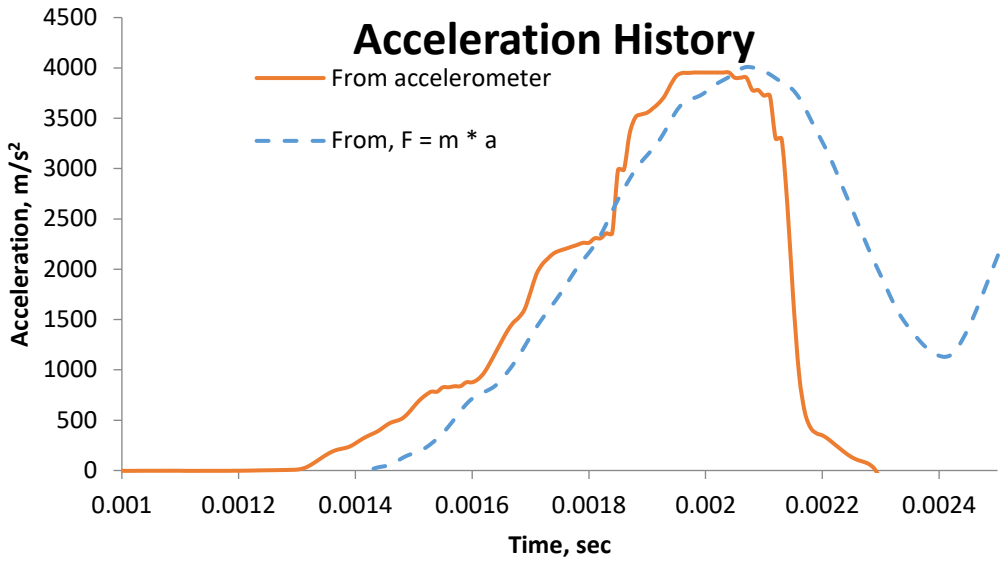

CR25F1 OPC and Silica Fume, Drop Height 250 mm

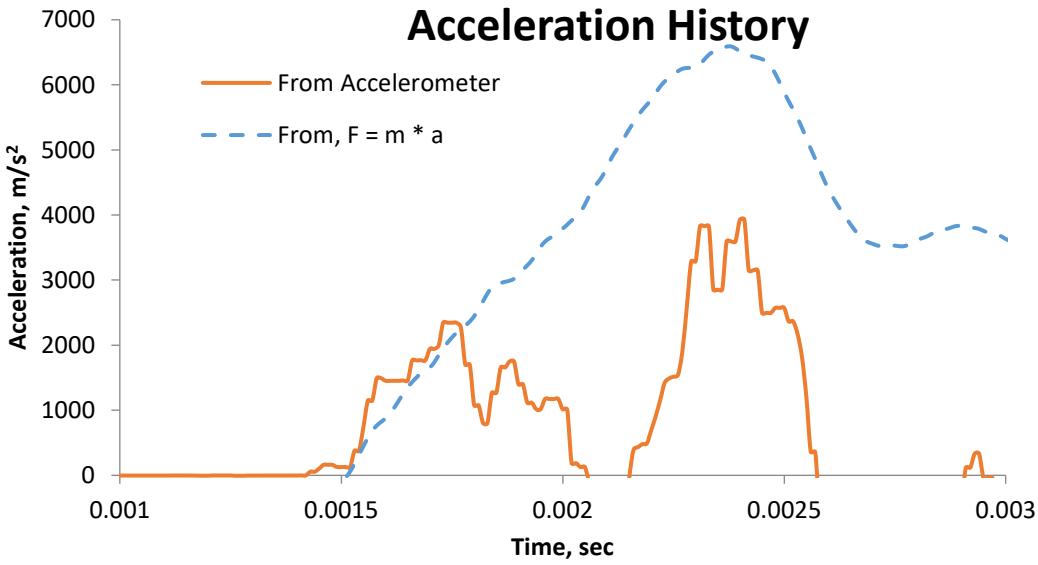

CR25F1 OPC and Metakaolin, Drop Height 250 mm

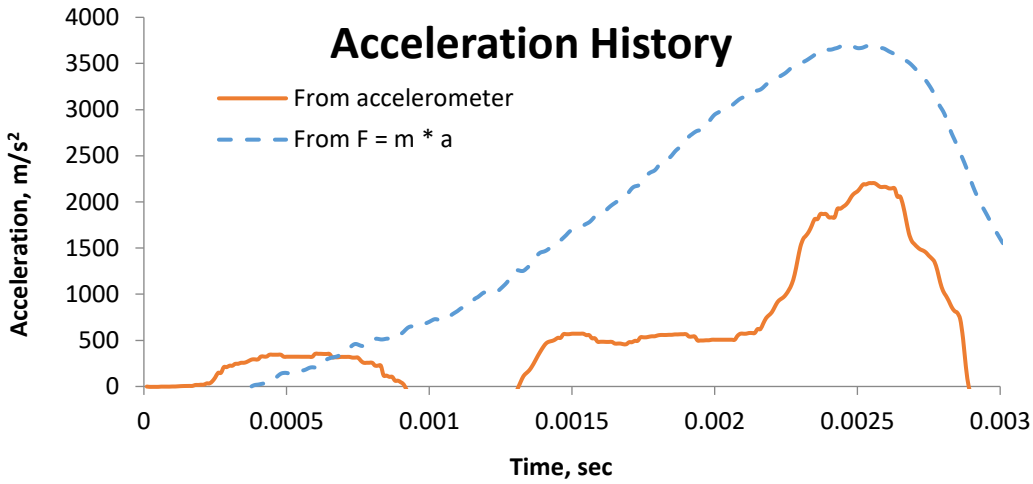

CR75F1 Only OPC, Drop Height 250 mm

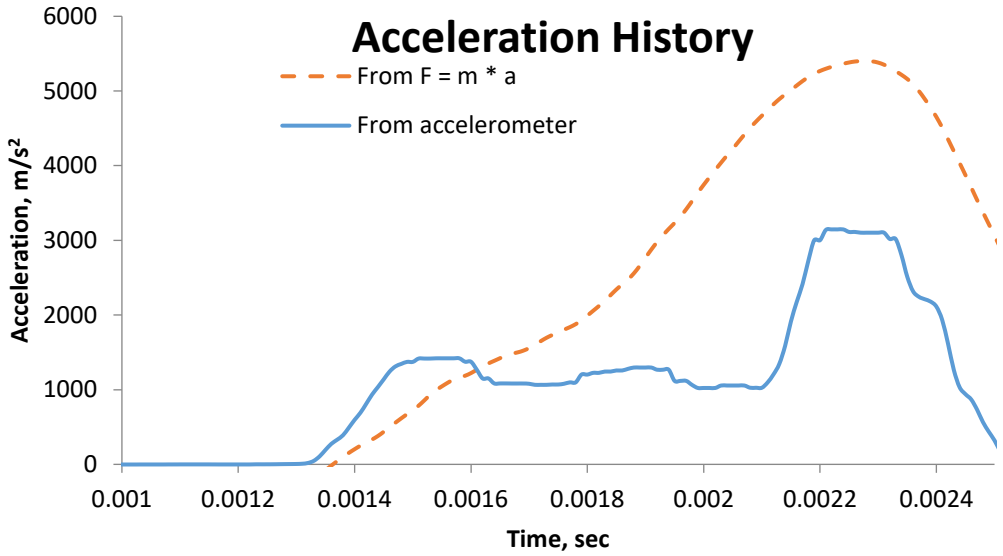

CR75F1 OPC and Silica Fume, Drop Height 250 mm

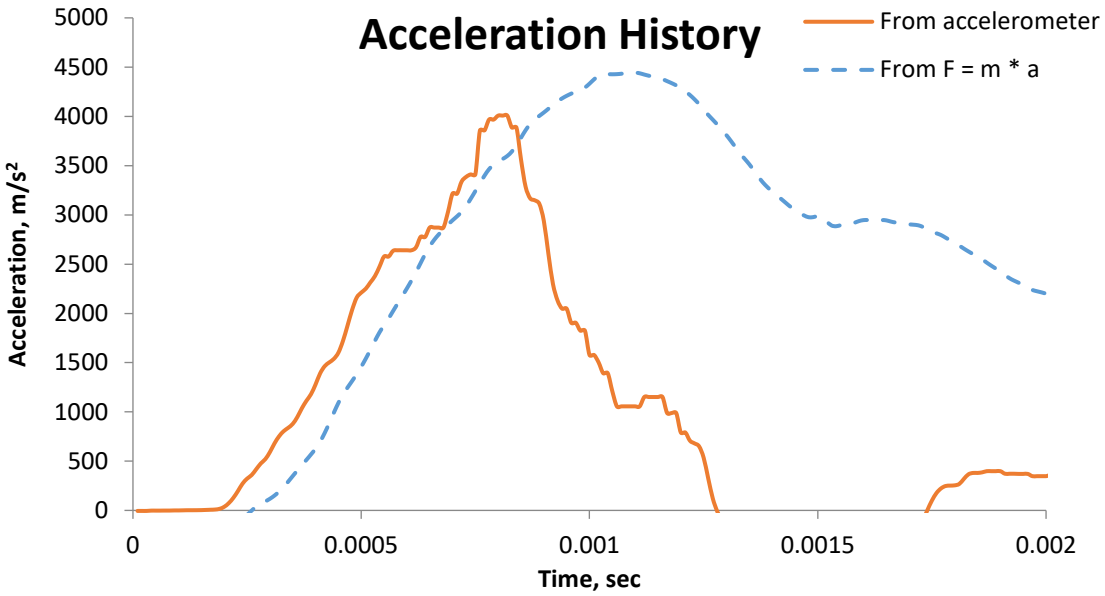

CR75F1 OPC and Metakaolin, Drop Height 250 mm